PROJEKTOWANIE
Z WYKORZYSTANIEM WYBRANYCH
STALOWYCH PROFILI CIENKOŚCIENNYCH
– PROCEDURY OPRACOWANE
W RAMACH PROJEKTU
„GRISPE PLUS"

TOM 1
PREZENTACJE

REDAKCJA NAUKOWA
MARIUSZ MAŚLAK

POLITECHNIKA KRAKOWSKA
KRAKÓW 2018

Materiały prezentowane w książce zostały opracowane w ramach
międzynarodowego projektu badawczego
„**Grispe Plus - Valorisation of knowledge for specific profiled steel sheets**”
finansowanego przez Unię Europejską w ramach funduszu
Research Fund for Coal and Steel (grant agreement **RFCS-2016 No 754092**).

Redakcja naukowa
Mariusz Maślak
Katedra Konstrukcji Metalowych,
Instytut Materiałów i Konstrukcji Budowlanych,
Wydział Inżynierii Lądowej,
Politechnika Krakowska,
ul. Warszawska 24, 31-155 Kraków,
e-mail: mmaslak@pk.edu.pl.

ISBN 978-83-953563-2-2 Tomy 1 i 2
w tym:
ISBN 978-953563-0-8 Tom 1: Prezentacje

Nakład 100 egz.
Druk i oprawa: Wydawnictwo PiT, 31-455 Kraków, ul. Ułanów 54/51
e-mail: wydawnictwopit@op.pl

Spis treści

Tom 1

1. Wprowadzenie 5
2. Partnerzy współpracujący w projekcie „Grispe Plus” 11
3. Uczestnicy seminarium „Grispe Plus” w Krakowie, 14.06.2018 21
4. Profile cienkościenne analizowane w projekcie 27
5. State-of-the-art 29
    5.1. Steel decks (Anna Palisson) 31
    5.2. Liner trays + assembled profiles + corrugated sheets + curved profiles (Christian Fauth) 49
    5.3. Perforated and holed profiles (Anna Palisson) 75
    5.4. Interlocking planks (Mickael Blanc, Thibault Renaux) 97
6. Prezentacje omawiane podczas seminarium w Krakowie 117
    6.1. Wprowadzenie do projektu „Grispe Plus” 119
    6.2. Steel decks with embossments/indentations and/or outwards stiffener (Anna Palisson) 127
    6.3. Corrugated sheeting (Thibault Renaux) 159
    6.4. Curved profiles (Irene Puncello, Silvia Caprili, Walter Salvatore) 209
    6.5. Assembled profiles (Thibault Renaux) 251
    6.6. Grispe Workshop – Interactive section (David Izabel) 311
    6.7. Grispe Workshop – Proposals for the inclusion of 9 calculation methods into EN1993-1-3 (David Izabel) 335

Tom 2

7. Szczegółowe instrukcje projektowania 5
    7.1. Steel decks with embossments – autor wersji oryginalnej: Anna Palisson, tłumaczenie na język polski: Anna Palisson 7
    7.2. Steel decks with outwards stiffeners – autor wersji oryginalnej: Anna Palisson, tłumaczenie na język polski: Anna Palisson 61
    7.3. Liner trays – autorzy wersji oryginalnej: Markus Kuhnhenne, Dominik Pyschny, Lisa Kramer, tłumaczenie na język polski: Mariusz Maślak 103
    7.4. Corrugated sheeting – autor wersji oryginalnej: Thibault Renaux, tłumaczenie na język polski: Mariusz Maślak 141
    7.5. Curved profiles – autorzy wersji oryginalnej: Walter Salvatore, Silvia Caprili, Irene Puncello, tłumaczenie na język polski: Mariusz Maślak 175

7.6. Assembled profiles – autor wersji oryginalnej: Thibault Renaux,
tłumaczenie na język polski: Mariusz Maślak 211
7.7. Perforated profiles – autor wersji oryginalnej: Anna Palisson,
tłumaczenie na język polski: Anna Palisson 269
7.8. Profiles with holes – autor wersji oryginalnej: Anna Palisson,
tłumaczenie na język polski: Anna Palisson 309
7.9. Interlocking planks – autor wersji oryginalnej: Mickael Blanc,
tłumaczenie na język polski: Mariusz Maślak 347

1.
WPROWADZENIE

W dniu 14 czerwca 2018 roku w Sali Senackiej Politechniki Krakowskiej odbyło się seminarium naukowe w ramach którego zaprezentowano wyniki uzyskane w międzynarodowym projekcie badawczym **„Grispe Plus – Valorisation of knowledge for specific profiled steel sheets”** („Grispe Plus – waloryzacja stanu wiedzy na temat specyficznie profilowanych blach stalowych”). W seminarium tym wzięło udział około 50 osób, w tym zagraniczni wykładowcy, pracownicy krajowych uczelni technicznych, projektanci i wykonawcy zainteresowani prezentowaną tematyką. Szeroko reprezentowani byli również przedstawicieli organizacji i stowarzyszeń branżowych.

Nazwa **„Grispe Plus”** jest akronimem grantu naukowego finansowanego przez Unię Europejską w ramach funduszu Research Fund for Coal and Steel (grant agreement **RFCS-2016 No 754092**). **Politechnika Krakowska** jest pełnoprawnym partnerem w tym programie jako tak zwany „Participant No 3”. Pozostałymi partnerami są:

- **L’Enveloppe Metallique du Batiment** (Paryż, Francja) – stowarzyszenie reprezentujące francuskich producentów profili stalowych i płyt warstwowych z okładzinami stalowymi - koordynator programu,
- **Bacacier** (Aigueperse, Francja) – francuski wytwórca i eksporter stalowych blach profilowanych,
- **Joris Ide** (Zwevezele, Belgia) – międzynarodowa grupa łącząca producentów stalowych pokryć dachowych i systemów obudowy ściennej stosowanych w budynkach,
- **Sokol Palisson Consultants** (Paryż, Francja) – francuskie biuro projektowo – doradcze specjalizujące się w ekspertyzach wykonywanych w zakresie konstrukcji metalowych,

- **RWTH Aachen University** (Akwizgran, Niemcy) – wiodący uniwersytet techniczny Nadrenii - Westfalii,
- **Universita di Pisa** (Piza, Włochy) – założony 1343 roku uniwersytet włoski,
- **Tampere University of Technology** (Tampere, Finlandia) – wiodąca politechnika fińska.

Projekt **"Grispe Plus"** to formalnie kontynuacja projektu **"Grispe"** prowadzonego w latach 2013-2016 pod nazwą **"Guidelines and recommendations for integrating specific profiled steel sheets in the Eurocodes"** („Wytyczne i zalecenia odnośnie zintegrowania specyficznie profilowanych blach stalowych z programem eurokodów"). Raport końcowy z tego projektu, opublikowany 15 maja 2018 roku, można pobrać ze strony https://publications.europa.eu.

Podstawowym celem współpracy w ramach projektu **„Grispe Plus"** było zaproponowanie miarodajnych metod projektowania odniesionych do siedmiu klas stalowych wyrobów cienkościennych dotychczas słabo obecnych w normalizacji. Zestawienie typów wyrobów wybranych do szczegółowej analizy odpowiada kolejnym tytułom referatów wygłoszonych podczas obrad. Pełny spis tych wystąpień podano poniżej. Dla każdej z rozważanych klas opracowano odpowiednią procedurę obliczeniową wraz z wnioskiem o jej wdrożenie do nowelizowanej normy EN 1993-1-3.

Spotkanie w Krakowie było czwartym z tego rodzaju warsztatów organizowanych kolejno w każdym z krajów biorących udział w programie. Pierwsze z nich miało miejsce 5 października 2017 roku w Paryżu, drugie 23 stycznia 2018 roku w Aachen natomiast trzecie 15 marca 2018 roku w Pizie. Piąte spotkanie odbyło się w Helsinkach 21 listopada 2018 roku.

Warsztaty zorganizowane w Krakowie miały charakter wykładów rozdzielonych tak zwanymi sesjami interaktywnymi, podczas których prowadzona była merytoryczna dyskusja nad przedstawionymi propozycjami. Moderatorem tych sesji był *David Izabel*, Dyrektor Techniczny L'Enveloppe Metallique du Batiment. Zarówno wykłady jak i dyskusja odbywały się w całości w języku angielskim. Wszyscy słuchacze otrzymali specjalnie przygotowane certyfikaty uczestnictwa.

Spotkanie otworzył dziekan Wydziału Inżynierii Lądowej Politechniki Krakowskiej dr hab. inż. *Andrzej Szarata*, prof. PK krótką prezentacją na temat specyfiki i osiągnięć kierowanego przez niego Wydziału. W trakcie obrad przedstawiono następujące wykłady:

- **The Grispe & Grispe Plus projects** (Projekty Grispe i Grispe Plus) – prezentował *David Izabel*, L'Enveloppe Metallique du Batiment,
- **E-teaching Grispe Plus: Using e-lectures to disseminate Grispe results** (Użycie technik e-nauczania do celów pularyzacji rezultatów uzyskanych w ramach projektu Grispe Plus) – prezentował *Roman Breuer*, RWTH University Aachen,
- **Steel decks with embossments/indentations and/or outwards stiffener** (Panele stalowe z przetłoczeniami i/lub z zewnętrznymi usztywnieniami) – przentowała *Anna Palisson*, SPC Consultans,
- **Corrugated sheeting** (Pokrycia z blach fałdowych) – prezentował *Thibault Renaux* – Joris Ide,
- **Liner trays** (Cienkościenne kasety ścienne) – prezentował *Dominik Pyschny*, RWTH University Aachen,
- **Cladding & roof profiles assemblies** (Zestawy cienkościennych okładzin i profili dachowych) – prezentował *Thibault Renaux*, Joris Ide,
- **Curved profiles** (Łukowe profilowane panele cienkościenne) – prezentowała *Irene Puncello*, Universita di Pisa,
- **Perforated and holed profiles** (Cienkościenne profile perforowane i z pojedynczymi otworami) – prezentowała *Anna Palisson*, SPC Consultans,

- **External interlocking planks and their assemblies** (Zewnętrzne cienkościenne panele linearne i ich zestawy) – prezentował *Mickael Blanc*, Bacacier,
- **Proposals for the inclusion of seven calculation methods into EN 1993-1-3** (Propozycje włączenia siedmiu procedur obliczeniowych proponowanych w projekcie do normy EN 1993-1-3) – prezentował *David Izabel*, L'Enveloppe Metallique du Batiment.

W przeddzień seminarium, to jest 13 czerwca 2018 roku, w godzinach popołudniowych, w sali seminaryjnej Katedry Konstrukcji Metalowych działającej w strukturach Wydziału Inżynierii Lądowej Politechniki Krakowskiej, miało miejsce robocze spotkanie międzynarodowego komitetu zarządzającego projektem. Obrady prowadził *David Izabel* z L'Enveloppe Metallique du Batiment. Czynny udział w nich wzięli wszyscy polscy współpracownicy uczestniczący w projekcie, to znaczy *Mariusz Maślak*, *Maciej Suchodoła*, *Izabela Tylek* i *Paweł Żwirek*.

Niniejsze opracowanie zawiera szczegółowe instrukcje projektowania oraz przykłady obliczeniowe odnoszące się do propozycji prezentowanych podczas spotkania w Krakowie. Ze względu na wygodę czytelnika podzielono go na dwa tomy. W pierwszym z nich, za zgodą autorów, zestawiono slajdy omawiane podczas poszczególnych wykładów oraz przypisane do tych slajdów prezentacje z opisem aktualnego stanu wiedzy (tak zwane *state-of-the-arts*). Publikujemy je w oryginalnej, angielskiej wersji językowej. Drugi tom zawiera tłumaczone na język polski tak zwane *design manuals*, opracowane osobno dla każdego typu profilu rozważanego w projekcie i dla skojarzonych z nim procedur obliczeniowych rekomendowanych do stosowania w praktyce. Oryginalne, angielskie wersje tych instrukcji oraz ich tłumaczenia na języki: francuski, niemiecki i włoski można pobrać ze strony www.grispeplus.eu. W zakładce tej znajdują się również dodatkowe materiały pomocne przy projektowaniu, w tym między innymi arkusze kalkulacyjne, o których mowa w niektórych *design manuals*.

Mamy nadzieję, że przekazywane Państwu materiały okażą się być przydatne w praktyce inżynierskiej. Liczymy również na to, że zaproponowane w nich algorytmy obliczeniowe zostaną wprowadzone do nowelizowanych eurokodów. Dopiero spełnienie obu tych postulatów jednocześnie sprawi, że w naszym odczuciu zdefiniowany na wstępie podstawowy cel postawiony przed nami jako współuczestnikami projektu **„Grispe Plus”** zostanie z sukcesem osiągnięty.

Mariusz Maślak

Kraków, grudzień, 2018

2.
PARTNERZY
WSPÓŁPRACUJĄCY W PROJEKCIE
„GRISPE PLUS”

L'ENVELOPPE MÉTALLIQUE DU BÂTIMENT

L'Enveloppe Metallique du Batiment is the French professional organization representing the producers of steel profiles and sandwich panels. Its membership represents 95% of the manufacturers in France. L'Enveloppe Metallique is member of numerous European committees including CEN TC 250 SC3 (revision of Eurocode EN 1993-1-3), CEN TC 128 SC7 (profiles steel sheet), CEN TC 127 WG4 (fire), CEN TC 135 WG 14 (Eurocode 1090-4), CEN TC 351 and CENT TC 350 (dangerous substances and life cycle). L'Enveloppe Metallique organizes training seminars on profiles (design with Eurocodes, application of new regulations, etc.) for manufacturers, installers and end users, with a portfolio of 65 such industrial seminar programmes available. L'Enveloppe Metallique manages and coordinates many experimental programmes and technical studies on profiles of interest to its members and to the industry at large (e.g. seismic tests, thermal studies, EPD, BIM objects, etc.). L'Enveloppe Metallique was the coordinator in the RFCS GRISPE project (Guidelines and Recommendations for Integrating Specific Profiled steel sheets in the Eurocodes) on steel profiles on which GRISPE PLUS is based.

BACACIER is a French manufacturer of profiled sheets for the construction industry which exports to the European Union and beyond. The company is now 20 years old and provides products for steel cladding, covering, roofing and decking. BACACIER is an independent group and can count on its 150 field agents to fulfill its promise: “be there”. The company transforms 80,000 tons of steel per year, making it the 3^{rd} actor on the French cladding and roofing market. Its team of 5 engineers is constantly working on innovation to make the vision “industrial building differently” come true. BACACIER was a partner in the European RFCS GRISPE project (Guidelines and Recommendations for Integrating Specific Profiled steel sheets in the Eurocodes). In particular, it was involved in the development of a calculation method for external interlocking planks and their assemblies, in the preparation of an Excel software sheet for the cladding system and in the proposal for an amendment to EN 1993-1-3 for plank systems. It also furnished the samples for half of the other GRISPE subjects, making it a major industrial partner of this project.

Joris Ide is an international group and one of the leading manufacturer of steel roof and wall systems and cladding products for buildings. It is present in a range of markets across the European Union including Belgium, France, the Netherlands, the United Kingdom, Ireland, Hungary, Germany, Croatia and Scandinavia. It has major manufacturing facilities in five different European countries with a staff of over 1000 employees. Joris Ide was one of the key industrial participant in the RFCS GRISPE project through its subsidiary Joris Ide Bretagne in France. It was in particular involved in the work on planks and cladding.

Sokol Palisson Consultants is a French SME created in 2007, it offers consultancy and expertise to metal manufacturers and builders to design, develop and optimize their products in compliance with European Standards Eurocodes. The company is approved with the French research tax credit (CIR). Anna Palisson, owner of Sokol Palisson Consultants, is an engineer. She graduated in 1996 from the Ecole Nationale Superieure des Arts et Metiers (ENSAM). For over ten years she perfected her expertise and knowledge in structure analysis and testing by leading a number of major industrial R&D. In 2007 she created Sokol Palisson Consultants (SPC) to offer metal manufacturers and users her technical skills and expertise in the field of cold formed products. In addition to supporting manufacturers in their projects, she participates in the development and promotion of steel products through publications and training. She contributes to the development of Eurocodes on the one hand as a member of CNC2M (Commission de Normalisation de la Construction Métallique et Mixte) and on the other hand as a partner of the GRISPE project (Guidelines and Recommendations for Integrating Specific Profiled steel sheets in the Eurocodes) where she was WP leader responsible for the work on steel decks and for perforated and holed profiles. In this capacity she developed design methods for steel profiles which although frequently used in steel –framed construction, were not covered by the design rules defined in the Eurocodes.

Cracow University of Technology

Cracow University of Technology is the younger of two technical universities currently operating in Cracow, the former capital of the kings of Poland. After the Second World War it emerged from the older AGH University of Science and Technology as the so-called Polytechnic Faculties which in 1947 were relocated to the separate campus near the city centre. At present, more than 15,000 students are educated here at seven faculties including the following: Architecture; Chemical Engineering and Technology; Civil Engineering; Electrical and Computer Engineering; Environmental Engineering; Mechanical Engineering; Physics, Mathematics and Computer Science.

RWTH Aachen University is recognized to be one of the top technical universities within Germany. With about 260 institutes, 550 professors and 45.000 students, RWTH Aachen is one of Europe's premier educational and research institutions. The Institute of Steel Construction is one of the major institutes within the Faculty of Civil Engineering of RWTH Aachen. It comprises a staff of about 70 and covers a wide range of research activities and 3 professorships with working groups e.g. for structural design, dynamics, wind engineering, building physics and envelopes. » The department of Engineering Hydrology, RWTH Aachen University (LFI) is leading the eLearning group of the RWTH since 2004. LFI develops eLearning modules in form of Online-Courses and Games to learn to support University lectures since then and will lead the development of the GRISPE+-eLearning components.

The University of Pisa is a public institution with a total amount, actually, of twenty departments, with high level research centres in the sectors of agriculture, astrophysics, computer science, engineering, medicine and veterinary medicine. The University has close relations with the Pisan Institutes of the National Board of Research, with many cultural institutions of national and international importance, and with industry, especially that of information technology, which went through a phase of rapid expansion in Pisa during the nineteen sixties and seventies. The University of Pisa was officially established in 1343, although a number of scholars claim its origin dates back to the 11th century. With the birth of the Kingdom of Italy, the University of Pisa became one of the new state's most prestigious cultural institutions. Between the second half of the nineteenth and first half of the twentieth centuries the following prestigious lecturers taught at Pisa: the lawyers Francesco Carrara and Francesco Buonamici, philologists Domenico Comparetti and Giovanni D'Ancona, historians Pasquale Villari, Gioacchino Volpe and Luigi Russo, philosopher Giovanni Gentile, economist Giuseppe Toniolo and mathematicians Ulisse Dini and Antonio Pacinotti. The Department of Civil and Industrial Engineering (DICI) was established in 2012, following a major reform of the Italian higher education system, as a merger of the former departments of aerospace engineering, chemical engineering, industrial engineering, chemistry and materials science, mechanical engineering, nuclear and production engineering and Civil Engineering.

TAMPERE UNIVERSITY OF TECHNOLOGY

Tampere University of Technology (TUT) is at the leading edge of technological development and a sought-after collaboration partner among the scientific and business communities. We educate skillful graduates to serve the needs of society. Our University is a fertile breeding ground for innovations and new research- and knowledge-based companies. We generate new knowledge and expertise for the benefit of society. We foster the well-being of people and the environment through research and education. We develop technologies that reshape the competitive landscape of Finnish industry.

3.
UCZESTNICY SEMINARIUM „GRISPE PLUS" W KRAKOWIE 14.06.2018

WYKŁADOWCY

Lp.	NAZWISKO I IMIĘ	PARTNER
1.	**Blanc Mickael**	Bacacier, Francja
2.	**Breuer Roman**	RWTH Aachen, Niemcy
3.	**Izabel David**	L'Enveloppe Metallique du Batiment, Francja
4.	**Palisson Anna**	SPC Consultans, Francja
5.	**Puncello Irene**	Universita di Pisa, Włochy
6.	**Pyschny Dominik**	RWTH Aachen, Niemcy
7.	**Renaux Thibault**	Joris Ide, Belgia
8.	**Sokol Leopold**	SPC Consultans, Francja
9.	**Spagni Daniel**	L'Enveloppe Metallique du Batiment, Francja

UCZESTNICY

Lp.	NAZWISKO I IMIĘ	PRZEDSIĘBIORSTWO LUB UCZELNIA
1.	**Baran Paweł**	AKE Studio Sp. z o.o., Tarnobrzeg
2.	**Boryczko Mirosław**	Politechnika Krakowska
3.	**Bieliński Marcin**	BALEX METAL Sp. z o.o., Bolszewo
4.	**Domański Tomasz**	Politechnika Krakowska
5.	**Fiszer Paweł**	ME Sp. z o.o., Kraków

6.	**Górecki Marcin**	Politechnika Lubelska
7.	**Górski Marcin**	Politechnika Rzeszowska
8.	**Grabowski Michał**	Blachprofil 2 Sp. z o.o., Kraków
9.	**Gremza Grzegorz**	Politechnika Śląska
10.	**Gwóźdź Marian**	Politechnika Krakowska
11	**Jamro Szymon**	Gór-Stal Sp. z o.o., Gorlice
12	**Janicki Marcin**	Politechnika Krakowska, student
13	**Jarosiński Patryk**	ME Polska Sp. z o.o., Kraków
14.	**Kozłowski Aleksander**	Politechnika Rzeszowska
15.	**Kmiecik Kamil**	Politechnika Krakowska
16.	**Król Paweł**	Politechnika Warszawska
17.	**Kuchta Krzysztof**	AGH Kraków
18.	**Kucharski Andrzej**	Krakowska Rada Federacji Stowarzyszeń Naukowo – Technicznych NOT
19.	**Machowski Andrzej**	Politechnika Krakowska
20.	**Maślak Mariusz**	Politechnika Krakowska

21.	**Mazur Andrzej**	Blachprofil 2 Sp. z o.o., Kraków
22.	**Michałowski Tomasz**	Politechnika Krakowska
23	**Urbańska - Galewska Elżbieta**	Politechnika Gdańska
24.	**Pelczar - Zajdel Paulina**	Politechnika Krakowska
25.	**Piekarczyk Marek**	Politechnika Krakowska
26.	**Pięciorak Edyta**	AGH Kraków
27.	**Przęczek Bartłomiej**	GSBK Biuro Konstrukcyjne Sp. z o.o., Kraków
28.	**Pisarek Zdzisław**	Politechnika Rzeszowska
29.	**Rawska - Skotniczny Anna**	Politechnika Opolska
30.	**Rusek Janusz**	AGH Kraków
31.	**Ruchała Przemysław**	GSBK Biuro Konstrukcyjne Sp. z o.o., Kraków
32	**Rzeszut Katarzyna**	Politechnika Poznańska
33	**Sendkowski Jerzy**	BIURO BUDOWLANE „ANKRA" Sp. z o. o., Kielce
34.	**Słowiński Kamil**	AGH Kraków

35.	**Suchodoła Maciej**	Politechnika Krakowska
36.	**Snela Małgorzata**	Politechnika Lubelska
37.	**Szczecina Michał**	Politechnika Świętokrzyska
38.	**Szczęsny Marek**	Arcelor Mittal Europe, Świętochłowice
39.	**Szumigała Maciej**	Politechnika Poznańska
40.	**Świerczyna Szymon**	Politechnika Śląska
41.	**Tylek Izabela**	Politechnika Krakowska
42.	**Woźniczka Piotr**	Politechnika Krakowska
43.	**Wilk Michał**	Przedsiębiorstwo Techniczno - Usługowe "CON-BUD", Chorzów
44.	**Żwirek Paweł**	Politechnika Krakowska

4.
PROFILE CIENKOŚCIENNE ANALIZOWANE W PROJEKCIE

SIEDEM GRUP PROFILI CIENKOŚCIENNYCH

- **Steel decks with embossments/indentations and/or outwards stiffeners** - Panele stalowe z przetłoczeniami i/lub z zewnętrznymi usztywnieniami,
- **Liner trays** - Cienkościenne kasety ścienne,
- **Corrugated sheeting** - Pokrycia z blach falistych,
- **Curved profiles** - Łukowe profilowane panele cienkościenne
- **Cladding & roof profiles assemblies -** Zestawy cienkościennych okładzin i profili dachowych,
- **Perforated and holed profiles** - Cienkościenne profile perforowane i z pojedynczymi otworami,
- **External interlocking planks and their assemblies -** Zewnętrzne cienkościenne panele linearne i ich zestawy.

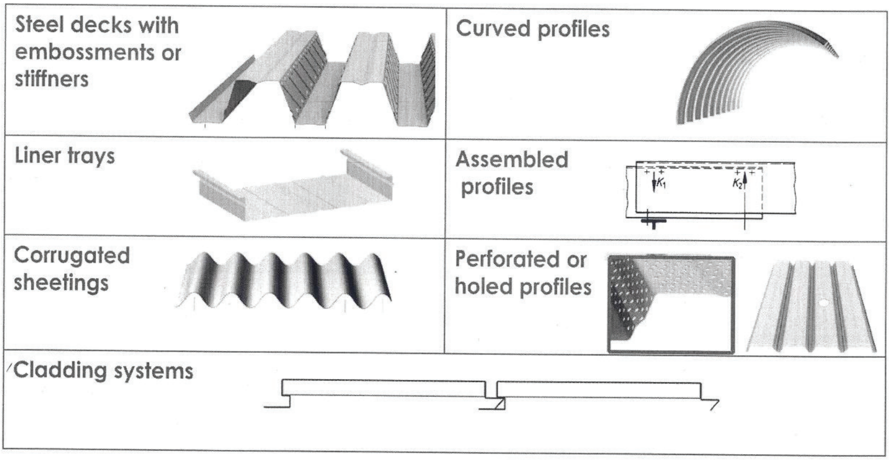

5.
STATE-OF-THE-ART

w tym:

5.1. Steel decks –
autor: *Anna Palisson*
(*Sokol Palisson Consultans*)

5.2. Liner Trays + Assembled profiles
+ Corrugated sheets + Curved profiles –
autor: *Christian Fauth*
(*Karlsruher Institut für Technologie*)

5.3. Perforated and holed profiles –
autor: Anna Palisson
(*Sokol Palisson Consultans*)

5.4. Interlocking planks –
autorzy: Mickael Blanc (*Bacacier*),
Thibault Renaux (*Joris Ide*).

GRISPE

Guidelines and **R**ecommendations for **I**ntegrating **S**pecific **P**rofiled steel sheets in the **E**urocodes
(**GRISPE**)

WP1 Doc 1 Final Version 01

WP1 Background document

Working Package 1

Deliverable D 1.1

DOCUMENT CONTROL INFORMATION AND ARCHIVING

Guidelines and Recommandations for Integrating Specific Profiled Steels sheets in the Eurocodes (GRISPE)

Project co-funded under the Research Fund for Coal and Steel
Grant agreement No RFCS-CT-2013-00018
Proposal No RFS-PR-12027

Author(s)	
Palisson Anna, Sokol Palisson Consultants	
Drafting history	
Draft Version 1	*9th December 2013*
Draft Version 2	*27th December 2013*
Final Version Revision 01	*28th December 2013*
Final Version Revision 02	*Day Month Year*
Final Version Revision 03	*Day Month Year*
Final Version Revision xx	*Day Month Year*
Final Version CO	*Day Month Year*

Dissemination Level		
PU	*Public*	
PP	*Restricted to the Commission Services, the Coal and Steel Technical Groups and the European Committee for Standardisation (CEN)*	
RE	*Restricted to a group specified by the Beneficiaries*	
CO	*Confidential, only for Beneficiaries (including the Commission services)*	***x***

Verification and Approval
Coordinator David Izabel, SNPPA
WP1 Leader SOKOL PALISSON CONSULTANTS
Other Beneficiaries SNPPA, Bac Acier, IFL, Joris Ide, KIT, PUT

Deliverable	
D 1.1 WP1 Background document	***Due date : 30.11.2013*** ***Completion date: 28.12.2013***

1. INTRODUCTION

Due to its many construction advantages steel decking is frequently used in steel-framed construction for both roofs and floors for interior design, commercial and industrial refurbishments and for the building trade. In order to increase the shear connection between the steel and the concrete in the composite slabs, steel decks are reinforced with connectors such as embossments (Fig. 1) or indentations (Fig.2) on the webs, or outwards stiffeners (Fig.3) on the edge.

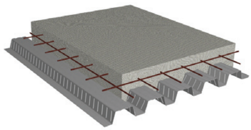

Fig. 1 - Indentations in a composite slab

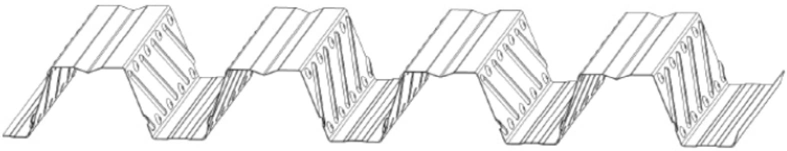

Fig. 2 - PCB 80 deck from BACACIER SAS, with embossments and indentations

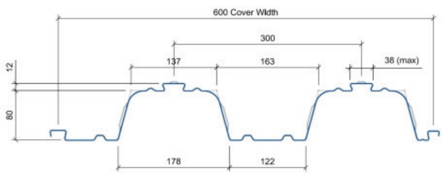

Fig. 3 - TR80 deck from SMD

At the composite stage the behavior of composite slabs with embossments has been determined by numerous studies [1] to [7], embossments increase for the composite steel-concrete slab shear connection, moment capacity, mid-span deflections and end slips.

At the construction stage the sheeting used as shuttering has to support the fresh concrete weight and the construction loads, and in this case the effect of the embossments and indentations is not favorable. Unfortunately the European Standard EN 1993-1-3 dealing with design rules for cold-formed members and sheeting doesn't cover profiles with embossments, indentations or outwards stiffeners. Moreover the existing studies and researches on this type of profile don't allow to quantify precisely by calculation the effect of embossment and indentations on the steel deck resistance and stiffness and to analyse the bending resistance of sheeting with outwards stiffener in the upper flange. A study performed by P. Luure and M. Crisinel [8] shows an influence of about 10% on the resistance and on the stiffness. J. M. Davies [9] found in his finite element analysis a decrease of 8 to 10% of the bending strength for dimples in top flange, for dimples in the webs the decrease of bending strength was less important, about 3%. Unfortunately both studies don't take into account the effect of combined action of support reaction and negative moment whereas the interactive resistance M–F would be lower from the resistance of pure bending M_R or contact pure pressure F_R, as it could be shown for corrugated sheets by A. Biegus [10].

The aim of this document is to give a state of the art of the current European Standard EN and of the background information about steel decks with embossments, indentations and outwards stiffeners, and to emphasize the lack of data and knowledge.

2. EUROCODE

2.1. EN 1994-1-1

The profiled steel sheet with embossments and indentations are within the scope of the European standard EN 1994-1-1 for design of composite steel and concrete structures, as in the Part 9.1.2.1, embossments and indentations are defined as mechanical interlocks (Key 1 in Fig.4).

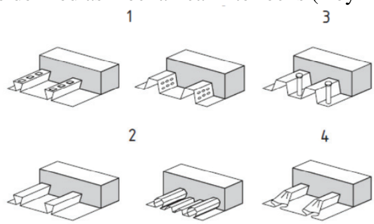

Key

1 mechanical interlock

2 frictional interlock

3 end anchorage by through-deck welded studs

4 end anchorage by deformation of the ribs

Fig. 4 - Typical forms of interlock in composite slabs

The methods of verifications of composite slabs for the ultimate states are determined in part 9.7. In case of flexure the standard specifies:
- in part 9.7.2 (3) that for the effective area of the steel sheeting, the width of embossments and indentations in the sheet should be neglected, unless it is shown by tests that a larger area is effective
- in part 9.7.2 (5) and 9.7.2 (6) the stress distribution to calculate the sagging bending resistance of a cross-section with a neutral axis above the sheeting (Fig.5) and with a neutral axis in the sheeting (Fig. 6).

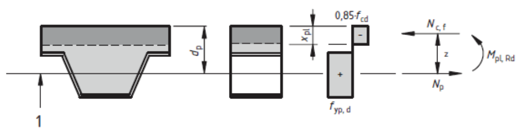

Key

1 centroidal axis of the profiled steel sheeting

Fig. 5 - Stress distribution for sagging bending if the neutral axis is above the steel sheeting

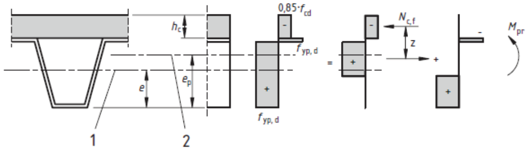

Key

1 centroidal axis of the profiled steel sheeting

2 plastic neutral axis of the profiled steel sheeting

Fig. 6 - Stress distribution for sagging bending if the neutral axis is in the steel sheeting.

- in part9.7.2 (7) the stress distribution to calculate the hogging bending resistance of a cross-section if the contribution of the steel sheeting is neglected (Fig. 7).

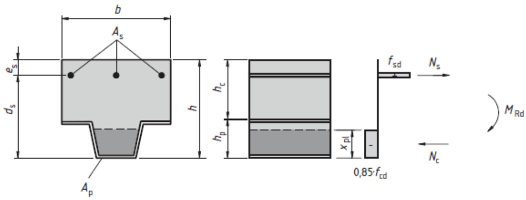

Fig. 7 - Stress distribution for hogging bending

The part 9.7.3 of this standard determines longitudinal shear for composite slabs without and anchorage and part 9.7.4 with end anchorage.

In several parts EN 1994-1-1 specifies that the steel sheeting alone, should be designed (part 9.4.1), verified for ultimate limit states (part 9.5. (1)) and for serviceability limit states (part 9.8), and determined (part 9.6. (1)) in accordance with EN 1993-1-3, but EN 1993-1-3 doesn't provide any information about design and verification of profiles with indentations, embossments or outwards stiffeners.

2.2. EN 1993-1-3

The European standard EN 1993-1-3 gives, for cold-formed members and sheeting, methods for design by calculation and for design assisted by testing. The design by calculation apply only within stated ranges of material properties and geometrical proportions for which sufficient experience and test evidence is available. These limitations do not apply to design assisted by testing. Examples of cross-sections for cold-formed members and sheets covered by EN 1993-1-3 are illustrated in figure 8 (part 1.5.1).

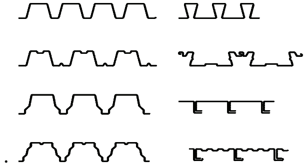

Fig. 8 - Examples of cold-formed members and profiled sheets

It is written in part 1.5.1. (5) that cross-sections of cold-formed members and sheets may either be unstiffened or incorporate longitudinal stiffeners in their webs or flanges, or in both. Unfortunately the form of stiffeners defined in part 1.5.2 don't include indentations, embossments, outwards stiffeners (Fig.9 and Fig. 10), in the flange only inwards stiffeners are defined.

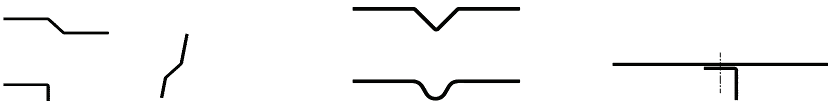

Folds and bends — Folded groove and curved groove — Bolted angle stiffener

Fig. 9 - Typical forms of stiffeners for cold-formed members and sheeting

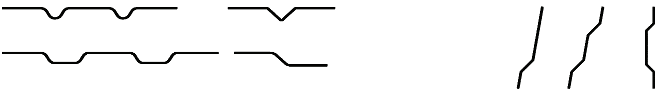

Intermediate flange stiffeners — Intermediate web stiffeners

Fig. 10 - Typical intermediate longitudinal stiffeners

To design a steel sheeting <u>two criteria of verification must be determined</u>, resistance at ultimate limit states and flexion stiffness at serviceability limit states. EN 1993-1-3 provides the methodology to determine those criteria for steel sheeting only with typical stiffeners.

First, effective section properties must be calculated. Buckling of plane elements and flexural buckling of a stiffener reduce resistance therefore an effective width of the element (Fig. 11) and a reduced thickness of the stiffener must be determined in accordance with part 5.5.

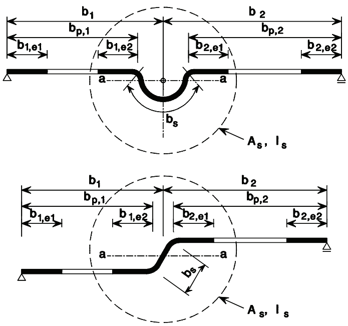

Figure 11 - Intermediate stiffeners

In the case of sheeting with intermediate stiffeners in the flanges and in the webs (Fig. 12), interaction between the flexural buckling of the flange stiffeners and the web stiffeners must be taken into account (part 5.5.3.4.4).

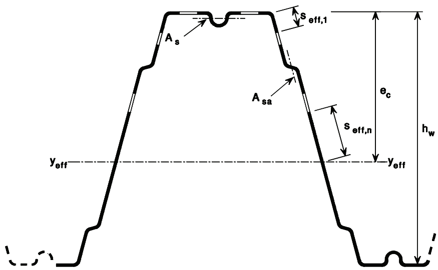

Figure 12 - Trapezoidal profiled sheeting with flange stiffeners and web stiffeners

Next, resistance of cross-sections at ultimate limit states must be calculated. Resistance to axial tension, to axial compression (Fig. 13), to bending moment (Fig. 14), to shear force, to torsional moment, local transverse forces (Fig. 15) and to combined forces and moments must be determined with the effective cross-section.

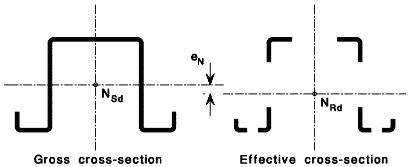

Figure - 13 Effective cross-section under compression

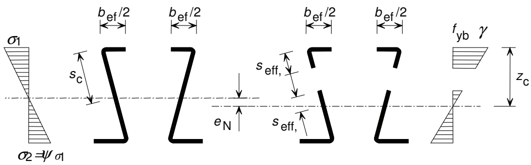

Figure 14 - Effective cross-section for resistance to bending moments

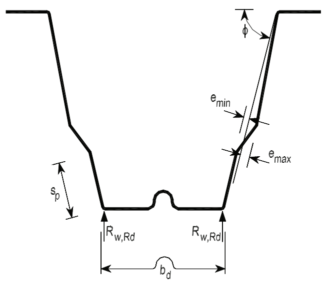

Figure 15 - Stiffened webs for local transverse forces

At least flexion stiffness at serviceability limit states must be calculated in accordance with part 7. All serviceability limit state calculations must use the properties of the effective cross-section obtained from Section 5.1, as in the expression of moment of area :

$$I_{\text{fic}} = I_{\text{gr}} - \frac{\sigma_{\text{gr}}}{\sigma}(I_{\text{gr}} - I(\sigma)_{\text{eff}}) \qquad \dots (7.1)$$

where

I_{gr} is second moment of area of the gross cross-section;

σ_{gr} is maximum compressive bending stress in the serviceability limit state, based on the gross cross-section (positive in formula);

$I(\sigma)_{\text{eff}}$ is the second moment of area of the effective cross-section with allowance for local buckling calculated for a maximum stress $\sigma \geq \sigma_{\text{gr}}$, in which the maximum stress is the largest absolute value of stresses within the calculation length considered.

Therefore calculation of the deflection also takes into account the effective cross-section.

As we see above, the criteria of verification of a steel sheeting must take into account the effective cross-section which is impacted by the web and flange stiffeners, therefore the absence of indentations, embossments and outwards stiffeners in the standard EN 1993-1-3 is a real lack to correctly determine and verify the resistance of a steel sheeting for composite slabs by calculation approach. And this lack is even more disturbing and serious as several previous studies have shown that the effect of embossments unfavorable to certain criteria as bending resistance. In the next chapter we will focus on studies performed on sheeting with indentations, embossments and outwards stiffeners.

3. STATE OF THE ART

The review of the existing published and on-going works allowed to find few studies on steel sheeting with embossments and indentations and no study on sheeting with outwards stiffeners.

Two finite element analysis of the effect of embossment in the structural behavior of the steel deck profile strength and stiffness were reported.

The first one [11], made by O. T. BAIAO FILHO, presents the effect of the embossments in a profile element when subjected to axial load and to bending moment. A model (Fig. 16) of a trapezoidal deck profile having 0.316 in. thickness is considered. Its structural behavior, in axial tension and bending is approximately the same as the real deck's.

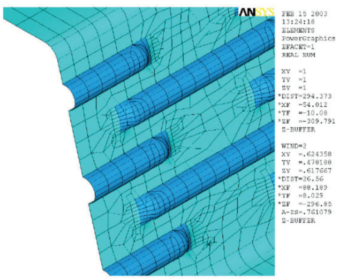

Figure 16 - Embossment model

A comparison between deck without and with embossments is presented for axial tension (Fig. 17) and for bending moment (Fig. 18)

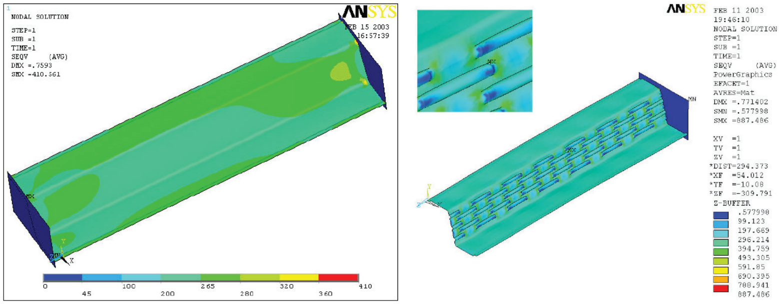

Figure 17 - Models without and with embossments subject to axial tension force - SEQV

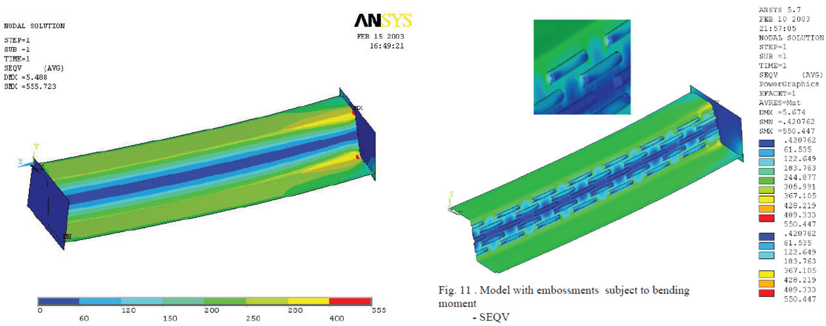

Figure 18 - Models without and with embossments subject to bending moment - SEQV

The author finds that the maximum perpendicular displacement to the model axis is 0.216 in. for the flat plate model and 0.223 in. for the model with embossments (difference of about 3.4%). He concludes that the presence of embossments have a very small effect in the structural behavior of the model, when subject to a bending moment, and that making embossments causes only a small loss in the steel deck profile stiffness, nevertheless he doesn't specify if it concerns moment of inertia, bending or shear resistance. These analyses are rather approximate and the validation must be done with the full-scale test results.

The reviewer notes:

- The small impact of the embossment is predictable, because of relatively small part of cross section impacted by the embossment.

- The effect of combined action of support reaction and negative moment was not studied in this paper

- No global conclusion can be drawn because only one type of profile and one type of embossments was analyzed

The second finite element analysis [12] made by E. S. Mistakidis, K.G. Dimitriadis, presents the contribution of the embossed areas of the steel sheeting to the total strength in pure tension and in pure bending. It is based on three-dimensional models of the steel sheeting (Fig. 19)

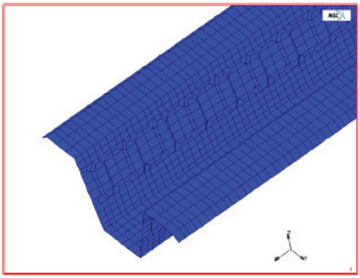

Figure 19 - Details of the F.E. discretization of the embossments

Two series of analyses were performed, with the steel profile subjected to pure tension and to pure bending. The studied trapezoidal profile was SYMDECK 73. A parametric analysis was performed in order to study the effect of the depth of the embossments or the indentations to the strength and the stiffness of the steel sheeting, four different depth were used (0.5, 1.0, 1.5, 2.5 mm). The MARC FE code was used.

In pure tension for the different depth of embossment a diagram was given of the percentage of the area of the full cross-section that is active for every value of the strain (Fig. 20). Based on these results the following formula is proposed of the axial strength of the steel profile with embossments in terms of an "effective thickness" of the region of the cross -section that corresponds to the positions of embossments:

$$N_{Rd} = A_{p,eff}\frac{f_{yp}}{\gamma_{ap}} = \left(A_{net} + A_{emb}\frac{t_{eff,N}}{t}\right)\frac{f_{yp}}{\gamma_{ap}}, \qquad (2)$$

where $A_{p,eff}$ is the effective cross-sectional area of the steel profile in tension, $A_{p,emb}$ the cross-sectional area of the steel profile that corresponds to the region of the embossments, $A_{p,net}$ the cross-sectional area of the steel profile excluding the region of the embossments, i.e. $A_{p,net} = A_{p,full} - A_{p,emb}$, where $A_{p,full}$ is the full cross-sectional area of the steel profile, f_{yp} the yield strength of the profile steel sheeting, and γ_{ap} the partial safety factor for the profile steel sheeting.

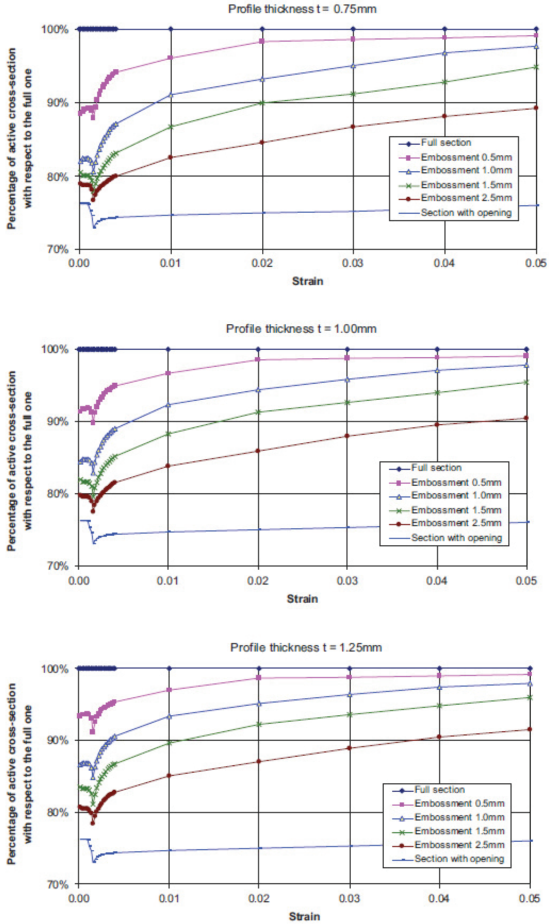

Figure 20 - Percentage of active cross-section (with respect to the full one) - strain diagram

In pure bending tension for the different depth of embossment a diagram was given of bending strength ratio (with respect to full section) for various embossment depths (Fig. 21).

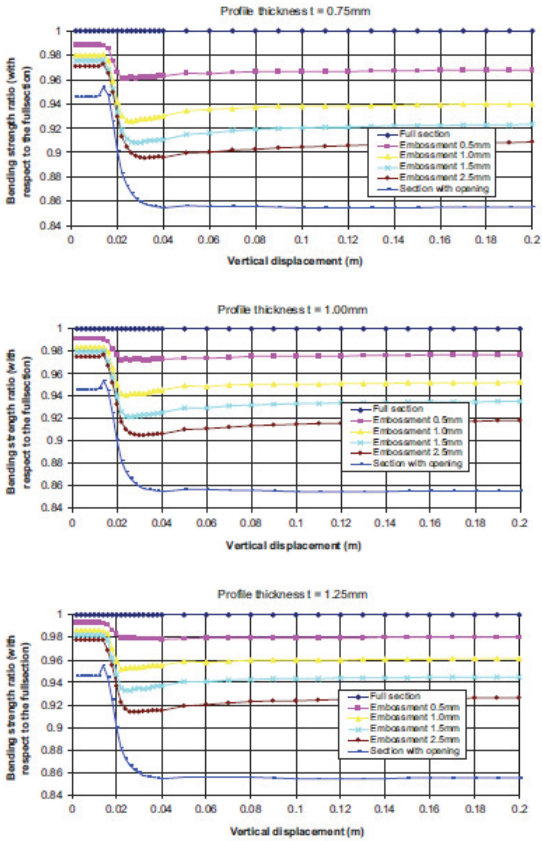

Figure 21 - Bending strength ratio (with respect to full section) for various embossment depths

The effective thickness was calculated as a function of the depth of the embossment, in the elastic range, on the left of Figure 22 and in the plastic range on the right of Figure 22.

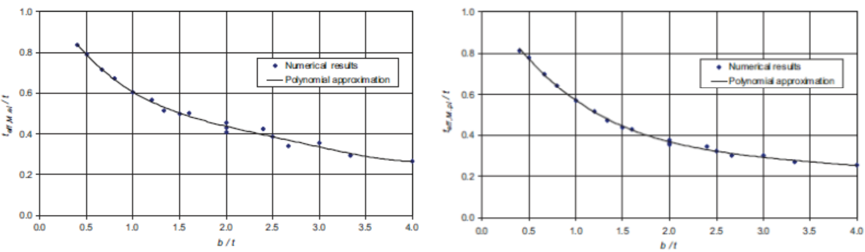

Figure 22 - Relationship between the ratios b/t and $t_{eff,M/t}$ in elastic and plastic ranges

The authors specify that the elastic bending resistances can be used together with the provisions of EN 1993-1-3 for the design of cold formed sections, while the plastic bending resistance is used for the design of composite slabs in bending.

According to the authors the following formula should be used:

- when the neutral axis lies within the sheeting

$$M_{p,Rd} = N_{cf} z + 1.25 M_{pa}\left(1 - \frac{N_{cf}}{A_{pf} f_{yp}/\gamma_{ap}}\right), \qquad (4)$$

where, z is the lever arm of the internal tension and compression forces of the cross-section, N_{cf} the design value of the compressive normal force in the concrete flange and M_{pa} the design value of the plastic resistance moment of the effective cross-section of the profile steel sheeting.

- and when the neutral axis lies within the sheeting the following formula should be used:

$$M_{p,Rd} = N_{cf} z + 1.25 M_{pa,eff}\left(1 - \frac{N_{cf}}{A_{p,eff} f_{yp}/\gamma_{ap}}\right).$$

The reviewer notes

The above equation may be presented under the following form:

$$M_{pr} = N_{pa}\eta\frac{z}{2} * \mathrm{Min}[1.25(1-\eta),1)]$$

As it was demonstrated in [12] the above equation (4) adopted in the EN 1994-1-1 is not exact, because it is based on some arbitrary hypotheses and assumptions.

The more realistic formula, given by A. Palisson and L. Sokol in [13] is $M_{pr} = N_{pa} z_{pr} \dfrac{(1-\eta)(\chi+\eta)}{1+\chi}$

In this paper it was demonstrated that the contribution of the embossment seems significant the area of the embossments region can be considered as active. There was a strong relation between the area of the embossment region and the ratio between the depth of the embossment and the thickness of the profile, for both cases of tension and bending of the profile. Modified formulas are proposed for the calculation of the sagging bending resistance of composite slabs, taking into account the effective area of the embossments region and leading to an increase of the bending strength of the order of 15%.

The reviewer notes:
The effect of combined action of support reaction and negative moment was not studied in this paper.

The single testing study was performed by P. Luure and M. Crisinel [8] who conducted tests to determine the influence of web embossments/indentations on the resistance of two types of

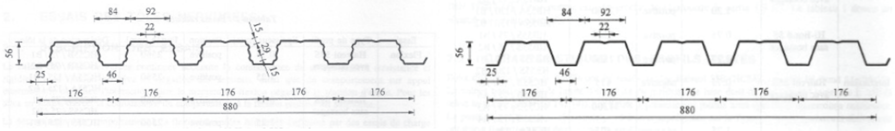

Figure 23 - HAIRCOL 55S with and without embossments

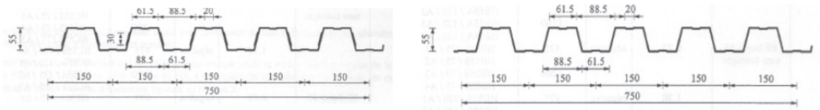

Figure 24- HI-BOND 55 with and without indentations

In total 16 bending and 32 bending - support reaction interaction tests were carried out. The same profiles with and without embossments/indentations were tested, with two different thicknesses of the sheets t=0.75mm and t=1.25mm. Tests were performed in accordance with Standard DIN 18807 [14], very close to EN 1993-1-3.

The aim of bending tests (Fig. 25) was to determine bending moment resistance and the flexion stiffness.

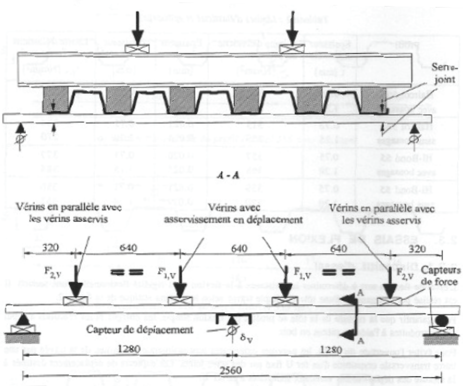

Figure 25- Bending test set-up

The bending moment was calculated with the following equation:

$M_v = \left[3 \cdot \left(F_{1,v} + F'_{1,v}\right) + F_{2,v} + F'_{2,v}\right] \cdot \frac{L}{16} + M_0$ where:

$F_{i,v}$ are measured forces; L is test span (L = 2560 mm); M = sheet own weight +accessories weigth

The stiffness was calculated with the following equation:

$$EI_v = \frac{0.9141\cdot(\Delta F_{1,v} + \Delta F'_{1,v}) + 0.3672\cdot(\Delta F_{2,v} + \Delta F'_{2,v})}{48}\cdot\frac{L^3}{\Delta\delta_v}$$ where:

$\Delta F_{i,v}$ are force differences corresponding to moment difference; $\Delta\delta v$ are deflection differences; L is test span (L = 2560 mm) (Fig. 26)

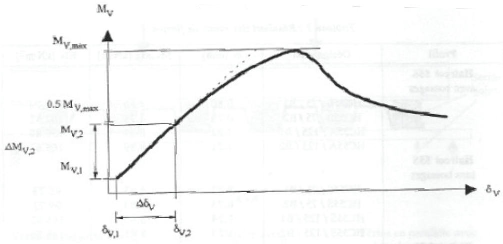

Figure 26 - Flexion stiffness determination

The aim of interaction tests (Fig. 27) was to simulate the behavior on the intermediate support.

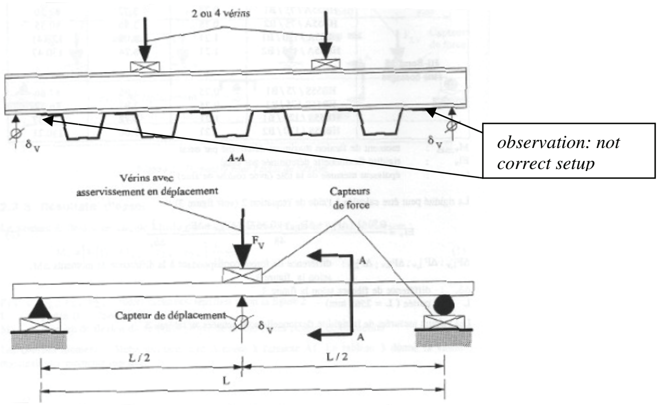

Figure 27- Interaction test set-up

The reaction and the bending moment are calculated with the following equations:

$$R_v = F_v + R_0$$
$$M_v = \frac{F_v \cdot L}{4} + M_0$$ where:

Fv is the measured force; R0 is the initial load due to sheet own weight +accessories weight; M0 is the initial moment due to sheet own weight +accessories weight; L is test span (L = 475 or 1200 mm).

The results of these tests showed that embossments decrease the bending resistance of the profiled sheeting of 10% On the contrary the tests showed that embossments increase the web crippling resistance of 10%. But to draw any global conclusions a test program even more complete should be carried out, with different types of profiles and embossments.

The reviewer notes:
- The effect of combined action of support reaction and negative moment was not studied in this paper
- The conclusion of this study does not permit to predict the impact of the embossment in function of its type and positioning

J. M. Davies [9] investigated the effect of dimples on the bending strength using the finite element method. Two decking profiles have been analysed: the Holorib profile with square dimples in the flanges and the Metecno profile with rectangular dimples in the webs (Fig. 28).

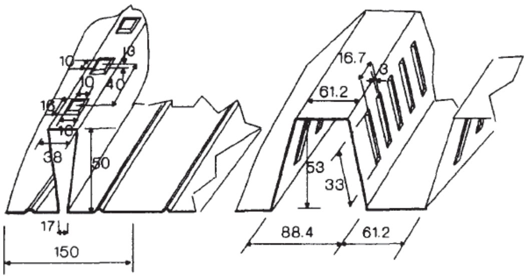

Fig. 28 - Holorib profile with square dimples in the flanges and the Metecno profile with rectangular dimples in the webs

The authors found that the dimples decrease the bending strength. In the case of the dimples in the webs the reduction was about 3%, in the case of the dimples in the flange the reduction was 8.21% for the Holorib 0.9/50 profile and 10.96% for the Holorib 1.2/50 profile. This decrease was approximately inversely proportional to $\lambda_p = b/t\sqrt{F_y/E}$. The author noted that if elastic buckling of flange dominates the strength of a steel deck, λ_p has a relatively large value, dimples in the compression flanges can increase the bending strength. The author intends, in further parametric studies, to investigate relationship between compression flange dimples, λ_p and bending strength.

The reviewer notes:
- The effect of combined action of support reaction and negative moment was not studied for decks with dimples
- The conclusion of this study is that the influence on bending strength depends on type and positioning of stiffeners, but the relationship was not established.

4. CONCLUSIONS

As we could see in this state of the art there is a real lack of data and knowledge about the effect of embossments, indentations and outwards stiffeners on the steel deck resistance and stiffness it means on the bending strength ($M_{c,Rd}$) on the shear ($V_{w,Rd}$) and on support strength ($R_{w,Rd}$). The European Standard EN 1993-1-3 dealing with design rules for cold-formed members and sheeting doesn't cover profiles with embossments, indentations or outwards stiffeners. The background information for the effect of such stiffeners is that embossments decrease of about 10% the

bending resistance of the profiled sheeting and that embossments increase of about 10% the web crippling resistance. But the test program which led to these tendencies was not important enough to establish global conclusions.
Therefore a series of tests should be performed in order to acquire data on resistance and stiffness of the steel decks with embossment and indentations or with outwards stiffener in the upper flange.

REFERENCES

[1] P. REN, G. COUCHMAN, M. CRISINEL "COMPARISON BETWEEN THEORETICAL MODEL COMPCAL AND TEST RESULTS" 1993

[2] B. DANIELS, M. CRISINEL "ESSAIS DE DALLES MIXTES AVEC TOLES PROFILEE HIBOND 55" 1987

[3] B. J. DANIELS, A. ISLER, M. CRISINEL "MODELLING OF COMPOSITE SLABS WITH THIN-WALLED COLD-FORMED DECKING, 1990

[4] M. CRISINEL, 2004, "A NEW SIMPLIFIED METHOD FOR THE DESIGN OF COMPOSITE SLABS", JOURNAL OF CONSTRUCTIONAL STEEL RESEARCH 60 481–491, 2004

[5] L.D. LUTTRELL, S. PRASANNAN," STRENGTH FORMULATIONS FOR COMPOSITE SLABS" SEVENTH INTERNATIONAL SPECIALTY CONFERENCE ON COLD·FORMED STEEL STRUCTURES ST. LOUIS, MISSOURI, U.S.A., NOVEMBER 13·14, 1984

[6] P; MÄKELÄINEN "THE LONGITUDINAL SHEAR BEHAVIOUR OF A NEW STEEL SHEETING PROFILE FOR COMPOSITE FLOOR SLABS, JOURNAL OF CONSTRUCTIONAL STEEL RESEARCH" JOURNAL OF CONSTRUCTIONAL STEEL RESEARCH 49, 117-128., 1999

[7] V.MARIMUTHU, "EXPERIMENTAL STUDIES ON COMPOSITE DECK SLABS TO DETERMINE THE SHEAR-BOND CHARACTERISTIC (M–K) VALUES OF THE EMBOSSED PROFILED SHEET", JOURNAL OF CONSTRUCTIONAL STEEL RESEARCH 63, 791-803, 2007

[8] P. LUURE AND M. CRISINEL "ESSAIS COMPARATIFS SUR TÔLES NERVUREES DE PLANCHERS MIXTES AVEC ET SANS BOSSAGES" 1993

[9] J. M. DAVIES, C. JIANG " DESIGN PROCEDURES FOR PROFILED METAL SHEETING AND DECKING", *THIN-WALLED STRUCTURES* VOL. 27, NO. I, PP. 43-53, 1997

[10] A. BIEGUS, D. CZEPIZAK " RESEARCH ON THE INTERACTIVE RESISTANCE OF CORRUGATED SHEETS UNDER COMBINED BENDING AND CONTACT PRESSURE", THIN-WALLED STRUCTURES 44, 825–831, 2006

[11] O. T. BAIAO FILHO "EMBOSSMENTS CONSIDERATIONS ON THE STEEL DECK PROFILE STRENGTH AND STIFFNESS",

[121] E. S. MISTAKIDIS, K. G. DIMITRIADIS "BENDING RESISTANCE OF COMPOSITE SLABS MADE WITH THIN-WALLED STEEL SHEETING WITH INDENTATIONS OR EMBOSSMENTS" 2007

[13] A. PALISSON, L. SOKOL "RESISTANCE PLASTIQUE DES DALLES MIXTES EN CONNEXION PARTIELLE, CONSTRUCTION METALLIQUE" N° 2-2011, CTICM

[14] DIN 18807, TEILS 1, 2, 3, TRAPEZPROFILE IM HOCHBAU, STAHLTRAPEZPROFILE. DEUTSCHES INSTITUT FUR NORMUNG, BERLIN

GRISPE

Guidelines and **R**ecommendations for **I**ntegrating **S**pecific **P**rofiled steel sheets in the **E**urocodes (**GRISPE**)

WP2 Doc 1 Version 02

Background Document

Working Package 2

Deliverable D 2.1

Guidelines and Recommandations for Integrating Specific Profiled Steels sheets in the Eurocodes (GRISPE)

Project co-funded under the Research Fund for Coal and Steel
Grant agreement No RFCS-CT-2013-00018
Proposal No RFS-PR-12027

Author(s)	
C. Fauth, KIT	
Drafting history	
Draft Version 1	*28th November 2013*
Final Version 1	*30th November 2013*

Dissemination Level		
PU	*Public*	
PP	*Restricted to the Commission Services, the Coal and Steel Technical Groups and the European Committee for Standardisation (CEN)*	
RE	*Restricted to a group specified by the Beneficiaries*	
CO	*Confidential, only for Beneficiaries (including the Commission services)*	***X***

Verification and Approval
Coordinator: David Izabel, SNPPA, 30.11.2013
WP2 Leader: Rainer Holz, IFL. 30.11.2013
Other Beneficiaries

Deliverable	
D 2.1 Backround Document	***Due date: 30th Nov. 2013*** ***Completion date: 30th Nov. 2013***

Summary

1 Liner Trays 4
1.1 Component description 4
1.2 Design model according to DIN EN 1993-1-3 6
1.3 Design by testing according to DIN EN 1993-1-3 and DIN 18807 10
1.4 State of the art 12
1.5 Conclusion 16
2 Assembled profiles 17
2.1 Component description 17
2.2 DIN 18807 (state of the art) 17
2.3 Conclusion 19
3 Corrugated sheets 19
3.1 Component description 19
3.2 State of the art 19
3.3 Conclusion 23
4 Curved profiles 23
4.1 Component description 23
4.2 State of the art 24
4.3 Conclusion 25
5 References 25

1 Liner Trays

1.1 Component description

A liner tray is a trough-like cold formed steel component with a wide flange with two webs and two smaller flanges. The two small flanges are stiffened with outward profiles which span at right angle to the span of the liner trays, for example trapezoidal or corrugated sheets. There could be also wall panels instead of the trapezoidal or corrugated profiles. The width is normally between 500 mm and 600 mm. The height is normally between 90 mm and 160 mm. Typically they are used for inner sheets of walls, but they can also be used for roof lower sheets. To increase the load bearing capacity the flanges and webs are reinforced with stiffeners. The liner trays can be spanning vertically or horizontally. When they are spanning horizontally they form a two layer built-up cladding system. When they span vertically they build a cassette wall system.

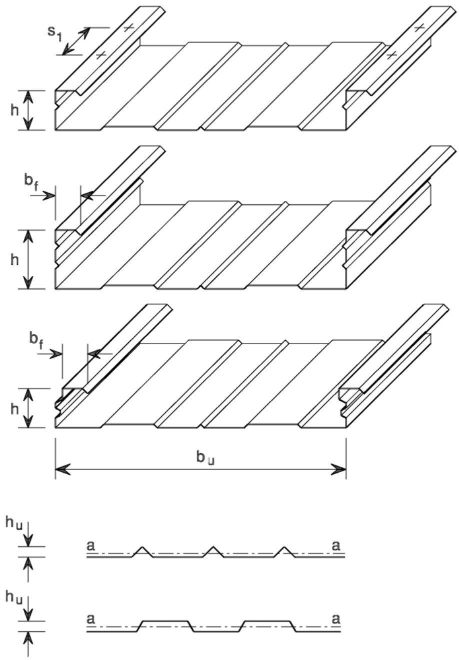

Fig.1: Typical design of liner trays [DIN EN 1993-1-3]

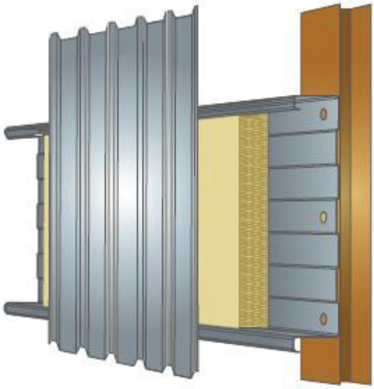

Fig. 2a: Typically two layer build-up wall cladding system [product catalog of Joris IDE]

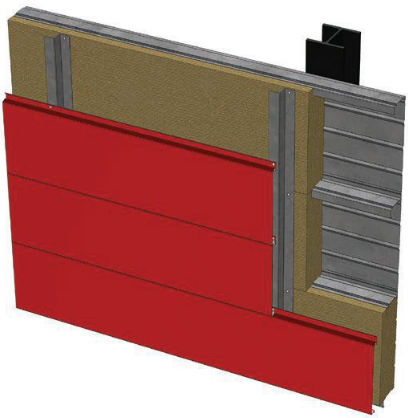

Fig. 2b: Two layer build-up wall cladding system with outward panels instead of trapezoidal sheets [product catalog of Bacacier]

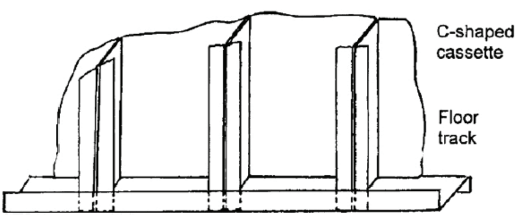

Fig. 2c: Cassette wall construction [1]

The determination of the load bearing capacity is carried out via experiments. In Germany the test procedures are governed by the following documents:

- DIN EN 1993-1-3
- DIN EN 1993-1-3/NA
- DIN 18807-2
- DIN 18807-2/A1
- "Ergänzende Prüfgrundsätze für Stahlkassettenprofiltafen"

1.2 Design model according to DIN EN 1993-1-3

A design method is given in Eurocode EN 1993-1-3. Axial compression is not explicitly considered in En 1993-1-3. The design procedure is similar to that for bending with the narrow flanges in compression.
For wide flange and web, the effective width approach will be applied, while for the smaller flanges and the adjacent edge stiffener the iterative procedure has to be used.
The resistance of the webs is given in section 6.1.5 "shear force" and for local transverse forces section 6.5.11 "Combined bending moment and local load or support reaction". The load bearing capacity in bending is given in section 10.2.2 "Moment resistance". The shear resistance should be determined by the following expression

$$V_{b,Rd} = \frac{\frac{h_w}{\sin\varphi} * t * f_{bv}}{\gamma_{mo}}$$

The shear buckling strength f_{bv} can be determined with the following table

Relative web slenderness	Web without stiffening at the support	Web with stiffening at the support [1)]
$\bar{\lambda}_w \leq 0{,}83$	$0{,}58\ f_{yb}$	$0{,}58\ f_{yb}$
$0{,}83 < \bar{\lambda}_w < 1{,}40$	$0{,}48 f_{yb} / \bar{\lambda}_w$	$0{,}48 f_{yb} / \bar{\lambda}_w$
$\bar{\lambda}_w \geq 1{,}40$	$0{,}67 f_{yb} / \bar{\lambda}_w^2$	$0{,}48 f_{yb} / \bar{\lambda}_w$
[1)] Stiffening at the support, such as cleats, arranged to prevent distortion of the web and designed to resist the support reaction.		

Table 1: shear buckling strength f_{bv} according to EN 1993-1-3

The relative web slenderness $\bar{\lambda}_w$ for webs without longitudinal stiffeners can be determined with

$$\bar{\lambda}_w = 0{,}346 * \frac{s_w}{t} * \sqrt{\frac{f_{yb}}{E}}$$

for webs with longitudinal stiffeners the web slenderness is given below

$$\bar{\lambda}_w = 0{,}346 * \frac{s_d}{t} * \sqrt{\frac{5{,}34 * f_{yb}}{\kappa_\tau * E}}$$

with

$$\kappa_\tau = 5{,}34 + \frac{2{,}10}{t} * \left(\frac{\sum I_s}{s_d}\right)^{1/3}$$

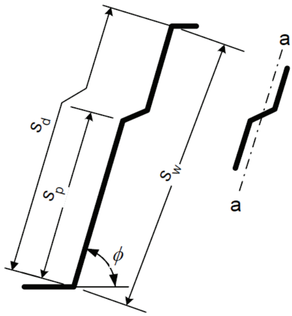

Fig. 3: Longitudinally stiffened web

The resistance in bending $M_{c,Rd}$ is given below when the following conditions are complied:

- the geometry values are within the following range (see Ill. 4)
- the depth of the corrugations of the wide flange does not exceed h/8, where h is the overall depth of the liner tray

0,75 mm	≤	t_{nom}	≤	1,5 mm
30 mm	≤	b_f	≤	60 mm
60 mm	≤	h	≤	200 mm
300 mm	≤	b_u	≤	600 mm
		I_a / b_u	≤	10 mm^4 / mm
		s_1	≤	1000 mm

Fig. 4: Range of validity

If the conditions are not fulfilled the determination of the resistance can be carried out by testing. When the wide flange is in compression you should determine the moment resistance with the step by step method given in the following figure

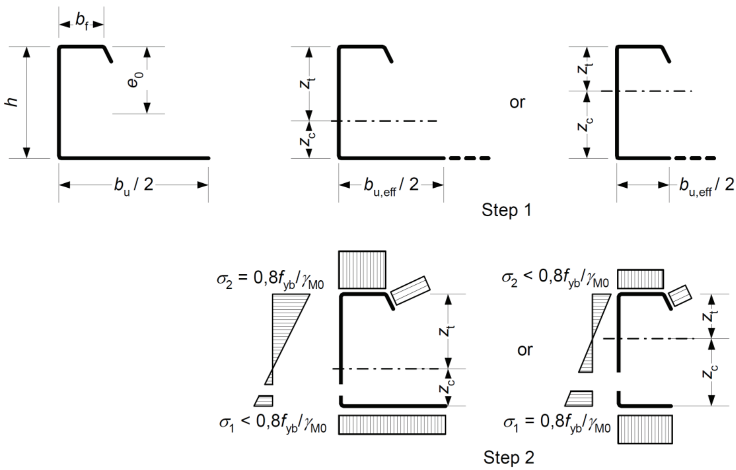

Fig. 5: Determination of moment resistance – wide flange under compression

- Step 1: Determination of the centroid of the cross-section considering the effective areas in cross-sections under compression (Eurocode EN 1993-1-5) with the effective areas of the wide flange and the complete area of the web
- Step 2: Determine the centroid of the new effective cross-section with the effective areas of the web, then determine the moment resistance $M_{c,Rd}$:

$$M_{c,Rd} = 0,8 * \frac{W_{eff,min} * f_{yb}}{\gamma_{mo}}$$

When the wide flange is in tension you should determine the moment resistance with the step by step method given in the following figure

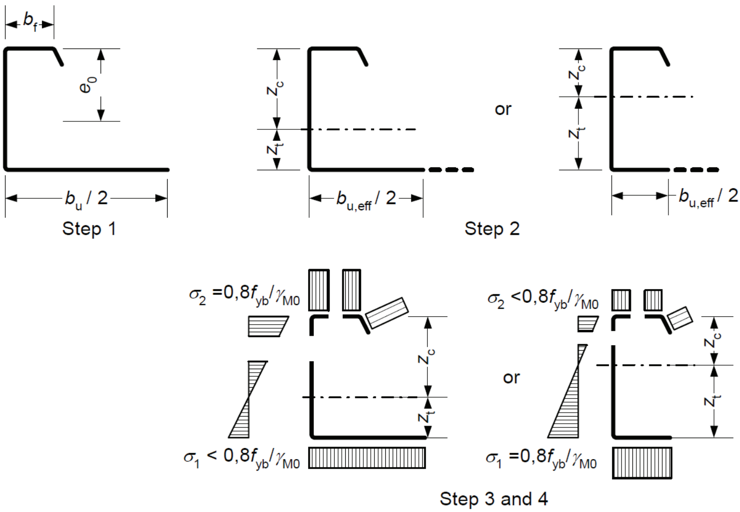

Fig. 6: Determination of moment resistance – wide flange under tension

- Step 1: Determine the centroid of the whole cross-section (fully effective wide flange and web)
- Step 2: Determine the effective width of the wide flange $b_{u,eff}$ (considering flange curling)

$$b_{u,eff} = \frac{53,3 * 10^{10} * {e_0}^2 * t^3 * t_{eq}}{h * L * {b_u}^3}$$

with

$t_{eq} = (12*I_a/b_u)^{1/3}$

- Step 3: Determination of the centroid of the cross-section considering the effective areas in cross-sections under compression (Eurocode EN 1993-1-5) with the effective areas of the wide flange and the complete area of the web
- Step 4: Determine the centroid of the new effective cross-section with the effective areas of the web, then determine the moment resistance $M_{b,Rd}$:

$$M_{b,Rd} = 0,8 * \beta_b * \frac{W_{eff,com} * f_{yb}}{\gamma_{mo}} \text{ but } M_{b,Rd} = 0,8 * \beta_b * \frac{W_{eff,t} * f_{yb}}{\gamma_{mo}}$$

with the correlation factor β_b:

$\beta_b = 1,0$ ($s_1 \leq 300$ mm)
or
$\beta_b = 1,15 - s_1/2000$ ($300 \leq s_1 \leq 1000$ mm)

Shear lag need not be considered if $L/b_{u,eff} \geq 25$. Otherwise a reduction of the value with ρ (section 6.1.4.3) needs to be considered.

1.3 Design by testing according to DIN EN 1993-1-3 and DIN 18807

The test procedures in Eurocode EN 1993-1-3 section A2 are presented with profiled sheets, but they are also for liner trays. The test procedures are equal to DIN 18807-2.
There are 4 types of tests, the single span test, the double span test, the internal support test and the end support test. The double span and the internal support test are both for liner trays which are over two or more spans to determine combination of the bending moment and the support reaction resistance. In the following figures the test setups of the single span, the internal support and the end support test are shown.

Single span test:

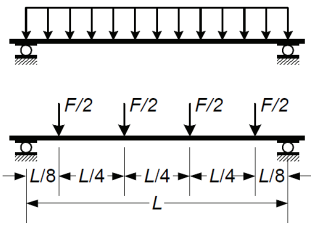

a) Uniformly distributed loading and an example of alternative equivalent line loads

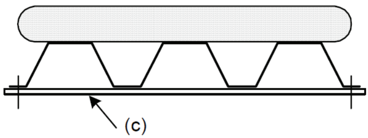

b) Distributed loading applied by an airbag (alternatively by a vacuum test rig)

(c) Transverse tie

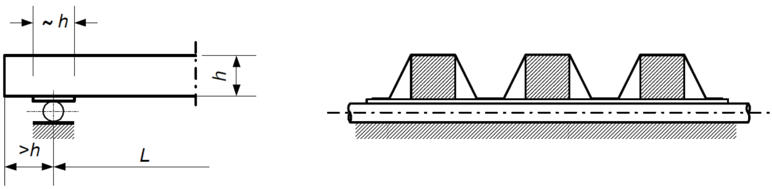

c) Example of support arrangements for preventing distortion

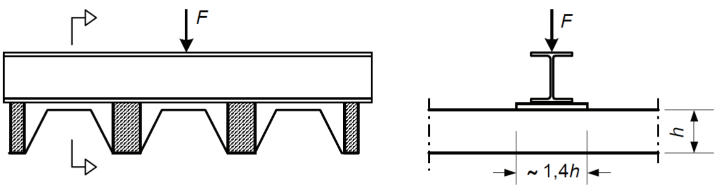

d) Example of method of applying a line load

Fig. 7: Test setup for single span test

Internal support test:

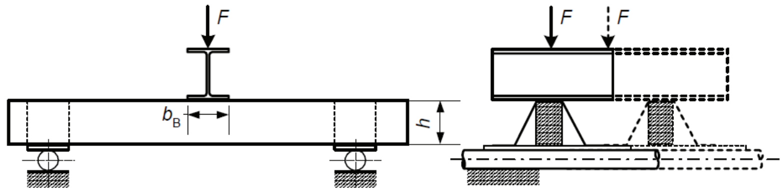

a) Internal support under gravity loading

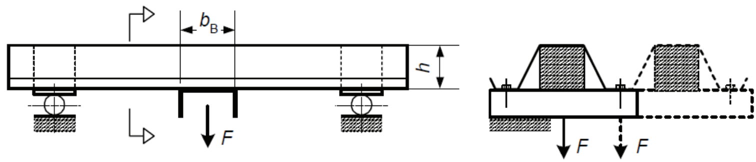

b) Internal support under uplift loading

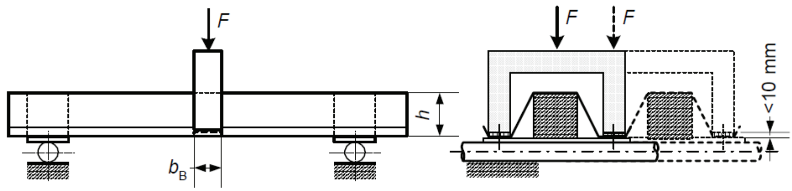

c) Internal support with loading applied to tension flange

Fig. 8: Test setup for the internal support test

End support test:

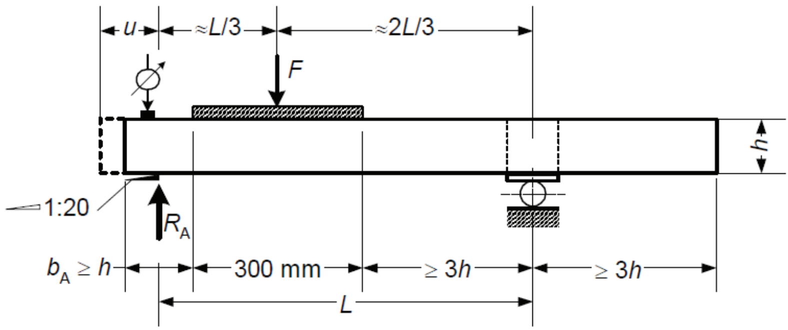

Fig. 9: Test setup for the end support test

In Germany there are additions to the test procedures given by the “Deutsches Institut für Bautechnik” (DIBt) which must be taken into account.

1.4 State of the art

The behavior of liner tray sections under the three primary load systems of axial compression, bending and shear was researched by Baehre in Karlsruhe at the research center of steel, timber and masonry.

The developed test based approach by Baehre [2], [3] and [4] was expanded by studies carried out by Davies at the University of Manchester [5], [6], [7], [8] and [9].

The results are the basis of the design procedure in Eurocode EN 1993-1-3. The geometrical restrictions for these design procedure (see fig. 4) were caused through the limits of the tests by Baehre.

By the design for bending with the wide flange under tension there are three effects which should be considered:

- local buckling of the web and smaller flanges
- distortional buckling of the smaller flanges assembly
- flange curling of the wide flange

The distance s_l between the fasteners controls the distortional buckling of the small flanges.

In Baehre`s test panels this effect was considered up to a distance s_l = 1000 mm.

By the design for bending with the wide flange under compression the flange curling of the wide flange interacts with local buckling of the wide flange. The EC 3 deals not with this interaction. The conventional procedure of effective widths should be used.

Because of flange curling there is more scatter between the experimental results and the theory than it is customary by cold formed steel sections in bending. Therefore the EC 3 required a material factor 1,25 instead of 1,0. The higher material factor is considered with a factor 1,00/1,25 = 0,80 in the two formulas for bending resistance $M_{c,Rd}$ and $M_{b,\,Rd}$.

In [10] Jönsson developed a flange curling model (FCM) and compared it in an analysis of a liner tray with wide flange under tension with a Finite Element Analysis (FEA), the method form EC 3 and tests from Bernard [11].

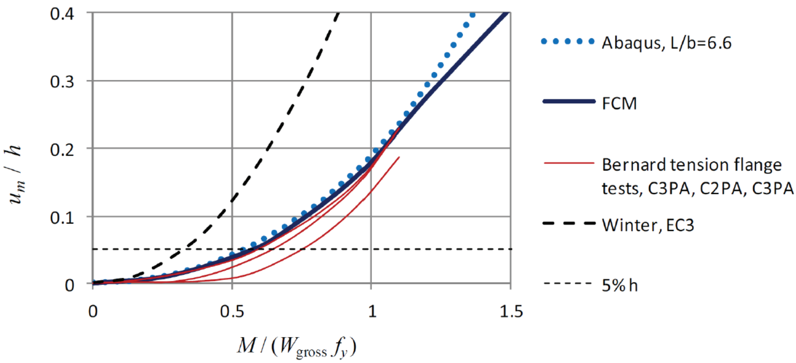

Fig. 10: flange curling displacements of Bernard tests, EC 3, FEA and Jönsson [10]

The conclusion of the author is

- the FCM reproduces the non-linear flange curling displacement behavior for tension flanges for a practical range of slenderness values
- the FCM approximates the stress distribution in the curled flange with reasonable accuracy

- for wide flange in tension the effective moment arm reduction and the effective width have been given
- stiffeners in tension flanges are taken into account by using the full developed width of the flanges
- the use of the FCM in compression flanges should be investigate in further research

The FCM is briefly described in the following lines:
The flange curling phenomenon is initiated by the curvature of the beam, which rotates the axial flange stress resulting towards the neutral axis of the section. The curvature can be found from

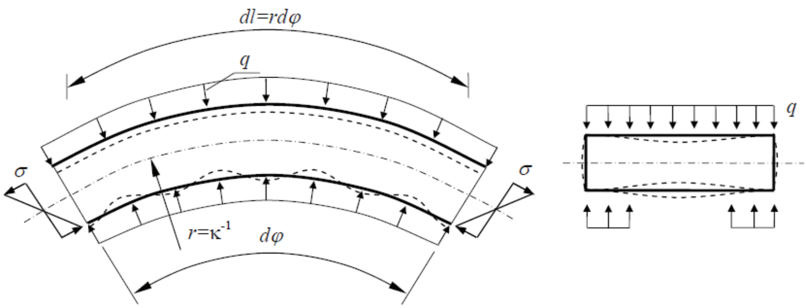

Fig. 11: Second order transverse load action on the flanges

$$\kappa = \frac{\sigma_e}{E * z_e} \quad \text{or} \quad \kappa = \frac{M}{E * I_{ef}}$$

The transverse flange load q is

$$q = t * \sigma * \kappa$$

With the main assumption that “distorted cross-sections remain plain” you can determine the flange stress as a function of the distance x from the corner:

$$\sigma\langle x \rangle = \sigma_e * \left(1 - \frac{u(x)}{z_e}\right)$$

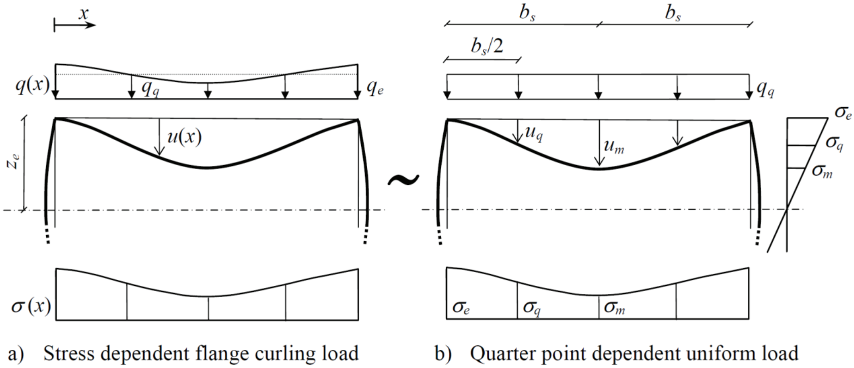

Fig. 12: modelling of second order transverse load action on the flanges [10]

There is a simplification of the problem (see fig. 12b) so that the flange curling load q_q is uniform and determined by the displacement u_q at the quarter points of the flanges

$$q_q = q_e\left(1 - \frac{u_q}{z_e}\right) \ \ with \ \ q_e = t * \sigma_e * \kappa$$

The displacements from a uniform flange load q_q may be found by using the model shown in the following figure.

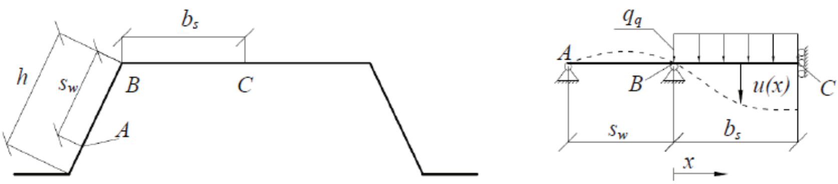

Fig 13: Curling displacements bases on approximate flange support conditions

With the ordinary beam differential equation you can determine the displacement at the quarter point and insert this solution in the previous equation of the flange load q_q so that you can find the approximated uniform flange curling load

$$\mathrm{q_q} = \mathrm{q_e} * \left(1 - \frac{\mathrm{C_q} * \mathrm{q_e}}{\mathrm{z_e} + \mathrm{C_q} * \mathrm{q_e}}\right)$$

with

$$q_e = t * \sigma_e * \kappa$$

and

$$\mathrm{C_q} = \frac{\mathrm{b_s^4}}{24 * \mathrm{D}} * \left(\frac{57}{16} - \frac{3}{1 + \mathrm{s_w}/(3 * \mathrm{b_s})}\right)$$

with

$$\mathrm{D} = \frac{\mathrm{E} * \mathrm{t}}{12(1 - \nu^2)}$$

With the equation of q_q, C_q and q_e you can find the flange curling displacement with

$$u_q = C_q * q_q$$

The effective widths b_{ef} and the effective moment arm z_{ef} (see fig. 14) can be found by demanding equal moment and equal normal force for the flange curled cross section with the approximate stress distribution.

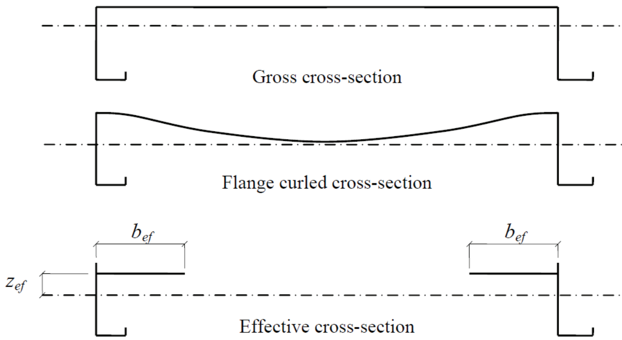

Fig. 14: Flange curling of slender tension flanges

$$\frac{z_{ef}}{z_e} = \frac{{z_e}^2 - 2 * \beta_1 * z_e + \beta_2}{(z_e - \beta_1) * z_e} \quad \text{and} \quad \frac{b_{ef}}{b_s} = \frac{z_e}{z_{ef}}\left(\frac{z_e - \beta_1}{z_e}\right)$$

with

$$\beta_1 = \frac{1 + 2 * s_w / b_s}{15(1 + \frac{s_w}{3 * b_s})} * \left(\frac{q_q * b_s^4}{3 * D}\right)$$

and

$$\beta_2 = \frac{1}{20160} * \left(3968 - \frac{6528}{1 + \frac{s_w}{3 * b_s}} + \frac{2688}{\left(1 + \frac{s_w}{3 * b_s}\right)^2}\right) * \left(\frac{q_q * b_s^4}{3 * D}\right)^2$$

and

$$s_w = 0{,}9 * h$$

These equations can be directly introduced into the iterative scheme for determination of effective cross section properties.

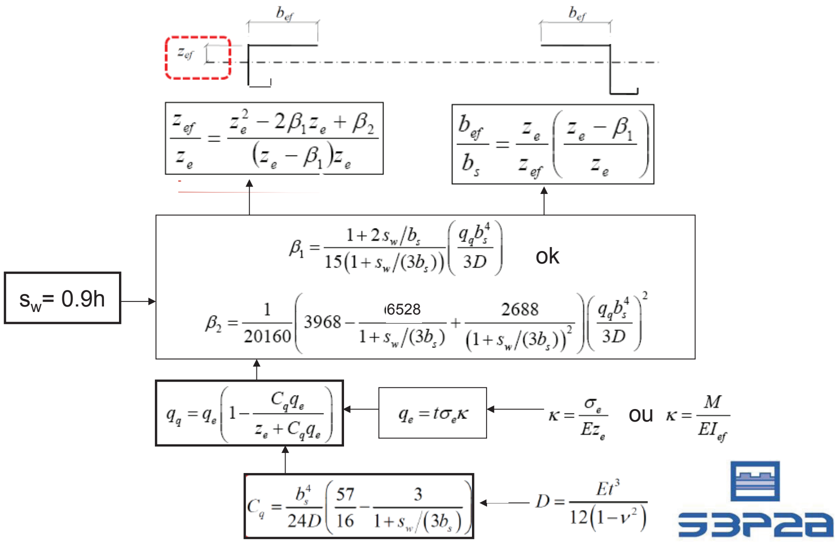

Fig. 15: comparison of FCM

1.5 Conclusion

The restriction of the fasteners distance $s_1 \leq 1000$ mm, which should control distortional buckling, came from the limits of Baehre`s tests (because trapezoidal sheets have normally a width $b \leq 1000$ mm). To extend the design rules for spacer distance $s_1 > 1000$ mm a number of series of tests should be performed to analyse the distortional buckling effects. If the spacer distances increase over $s_1 = 1000$ mm, the “normal” setup liner tray with outward trapezoidal sheets can`t be realized in reality. There must be a cassette wall construction like in figure 2b with outward panels for cladding panels.
The test series will be also used to confirm the FCM method (to acquire data of the flange curling effect to improve the determination of $b_{u,eff}$)
In addition a series of tests should be performed to acquire data of the system behavior (see fig. 16). Dependent of the lateral stiffness of the spacers, this system works like a composite beam with elastic shear bond between the inner layer (liner trays) and the outer layer (profiled sheeting).

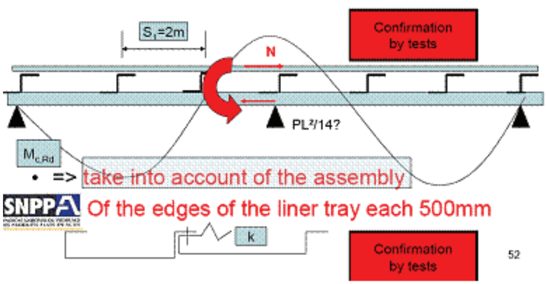

Fig. 16: system behavior of liner trays

2 Assembled profiles

2.1 Component description

There are three types of assemblies (see fig. 10). The resistance of the first joint is equal to a single profile. The resistance by the second and third joint is higher than the load bearing capacity of a single profile. The second joint and third joint are often used to repair buildings or to solve deflection in span. A second reason is to improve the load bearing capacity below snow accumulation
In DIN 18807 there is a design procedure for the fasteners and the web for the clamped joint. In prEN 1090-4 the same procedure is mentioned.

Clamped joint, moving resisting connection (EN 1090-4)	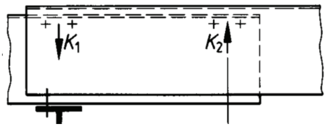
Overlap joint	
Continous profile with local reinforcement	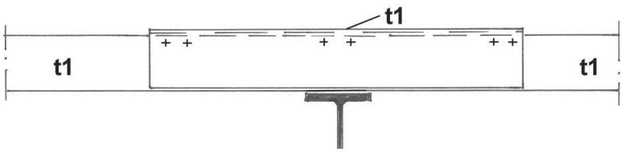

Fig.17: Three various profile assemblies

2.2 DIN 18807 (state of the art)

In DIN 18807 there is a solution for overlapping profiles. They are only allowed at the supports. If powers are to be worn over contact, tests must be performed. In the overlapping field the resistance is equal to a continuous profile. In the following figures 11 and 12 are the two possibilities of this clamped joint.

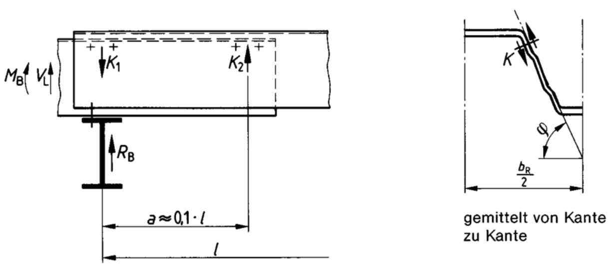

Fig. 18: overlapping profiles according to DIN 18807-3

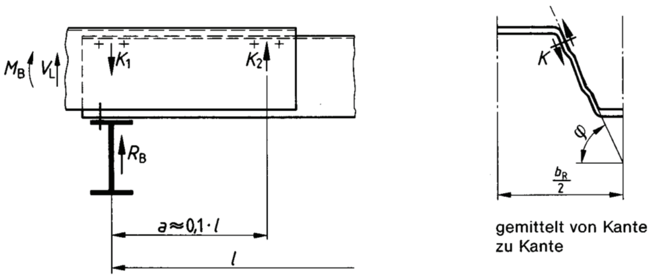

Fig. 19: overlapping profiles according to DIN 18807-3

The force on the fastener is given to

$$K = \max K_i = \frac{|M_B|}{2 * a * \sin\varphi} * b_R \quad \text{(Fig. 11)}$$

or

$$K = \max K_i = \frac{\left|\frac{M_B}{a} + V_L\right|}{2 * \sin\varphi} * b_R \quad \text{(Fig. 12)}$$

A maximum of two fasteners may be recognized in horizontal and vertical direction in each compound (maximum 4 fasteners). The required fastener edge spacings and hole spacings shall be complied with

- hole spacing in direction of force	≥ 3d
	≥ 20 mm
- hole spacing at right angles to direction to force	≥ 30 mm
- hole spacing p	≥ 4d
	≥ 40 mm
	≥ 10d

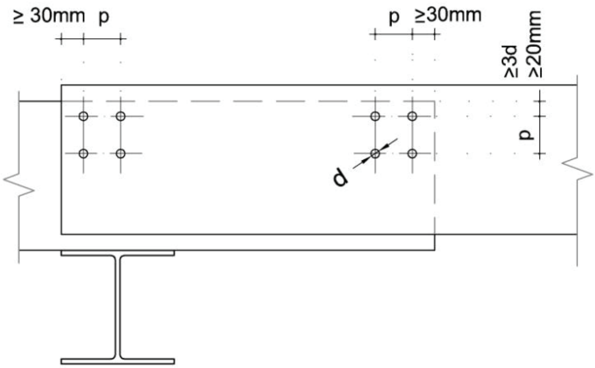

Fig. 20: the distances of the fasteners according to DIN 18807-3 for a statically effective overlapping

2.3 Conclusion

There are design procedures in DIN 18807 and further in EN 1090-4. The design rules are similar to each other. To confirm this procedure there should be a series of tests at the clamped joint to confirm this design procedure. In addition there should be a number of tests at the overlap joint to acquire data about the load bearing capacity.

3 Corrugated sheets

3.1 Component description

Corrugates steel sheets are the oldest cold formed steel sheets, they have a continuous curve instead of the flat sections like trapezoidal profiles.

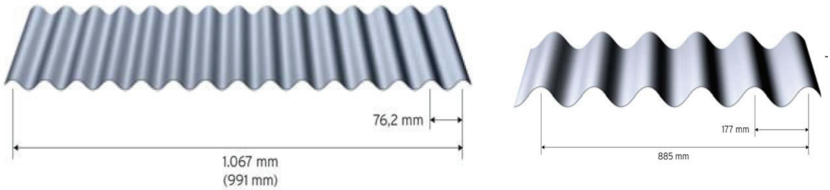

Fig. 21: Corrugated sheets

3.2 State of the art

The conventional bending theory can be used for corrugated steel sheets, because of the continuous curvature no local buckling is to be expected. In DIN 59231 [12] is a parameter range of the d/r-ratio where no buckling is expected.
In [13] there`s a calculation method which is developed from the comparison with FE calculations. This procedure corresponds to the usual procedure for buckling problems. Parameters are developed from the comparison with FE calculations with which the reduction factor χ between the limits for flat plates and circular cylinders can be calculated. With the help of this reduction factor χ you get finally the bearing stress of the cylinder segment. I. a. the influence of the boundary conditions of the longitudinal edges and various forms of predeformations are investigated.
It remains to check whether corrugated profiled sheets fit into the curvature of field of CTICM study. The different steps are shown in the following:

- Parameter of curvature:

$$Z = \frac{b^2}{R * t}$$

- critical buckling strength:

$$\sigma_{cr}{}^{z} = k_c^z * \sigma_E$$

with

$$\sigma_E = \frac{\pi^2 * E}{12 * (1-\nu^2)} * \left(\frac{t}{b}\right)^2 \quad \text{and} \quad k_c^z = \frac{k_c^{plate}}{2} * \left(1 + \sqrt{1 + \frac{48 * (1-\nu^2)}{\pi^4 * \left(k_c^{plate}\right)^2} * Z^2}\right)$$

- parameters $\bar{\lambda}$, β, $\overline{\lambda_0}$ and $\alpha_{Z,s}$:

$$\bar{\lambda} = \sqrt{\frac{f_y}{\sigma_{cr}^Z}}$$

$$\beta = \frac{1 + 0{,}97^Z}{2}$$

$$\overline{\lambda_0} = 0{,}2 + 0{,}473 * 0{,}95^Z$$

α_{z}: table:

Z	0	10	20	30	≥40
α_z	0,28	0,38	0,33	0,21	0,13

- reduction coefficient χ

$$\chi = \frac{2 * \beta}{\beta + \bar{\lambda} + \sqrt{(\beta + \bar{\lambda})^2 - 4 * \beta * \left(\bar{\lambda} - \alpha_z * (\bar{\lambda} - \bar{\lambda}_0)\right)}}$$

- ultimate stress σ_u

$$\sigma_u = \chi * f_y$$

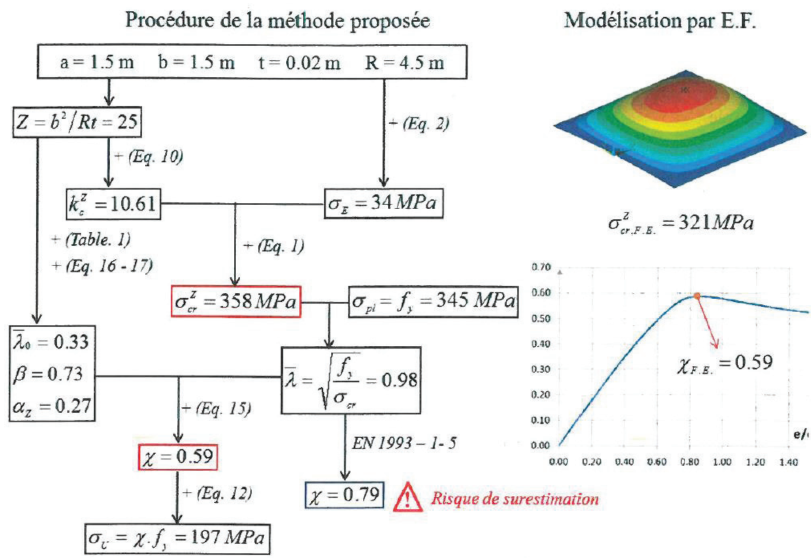

Fig. 22: An example of the proposed calculation method [13]

The effective second moment of area can be determined with the following approximate function

$$I = I_{eff} = \frac{2}{105} * h^2 * n * b_r * t * \left(\frac{1}{\cos\left(\arctan\left(\frac{4 * h}{b_r}\right)\right)} + 6 \right)$$

This equation is based on a parabolic curvature. The geometrical parameters n, h and b_r are explained in the following figure.

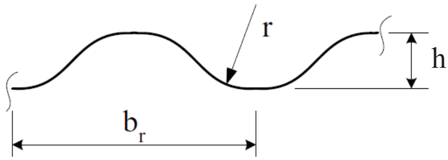

Fig. 23: Corrugated sheet

In DIN EN 1993-4-1 there`s another equation to determine the stiffness of corrugated sheets in steel silos. The stiffness for axial compression can be determined with the following equation

$$C_y = E * t * \left(1 + \frac{\pi^2 * d^2}{a * l^2}\right)$$

The second moment of area can be determined with the notation from shell structures with the following equation to

$$I_y = 0{,}13 * t * d^2$$

With the notation according to DIN EN 1993-1-3 you receive

$$I_x = 0{,}13 * t * {h_w}^2$$

Therefore moment resistance $M_{c,Rd}$ can be obtained with the following equation

$$M_{c,Rd} = \frac{130 * t * {h_w}^2}{\frac{h_w}{2}} * \frac{f_{yb}}{\gamma_{m0}} \quad (\text{Nmm/mm})$$

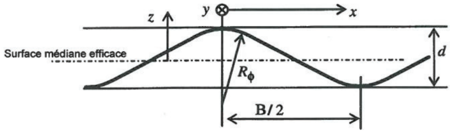

Fig. 24: corrugated sheet according to DIN EN 1993-4-1

Normally the corrugated sheets are designed by testing.
The tests are in accordance with DIN 18807 (see 1.3). Further informations are given in [14].

The pull-through resistance of fixings of steel sheeting can be determined according to DIN EN 1993-1-3 with

$$R_k = t * d_w * f_u * \alpha_{cycl} * \alpha_E$$

with

t	steel thickness
d_w	washer diameter
f_u	tensile strength
α_{cycl}	parameter for cyclic loads due the tensile loads (e.g. wind loading)
α_E	parameter for special cases of application

At the KIT tests with V-shaped specimen were recalculated and evaluated statistically (see fig. 16).

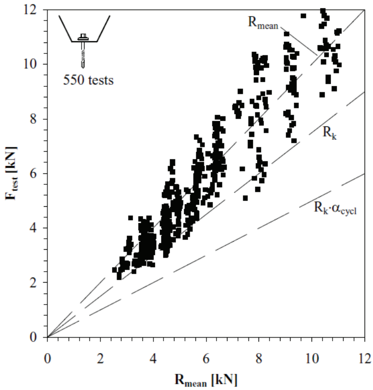

Fig. 25: Comparison of calculated load-bearing capacity with test results.

The characteristic value of load bearing capacity resulted in

$$R_k = 1{,}12 * t * d_w * f_u * \alpha_{cycl} * \alpha_E$$

The resistance can also be determined by tests. The test setups for trapezoidal and corrugated steel sheets are equal. Because the profile geometry for the profiled steel sheets treated in [15] has no or negligible influence. The standardized V-shaped specimen is shown in the following figure.

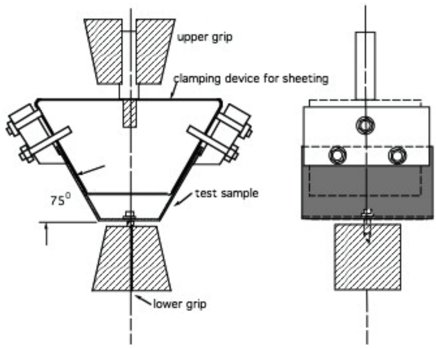

Fig. 26: Test setup according to [16]

3.3 Conclusion

There will be a number of test series to confirm the mentioned formulas and equations.

4 Curved profiles

4.1 Component description

There are three forms of curved profiles. The difference between the three forms is the method of curving. The shaping can be done by roll forming the profiles, by crushing the inner flange of the profiles or by bending the profiles on site.

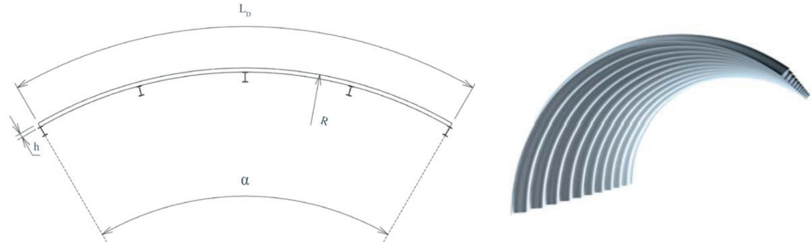

Fig. 27: curved profile by roll forming (variant A)

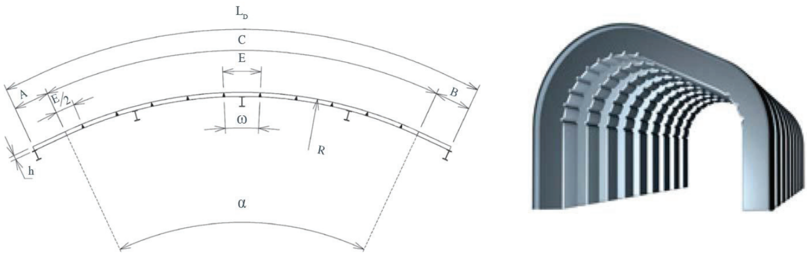

Fig. 28: curved profile by crushing the inner flange (variant B)

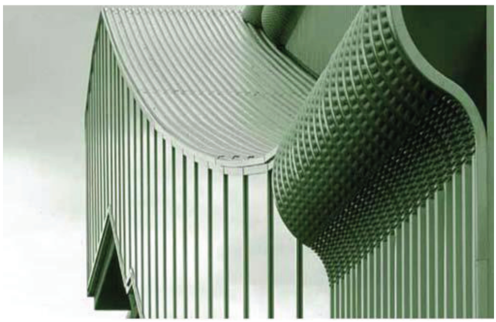

Fig. 29: curved profile by bending on site (variant C)

4.2 State of the art

Curved profiles

The bending load bearing capacity of variant B is not important because of the small spans.
Variant C can be designed according to the EN 1993-1-3 because of the large bending radius. Here, no change is expected in the bearing capacity compared to conventional profiles. There will be a focus on variant A in this project. In the following only variant A is considered.
The influence of residual stresses from the manufacturing was examined in the past at the research center of steel, timber and masonry in Germany.
A variety of tests according to DIN 18807-2 on curved trapezoidal profiles from different producers were performed. The bending radius was between 4 m and 19 m. The supports were not both fixed in the tests.
The difference in bending bearing capacity between a plane profile and a curved profile was between zero and ten percent.
In the literature you can find a reduction in the bearing capacity by 20% (narrow flange in compression) to 30% (wide flange in compression) [17].
If both supports are fixed, the bending theory is no longer applicable, the profile behaves like an arch.

Arch profiles

The arch actions produce high normal forces in the profile and thus high horizontal loads acting on the supports. These should be compensated by the substructure. Usually these systems are executed with tie rods. These compensate the horizontal arch forces from surcharges so that the substructure is merely loaded vertically, not taking into account wind suction load.
The company “Hoesch Building systems” has such a system developed in the past, it`s called “Legato Arch System”.

Fig. 30: Hoesch arch roof [www.hoesch-bau.com]

In DIN 18807-3 there is an interaction formula for bending and normal force in trapezoidal profiled sheets.

In case of compression force the following is applied

$$\frac{N_D}{N_{dD}} * \left[1 + 0{,}5 * \alpha \left(1 - \frac{N_D}{N_{dD}}\right)\right] + \frac{M}{M_d} \leq 1$$

in case of tension force

$$\frac{N_Z}{N_{dZ}} + \frac{M}{M_d} \leq 1$$

is applied with

N_Z design value of tensile force
N_D design value of compressive force
M design value of bending moment
M_d design resistance of bending moment
N_{dZ} design resistance of tensile force
N_{dD} design resistance of compressive force

and

$$\alpha = \frac{L_{cr}}{i_{ef} * \pi} * \sqrt{\frac{f_{y,k}}{E}}$$

with

L_{cr} buckling length
i_{ef} radius of inertia of the effective cross section

4.3 Conclusion

There will be a number of test series to confirm the mentioned formulas and equations.
This will be the influence of the curvature by the curved profile and the verification of the interaction formula by the arch.

5 References

[1] Davies J. M. (2006b). Light gauge steel cassette wall construction – theory and practice, Journal of Constructional Steel Research, 62 (2006)
[2] Baehre R., Buca J. (1986). Die wirksame Breite des Zuggurtes von biegebeanspruchten Kassetten, Stahlbau 55 (9), 1986
[3] Baehre R. (1987). Zur Schubfeldwirkung und –bemessung von Kassettenkonstruktionen, Stahlbau 56 (7)
[4] Baehre R., Buca J., Egner R. (1990). Empfehlungen zur Bemessung von Kassettenprofilen, R. Schardt Festschrift, University of Darmstadt
[5] Davies J. M., Dewhust D.W. (1997). The shear behavior of thin-walled cassette sections infilled with rigid insulation, Proceedings of International Conference on Experimental Model Research and Testing of Thin-Walled Structures, Prague, Czech Republic, September 1997)
[6] Davis J. M., Fragos A. S. (2002). The local shear buckling of thin-walled cassettes infilled by rigid insulations – 1. Tests, proceedings of 3rd European Conference on Steel Structures – Eurosteel 2002, Coimbra, Portugal 19-20 September (2002)
[7] Davies J. M., Fragos D.W. (2004). The local shear buckling of thin-walled cassettes infilled by rigid insulation, Journal of Constructional Steel Research, 60 (3-5)
[8] Davies J. M. (2002). Cassette wall construction, Current Research and Practice – Advance in Steel Structures – ICASS`02, Vol. 1(Chan S.L., Teng J.G. and Chung K.F., Eds), Elsevier Ltd., Oxford
[9] Voutay P.A., Davis J.M. (2002). Analysis of Cassette Sections in compression, Current Research and Practice – Advance in Steel Structures – ICASS`02, Vol. 1 (Chan S.L., Teng J.G. and Chung K.F., Eds.), Elsevier Science Ltd., Oxford
[10] Jönsson J., Ramonas G. (2012). Flange curling in cold formed profiles – Nordic Steel Construction Conference 2012, Hotel Bristol, Oslo Norway 5-7 September (2012)

[11] Bernard E.S., Bridge R.Q. (1995). Flange curling in profiled steel decks – Thin-Walled Structures
[12] DIN 59321 2003:11. Wellbleche und Pfannenbleche
[13] Le Tran K., Davaine L., et al.: Etude de la Resistance et de la Stabilite des Panneaux cylindriques non-raidis soumis a une Compression uniforme: application aux ouvrages d`arts, Revenue Construction Metallique, 01-2012
[14] Touchard, R.: Wellbleche, moderne Bauelemente mit genormter Tragfähigkeit. Deutscher Verzinkerei Verband e. V., Düsseldorf, Dezember 1988
[15] Misiek. T., et al.: Pull-through resistance of tensile-loaded srew-fastenings of thin-walled sheeting and sandwich panels, Stability and Ductility of Steel Structures, Rio de Janeiro, Brazil, 8-10 September
[16] ECCS TC 7, The Testing of Connections with Mechanical Fasteners in Steel Sheeting and Sections, ECCS publication no. 124, Brussels, 2009.
[17] James L. Jorgenson J.L., Chowdhury A.H.. Buckling Strenght of cold formed steel curved panels

GRISPE

Guidelines and **R**ecommendations for **I**ntegrating **S**pecific **P**rofiled steel sheets in the **E**urocodes (**GRISPE**)

WP3 Doc 1 Final Version 01

WP3 Background document

Working Package 3

Deliverable D 3.1

DOCUMENT CONTROL INFORMATION AND ARCHIVING

Guidelines and Recommandations for Integrating Specific Profiled Steels sheets in the Eurocodes (GRISPE)

Project co-funded under the Research Fund for Coal and Steel
Grant agreement No RFCS-CT-2013-00018
Proposal No RFS-PR-12027

Author(s)	
Palisson Anna, Sokol Palisson Consultants	
Drafting history	
Draft Version 1	*20th December 2013*
Draft Version xx	*Day Month Year*
Final Version Revision 01	*25th December 201*
Final Version Revision 02	*Day Month Year*
Final Version Revision 03	*Day Month Year*
Final Version Revision xx	*Day Month Year*
Final Version CO	*Day Month Year*

Dissemination Level		
PU	*Public*	
PP	*Restricted to the Commission Services, the Coal and Steel Technical Groups and the European Committee for Standardisation (CEN)*	
RE	*Restricted to a group specified by the Beneficiaries*	
CO	*Confidential, only for Beneficiaries (including the Commission services)*	***x***

Verification and Approval
Coordinator David Izabel, SNPPA
WP1 Leader SOKOL PALISSON CONSULTANTS
Other Beneficiaries SNPPA, Bac Acier, IFL, Joris Ide, KIT, PUT

Deliverable	
D 3.1 WP3Background document	***Due date : 30.11.2013*** ***Completion date: 25.12.2013***

1. INTRODUCTION

For architectural reasons and also in order to improve the acoustic performance perforated profiles (Fig. 1), with different types, geometries and distribution of micro-perforations on the profile web and flange, are increasingly developed and used.

Fig. 1 - Trapezoidal sheet with perforated web (Montana Bausysteme AG, Villemergen [1])

European Standard EN 1993-1-3 dealing with design rules for cold-formed members and sheeting covers only the triangular distribution of such perforations while many exist on the market.

As far as round or square holes in the flange of sheeting are concerned, they are often required for the passage of services (Fig. 2). But only plane walls without holes are covered by EN 1993-1-3.

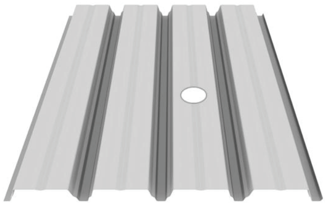

Fig. 2 - Round holes in the flange of sheeting

The aim of this document is to give a state of the art of the current European Standard EN and of the background information about steel perforated profiles and about sheeting with holes in the flange, and to emphasize the lack of data and knowledge.

2. EUROCODE

The European standard EN 1993-1-3 gives, for cold-formed members and sheeting, methods for design by calculation and for design assisted by testing. The design by calculation applies only within stated ranges of material properties and geometrical proportions for which sufficient experience and test evidence is available. These limitations do not apply to design assisted by testing.

To design steel sheeting two criteria of verification must be determined, resistance and flexion stiffness. EN 1993-1-3 provides the methodology to determine those criteria for steel sheeting only with:

- plane walls without holes
- plane walls with equilateral triangular perforation pattern (Fig. 3)

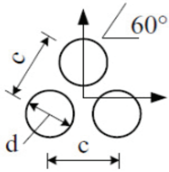

Fig. 3 - Equilateral triangular pattern

2.1. Plane without holes

The sheeting thin elements may buckle locally at a stress level lower than the yield point of steel when they are subject to compression in flexural bending and axial compression as shown in Fig. 4 [2].

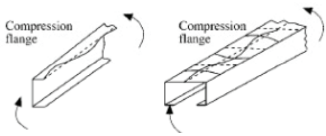

Fig. 4 - Local buckling of compression beam

An additional load can be carried by the element when the local buckling stress is reached, this phenomenon is the postbuckling strength, as shown in Fig. 5.

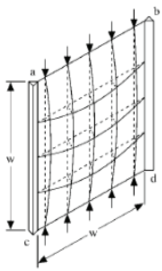

Fig. 5 - Postbuckling strength model

A nonuniform stress distribution is developed (Fig. 6)

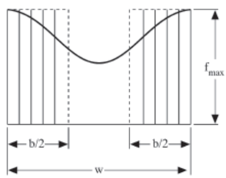

Fig. 6 - Stress distribution in stiffened compression elements

Von Karman traduced in 1910 this buckling by the following equation

$$\frac{\delta^4 w}{\delta x^4}+2\frac{\delta^4 w}{\delta x^2 \delta y^2}+\frac{\delta^4 w}{\delta y^4}=\frac{1}{D}\left(N_x\frac{\delta^2 w}{\delta x^2}+2N_{xy}\frac{\delta^2 w}{\delta x \delta y}+N_y\frac{\delta^2 w}{\delta y^2}\right)$$

$$D=\frac{Et^3}{12\left(1-\nu^2\right)}$$

The elastic local buckling stress for simply supported plate can be determined as follow:

$$f_y=\frac{\pi^2 E}{12\left(1-\nu^2\right)}*\frac{kt^2}{b_e^2}$$

This leaded Von Karman to the effective width (b_e) notion where the buckled intern part of the plate is neglected (Fig. 7)

$$\rho=\frac{b_e}{b}=\sqrt{\frac{\sigma_{cr}}{f_y}}$$

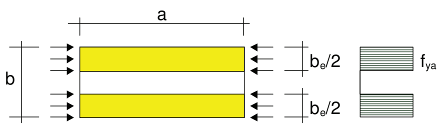

Fig. 7 - Effective width of stiffened compression elements

This theory was adapted in EN 1993-1-3 and 1993-1-5 where the effects of local and distortional buckling are taken into account in determining the resistance and stiffness of cold-formed members and sheeting. The effect of holes on the effective width is not taken into account.

2.2. Perforated sheeting

In section 10.4 of EN 1993-1-3 it is specified that perforated sheeting with the holes arranged in the shape of equilateral triangles may be designed by calculation, provided that the rules for non-perforated sheeting are modified by introducing the effective thicknesses given below.

- gross section properties may be calculated using part 5.1, but replacing t by $t_{a,eff}$ obtained from:

$$t_{a,eff} = 1{,}18\,t\left(1-\frac{d}{0{,}9a}\right)$$

where:

d	is	the diameter of the perforations;
a	is	the spacing between the centers of the perforations.

- effective section properties may be calculated using Section 5, but replacing t by $t_{b,eff}$ obtained from:

$$t_{b,eff} = t\sqrt[3]{1{,}18\left(1-d\ /a\right)}$$

- the resistance of a single web to local transverse forces may be calculated using part 6.1.9, but replacing t by $t_{c,eff}$ obtained from:

$$t_{c,eff} = t \left[1 - (d/a)^2 s_{per} / s_w\right]^{3/2}$$

where:

s_{per}	is	the slant height of the perforated portion of the web;
s_w	is	the total slant height of the web.

The criteria of verification of a steel sheeting must take into account the effective cross-section which is impacted by holes or perforations in the web and flanges, therefore this absence in the standard EN 1993-1-3 is a real lack to correctly determine and verify the resistance of a steel sheeting. And this lack is even more disturbing and serious as several previous studies have shown that holes [3] to [8], and perforations [9] to [11] reduce the strength locally and globally and have an impact on its bending resistance [12], [13]. In the next chapter we will focus on studies performed on sheeting with holes and perforations in the webs or flanges.

3. STATE OF THE ART

3.1. Plane with holes

The review of the existing published and on-going works allowed to find several studies on steel sheeting with holes. As we will see below these studies deal on the effect of holes on local buckling and postbuckling of plates subjected to compression or shear loading.

M. Azhari [3] established a nonlinear mathematical theory for initial and post local buckling analysis of perforated thin plates based on the principle of virtual work. The results of local buckling coefficient of plates subjected to uniaxial and biaxial compressions were compared with known solutions (Fig. 8).

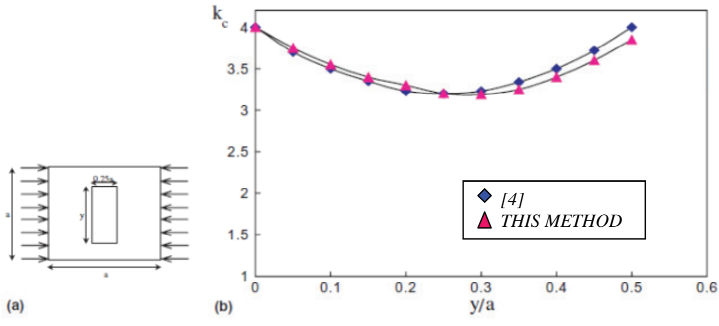

Fig. 8 - Local buckling coefficient of the perforated plate subjected to uniform compressions in one direction versus normalized rectangular hole dimension y/a.

He found that the presence of holes in structural members resulted in changes in the stress distribution within the member and consequently a reduction in the local buckling capacity of the plate. Therefore with increasing hole size parameters, strength of the perforated plate in the post local buckling phase decreased.

F-Y. Chow investigated the buckling behaviour of square plates containing holes and subjected to uniaxial or biaxial compression [5] or to in-plane shear loading [6]. He carried out parallel studies using experimental and computational methods. He found that the buckling coefficient decreased when both holes, square and circular, increased, and observed that introduction of considered types and sizes of holes rapidly reduces the strength of the plate in which the ratio width/thickness (a/t) is smaller than 50, while for higher value reduces of strength is progressive (Fig. 9).

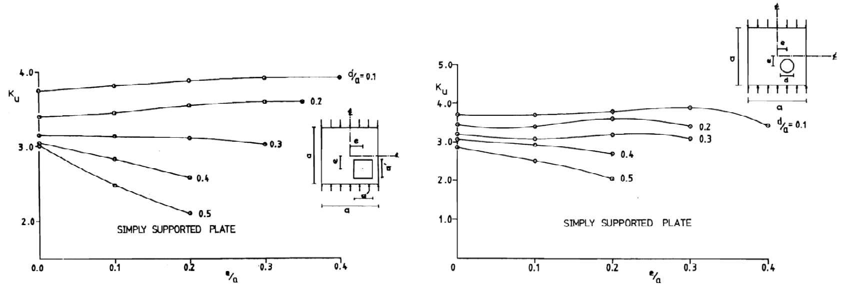

Fig. 9 Buckling coefficients for uniaxial loading for a plate with square and circular hole

The eight types of curves presented in the paper [6] can be directly used in the design process. The method can be applied for rectangular plates also.
For plates under uniform shear loading, two opposing results were obtained for holes located in the compression and tension diagonals; in the former case, the eccentricity reduced the buckling coefficient and in the latter, increased it.

J.K. Paik [7] investigated the ultimate strength characteristics of perforated steel plates under edge shear loads. He carried out a series of ANSYS elastic–plastic large deflection FEA with varying the cutout size as well as plate dimensions (aspect ratio and plate thickness). He confirmed that the cutout significantly reduced the plate ultimate strength. He found that the plate aspect ratio affected the ultimate strength of perforated plates to some extent when edge shear loads were predominant, while the plate thickness was not a sensitive parameter to the normalized ultimate shear strength when holding the cutout size constant.

Also, he found that the traditional approach of the plasticity correction with elastic buckling strength to estimate the so-called critical buckling strength may not be valid for perforated plates, specifically when the cutout size and/or the plate thickness are relatively large.

He developed, by regression analysis of FEA results, a closed-form empirical formula to predict the ultimate shear strength of perforated plate as a function of cutout size as well as plate dimensions.

He concluded that further studies were required for different types of loads or their combination loads or with different types or locations of cutout.

N.E. Shanmugam [8] studied post-buckling behaviour and ultimate load capacity of plates with holes (square and circular), with different boundary conditions and subjected to uniaxial or biaxial compression. Plates were analysed using the finite element method (FEM), and extensive studies were carried out covering parameters such as plate slenderness, opening size, boundary conditions and the nature of loading. He established a design formula to determine the ultimate load carrying capacity based on a best-fit regression analysis using the results from the finite element analyses.

The accuracy of the proposed formula was established by comparison with experimental values of ultimate capacity and similar finite element values. Ultimate load values are also presented in the form of charts for various values of plate slenderness and opening size. The ultimate load carrying capacity of perforated plates was found to be affected by various parameters studied. The increase in hole size and slenderness ratio resulted in a significant loss in the ultimate strength of perforated plates. The strength of perforated plates with simply supported edges was lower as compared to that of plates with clamped edges. The plates with circular holes generally had higher ultimate loads compared to the square perforated plates.

<u>The reviewer notes:</u>
The whole studies above investigated local buckling and postbuckling of plates subjected to axial compression and shear loading. There is no existing study which establishes for sheeting with holes:

- moment resistance under flexion
- web crippling resistance
- effect of combined action of support reaction and negative moment

3.2. Perforated sheeting

Several studies on sheets with triangular pattern perforations were performed.

S. C. Baik [9] proposed the following yield criterion in terms of apparent stresses of sheets with a uniform triangular pattern of round holes under biaxial loading and confirmed it by finite element analysis results (Fig. 10).

$$f_s^2 \sigma_s^{*2} + \sigma_n^{*2} - f_s \sigma_s^* \sigma_n^* + 3\sigma_{sn}^{*2} = \sigma_b^{*2}.$$

Further incorporating this yield stress he obtained a yield function containing anisotropic coefficients.

$$7.56|\sigma_{xy}^*|^{2.1} + 1.36|\sigma_x^*|^{2.1} + 1.39|\sigma_y^*|^{2.1} + |\sigma_x^* - \sigma_y^*|^{2.1} = (0.31\,\sigma_b)^{2.1}.$$

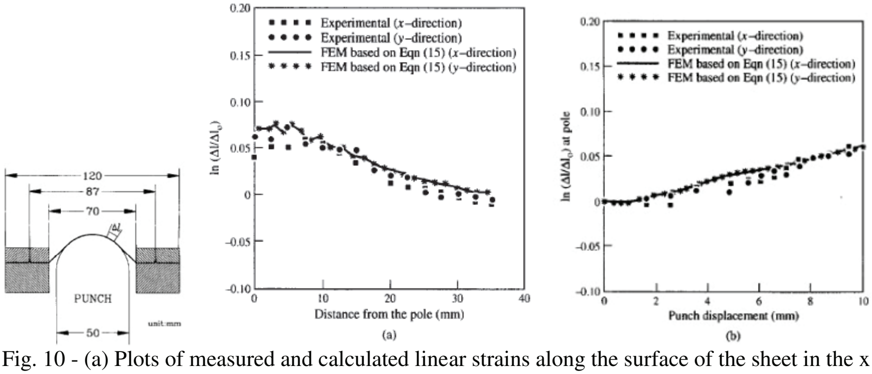

Fig. 10 - (a) Plots of measured and calculated linear strains along the surface of the sheet in the x and y directions at a dome height of 9.3 mm; and (b) the measured and calculated strains at the pole as a function of punch displacement in the x and y directions.

Y-C. Lee [10] investigated the plastic behavior of perforated sheets with low ligament ratios (Fig. 11) , he proposed a yield criterion for the perforated sheets in terms of apparent stresses by employing the equivalent-continuum approach.

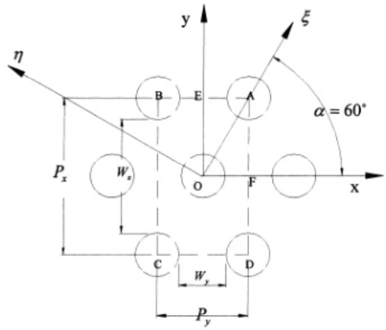

Fig. 11 - Round holes arranged in a triangular pattern.

Obtained yield criteria:

- For yielding along AB

$$\left(\frac{f}{\rho_x}\right)^2 S_x^2 - \left(\frac{f}{\rho_x\rho_y}\right) S_x S_y + \left(\frac{1}{\rho_y^2}\right) S_y^2 = Y_b^2.$$

- For yielding along AO:

$$\begin{aligned}&\frac{1}{16}\left[\left(\frac{f}{\rho_x}\right)^2 - \frac{3f}{\rho_x\rho_y} + \frac{9}{\rho_y^2} + \frac{9}{\rho_y^2}\right] S_x^2 \\ &+ \frac{1}{16}\left[6\left(\frac{f}{\rho_x}\right)^2 - \frac{10f}{\rho_x\rho_y} + \frac{6}{\rho_y^2} - \frac{18}{\rho_y^2}\right] S_x S_y \\ &+ \frac{1}{16}\left[9\left(\frac{f}{\rho_x}\right)^2 - \frac{3f}{\rho_x\rho_y} + \frac{1}{\rho_y^2} + \frac{9}{\rho_y^2}\right] S_y^2 = Y_b^2.\end{aligned}$$

The effectiveness of the proposed yield criterion was then demonstrated by comparing the predicted values of apparent yield stresses and apparent strain ratios with results obtained from finite-element analysis and experiment (Fig.12).

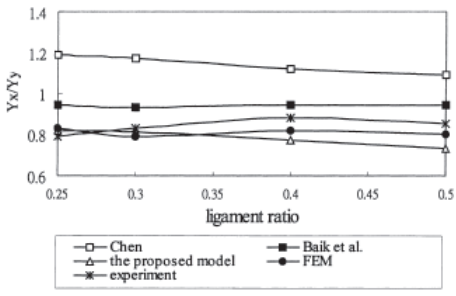

Fig. 12 - Comparison of the apparent yield stress ratio (Yx/Yy).

V. V. Degtyarev [11] studied critical elastic buckling load of uniformly uniaxial compressed isotropic plates perforated in equilateral triangular patterns using FEM (Fig. 13).

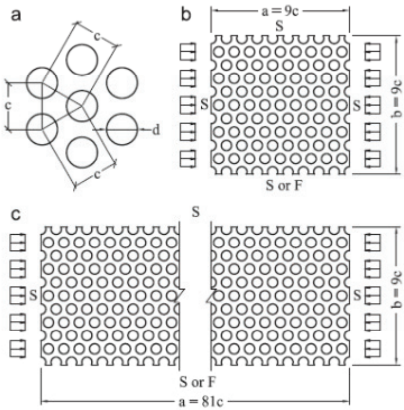

Fig. 13 -Studiedperforatedplates.(a)Equilateraltriangularperforationpattern; (b)Squareplates;and(c)Rectangularplates.S¼simplysupportedside;F¼freeside

The effect of perforations on the critical elastic buckling load was determined. His main conclusions were:

- Critical elastic buckling load of perforated plates decreased as the hole diameter-to-spacing ratio, d/c, increased (Fig. 14)

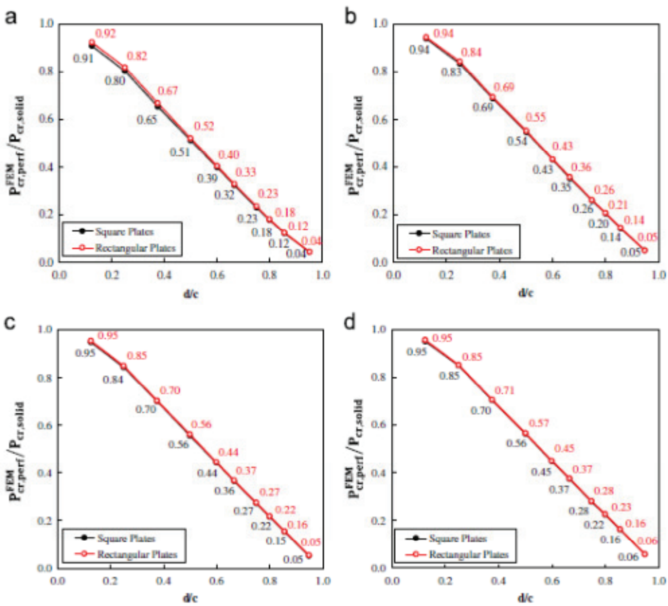

Fig. 14 - Effect of hole diameter-to-spacing ratio on critical elastic buckling load of perforated stiffened elements.(a) t¼b/20; (b) t¼b/40; (c) t¼b/60; and(d) t¼b/80.

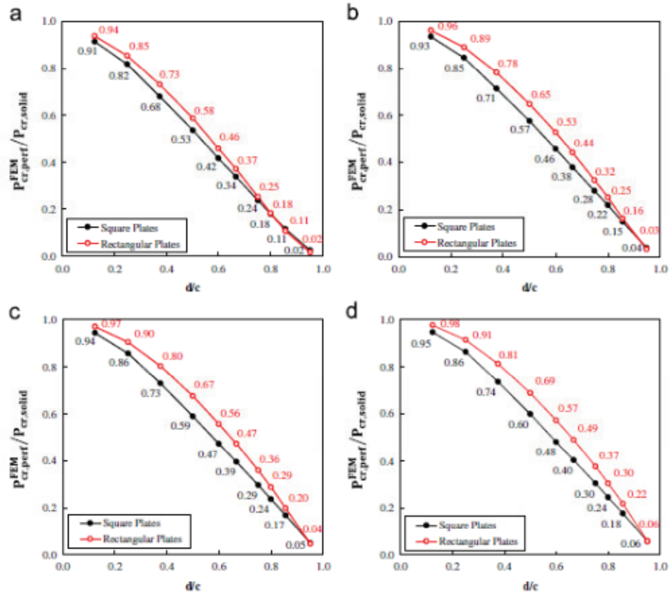

Fig.15 - Effect of hole diameter-to-spacing ratio on critical elastic buckling load of perforated unstiffened elements.(a) t¼b/20; (b) t¼b/40; (c) t¼b/60; and(d) t¼b/80.

- Stiffened square and rectangular elements demonstrated approximately the same critical elastic buckling load reduction for each considered d/c ratio.
- Unstiffened square elements demonstrated up to 30% greater critical elastic buckling load reduction due to the perforations when compared to unstiffened rectangular elements.
- For the most d/c values, the difference in the critical elastic buckling load reduction of the stiffened and unstiffened square elements was within 9%, but it achieved 88% for d/c=0.95 and b/t=20 (Fig. 14 and Fig. 15).
- A series of design formulas for predicting critical elastic buckling stress based on reduction coefficient approach and equivalent thickness approach was developed using multiple nonlinear regression analysis of the FEM results. In the equivalent thickness approach, the critical elastic buckling stress of perforated plates is calculated as follows:

  $$f_{cr} = k\frac{\pi^2 E}{12(1-\nu^2)}\left(\frac{t_{eq}}{b}\right)^2,$$

  the equivalent thickness is determined as follows

  $$t_{eq} = \sqrt{k_p}t,$$

  The author noted that when critical elastic buckling is calculated not in term of stress but in terms of distributed or total loads w_{cr} and P_{cr} , the equivalent thickness shall be determined using the following t_{eq}.

$$w_{cr} = k\frac{\pi^2 E}{12(1-\nu^2)}\frac{t_{eq}^3}{b^2},$$

$$P_{cr} = k\frac{\pi^2 E}{12(1-\nu^2)}\frac{t_{eq}^3}{b},$$

$$t_{eq} = \sqrt[3]{k_p}\,t,$$

<u>The reviewer notes:</u>
These three studies above deal with plates perforated in triangular patterns and don't provide information about quadratic patterns.

Studies about different arrays of holes were performed in Germany by Th. Misiek [12], [13], and K. Kathage [14]. The latter carried out a numerical analysis of perforated trapezoidal sheeting with quadratic arrays of the holes. He determined effective stiffness and deformation behaviour. The buckling coefficients for perforated plates under uniform uniaxial compression-loading and for infinitely long perforated plates under shear loading were derived as a base for the calculation of the effective width of a cross-section.

Th. Misiek [12] investigated the structural behavior of perforated thin-walled components with different hole patterns (Fig. 16) and developed on this basis a calculation method to determine the bearing capacity of fully or partially perforated thin-walled components such as trapezoidal or corrugated profiles.

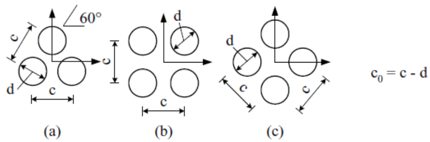

Fig. 16 - Perforation patterns

He normalized effective stiffness as a function of t/c for different perforation patterns, then he determined buckling stress and effective buckling stress which leaded to effective width and to bending moment, shear resistance and web crippling.

Here is a comparison of T. Misiek study, on the right column, with the Eurocode 3 rules on the left column

<u>Plane Elements with intermediate stiffeners EC3-1-3: 5.5.3.3 (4)</u>

<table>
<tr><td colspan="2">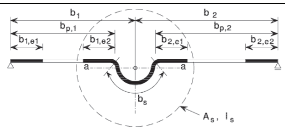
</td></tr>
<tr><th>EUROCODE RULES</th><th>T. MISIEK STUDY</th></tr>
<tr><td>Plate slenderness $\bar{\lambda}_p$ according to EN 1993-1-5

Plane Elements (part 4.4)</td><td>$$\bar{\lambda}_{p,p} = \sqrt{\frac{\frac{c_0}{c}\cdot f_y}{\sigma_{ki,p}}}$$</td></tr>
</table>

$$\bar{\lambda}_p = \sqrt{\frac{f_y}{\sigma_{cr}}} = \frac{\bar{b}/t}{28{,}4\ \varepsilon\ \sqrt{k_\sigma}}$$

$\bar{b} = b_p$

$$\varepsilon = \sqrt{\frac{235}{f_y \quad [\mathrm{N/mm^2}]}}\ .$$

internal compression elements:

$\rho = 1{,}0$ for $\bar{\lambda}_p \leq 0{,}673$

$\rho = \dfrac{\bar{\lambda}_p - 0{,}055\,(3+\psi)}{\bar{\lambda}_p^2} \leq 1{,}0$ for $\bar{\lambda}_p > 0{,}673$, where $(3+\psi) \geq 0$

$$\sigma_{ki,p} = \sigma_{cr,p} = k_\sigma\,(\psi) \cdot k_{11} \cdot \sigma_E$$

$$k_\sigma(\psi = 1) = \left(\frac{m^2}{\bar{\alpha}^2} + q \cdot \frac{\bar{\alpha}^2}{m^2}\right) + p \cdot \varsigma = 2 + 2 \cdot \varsigma$$

$$\varsigma = \frac{K_{12} + 2 \cdot K_{44}}{\sqrt{K_{11} \cdot K_{22}}}$$

(EC3-1-5:A1):

$$\sigma_E = \frac{\pi^2\ E\ t^2}{12\left(1-\nu^2\right)b^2}$$

$$\rho = \frac{b_{eff}}{b} = \frac{c_0}{c} \cdot \left(\frac{1}{\bar{\lambda}_{p,p}} - \frac{0{,}22}{\bar{\lambda}_{p,p}^2}\right) \leq \frac{c_0}{c}\ .$$

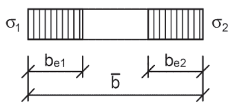

$\psi = 1$: $\quad b_{eff} = \rho\ \bar{b}$

$b_{e1} = 0{,}5\ b_{eff} \qquad b_{e2} = 0{,}5\ b_{eff}$

Flange with intermediate stiffener (5.5.3.4.2)

(2) For one central flange stiffener, the elastic critical buckling stress $\sigma_{cr,s}$ should be obtained from:

$$\sigma_{cr,s} = \frac{4{,}2\,k_w\,E}{A_s}\sqrt{\frac{I_s\ t^3}{4\ b_p^2\ (\ 2\ b_p\ +\ 3\ b_s\ )}}$$

with

$$A_s = t\,(b_{1,e2} + b_{2,e1} + b_s)$$

(3) For two symmetrically placed flange stiffeners, the elastic critical buckling stress $\sigma_{cr,s}$ should be obtained from:

$$\sigma_{cr,s} = \frac{4{,}2\ k_w\ E}{A_s}\sqrt{\frac{I_s\ t^3}{8\ b_1^2\ (\ 3\ b_e\ -\ 4\ b_1\ )}}$$

with:

$$b_e = 2b_{p,1} + b_{p,2} + 2b_s$$

$$b_1 = b_{p,1} + 0{,}5\,b_r$$

with

$$A_s = t\,(b_{1,e2} + b_{2,e1} + b_s)$$

$$\sigma_{cr,s,p} = \sqrt{k_{11} \cdot d_{11}} \cdot \sigma_{cr,s}$$

with

$$A_s = A_{s,p}$$

<table>
<tr><td>K_w is a coefficient that allows for partial rotational restraint of the stiffened flange by the webs or other adjacent elements, see (5) and (6). For the calculation of the effective cross-section in axial compression the value kw = 1,0

(5)
- if $l_b / s_w \geq 2$:
$$k_w = k_{wo}$$
- if $l_b / s_w < 2$:
$$k_w = k_{wo} - (k_{wo} - 1)\left[\frac{2 l_b}{s_w} - \left(\frac{l_b}{s_w}\right)^2\right]$$</td><td colspan="2">$$k_w = \begin{cases} k_{w0} + (k_{w0} - 1) \cdot \left(\left(\frac{l_{b,p}}{s_w}\right)^2 - 2 \cdot \frac{l_{b,p}}{s_w}\right) & \text{für } \frac{l_b}{s_w} < 2 \\ k_{w0} & \frac{l_b}{s_w} \geq 2 \end{cases}$$</td></tr>
<tr><td>for a compression flange with one intermediate stiffener:
$$l_b = 3{,}07 \sqrt[4]{\frac{I_s\ b_p^2\ (2\ b_p + 3\ b_s)}{t^3}}$$
$$k_{wo} = \sqrt{\frac{s_w + 2\ b_d}{s_w + 0{,}5\ b_d}}$$</td><td colspan="2">$$k_{w0} = \sqrt{\frac{\frac{k_{11,1}}{k_{11,2}} \cdot s_w + 2 \cdot b_1}{\frac{k_{11,1}}{k_{11,2}} \cdot s_w + 0{,}5 \cdot b_1}}$$
$$l_b = 3{,}65 \cdot \sqrt[4]{I_r \cdot b_p^3 \cdot \frac{1 + 3 \cdot s_r / b_p}{k_{11,1} \cdot t^3}} = 3{,}65 \cdot \sqrt[4]{\frac{d_{11}}{k_{11,1}} \cdot I_r \cdot b_p^3 \cdot \frac{1 + 3 \cdot s_r / b_p}{t^3}}$$
with
$s_r = 0{,}5 * b_s$
$b_1 = b_0$</td></tr>
<tr><td>for a compression flange with two intermediate stiffeners:
$$l_b = 3{,}65 \sqrt[4]{I_s\ b_1^2\ (3\ b_e - 4\ b_1)\ /\ t^3}$$
$$k_{wo} = \sqrt{\frac{(2\ b_e + s_w)\ (3\ b_e - 4\ b_1)}{b_1\ (4\ b_e - 6\ b_1) + s_w\ (3\ b_e - 4\ b_1)}}$$</td><td colspan="2">$$k_{w0} = \sqrt{\frac{\left(2 \cdot b_1 + \frac{k_{11,1}}{k_{11,2}} \cdot s_w\right) \cdot (3 \cdot b_1 - 4 \cdot b_k)}{b_k \cdot (4 - b_1 - 6 \cdot b_k) + \frac{k_{11,1}}{k_{11,2}} \cdot s_w \cdot (3 \cdot b_1 - 4 \cdot b_k)}}$$
$$l_b = 3{,}65 \cdot \sqrt[4]{I_{r,p} \cdot b_p^3 \cdot \frac{3 \cdot b_1 / b_k - 4}{k_{11,1} \cdot t^3}} = 3{,}65 \cdot \sqrt[4]{\frac{d_{11}}{k_{11,1}} \cdot I_r \cdot b_p^3 \cdot \frac{3 \cdot b_1 / b_k - 4}{t^3}}$$
with
$b_k = b_p + b_r/2$
$b_1 = b_0$
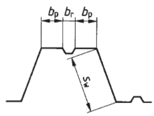
</td></tr>
<tr><td>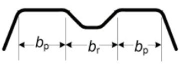
</td><td>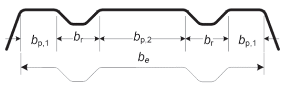
</td><td>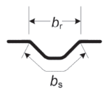
</td></tr>
</table>

Reduction factor χ_d 5.5.3.1 (7):

$\chi_d = 1{,}0$	if $\bar{\lambda}_d \leq 0{,}65$
$\chi_d = 1{,}47 - 0{,}723\bar{\lambda}_d$	if $0{,}65 < \bar{\lambda}_d < 1{,}38$
$\chi_d = \frac{0{,}66}{\bar{\lambda}_d}$	if $\bar{\lambda}_d \geq 1{,}38$

$\bar{\lambda}_d = \sqrt{f_{yb}/\sigma_{cr,s}}$	$\bar{\lambda}_d = \sqrt{f_{yb}/\sigma_{cr,s,p}}$

Webs with up to tow intermediate stiffeners (5.5.3.4.3)

EC3-1-3:5.5.3.4.3 (5):

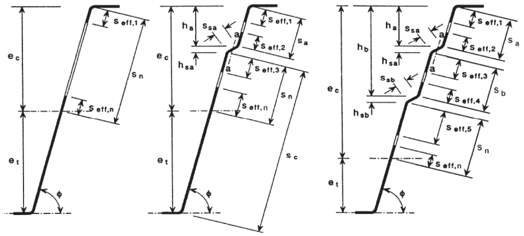

(5)

$$s_{eff,0} = 0{,}76\, t \sqrt{E / (\gamma_{M0}\, \sigma_{com,Ed})}$$

$s_{eff,1} = s_{eff,0}$

$s_{eff,2} = (1 + 0{,}5 h_a / e_c)\, s_{eff,0}$

$s_{eff,3} = [1 + 0{,}5 (h_a + h_{sa}) / e_c]\, s_{eff,0}$

$s_{eff,4} = (1 + 0{,}5 h_b / e_c)\, s_{eff,0}$

$s_{eff,5} = [1 + 0{,}5 (h_b + h_{sb}) / e_c]\, s_{eff,0}$

$s_{eff,n} = 1{,}5 s_{eff,0}$

→ EC3-1-3:5.5.3.4.3 (6)

$$s_{ef1,p} = 0{,}54 \cdot t \cdot \sqrt{\frac{k_{11} \cdot E}{\sigma_1} \cdot (\varsigma + 1)}$$

$$s_{efn,p} = \left(1{,}18 \cdot \sqrt{\frac{4 \cdot \varsigma + 5}{\varsigma + 1}} - 1\right) \cdot s_{ef1,p}$$

$$s_{efi,tp} = s_{efn,tp} + \left(s_{ef1,tp} - s_{efn,tp}\right) \cdot \frac{\sigma_i}{\sigma_1}$$

$$\varsigma = \frac{k_{44} + 0{,}3 \cdot (k_{12} - k_{44})}{k_{11}}$$

triangular holes $\zeta = 1{,}0$

(7) For a single stiffener, or for the stiffener closer to the compression flange in webs with two stiffeners, the elastic critical buckling stress $\sigma_{cr,sa}$ should be determined using:

$$\sigma_{cr,sa} = \frac{1{,}05\, k_f\, E \sqrt{I_s\, t^3\, s_1}}{A_{sa}\, s_2\, (s_1 - s_2)}$$

with

$s_2 = s_1 - s_a - 0{,}5\, s_{sa}$

for a singel stiffener

$s_1 = 0{,}9\, (s_a + s_{sa} + s_c)$

For the stiffener closer to the comression flange, in webs with two stiffeners

$s_1 = s_a + s_{sa} + s_b + 0{,}5 (s_{sb} + s_c)$

with

$$\sigma_{cr,sa,p} = \sqrt{k_{11} \cdot d_{11}} \cdot \sigma_{cr,sa}$$

$$A_{sa} = A_{sa,p}$$

and

$$A_{sb} = A_{sb,p}$$

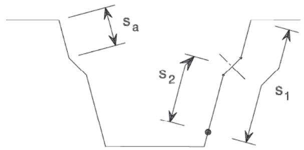

The effective area shoul be obtained from the following:

For a single stiffener, or for the stiffener closer to the compression flange

$A_{sa} = t\,(s_{eff,2} + s_{eff,3} + s_{sa})$

For a second stiffener

$A_{sb} = t\,(s_{eff,4} + s_{eff,5} + s_{sb})$

(9) For a single stiffener, or for the stiffener closer to the compression flange in webs with two stiffeners, the reduced effective area $A_{sa,red}$ should be determinded from:

$$A_{sa,red} = \frac{\chi_d\, A_{sa}}{1-(h_a + 0{,}5h_{sa})/e_c} \quad \text{but } A_{sa,red} \leq A_{sa}$$

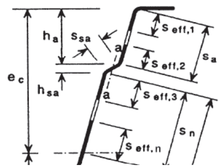

Sheeting with flange stiffeners and web stiffeners: (5.5.3.4.4)

(1) Interaction between the distortional buckling (flexural buckling of the flange stiffeners and the web stiffeners) should be obtained from

$$\sigma_{cr,mod} = \frac{\sigma_{cr,s}}{\sqrt[4]{1+\left[\beta_s \dfrac{\sigma_{cr,s}}{\sigma_{cr,sa}}\right]^4}}$$

with

$\beta_s \;=\; 1 - (h_a + 0{,}5\, h_{ha}) / e_c$ for a profile in bending;

$\beta_s \;=\; 1$ for a profile in axial compression.

$$N_{el,p} = \left(\frac{1}{N_{rel,p}^4} + \frac{\delta^4}{N_{sel,p}^4}\right)^{-\frac{1}{4}}$$

with

$$\delta = \frac{\sigma(h'_a)}{\sigma_1} \cdot \frac{A_{s,p}}{A_{r,p}}$$

$$\frac{N_{rel,p}}{A_{r,p}} = \sigma_{cr,s,p}$$

$$\frac{N_{sel,p}}{A_{s,p}} = \sigma_{cr,sa,p}$$

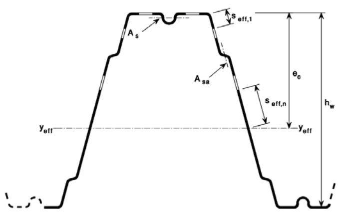

Figure 5.16: Trapezoidal profiled sheeting with flange stiffeners and web stiffeners

Bending Moment (6.1.4)

$M_{\mathrm{c,Rd}} = W_{\mathrm{eff}} f_{\mathrm{yb}} / \gamma_{\mathrm{M0}}$	Fully perforated trapezoidal sheeting $$M_{R,k} = W_{ef} \cdot \frac{c_0}{c} \cdot f_y$$
	Flanges without perforation and partially perforated webs: Moment resistance of the unperforated flange $$M_{R,k} = \frac{I_{ef}}{z_{\max}} \cdot f_y$$ Moment resistance of the web $$M_{R,k} = \frac{I_{ef}}{z_{tp}} \cdot \frac{1}{d_{11}} \cdot \frac{c_0}{c} \cdot f_y$$ with z_{tp}: maximum ordinate of the transition from the unperforated to the perforated section and $$\frac{1}{d_{11}} \cdot \frac{c_0}{c} \leq 1$$
	Flanges fully perforated and partially perforated webs: Moment resistance of the fully perforated flange $$M_{R,k} = \frac{I_{ef}}{z_{\max}} \cdot \frac{1}{d_{11}} \cdot \frac{c_0}{c} \cdot f_y$$ Moment resistance of the web $z \geq z_{tp}$ $$M_{R,k} = \frac{I_{ef}}{z_{tp}} \cdot \frac{1}{d_{11}} \cdot \frac{c_0}{c} \cdot f_y$$ or $$M_{R,k} = \frac{I_{ef}}{z_{tp}} \cdot f_y$$ with $$\frac{1}{d_{11}} \cdot \frac{c_0}{c} \leq 1$$

Shear Force (6.1.5)

(1) Shear resistance $$V_{\mathrm{b,Rd}} = \frac{\frac{h_{\mathrm{w}}}{\sin\phi} t f_{\mathrm{bv}}}{\gamma_{\mathrm{M0}}}$$ Webs without longitudinal stiffeners $$\bar{\lambda}_{\mathrm{w}} = 0{,}346 \frac{s_{\mathrm{w}}}{t} \sqrt{\frac{f_{\mathrm{yb}}}{E}}$$ Webs with longitudinal stiffeners	Shear resistance $$V_{d,p} = \frac{c_0}{c} \cdot \tau_d \cdot s_w \cdot t \cdot \sin\varphi$$ Webs without longitudinal stiffeners $$\lambda_{w,p} = \frac{s_w}{t} \cdot \frac{2{,}31}{\sqrt{k_{\tau,p}}} \cdot \sqrt{\frac{\frac{c_0}{c} \cdot f_y}{E}}$$ with

$$\bar{\lambda}_w = 0{,}346\,\frac{s_d}{t}\sqrt{\frac{5{,}34}{\kappa_\tau}\frac{f_{yb}}{E}} \geq 0{,}346\,\frac{s_p}{t}\sqrt{\frac{f_{yb}}{E}}$$

with

$$k_\tau = 5{,}34 + \frac{2{,}10}{t}\left(\frac{\Sigma I_s}{s_d}\right)^{1/3}$$

$$k_{\tau,p} = \begin{cases} k_{11}\cdot\left(3{,}293 + 2{,}286\cdot\varsigma - 0{,}24\cdot\varsigma^2\right) & \text{für } \varsigma \leq 1 \\ k_{11}\cdot\sqrt{\varsigma}\cdot\left(4{,}757 + \dfrac{0{,}874}{\varsigma^2} - \dfrac{0{,}283}{\varsigma^4}\right) & \text{für } \varsigma > 1 \end{cases}$$

Webs with longitudinal stiffeners

$$\bar{\lambda}_w = 2{,}31\,\frac{s_1}{t}\sqrt{\frac{\frac{c_0}{c}}{\kappa_{\tau,p}}\frac{f_y}{E}}$$

with

$$k_{\tau,p} = \begin{cases} k_{11}\cdot\left(3{,}293 + 2{,}286\cdot\varsigma - 0{,}24\cdot\varsigma^2\right) + \dfrac{2{,}1}{t}\cdot\sqrt[3]{k_{11}^2\cdot d_{11}\cdot\dfrac{I_s}{s_1}} & \text{für } \varsigma \leq 1 \\ k_{11}\cdot\sqrt{\varsigma}\cdot\left(4{,}757 + \dfrac{0{,}874}{\varsigma^2} - \dfrac{0{,}283}{\varsigma^4}\right) + \dfrac{2{,}1}{t}\cdot\sqrt[3]{k_{11}^2\cdot d_{11}\cdot\dfrac{I_s}{s_1}} & \text{für } \varsigma > 1 \end{cases}$$

and

$$\bar{\lambda}_w \geq 2{,}31\,\frac{s_m}{t}\sqrt{\frac{\frac{c_0}{c}}{\kappa_{\tau,p}}\frac{f_{yb}}{E}}$$

with

$$k_{\tau,p} = \begin{cases} k_{11}\cdot\left(3{,}293 + 2{,}286\cdot\varsigma - 0{,}24\cdot\varsigma^2\right) & \text{für } \varsigma \leq 1 \\ k_{11}\cdot\sqrt{\varsigma}\cdot\left(4{,}757 + \dfrac{0{,}874}{\varsigma^2} - \dfrac{0{,}283}{\varsigma^4}\right) & \text{für } \varsigma > 1 \end{cases}$$

Relative web slenderness	Web without stiffening at the support	Web with stiffening at the support [1]
$\bar{\lambda}_w \leq 0{,}83$	$0{,}58\,f_{yb}$	$0{,}58\,f_{yb}$
$0{,}83 < \bar{\lambda}_w < 1{,}40$	$0{,}48 f_{yb}/\bar{\lambda}_w$	$0{,}48 f_{yb}/\bar{\lambda}_w$
$\bar{\lambda}_w \geq 1{,}40$	$0{,}67 f_{yb}/\bar{\lambda}_w^2$	$0{,}48 f_{yb}/\bar{\lambda}_w$

[1] Stiffening at the support, such as cleats, arranged to prevent distortion of the web and designed to resist the support reaction.

	τ_d/β_S für Stege ohne Stützbleche über den Auflagern	τ_d/β_S für Stege mit Stützblechen über den Auflagern
$\lambda_w \leq 2{,}1$ $2{,}1 < \lambda_w \leq 4{,}0$ $4{,}0 < \lambda_w$	0,67 $1{,}4/\lambda_w$ $5{,}6/\lambda_w^2$	0,67 $1{,}4/\lambda_w$ $1{,}4/\lambda_w$

Based on comprehensive numerical and experimental investigations on web crippling (Fig. 17), it

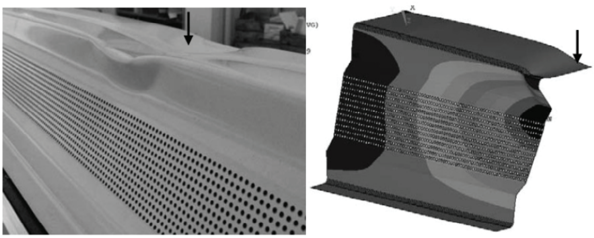

Fig. 17 - Web crippling failure at supports

could be shown for fully and partially perforated trapezoidal profiles, that the influence of the perforation can be expressed with the application according to DIN 18807-1 [15] and DIN 18807-6 [16] of a factor Cp for fully perforated webs.

$$R_{w,Rd,p} = C_p \cdot R_{w,Rd}$$

$$C_p = \sqrt{\frac{c_0}{c}\cdot\frac{k_{\sigma,p}}{4}} = \sqrt{\frac{c_0}{c}\cdot\frac{k_{11} + k_{44} + 0.3\cdot(k_{12} - k_{44})}{2}}$$

And C_{tp} for partially perforated webs to the capacities of the unperforated sheeting according to EN 1993-1-3 and EN 1999-1-4.

$$R_{w,Rd,tp} = C_{tp} \cdot R_{w,Rd}$$

$$C_{tp} = \begin{cases} 1.0 & b_1 > \beta_{tp} \cdot b \\ \frac{\beta_1}{\beta_{tp}} \cdot \frac{s_w}{b_B} + C_{tp}^* \cdot \left(1 - \frac{\beta_1}{\beta_{tp}} \cdot \frac{s_w}{b_B}\right) & \text{for } r \cdot \tan\frac{\phi}{2} < b_1 \le \beta_{tp} \cdot b_B \\ C_p & b_1 \le r \cdot \tan\frac{\phi}{2} \end{cases}$$

with

$$C_{tp}^* = 0.59 + 0.41 \cdot \sqrt{\frac{c_0}{c} \cdot \frac{k_{\sigma,p}}{4}}$$

and

$$\beta_{tp} = 2.57 \cdot \left(0.70 - 0.09 \cdot \sqrt{\frac{r}{t}}\right) \cdot \left(0.57 - 0.37 \cdot \left(\frac{\phi}{90}\right)^2\right)$$

For stiffened webs:

$$R_{w,Rd} = \kappa_s \cdot R_{w,Rd}$$

with

$$\kappa_s = 1{,}0$$

For design purpose, to take into account the scatter of results, the characteristic values should be used with the following equations.

$$C_{tp,k}^* = 0.92 \cdot C_{tp}^*$$

$$\beta_{tp,k} = \beta_{tp} \cdot \frac{1 - C_{tp,k}^*}{1 - C_{tp}^*}$$

A calculation procedure for these factors was described (Fig. 18).

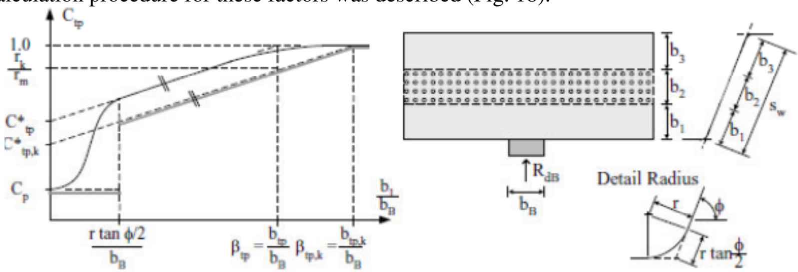

Fig. 18 - C_{tp} in dependence of b1 to b_B and the corresponding dimensions of the sheeting

Numerical investigations with the finite-elements method allow the verification of these theoretically derived calculation procedures. And all theoretical considerations or numerical studies results could be verified by comparison with experimental results from a extensive database as well as specially conducted for this work attempts (Fig. 19).

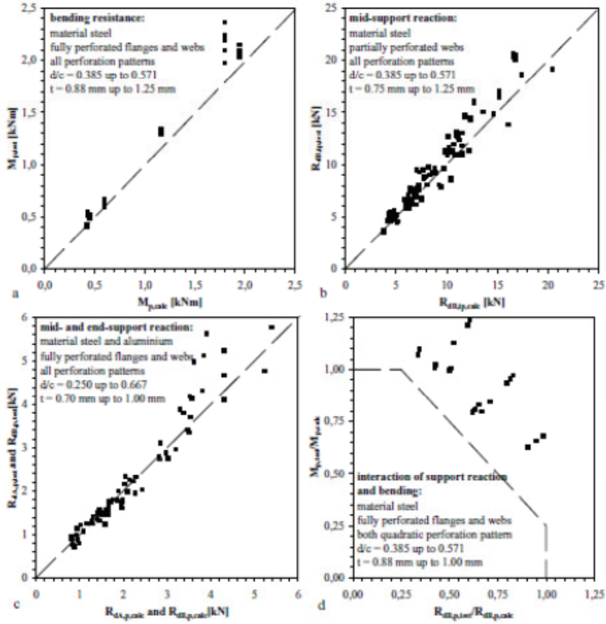

Fig. 19 - Comparison of calculated load-bearing capacities with test results

4. CONCLUSIONS

As we could see in this state of the art the European Standard EN 1993-1-3 dealing with design rules for cold-formed members and sheeting only covers plane walls without holes and plane walls with equilateral triangular perforation pattern. The background information about sheeting with holes only deals with buckling and postbuckling of plates with holes subjected to compression and shear loadings, and doesn't give any data about moment resistance, web crippling resistance and interaction moment-reaction resistance. As far as are perforated sheeting with triangular and quadratic pattern perforations are concerned, some useful information found in the literature was given by Th. Misiek investigations on the effective width and web crippling resistance. However, this investigation was based on numerical computer analysis that doesn't lead directly to the analytical formulation.

Therefore a series of tests and analytical investigations should be performed in order to acquire data on resistance and stiffness of the steel decks with holes and in order to confirm and complete design rules determined by the unique investigation about triangular and quadratic pattern perforations, existing in the background.

REFERENCES

[1] TH. MISIEK, H. SAAL, K. KATHAGE "TRAGFAHIGKEIT PERFORIERTER DUNNWANDIGER BAUTEILE" STAHLBAU 78, 2009

[2] YU, W.W. “COLD-FORMED STEEL STRUCTURES” *STRUCTURAL ENGINEERING HANDBOOK,* ED. CHEN WAI-FAH BOCA RATON: CRC PRESS LLC, 1999

[3] M. AZHARI, A. R. SHAHIDI, M. M. SAADATPOUR "LOCAL AND POST LOCAL BUCKLING OF STEPPED AND PERFORATED THIN PLATES" 2005

[4] C.J. BROWN, A.L. YETTRAM, M. BURNETT, STABILITY OF PLATES WITH RECTANGULAR HOLES, J. STRUCT. ENG. 1131111–1116, 1987

[5] F-Y. CHOW, R. NARAYANAN "BUCKLING OF PLATES CONTAINING OPENINGS" 1984

[6] R. NARAYANAN, F-Y. CHOW "STRENGTH OF BIAXIALLY COMPRESSED PERFORATED PLATES" 1984

[7] PAIK J.K. "ULTIMATE STRENGTH OF PERFORATED STEEL PLATES UNDER EDGE SHEAR LOADING", THIN-WALLED STRUCTURES 45, 2007

[8] SHANMUGAM N.E "DESIGN FORMULA FOR AXIALLY COMPRESSED ERFORATED PLATES" THIN-WALLED STRUCTURES 34, 1999

[9] SEUNG CHUL BAIK*, HEUNG NAM HAN*, SANG HEON LEE*, KYU HWAN OH * and DONG NYUNG LEE, "PLASTIC BEHAVIOUR OF PERFORATED SHEETS UNDER BIAXIAL STRESS STATE", LNT. J. MECH. SCI. VOL. 39, NO. 7, PP. 781- 793. 1997

[10] Y-C LEE, F-K. CHEN; "YIELD CRITERION FOR A PERFORATED SHEET WITH A UNIFORM TRIANGULAR PATTERN OF ROUND HOLES AND A LOW LIGAMENT RATIO", DEPARTMENT OF MECHANICAL ENGINEERING, NATIONAL TAIWAN UNIVERSITY, 1 ROOSEVELT ROAD, SECT. 4, TAIPEI 10764, TAIWAN, ROC, RECEIVED 28 FEBRUARY 1999

[11] V.V DEGTYAREV, N.V DEGTYAREVA "ELASTIC STABILITY OF UNIFORMLY COMPRESSED PLATES PERFORATED IN TRIANGULAR PATTERNS", THIN-WALLED STRUCTURES 52 (2012) 165–173

[12] T.MISIEK, 2008, TRAGVERHALTEN DÜNNWANDIGER BAUTEILE AUS PERFORIERTEN BLECHEN (DESCRIBED BY ZBP) PHD IN GERMAN, UNIVERSITÄT FRIDERICIANA ZU KARLSRUHE, 2008

[13] T.MISIEK, H. SAAL "LOAD-BEARING CAPACITY OF PERFORATED TRAPEZOIDAL SHEETING" STABILITY AND DUCTILITY OF STEEL STRUCTURES, RIO DE JANEIRO, BRAZIL, SEPTEMBER 8-10, 2010

[14] K. KATHAGE, Th. MISIEK, H. SAAL "STIFFNESS AND CRITICAL BUCKLING LOAD OF PERFORATED SHEETING" THIN-WALLED STRUCTURES 44, 2006

[15] DIN 18807-1:1987-06: TRAPEZPROFILE IM HOCHBAU; STAHLTRAPEZPROFILE; ALLGEMEINE ANFORDERUNGEN, ERMITTLUNG DER RAGFÄHIGKEITSWERTE DURCH BERECHNUNG.

[16] DIN 18807-6:1995-09: TRAPEZPROFILE IM HOCHBAU; ALUMINIUM-TRAPEZPROFILE UND IHRE VERBINDUNGEN; ERMITTLUNG DER TRAGFÄHIGKEITSWERTE DURCH BERECHNUNG

GRISPE

Guidelines and **R**ecommendations for **I**ntegrating **S**pecific **P**rofiled steel sheets in the **E**urocodes (**GRISPE**)

WP4 Doc 1 Version 01

Background document

Working Package 4

Deliverable D 4.1

Guidelines and Recommandations for Integrating Specific Profiled Steels sheets in the Eurocodes (GRISPE)

Project co-funded under the Research Fund for Coal and Steel
Grant agreement No RFCS-CT-2013-00018
Proposal No RFS-PR-12027

Author(s)
M. BLANC, BACACIER
T. RENAUX, Société Bretonne de Profilage – Groupe JORIS IDE

Drafting history	
Draft Version 1 (part 1)	*24th October 2013*
Draft Version 1 (part 2)	*31st October 2013*
Final Version	*30th November 2013*

Dissemination Level		
PU	*Public*	
PP	*Restricted to the Commission Services, the Coal and Steel Technical Groups and the European Committee for Standardisation (CEN)*	
RE	*Restricted to a group specified by the Beneficiaries*	
CO	*Confidential, only for Beneficiaries (including the Commission services)*	***X***

Verification and Approval
Coordinator
WP4 Leader
Other Beneficiaries

Deliverable	
D 4.1 Background document : synthesis of the state of art	***Due date : 30th Nov. 13*** ***Completion date:30th Nov. 13***

Summary

1. Context of WP 4 4
1.1. Actual European standards developed for steel sheets 4
1.2. Actual methods used for designing 6
1.2.1. Designing by tests 6
1.2.2. Designing by calculation [4] [5] 8
1.3. Introducing the second part of the synthesis of state of art 12
2. Critical description of reference [9] 13
2.1.1. Design and background 13
2.1.2. Effects of loading 14
2.1.3. Resistance of the cladding cassette [4] 14
2.1.4. Resistance of the screws at Ultimate Limit States 16
2.2. Analysis of the method showed 17
2.3. Interest and conclusion about the method for WP4 18
3. Conclusion and problematic of cladding planks with hidden longitudinal joints 18
References 19

1. Context of WP 4

In the story of steel building envelope, claddings planks and cassettes were developed for esthetical applications. Unlike the corrugated steel sheets for “traditional” cladding, consideration of aesthetics has taken over the mechanical aspect.
Indeed, research of performance compared to wind load resistance has been replaced by the research of hidden fixings solutions as below:

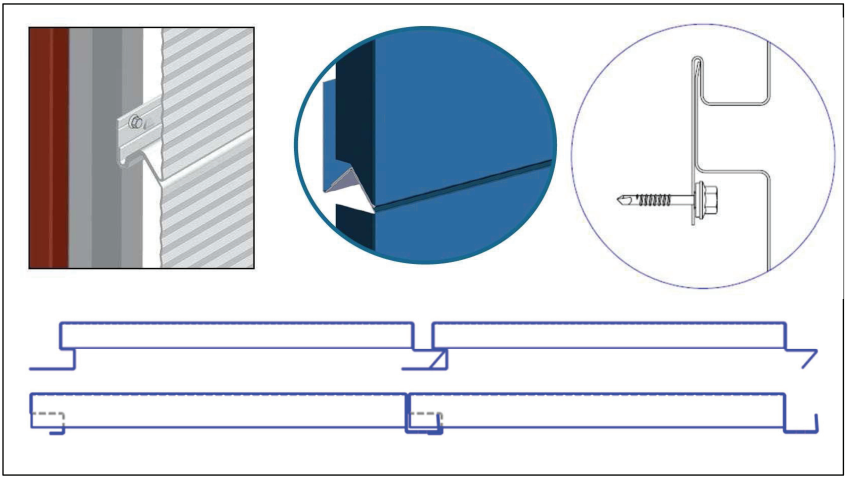

Figure 1: Examples of hidden fixing (non-limiting)

1.1. Actual European standards developed for steel sheets

Design of “classic” profiles for cladding uses two types of methods:

- By calculation
- And/or by tests

In Europe, before the arrival of the Eurocodes, the choice of one or two methods operated at national level. While in Germany the standards authorized the use of the calculations [1] and the experimental [2], the France retains only the method by testing [3].
The introduction of the Eurocodes provides a common method of design that allows the use of tests and/or analytical formulas [4] [5], but claddings planks are not covered by the scope (Figure 2 and Figure 3).

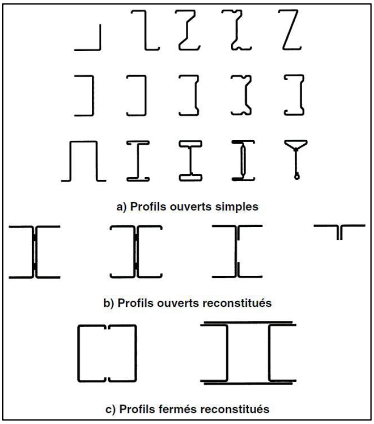

Figure 2: Common geometries of steel members

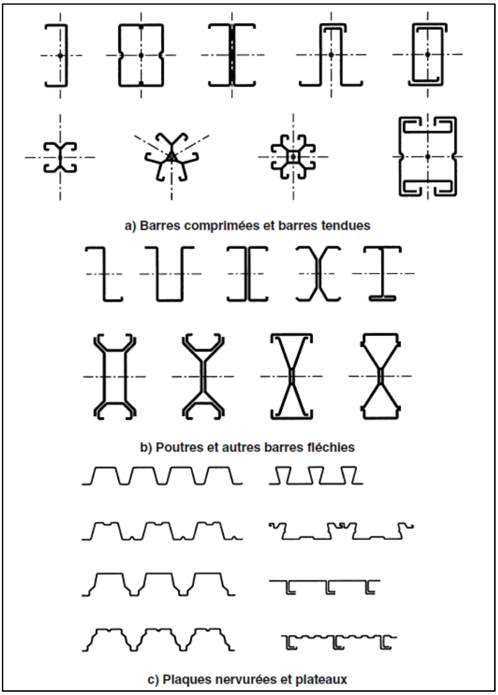

Figure 3: Examples of corrugated steel sheets and profiles

1.2. Actual methods used for designing

To overcome this situation, different strategies have been implemented.
At European level, cladding planks and cassettes can be designed across a European Technical Approval according the ETAG 34 part 1 and 2 [6] [7]. The wind load behaviour is determined by tests like method chosen in France [8] or across a French Technical Assessment (AT/DTA). But although these methods are loyal to the real assembly with a specific distance between supports, they don't allow interpolation or extrapolation to other spans. Moreover, this kind of test present a high cost and it's not possible to view and analyse the behaviour of the hidden joint on support and in span for cladding plank with hidden fixing.
For cladding cassettes, some manufacturers try with success to consider certain parts of Eurocode [9] but in situation of hidden fixings, this method is not applicable.

1.2.1. Designing by tests

Actual experimental method in France [3] adapted to cladding planks and cassettes helps to have accurate information about physical phenomena.
Apply and determine resistance under wind pressure drive to situation below (Figure 4 c)):

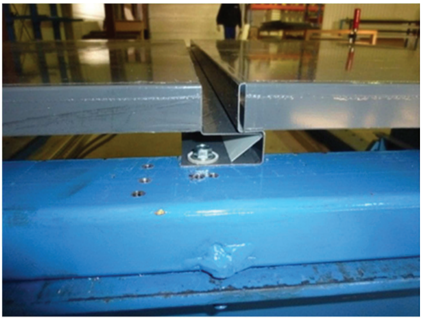

a) Before load application

b) During load application

c) End of the test

Figure 4: Wind pressure test with linear loads

Under wind depression loads, the behaviour and rupture is function of the technology of the hidden joint. In the situation of Figure 5, no rupture is found but in fact a progressive dislocation. In the situation of Figure 6, the dislocation is brutal.

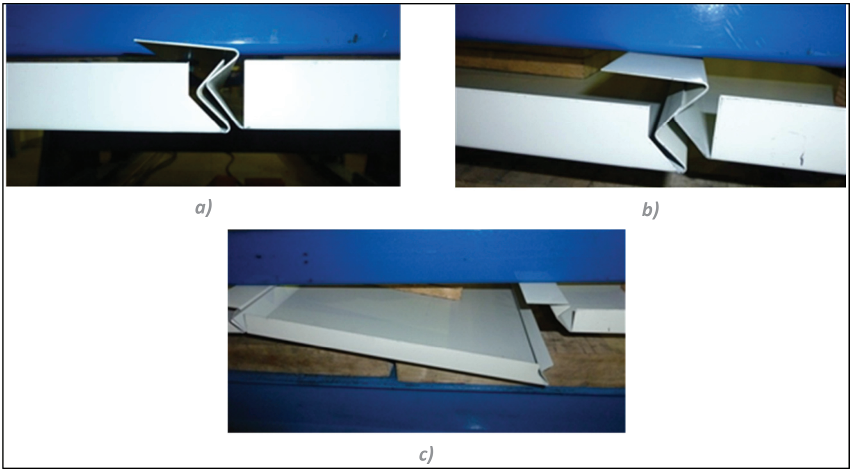

Figure 5: Cladding planks dislocation during wind suction tests

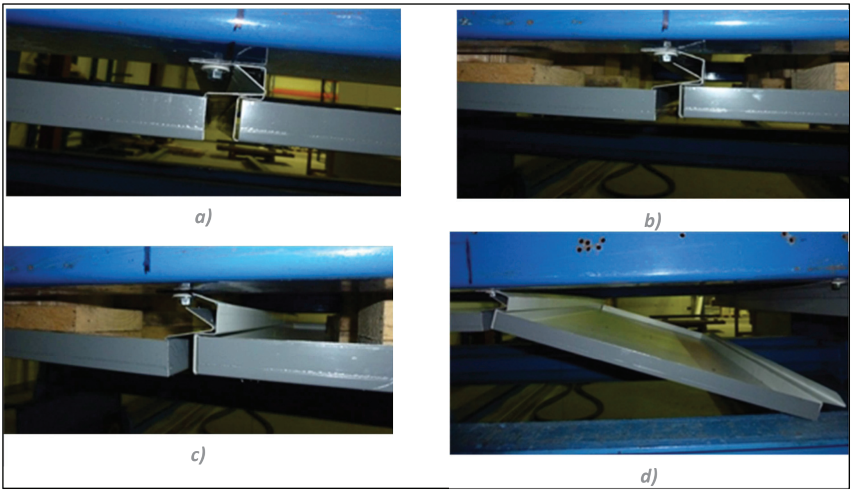

Figure 6: Cladding cassettes dislocation during wind suction tests

1.2.2. Designing by calculation [4] [5]

The closest form of section, for interlocking planks and cassettes, for which a design method is given in Eurocode EN 1993-1-3, is liner tray. In bending, this method should give good results.

The principle of this method is to consider that the wide flange (without stiffeners in our case) is not fully effective in bending, whether it is tensed or compressed. The section is then calculated as a beam considering this effective flange instead of the full wide one. The estimation of this effective part of the wide flange depends on the stress:

- In compression: both shear lag and plate buckling effects according to EN 1993-1-5 must be considered. These effects are evaluated with the wide flange simplified to a plate without any stiffeners.
- In tension: the possible flange curling is taken into account, considering the cross inertia of the flange due to the stiffeners. In our case, the wide flange is a plate. So we should determine the effective part of this only using shear lag effect according to EN 1993-1-5.

1.2.2.1. Behaviour of the wide flange

Shear lag effect

In our case, the effective width of the wide flange $b_{u,eff}$ for shear lag is determined from:

$$b_{u,eff} = \beta \cdot b_0$$

where:

- β: effective[s] factor of the flange;
- b_0: reference width of the flange.

In our case, it is to say for an internal flange, and the gross overall width b_u:

$$b_0 = \frac{b_u}{2}$$

The effective factor β for shear lag depends on the location of the studied cross section. Its determination relies on the slenderness of the flange which is linked to the effective length of the span. The values of effective lengths for different configurations of span are given below:

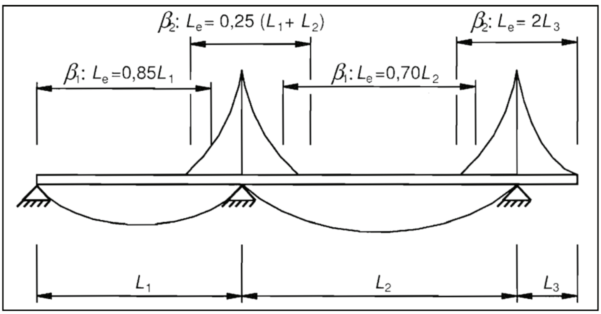

Figure 7: Effectives lengths for shear lag

As the wide flange is a plate without stiffeners, its slenderness κ is:

$$\kappa = \frac{b_0}{L_e}$$

The effective factor β is given in the table below:

κ	Verification	β – value
$\kappa \leq 0{,}02$		$\beta = 1{,}0$
$0{,}02 < \kappa \leq 0{,}70$	sagging bending	$\beta = \beta_1 = \dfrac{1}{1 + 6{,}4\,\kappa^2}$
	hogging bending	$\beta = \beta_2 = \dfrac{1}{1 + 6{,}0\left(\kappa - \dfrac{1}{2500\,\kappa}\right) + 1{,}6\,\kappa^2}$
$> 0{,}70$	sagging bending	$\beta = \beta_1 = \dfrac{1}{5{,}9\,\kappa}$
	hogging bending	$\beta = \beta_2 = \dfrac{1}{8{,}6\,\kappa}$
all κ	end support	$\beta_0 = (0{,}55 + 0{,}025 / \kappa)\,\beta_1$, but $\beta_0 < \beta_1$
all κ	Cantilever	$\beta = \beta_2$ at support and at the end

Figure 8: Values of effective factor β

This effect is to be considered for the wide flange whether it is in tension or in compression

Plate buckling effect on the wide flange

The effective area of the wide flange for the effects of plate buckling $A_{c,eff}$ is given below:

$$A_{c,eff} = \rho \cdot A_c$$

where:

- ρ: effective^{p} factor of the flange;
- A_c: area of the gross cross-sectional area of the flange (i.e. $b_u \times t$).

As for shear lag, the effective^{p} factor ρ depends on the slenderness $\bar{\lambda}_p$ which is:

$$\bar{\lambda}_p = \sqrt{\frac{f_y}{\sigma_{cr}}} = \frac{b_u/t}{28{,}4 \cdot \varepsilon \cdot \sqrt{k_\sigma}}$$

In our case, the wide flange is an internal element fully compressed with a constant stress, i.e. the stress ratio $\psi = 1$ and the corresponding buckling factor is:

$$k_\sigma = 4{,}0$$

In the formula above

$$\varepsilon = \sqrt{\frac{235}{f_y}}$$

f_y is the basic yield strength (N/mm^2)

Stress distribution (compression positive)	Effective[p] width b_{eff}
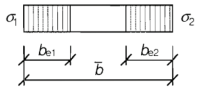	$\underline{\psi = 1}$: $b_{eff} = \rho\ \bar{b}$ $b_{e1} = 0{,}5\ b_{eff}$ $b_{e2} = 0{,}5\ b_{eff}$

Figure 9: Effectives parts of the wide flange

Then, each effective part of the flange, b_{e1} and b_{e2} given above, is associated to the closest web.

1.2.2.2. Buckling effect on the web

As for the wide flange, the effective area of the web $A_{c,eff}$ is given by:

$$A_{c,eff} = \rho \cdot A_c$$

The difference is that the stress ratio ψ is different because the web is part tensed and part compressed.

Stress distribution (compression positive)	Effective[p] width b_{eff}
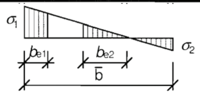	$b_{eff} = \rho\ b_c = \rho\ \bar{b}\ /\ (1\text{-}\psi)$ $b_{e1} = 0{,}4\ b_{eff}$ $b_{e2} = 0{,}6\ b_{eff}$

$\psi = \sigma_2/\sigma_1$	1	$1 > \psi > 0$	0	$0 > \psi > -1$	-1	AC1 $-1 > \psi \geq -3$ AC1
Buckling factor k_σ	4,0	$8{,}2\ /\ (1{,}05 + \psi)$	7,81	$7{,}81 - 6{,}29\psi + 9{,}78\psi^2$	23,9	$5{,}98\ (1 - \psi)^2$

Figure 10: Effectives parts of the web

As we can see above, the buckling factor k_σ depends on this stress ratio ψ and so does the slenderness $\bar{\lambda}_p$, i.e. they depend on the position of the centroid of the section.

1.2.2.3. Performances of the section

The moment resistance is determined using a step-by-step procedure. This procedure depends on the stress in the wide flange.

Wide flange in compression

Step 1: Determine the position of the centroid of the section, considering fully effective web and small flange, and the effective part of the wide flange (considering both shear lag and buckling effects)

Step 2: Find the centroid of the effective cross section, considering the effective part of the web calculated with the stress ration ψ deducted from the first centroid, and deduct the moment resistance $M_{c,Rd}$:

$$M_{c,Rd} = 0{,}8 \cdot W_{eff,\min} \cdot \frac{f_{yb}}{\gamma_{M0}}$$

where:

$$W_{eff,\min} = \frac{I_{y,eff}}{\max(z_c; z_t)}$$

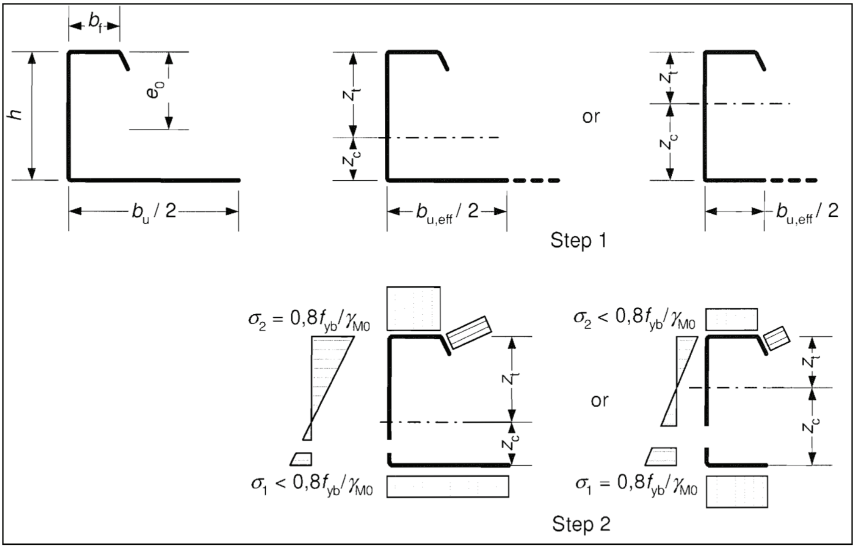

Figure 11: Calculation method for wide flange in compression

Wide flange in tension

Step 1: Determine the position of the centroid of the section, considering a fully effective web and the effective part of the wide flange (considering only shear lag effect)

Step 2: Determine the position of the centroid of the section considering the effective part of the web calculated with the stress ration ψ deducted from the first centroid and the effective part of the wide flange

Step 3: Find the centroid of the effective cross section considering the effective part of the web, of the wide flange and of the small flange, and deduct the moment resistance $M_{c,Rd}$:

$$M_{c,Rd} = 0,8 \cdot W_{eff,\min} \cdot \frac{f_{yb}}{\gamma_{M0}}$$

where:

$$W_{eff,\min} = \frac{I_{y,eff}}{\max(z_c; z_t)}$$

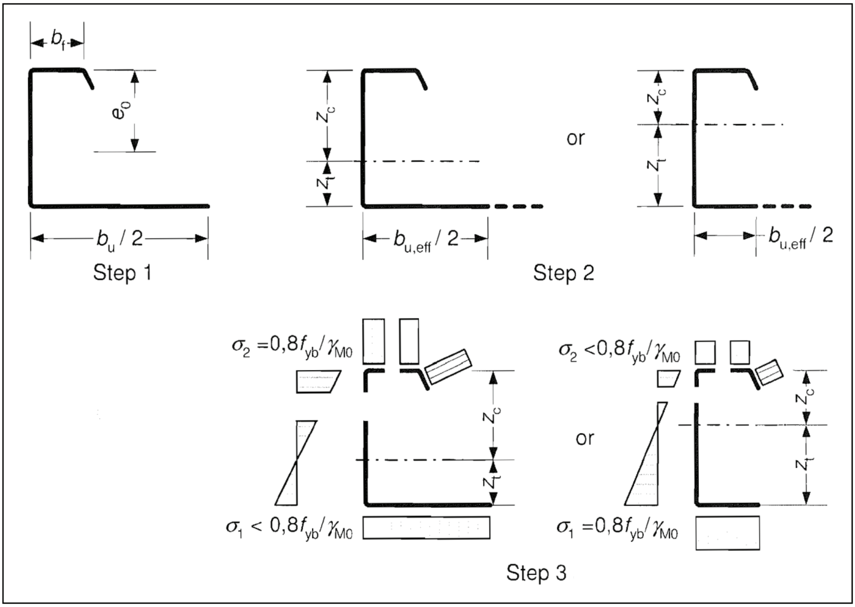

Figure 12: Calculation method for wide flange in tension

1.3. Introducing the second part of the synthesis of state of art

The main difficulty of WP 4 lies in determining suitable test campaigns to identify all conditions and characteristics governing dislocation phenomena that drive the behaviour under depression load of hidden fixed cladding planks and cassettes.
This also means that suitable measures devices must be implemented.
The establishment of analytical formulas characteristics of dislocation phenomena may appeal to parts of Eurocode 3 Part 1-3, paragraph 5 and 10.1 in particular, but also standard prefiguring Eurocodes [1] [10].

2. Critical description of reference [9]

Part of this document deals with the design of a cladding cassette that appeal to the classical theory of plates and certain formulas of EN 1993-1-3 (and correctly to EN 1993-1-5), similar to example below:

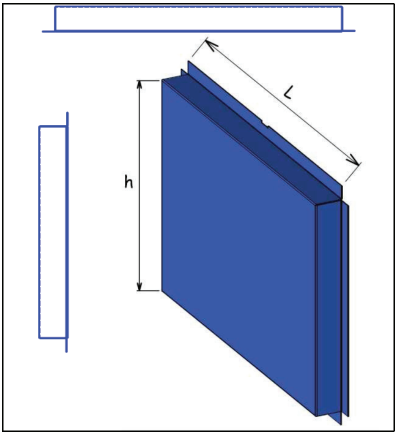

Figure 13: Cladding cassette similar the one studied

2.1.1. Design and background

The design of the cladding cassette needs especially to check the material thickness and the height.
Due to the type of product and its implementation, the cladding cassette is a rectangular simply supported thin plate with rotational springs at all four edges (Fig. 8).

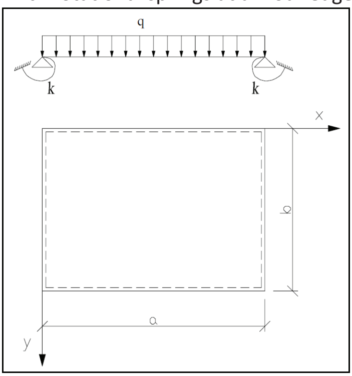

Figure 14: Mechanical model

2.1.2. Effects of loading

The first step to determine the final deflection is to consider a Navier's solution for deflection at any point of the plate:

$$v_q(x,y) = \frac{16 \cdot q}{D \cdot \pi^6} \cdot \sum_{m=1}^{\infty} \sum_{n=1}^{\infty} \frac{\sin \frac{m \cdot \pi \cdot x}{a} \cdot \sin \frac{n \cdot \pi \cdot y}{b}}{m \cdot n \cdot \left[\left(\frac{m}{a}\right)^2 + \left(\frac{n}{b}\right)^2\right]}$$

With q is the uniform applied distributed load, D the bending stiffness, E the Young's modulus, t the cassette thickness and ν the Poisson's ratio:

$$D = \frac{E \cdot t^3}{12 \cdot (1 - \nu^2)}$$

The rotational stiffness of edges is taken into account across a coefficient from beam theory:

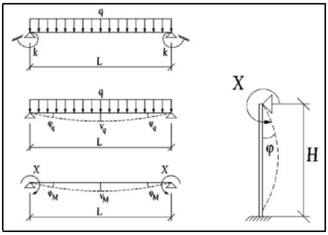

Figure 15: Models used for beam theory

And the maximum deflection to the centre of the plate is determined by:

$$v_m = v_m \cdot \left[1 - \frac{4}{5 \cdot \left(\frac{H}{2 \cdot L} + 1\right)}\right]$$

In addition, maximum stresses at mid-point of the plate are determined:

$$\sigma_x = \frac{6}{t^3} \cdot M_x$$

$$\sigma_y = \frac{6}{t^3} \cdot M_y$$

2.1.3. Resistance of the cladding cassette [4]

Resistance of the cladding cassette is determined considering the edge as showed below:

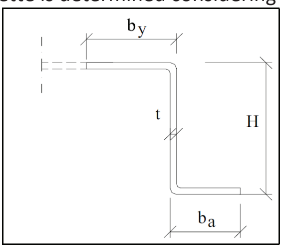

Figure 16: Edge of the cladding cassette

Under wind pressure, the top flange b_y is compressed and under wind suction is b_a.

To determine the effective part of b_a and b_y of this simulated simple supported beam, the outstanding element buckling value k_σ and the gross cross section is used with assume $k_\sigma = 0{,}43$:

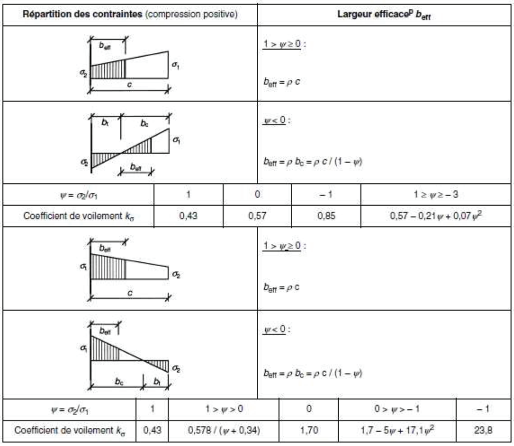

Répartition des contraintes (compression positive)	Largeur efficace[p] b_{eff}
	$1 > \psi \geq 0$: $b_{eff} = \rho\, c$
	$\psi < 0$: $b_{eff} = \rho\, b_c = \rho\, c\,/\,(1-\psi)$

$\psi = \sigma_2/\sigma_1$	1	0	−1	$1 \geq \psi \geq -3$
Coefficient de voilement k_σ	0,43	0,57	0,85	$0{,}57 - 0{,}21\psi + 0{,}07\psi^2$

Répartition des contraintes (compression positive)	Largeur efficace[p] b_{eff}
	$1 > \psi \geq 0$: $b_{eff} = \rho\, c$
	$\psi < 0$: $b_{eff} = \rho\, b_c = \rho\, c\,/\,(1-\psi)$

$\psi = \sigma_2/\sigma_1$	1	$1 > \psi > 0$	0	$0 > \psi > -1$	−1
Coefficient de voilement k_σ	0,43	$0{,}578\,/\,(\psi + 0{,}34)$	1,70	$1{,}7 - 5\psi + 17{,}1\psi^2$	23,8

Figure 17: Buckling coefficient defined in EN 1993–1–3

The effective widths b_{eff} are the minimum between effective b_a and effective by; and the new cross section presents both flanges fully effective:

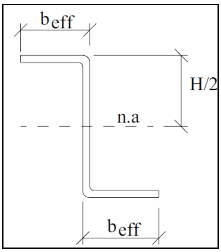

Figure 18: Section with two b_{eff} wide flanges

To determine the effective part of b_a and by, the reduction factor ρ, from ENV 1993-1-3, is used as following:

If $\quad \bar{\lambda}_p \leq 0.673$: $\quad \rho = 1.0$

If $\quad \bar{\lambda}_p > 0.673$: $\quad \rho = (1.0 - \dfrac{0.22}{\bar{\lambda}_p})/\bar{\lambda}_p$, where:

$$\bar{\lambda}_p = \sqrt{\frac{f_y}{\sigma_{cr}}} \equiv \frac{b_p}{t}\sqrt{\frac{12(1-v^2)f_y}{\pi^2 E k_\sigma}}$$

, where: b_p is the nominal width of the plate element under consideration and f_y is the yield stress (or, more precisely, 0.2% proof strength) for the copper sheet.

Figure 19: Reduction factor ρ

The effective parts of the web are calculated with $k_\sigma = 4$ like paragraph 1.2.2.2 above.
The final effective section of the cassette edge is yet represented following:

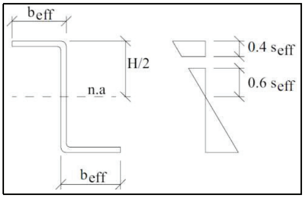

Figure 20: Effective section

The last step consists to determine the effective bending modulus W_{eff} and consequently the bending resistant moment:

$$M_{c,Rd} \leq W_{eff} \cdot \frac{f_y}{\gamma_{M1}}$$

2.1.4. Resistance of the screws at Ultimate Limit States

This design is made following the recommendations of ENV 1993-1-3. Dimensional criteria must be satisfied:

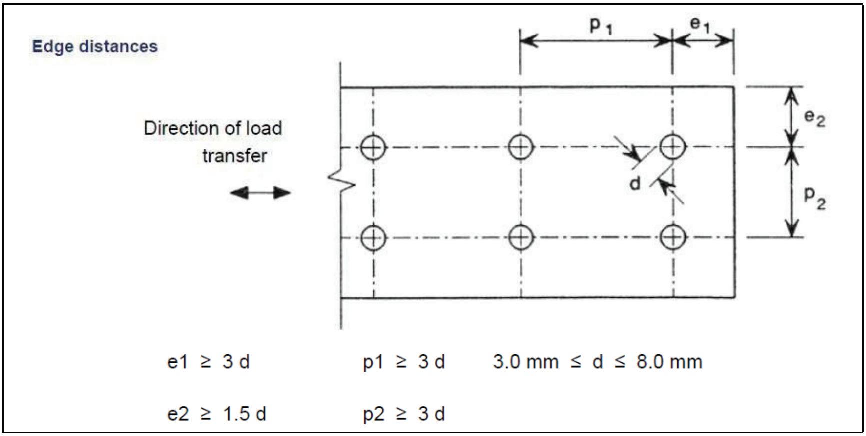

Figure 21: Edge and screw distances

Three kind of verification are established:

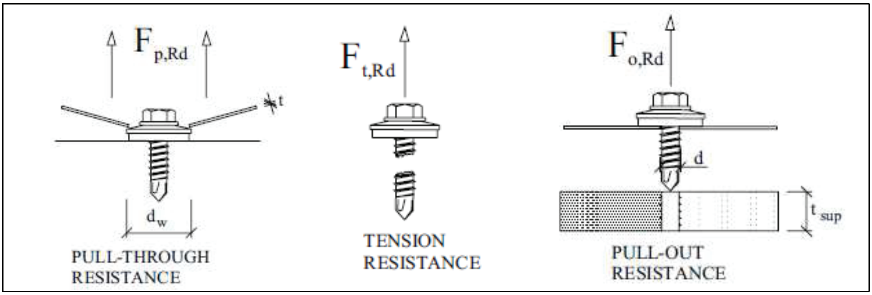

Figure 22: Type of fracture for screw

Using the following formulas:
For pull-through resistance:

$$F_{p,Rd} = 0{,}5 \cdot d_w \cdot t \cdot \frac{f_u}{\gamma_{M2}}$$

For pull-out resistance:

$$F_{o,Rd} = 0{,}65 \cdot d \cdot t_{\text{sup}} \cdot \frac{f_{u,\text{sup}}}{\gamma_{M2}}$$

Tension resistance, $F_{t,Rd}$ is given by the screw manufacturer (technical data by testing). With two conditions:

- $F_{t,Rd} \geq F_{p,Rd}$
- $F_{t,Rd} \geq F_{o,Rd}$

2.2. Analysis of the method showed

Method used to determine loading effects is limited to cassette on 4 simply supports, and this type of configuration not include cassettes on 2 simply supports and 2 others free.
Using Navier's solution is correct for plate on 4 supports. In this case, the deflection at the centre is:

$$v_q = \frac{5 \cdot q \cdot a^2 \cdot b^2}{384 \cdot D} \cdot f(\rho)$$

With:

$$\rho = a/b$$

The consequence of different boundary conditions could be appreciated using various models, for 2 simply supports and 2 free edges; Levy's model is one solution. In Reference [11] for square plate of a dimension, the author give for 4 simply supports a maximum displacement to the plate centre of (chapter II – paragraph 7):

$$v_q = 0{,}318 \cdot \frac{15 \cdot q \cdot a^4}{4 \cdot E \cdot I \cdot \pi^5}$$

Using Navier's solution, while Levy's solution gives for 2 simply supports combined with 2 free edges (chapter V – paragraph 15):

$$v_q = 0{,}994 \cdot \frac{15 \cdot q \cdot a^4}{4 \cdot E \cdot I \cdot \pi^5}$$

In addition, the method described here for calculating deflection not takes account of edges behaviour (and edges effective inertia). It could be appear secure but the obtained result is a deflection between the centre of the plate and these edges.

Concerning the determination of the resistance of the cassette, the references of the formulas aren't updated:

- Buckling coefficient k_σ into EN 1993-1-5,
- Reduction factor ρ into EN 1993-1-5,
- Relation to determine $\bar{\lambda}_p$ incorrect,
- New criteria for pull-out resistance for screw (depending of the thread).

2.3. Interest and conclusion about the method for WP4

The method is simple and use general knowledge of plate theory combined to Eurocode formulas.
Boundaries conditions must be taken into account in order to choose the correct model for the deflection using for example Levy's model or more recent solution.
Eurocodes reference formulas must be updated.
This method, after updating, should be a good estimation for behaviour of cladding cassette but not for cladding planks due to the specificity of the hidden longitudinal joint.

3. Conclusion and problematic of cladding planks with hidden longitudinal joints

The method described in paragraphs 1.2.2 and 2.1.3, after updating, should be a good estimation for behaviour of cladding cassette but not for cladding planks due to the specificity of the hidden longitudinal joint.
As we showed in paragraph 1.2.1, its design under wind suction is based on test and the main difficulty for WP4 will be to determine the behaviour of the longitudinal hidden joint between two planks (cf. Figure 1).

References

[1] DIN 18807-1, Trapezoidal sheeting in building; trapezoidal steel sheeting: general requirements and determination of loadbearing capacity by calculation

[2] DIN 18807-2, Trapezoidal sheeting in building; trapezoidal steel sheeting: determination of loadbearing capacity by testing.

[3] NF P 34-503, Profiled sheeting made of coated or non-coated steel sheet and panels – Bending tests under linear loads and/or under concentrated loads.

[4] EN 1993-1-3, Eurocode 3 – Design of steel structures – Part. 1-3: General rules – Supplementary rules for cold-formed members and sheeting.

[5] EN 1993-1-5, Design of steel structures – Part 1-5: Plated structural elements.

[6] ETAG 034, Guideline for European Technical Approval of kits for external wall claddings, Part I: Ventilated cladding kits comprising cladding components and associated fixings.

[7] ETAG 034, Guideline for European Technical Approval of kits for external wall claddings, Part II: Cladding kits comprising cladding components, associated fixings, subframe and possible insulation layer.

[8] Book CSTB 3517, Methods for testing resistance to wind load on cladding systems, claddings.

[9] LUVATA, Nordic systems copper – Facade, roof and rainwater structures.

[10] Book CSTB 1564, DTU P22-703, Design rules constructions with thin wall elements – Justification by designing the safety of buildings.

[11] E. ESTANAVE: Contribution to the study of elastic equilibrium of rectangular thin plate, Scientific Annals of E.N.S. 3th serial, tome 17 (1900) pp. 295-358.

6.
PREZENTACJE
OMAWIANE PODCZAS SEMINARIUM
W KRAKOWIE

w tym:

6.1. **Wprowadzenie do projektu „Grispe Plus”,**

6.2. **Steel decks with embossments/indentations and/or outwards stiffener**
(autor: *Anna Palisson*),

6.3. **Corrugated sheeting**
(autor: *Thibault Renaux*),

6.4. **Curved profiles**
(autorzy: *Irene Puncello, Silvia Caprili, Walter Salvatore*),

6.5. **Assembled profiles**
(autor: *Thibault Renaux*),

6.6. **Grispe Workshop – Interactive section**
(autor: *David Izabel*),

6.7. **Grispe Workshop – Proposals for the inclusion of 9 calculation methods into EN1993-1-3**
(autor: *David Izabel*).

GRISPE PLUS

VALORISATION OF KNOWLEDGE
FOR SPECIFIC PROFILED STEEL SHEETS

WORKSHOP, CRACOW UNIVERSITY OF TECHNOLOGY
WARSZAWSKA 24 - CRACOW
Thursday, 14th June 2018 from 9.00 am to 4.15 pm

DISCOVER EASY TO USE CALCULATION METHODS FOR 7 KEY FAMILIES OF STEEL PROFILES!

- steel decks with embossments/indentations and/or outwards stiffener
- liner trays
- assembled profiles
- corrugated sheeting
- curved profiles
- perforated and holed profiles
- interlocking planks

The project has received financial support from the European Community (RFCS programme) under grant agreement No 754092

GRISPE PLUS

VALORISATION OF KNOWLEDGE FOR SPECIFIC PROFILED STEEL SHEETS

PARTNERS

BACACIER

Route de Chaptuzat
63260 Aigueperse
France
www.bacacier.com

L'ENVELOPPE MÉTALLIQUE DU BÂTIMENT

6 -14, rue La Pérouse
75784 Paris Cedex 16
France
www.enveloppe-metallique.fr

SPC SOKOL PALISSON CONSULTANTS

53 avenue Hoche
75008 Paris
France
www.sokol-palisson.com

TAMPERE UNIVERSITY OF TECHNOLOGY

Korkeakoulunkatu 10
33720 Tampere
Finland
www.tut.fi

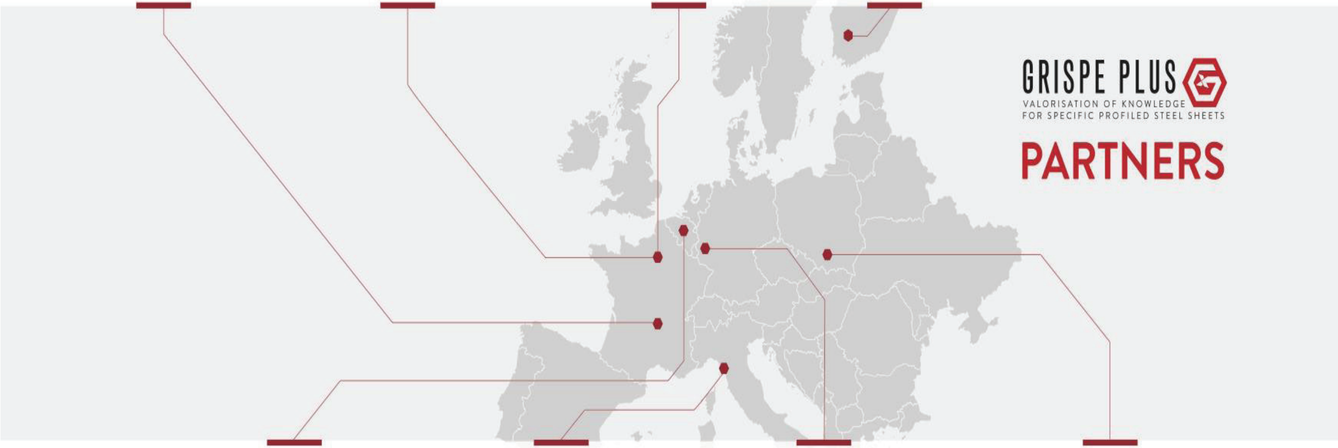

JORISIDE THE STEEL FUTURE

Hille 174
8750 Zwevezele
Belgium
www.joriside.com

UNIVERSITÀ DI PISA

Lungarno Pacinotti 43/44
56126 Pisa
Italy
www.unipi.it

RWTH AACHEN UNIVERSITY

Fakultät für Bauingenieurwesen /
Faculty of Civil Engineering
Mies-van-der-Rohe-Str. 1
52074 Aachen
Germany
www.rwth-aachen.de

Cracow University of Technology

Warszawska 24
31-155 Cracow
Poland
www.pk.edu.pl

The GRISPE & GRISPE PLUS projects

The GRISPE PLUS project has two objectives:

- Dissemination of value-added knowledge, acquired during an *earlier GRISPE project (2013-2016),* on seven key families of steel profiles widely used in construction and especially in non residential buildings .
  - Which kind of information and data will you be able to access thanks to the project ?
  - How easily can you access them?

- Incorporation of the seven key families of steel profiles into Eurocode EN 1993-1-3 as they are not considered in the current version of the code

The project has received financial support from the European Community (RFCS programme) under grant agreement No 754092

The seven key families of steel profiles

The GRISPE project aimed at providing technical data and calculation methods for seven widely used steel profiles not included in the current version of the Eurocode

STEEL DECKS WITH EMBOSSMENTS / INDENTATIONS OR STIFFENERS 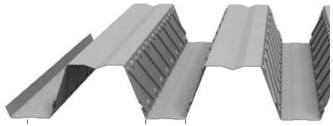	CURVED PROFILES 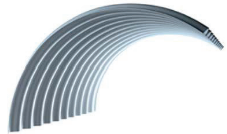
LINER TRAYS 	ASSEMBLED PROFILES 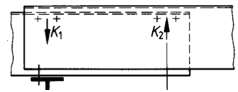
CORRUGATED SHEETINGS 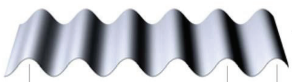	PERFORATED OR HOLED PROFILES 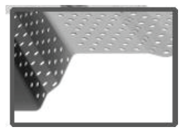 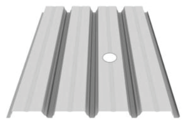
CLADDING SYSTEMS 	

The project has received financial support from the European Community (RFCS programme) under grant agreement No 754092

Which kind of value-added knowledge will you get ?

A previous EU funded project (GRISPE, 2013- 2016) has extensively studied and tested the seven families of steel profiles & a series of innovative calculation methods have been developed

The new GRISPE PLUS project explains in simple terms how to:

- ***apply and use all the research results***
- ***implement the various calculation methods***

The project has received financial support from the European Community (RFCS programme) under grant agreement No 754092

Which kind of value-added knowledge will you get ?

1. Critical review of the state of the art for the seven families of steel profiles
2. Results of the extensive experimental programme carried out from 2013 to 2016
3. Detailed analysis and validation of all the results
4. Innovative design and calculation methods developed in line with the experimental programme
5. Calculation methods backgrounds
6. Easy to use design Excel software sheets
7. European codification proposals to facilitate the inclusion of all the results of the work into EN 1993-1-3

The project has received financial support from the European Community (RFCS programme) under grant agreement No 754092

Where to find the information? How to access it easily ?

A series of tools give an easy access to the knowledge generated

On-line central resources:

www.grispeplus.eu

11 E-lectures:

- GRISPE PLUS summary
- General introduction
- 9 E-lectures on the seven families of profiles

7 Design manuals & worked examples into five languages

Five Workshops:

- France,
- Germany,
- Italy,
- Poland,
- Finland

The project has received financial support from the European Community (RFCS programme) under grant agreement No 754092

Thank you for
your attention

The project has received financial support from the European Community (RFCS programme) under grant agreement No 754092

GRISPE PLUS

VALORISATION OF KNOWLEDGE
FOR SPECIFIC PROFILED STEEL SHEETS

STEEL DECKS WITH EMBOSSMENTS / INDENTATIONS AND/OR OUTWARDS STIFFENERS

Anna PALISSON

KRAKOW 14th June 2018

The project has received financial support from the European Community (RFCS programme) under grant agreement No 754092

STEEL DECKS WITH EMBOSSMENTS / INDENTATIONS AND/OR OUTWARDS STIFFENERS

STEEL DECKS WITH EMBOSSMENTS / INDENTATIONS

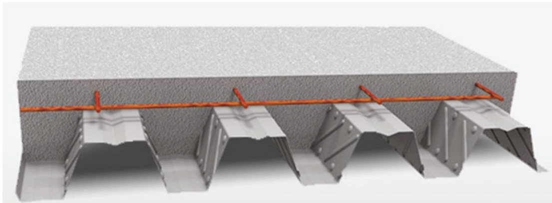

STEEL DECKS WITH OUTWARDS STIFFENERS

CONCLUSION

The project has received financial support from the European Community (RFCS programme) under grant agreement No 754092

STEEL DECKS WITH EMBOSSMENTS / INDENTATIONS

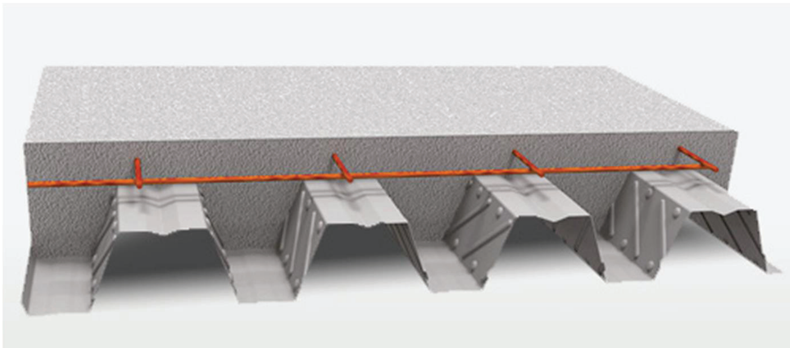

The project has received financial support from the European Community (RFCS programme) under grant agreement No 754092

STEEL DECKS WITH EMBOSSMENTS / INDENTATIONS

In order to increase the shear connection between the steel and the concrete in the composite slabs, steel decks are equipped with connectors such as embossments or indentations on the webs.

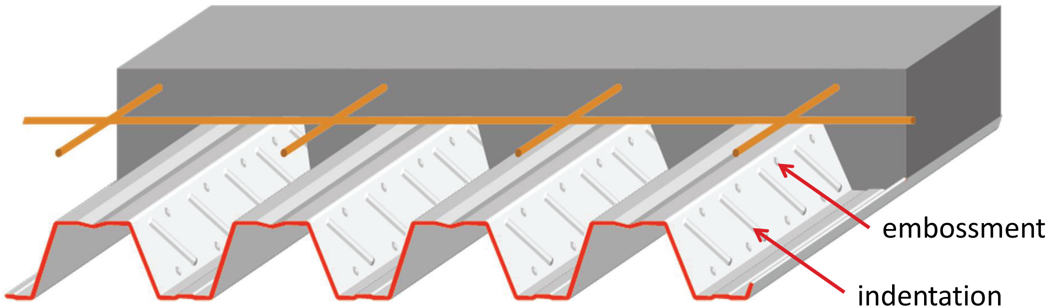

The project has received financial support from the European Community (RFCS programme) under grant agreement No 754092

STEEL DECKS WITH EMBOSSMENTS / INDENTATIONS

- At the construction stage the sheeting used as shuttering has to support the fresh concrete weight and the construction loads.
- EN 1994-1-1 specifies that steel sheeting should be designed in accordance with EN 1993-1-3.
- However, the current version EN 1993-1-3 does not provide any information on how to deal with the indentations or embossments in calculation of the effective section.

A design by calculation method of steel decks with embossments / indentations was developed within the GRISPE project.

The project has received financial support from the European Community (RFCS programme) under grant agreement No 754092

Development of the calculation method

This method is based on the results and analysis of many tests performed within the GRISPE project:

- Extensive global test programme on profiles
  - Without embossments / indentations
  - With embossments / indentations
- Local behaviour tests on samples
  - Without embossments / indentations
  - With embossments / indentations

The project has received financial support from the European Community (RFCS programme) under grant agreement No 754092

STEEL DECKS WITH EMBOSSMENTS / INDENTATIONS

Local behaviour testing

Local behaviour of profiles with embossments / indentations tested on samples:

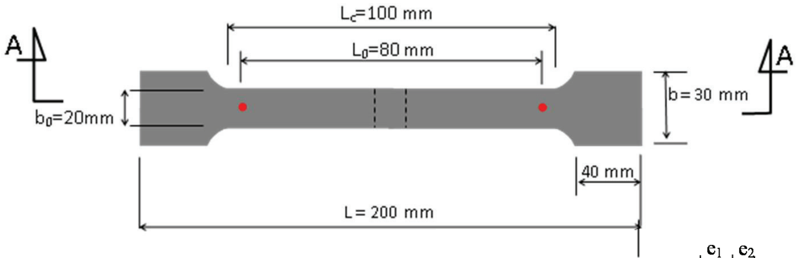

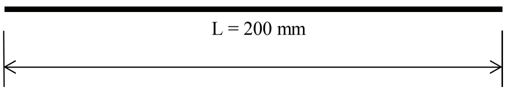

flat sample

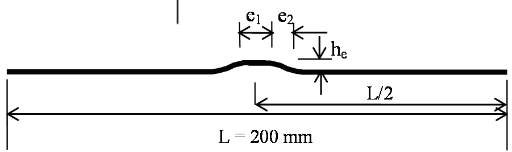

Sample with indentation

The project has received financial support from the European Community (RFCS programme) under grant agreement No 754092

STEEL DECKS WITH EMBOSSMENTS / INDENTATIONS

Local behaviour testing

Analysis of local tests led to a reduced thickness : $t_{red} = \rho * t$ where ρ depends on the height of the embossment h_e and on the thickness t:

t = 0,75 mm	
h_e (mm)	$\rho_p = K_{pe}/K_p$
1,5	0,200
2	0,150
2,5	0,080
2,75	0,060
3	0,053
3,5	0,041
4	0,029

Ratios ρ depending on the h_e dimensions for t = 0,75 mm

t = 1 mm	
h_e (mm)	$\rho_p = K_{pe}/K_p$
1,5	0,300
2	0,181
2,5	0,084
2,75	0,067
3	0,062
3,5	0,052
4	0,042

Ratios ρ depending on the h_e dimensions for t = 1 mm

The project has received financial support from the European Community (RFCS programme) under grant agreement No 754092

STEEL DECKS WITH EMBOSSMENTS / INDENTATIONS

Global behaviour testing

Extensive programme of global behaviour tests was performed at the KIT laboratory (Karlsruhe Technical University) in order to determine moment resistance, web crippling resistance and moment-reaction interaction of profiles :

- Without embossments / indentations
- With embossments / indentations

PCB 80 from Bacacier

PCB 60 from Bacacier

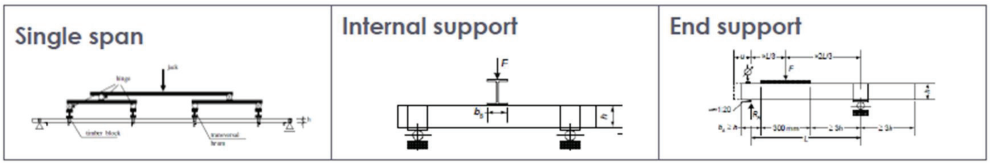

The project has received financial support from the European Community (RFCS programme) under grant agreement No 754092

STEEL DECKS WITH EMBOSSMENTS / INDENTATIONS

Global behaviour testing

Single span test results:

- Determination of the moment resistance

- Failure mode: buckling of the upper flange near the midspan (with and without embossments / indentations)

Test set-up

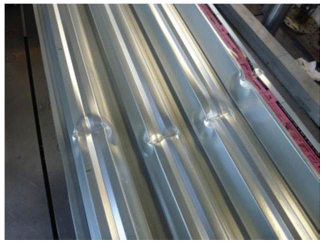

Without embossments/ indentations

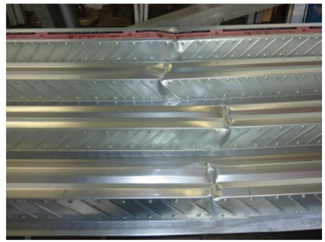

With embossments / indentations

The project has received financial support from the European Community (RFCS programme) under grant agreement No 754092

STEEL DECKS WITH EMBOSSMENTS / INDENTATIONS

Global behaviour testing

End support test results:

- Determination of the resistance at end support (web-crippling resistance)
- Failure mode: web-crippling (with and without embossments / indentations)

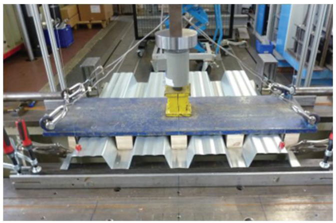

Test set-up

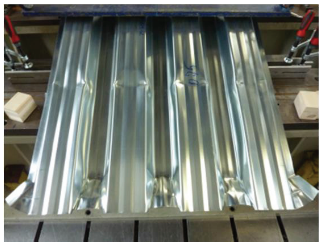

Without embossments/ indentations

With embossments / indentations

The project has received financial support from the European Community (RFCS programme) under grant agreement No 754092

STEEL DECKS WITH EMBOSSMENTS / INDENTATIONS

Global behaviour testing

Intermediate support test results:

- Determination of the resistance to combined moment and support reaction
- Failure mode: web-crippling and web + compressed flange buckling (with and without embossments / indentations)

Test set-up

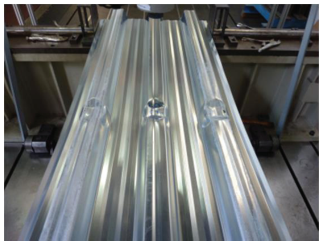

Without embossments/ indentations

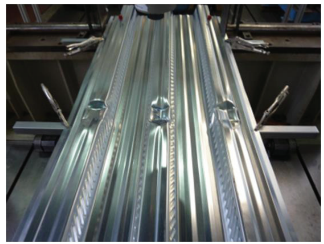

With embossments / indentations

The project has received financial support from the European Community (RFCS programme) under grant agreement No 754092

STEEL DECKS WITH EMBOSSMENTS / INDENTATIONS

Resistances determined by calculation

Moment resistance, web crippling resistance and moment-reaction interaction also determined by calculation:

- For profiles without embossments / indentations with usual EN 1993-1-3 formulas
- For profiles with embossments / indentations considering the embossments / indentations as plate elements with a reduced thickness as determined by the local testing
  $t_{red} = \rho * t$ where $\rho = A*h + B$, h is height of the embossments / indentations , A and B are coefficients given in next table:

The project has received financial support from the European Community (RFCS programme) under grant agreement No 754092

Global behaviour test analysis

Coefficients A and B :

Type of local deformation	t (mm)	h (mm)	A	B
Indentation	0.71	0 - 1.5	-0.533	1.000
		1.5 - 2.75	-0.112	0.368
		2.75 - 4.0	-0.025	0.128
	0.96	0 - 1.5	-0.467	1.000
		1.5 - 2.75	-0.186	0.580
		2.75 - 4.0	-0.020	0.122
	1.21	0 - 1.5	-0.401	1.000
		1.5 - 2.75	-0.260	0.792
		2.75 - 4.0	-0.015	0.116

Type of local deformation	t (mm)	h (mm)	A	B
Embossment	0.71	0 - 1.5	-0.267	1.000
		1.5 - 2.75	-0.056	0.684
		2.75 - 4.0	-0.013	0.564
	0.96	0 - 1.5	-0.234	1.000
		1.5 - 2.75	-0.093	0.790
		2.75 - 4.0	-0.010	0.561
	1.21	0 - 1.5	-0.201	1.000
		1.5 - 2.75	-0.130	0.896
		2.75 - 4.0	-0.008	0.558

The project has received financial support from the European Community (RFCS programme) under grant agreement No 754092

STEEL DECKS WITH EMBOSSMENTS / INDENTATIONS

Results

Moment resistance:

The moment resistance determined by calculation is compared to the moment resistance determined by testing

The comparison confirmed that considering the embossments / indentations as plate elements with a reduced thickness $t_{red} = \rho * t$ where $\rho = A*h + B$, h is height of the embossments / indentations , A and B are coefficients defined as before, gives coherent and safe results in relation with the testing results

The project has received financial support from the European Community (RFCS programme) under grant agreement No 754092

STEEL DECKS WITH EMBOSSMENTS / INDENTATIONS

Results

Web crippling resistance:

- The web crippling resistance determined by calculation is much bigger than the calculated one, for both profiles without embossments / indentations and with embossments / indentations
- The web crippling resistance of the profiles with embossments / indentations is slightly higher than this of the profiles without embossments / indentations,

Therefore as a safe simplification, the web crippling resistance may be determined without considering embossments / indentations

The project has received financial support from the European Community (RFCS programme) under grant agreement No 754092

Amendement proposal 1: Effective section of sheeting with indentation and/or embossment

(1) The effective width of plane wall with indentations (Fig. 5.15a) or embossments (Fig. 5.15b) should be first calculated according to 5.5.1(2)

(2) In the second step, the indentation or embossment should be taken into account considering the embossments / indentations (Fig. 5.15a / 5.15b) as plate elements with reduced thickness $t_{red} = \rho * t$ where:

- $\rho = A*h + B$
- h is height of the indentation / embossment in mm (see
- Figures 5.15a and 5.15b)

A and B are coefficients given in table 5.3.

The project has received financial support from the European Community (RFCS programme) under grant agreement No 754092

Amendement proposal 1: Effective section of sheeting with indentation and/or embossment

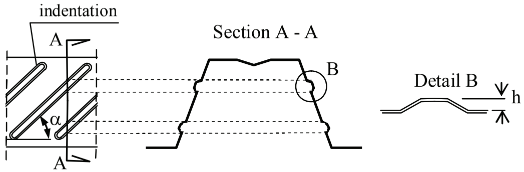

Figure 5.15a Exemple of sheeting with indentations

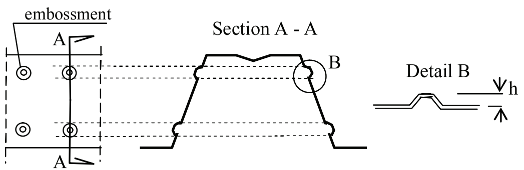

Figure 5.15b Exemple of sheeting with embossment

Table 5.3: Values of coefficients A and B (equation (5.43)

Type of local deformation	t (mm)	h (mm)	A	B
Indentation	0.71	0 - 1.5	-0.533	1.000
		1.5 - 2.75	-0.112	0.368
		2.75 - 4.0	-0.025	0.128
	0.96	0 - 1.5	-0.467	1.000
		1.5 - 2.75	-0.186	0.580
		2.75 - 4.0	-0.020	0.122
	1.21	0 - 1.5	-0.401	1.000
		1.5 - 2.75	-0.260	0.792
		2.75 - 4.0	-0.015	0.116
Embossment	0.71	0 - 1.5	-0.267	1.000
		1.5 - 2.75	-0.056	0.684
		2.75 - 4.0	-0.013	0.564
	0.96	0 - 1.5	-0.234	1.000
		1.5 - 2.75	-0.093	0.790
		2.75 - 4.0	-0.010	0.561
	1.21	0 - 1.5	-0.201	1.000
		1.5 - 2.75	-0.130	0.896
		2.75 - 4.0	-0.008	0.558

The project has received financial support from the European Community (RFCS programme) under grant agreement No 754092

Amendement proposal 1: Effective section of sheeting with indentation and/or embossment

(3) The cross section for calculation of the effective section should be positioned so as to cause the most unfavorable effect

(4) Range of validity

- $0{,}71\ \text{mm} \leq t \leq 1{,}21\ \text{mm}$
- $h \leq 4{,}0\ \text{mm}$
- $30° \leq \alpha \leq 60°$

(5) For intermediate thicknesses the reduction factor ρ may be determinated by means of linear interpolation between the neighbouring t values given in the Table 5.3.

For t > 1,21 mm the values given for t = 1,21 mm may be conservatively adopted.

The project has received financial support from the European Community (RFCS programme) under grant agreement No 754092

STEEL DECKS WITH EMBOSSMENTS / INDENTATIONS

<u>Amendement proposal 2: Resistance of sheeting with indentations or embossment to combined bending moment and local load or support reaction</u>

Add a new clause:

(2) In case of sheeting with indentations or embossments, the equations (6.28a), (6.28b) and (6.28c) from the AMD-1-3-2013-14 may be used with:

- $M_{c,Rd}$ = resistance moment determined considering the identations and/or embossments according to the Proposal 1
- $R_{w,Rd}$ = local transverse resistance determined without considering the identations and/or embossments

The project has received financial support from the European Community (RFCS programme) under grant agreement No 754092

Excel Files

Four Excel files were developed to provide a reliable design procedure in order to encourage and facilitate the use of steel decks with embossments / indentations.

- Profile with 1 stiffener in the upper flange, with longitudinal and conical embossments
    1) calculation of span moment resistance and end support reaction
    2) calculation of moment-reaction interaction at internal support
- Profile with 2 stiffeners in the upper flange, with longitudinal embossments
    3) calculation of span moment resistance and end support reaction
    4) calculation of moment-reaction interaction at internal support

The overall aim was to achieve simple, clear, easy to understand and easy to use excel files. The excel files were validated by the comparison of the calculation results with all the carried out tests. Moreover the excel files have been made available to a number of industry users to verify their fitness for purpose.

The project has received financial support from the European Community (RFCS programme) under grant agreement No 754092

STEEL DECKS WITH EMBOSSMENTS / INDENTATIONS AND/OR OUTWARDS STIFFENERS

STEEL DECKS WITH OUTWARDS STIFFENERS

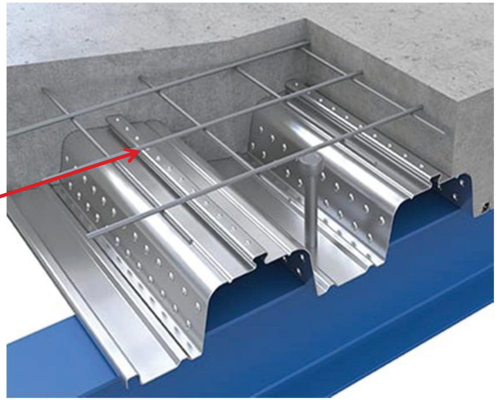

outwards
stiffener

The project has received financial support from the European Community (RFCS programme) under grant agreement No 754092

STEEL DECKS WITH OUTWARDS STIFFENERS

- In current practice of composite slabs, in order to increase the horizontal shear resistance between the steel sheeting and concrete, the outwards intermediate stiffeners in dovetail form are often used in the upper flange.
- However, the current version EN 1993-1-3 does not provide information on how to deal with this kind of stiffener in calculation of the moment resistance of the section.

A design by calculation method of steel decks with outwards stiffeners was developed within the GRISPE project. It is based on the results and analysis of tests performed within GRISPE.

The project has received financial support from the European Community (RFCS programme) under grant agreement No 754092

STEEL DECKS WITH OUTWARDS STIFFENERS

Testing

Global behaviour tests were performed in the KIT laboratory (Karlsruhe Technical University) in order to determine moment resistance on profile with outwards stiffeners

ComFlor® 80 from TataSteel

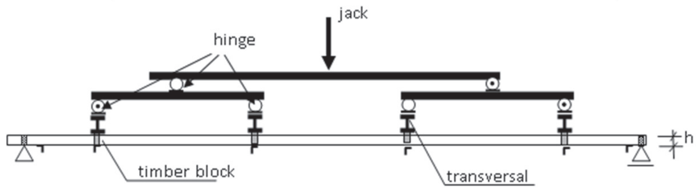

Single span test configuration

The project has received financial support from the European Community (RFCS programme) under grant agreement No 754092

STEEL DECKS WITH OUTWARDS STIFFENERS

Testing

Single span test results:

- Determination of the moment resistance

- Failure mode: buckling of the upper flange

The project has received financial support from the European Community (RFCS programme) under grant agreement No 754092

Calculation

The determination of the effective section modulus W_{eff} is based on an effective cross-section with a stress σ_1 in the upper flange and in the upper outwards stiffener and σ_2 in the bottom flange

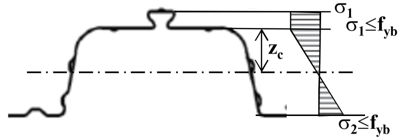

Depending on the distance z_c the yield stress is reached in the upper or lower flange.

- If the yield stress is reached in the lower flange then $\sigma_2 = f_{yb}$ and $\sigma_1 < f_{yb}$
- If the yield stress is reached in the upper flange then $\sigma_1 = f_{yb}$ and $\sigma_2 < f_{yb}$

The project has received financial support from the European Community (RFCS programme) under grant agreement No 754092

Results

The moment resistance determined by calculation with the effective section modulus W_{eff} defined in this way is compared to the moment resistance determined by testing

The comparison confirms that the definition of the effective section modulus W_{eff} based on an effective cross-section with:

- a stress σ_1 in the upper flange and in outwards stiffener
- a stress σ_2 in the bottom flange

gives results that are coherent and safe in relation with the testing results.

The project has received financial support from the European Community (RFCS programme) under grant agreement No 754092

<u>Amendement proposal:</u> Taking into account the intermediate outwards stiffener in the sheeting flange

Add a new clause in the section 5.5.3.3:

(12) For intermediate stiffeners facing outwards of sheeting flanges used for composite slabs, the calculations should be performed by taking the stress in the stiffener as equal to the stress in the flange.

The project has received financial support from the European Community (RFCS programme) under grant agreement No 754092

Excel File

An excel file was developed to provide a reliable design procedure in order to encourage and facilitate the use of steel decks with outwards stiffeners:

- Calculation of span moment resistance for a profile with 1 outwards stiffener in the upper flange

The overall aim was to achieve simple, clear, easy to understand and easy to use excel file. The excel file was validated by the comparison of the calculation results with all the carried out tests. Moreover the excel file has been made available to a number of industry users to verify their fitness for purpose.

The project has received financial support from the European Community (RFCS programme) under grant agreement No 754092

CONCLUSION

- The design by calculation methods of steel decks with embossments / indentations and of steel decks with outwards stiffeners presented here, were checked and validated by an extensive test programme performed within the GRISPE project.

- Five Excel files including these methods were developed for calculation of moment resistance, end support reaction and moment-reaction interaction at internal support

- These design by calculation methods were presented for proposal of Amendments on EN 1993-1-3 within CEN/TC250 Subcommittee 3 (SC3) “Steel Structures”.

The project has received financial support from the European Community (RFCS programme) under grant agreement No 754092

Thank you for your attention

The project has received financial support from the European Community (RFCS programme) under grant agreement No 754092

GRISPE PLUS

VALORISATION OF KNOWLEDGE
FOR SPECIFIC PROFILED STEEL SHEETS

Corrugated Sheeting

Ph. D. Thibault RENAUX – Joris Ide

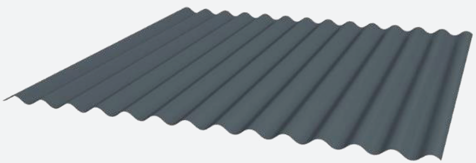

The project has received financial support from the European Community (RFCS programme) under grant agreement No 754092

Agenda

- Participant presentation
- Component description and context
- State of the art of design method
- Acquired data through GRISPE project
- Calculation method for corrugated sheets
- Conclusion

The project has received financial support from the European Community (RFCS programme) under grant agreement No 754092

Presentation of Joris Ide Group

The project has received financial support from the European Community (RFCS programme) under grant agreement No 754092

Presentation of Joris Ide Group

- 18 manufacturing in 8 countries
- More than 1000 employees
- 250 trucks delivering 1000 customers per day in Europe
- Export division worldwide
- Commercial presence spread over 16 countries

The project has received financial support from the European Community (RFCS programme) under grant agreement No 754092

Presentation of Joris Ide Group

- Insulated roof solution PIR/Mineral Wool
- Insulated wall solution PIR/Mineral Wool
- Non insulated architectural façade solutions
- Profiles and purlins:

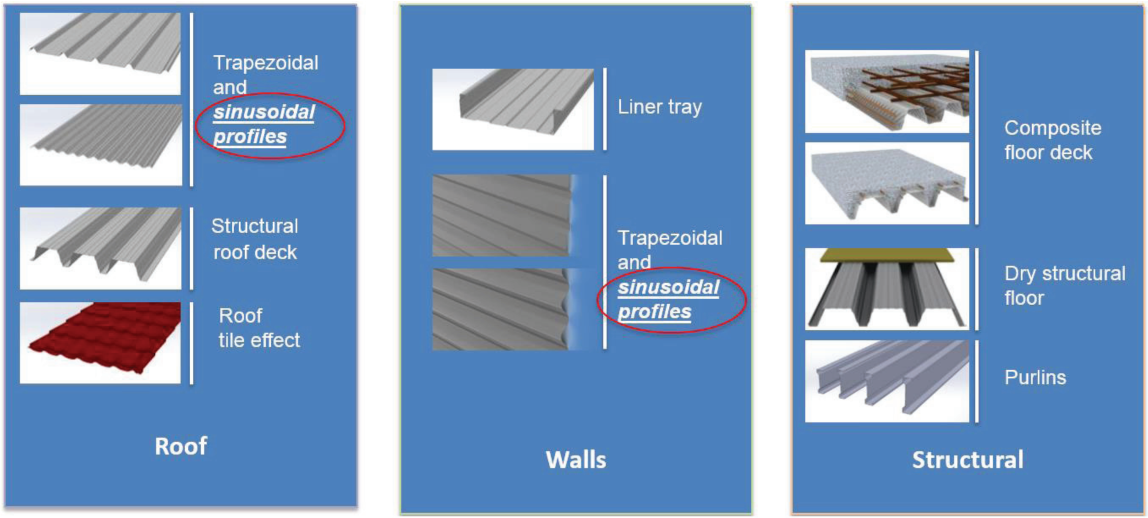

The project has received financial support from the European Community (RFCS programme) under grant agreement No 754092

Component description and context

The project has received financial support from the European Community (RFCS programme) under grant agreement No 754092

Component description and context

- What is a corrugated steel sheet ?

⇨Product having a continuous curve instead the flat section like trapezoidal profiles

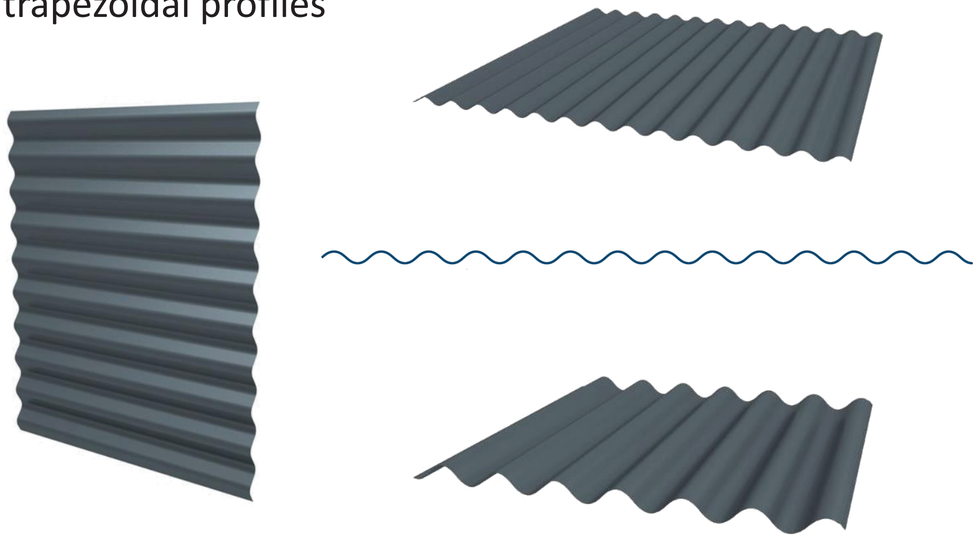

The project has received financial support from the European Community (RFCS programme) under grant agreement No 754092

Component description and context

- Corrugated steel sheet are common solutions for metallic roofing and cladding
  - Industrial buildings:

SNC Pont d'Ouit – Architect: DGA-Architecture

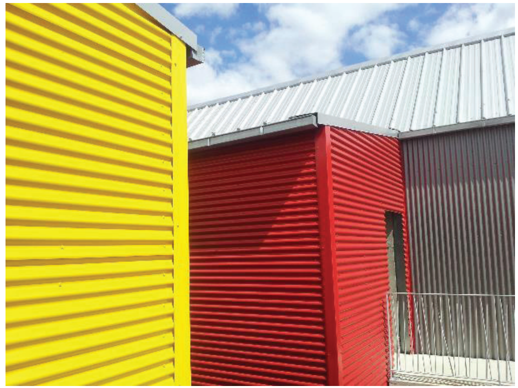

The project has received financial support from the European Community (RFCS programme) under grant agreement No 754092

Component description and context

- Residential buildings:

Aiguillon Construction
Architect: Christophe Rousselle Architecte

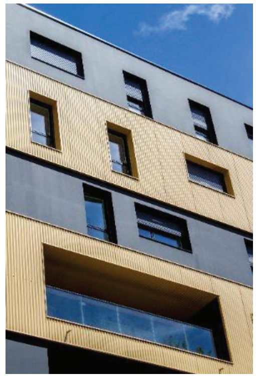

The project has received financial support from the European Community (RFCS programme) under grant agreement No 754092

Component description and context

- Commercial buildings:

The project has received financial support from the European Community (RFCS programme) under grant agreement No 754092

Component description and context

- Sports infrastructure buildings:

The project has received financial support from the European Community (RFCS programme) under grant agreement No 754092

Component description and context

- **But** actual European design rules don't prescribe calculation method (see EN 1993-1-3) !

The project has received financial support from the European Community (RFCS programme) under grant agreement No 754092

State of the art of design method

The project has received financial support from the European Community (RFCS programme) under grant agreement No 754092

State of the art of design methods

- Conventional bending theory can be used ⇦ no local buckling is expected for continuous curvature.

- DIN 59231 ⇨ parameter range of the d/r ratio where no buckling is expected (d the depth of profile and r the curve radius)

- Article in the revue “Revue de Construction Métallique” n°1-2012:

  - Calculation method developed in comparison with FEM
  - Procedure corresponding to the usual for buckling problems with parameters developed from the comparison with FEM

- Silo approach ⇨ EN 1993-4

- Swedish Code for Light Gauge Metal Structures StBK-N5

The project has received financial support from the European Community (RFCS programme) under grant agreement No 754092

Acquired data through GRISPE project

The project has received financial support from the European Community (RFCS programme) under grant agreement No 754092

Acquired data through GRISPE project

- 2 classical corrugated steel sheet are studied:
  - 18 mm depth / radius of 23 mm / 76 mm pitch

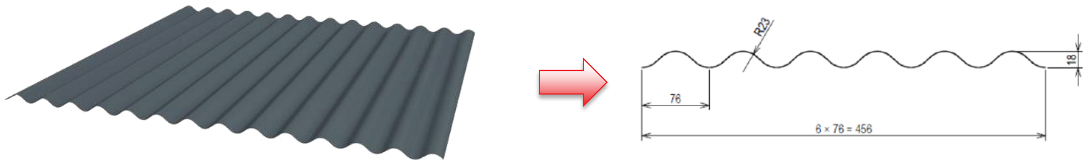

  - 46 mm depth / radius of 29,25 mm / 150 mm pitch

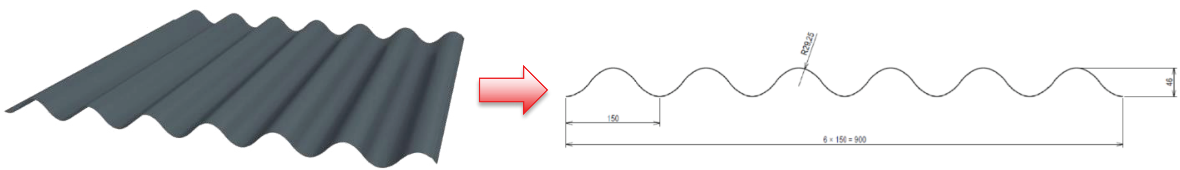

- Profiles are cut due to test consideration
- Supplier: Bacacier

The project has received financial support from the European Community (RFCS programme) under grant agreement No 754092

Acquired data through GRISPE project

- Test program:

According EN 1993-1-3

Type of test	Thickness [mm]	Support width [mm] / Fastening	Span [mm]		Number of tests	
			18/76	46/150	18/76	46/150
Single span test with gravity loading	0.63	-	1500	2000	3	6
	1.00	-	2000	3000	3	3
Internal support tests with gravity loading	0.63	10	400	600	2	2
			800	1000	2	2
		40	400	600	2	2
			800	1000	2	2
	1.00	10	400	600	2	2
			1000	1200	2	2
		40	400	600	2	2
			1000	1200	2	2
Internal support tests with uplift loading	0.63	valley	400	600	2	2
			800	1000	2	2
		crest	400	600	2	2
			800	1000	2	2
	1.00	valley	400	900	2	2
			1000	1400	2	2
		crest	400	900	2	2
			1000	1400	2	2
End support tests with gravity loading	0.63	-	1000	1050	4	3
	1.00	-	1000	1050	4	3
Shear test	0.63	-	1000	1000	1	1

- Supplemented by tensile tests

The project has received financial support from the European Community (RFCS programme) under grant agreement No 754092

Acquired data through GRISPE project

- Self weight of test specimens:

profile	thickness t (mm)	self-weight (kN/m²)
Bacacier 18/76	0,63	0,063
	1,00	0,099
Bacacier 46/150	0,63	0,067
	1,00	0,106

- Adjustment of test values considering real characteristics and number of tests:

  - According EN 1993-1-3 § A.6.2:

$$R_{adj,i} = R_{obs,i}/\mu_R \qquad \mu_R = \left(\frac{f_{yb,obs}}{f_{yb}}\right)^{\alpha}\left(\frac{t_{obs,cor}}{t_{cor}}\right)^{\beta}$$

  - According EN 1993-1-3 § A.6.3

$$R_k = R_m +/- k\,s$$

n	4	5	6	8	10	20	30	∞
k	2,63	2,33	2,18	2,00	1,92	1,76	1,73	1,64

$$s = \left[\sum_{i=1}^{n}\left(R_{adj,i} - R_m\right)^2 / (n-1)\right]^{0,5}$$

The project has received financial support from the European Community (RFCS programme) under grant agreement No 754092

Acquired data through GRISPE project

- Single span test (bending moment capacity):

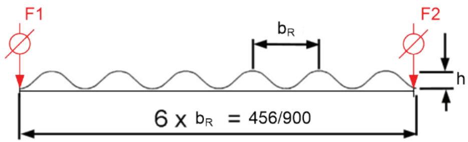

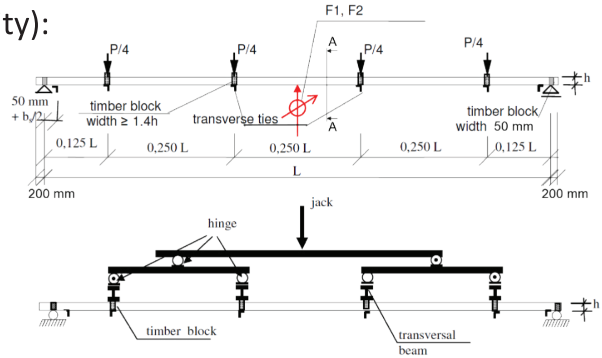

- Typical result – load/displacement curves for single span test:

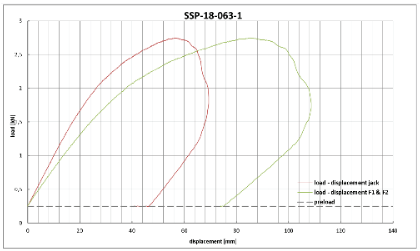

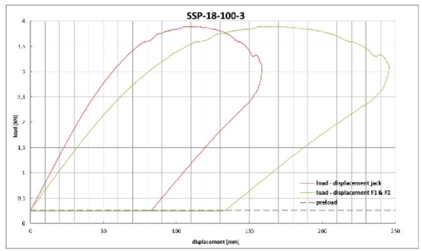

The project has received financial support from the European Community (RFCS programme) under grant agreement No 754092

Acquired data through GRISPE project

- Maximum bending moment in span (single span tests):

$$M_{c,Rk,F} = \frac{F_{u,k}}{b_V} \cdot \frac{L}{8} + \frac{g \cdot L_V \cdot (2 \cdot L - L_V)}{8}$$

  - $M_{c,Rk,F}$ characteristic bending moment in span
  - $F_{u,k}$ characteristic load (including preload)
  - b_V width of the test specimen (456 / 900 mm)
  - L_V length of the test specimen (1 900 / 2 400 / 3 400 mm)
  - L span length (1 500 / 2 000 / 3 000 mm)
  - q self-weight of the test specimen

- Test results:

Profile	nominal thickness t	steel core thickness t_{cor}	yield strength f_{yb}	span moment $M_{c,Rk,F}$
	mm	mm	N/mm²	kNm/m
Bacacier 18/76	0,63 1,00	0,523 0,943	333,7 402,0	1,09 2,08
Bacacier 46/150	0,63 1,00	0,520 0,933	364,3 409,0	2,41 5,47

- Two modes of failure occurred: Yielding or Buckling of the compressed part

The project has received financial support from the European Community (RFCS programme) under grant agreement No 754092

Acquired data through GRISPE project

- Examples of failure (by yielding):

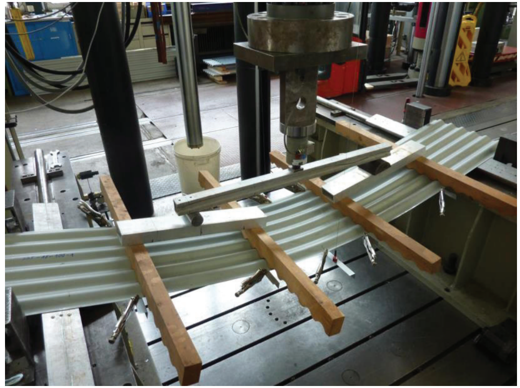

Profile 18.76 – 1,00 mm

- For small R/t ratio ⇨ failure by yielding in midspan (no buckling)

The project has received financial support from the European Community (RFCS programme) under grant agreement No 754092

Acquired data through GRISPE project

- Examples of failure (by buckling):

Profile 18.76 – 0,63 mm

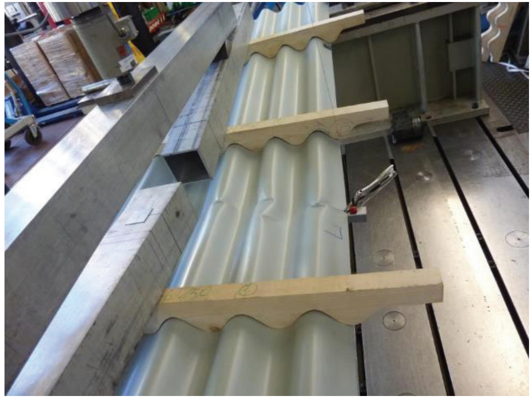

Profile 46.150 – 1,00 mm

- For great R/t ratio ⇨ failure by local buckling

The project has received financial support from the European Community (RFCS programme) under grant agreement No 754092

Acquired data through GRISPE project

- Intermediate support tests for downward loading:

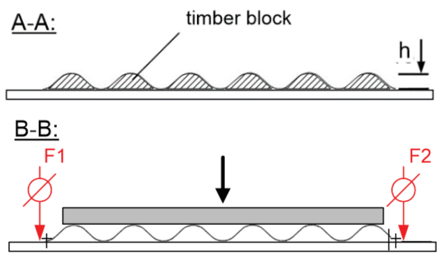

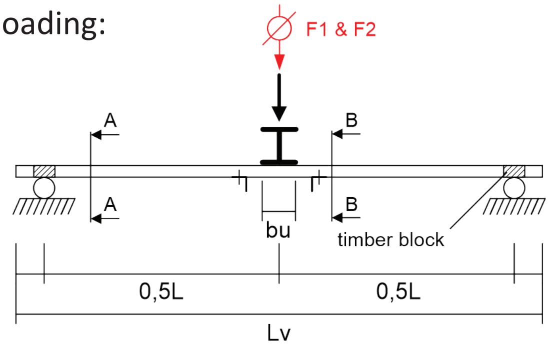

- Test setup and typical load/displacement curve:

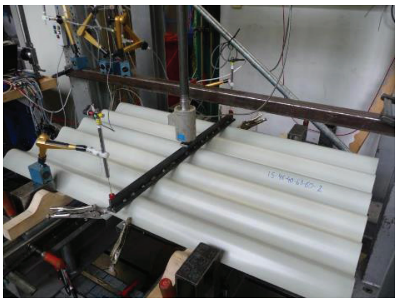

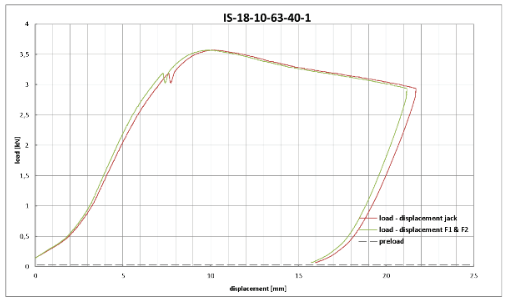

The project has received financial support from the European Community (RFCS programme) under grant agreement No 754092

Acquired data through GRISPE project

- Support reaction for intermediate support test: $R_{w,Rk,B} = F_{u,k}/b_V$

- Bending moment at support: $M_{c,Rk,B} = R_{w,Rk,B} \cdot \frac{L}{4} + \frac{g \cdot L_V \cdot (2L - L_V)}{8}$

  - $R_{w,Rk,B}$ characteristic support reaction at intermediate support
  - $M_{c,Rk,F}$ characteristic bending moment at intermediate support
  - $F_{u,k}$ characteristic load (including preload)
  - b_V width of the test specimen
  - L_V length of the test specimen
  - L span length (400 / 600 / 800 / 1 000 mm)
  - q self-weight of the test specimen

- Failure dominated by local deformations and buckling of the compressed part

The project has received financial support from the European Community (RFCS programme) under grant agreement No 754092

Acquired data through GRISPE project

- Characteristic M/R-combinations:

Profile	nominal thickness t	support width $L_{a,B}$	maximum bending moment $M_{c,Rk,B}$	corresp. support reaction R_1	corresp. bending moment M_2	max. support reaction $R_{w,Rk,B}$	interaction parameter $M^0_{Rk,B}$	interaction parameter $R^0_{Rk,B}$
	mm	mm	kNm/m	kN/m	kNm/m	kN/m	kNm/m	kN/m
Bacacier 18/76	0,63	10	0,88	4,40	0,77	7,81	1,02	32,00
		40	1,12	5,61	1,05	10,58	1,21	81,80
	1,00	10	2,27	9,06	2,01	20,15	2,49	104,44
		40	2,44	9,75	2,58	25,88	2,44	∞
Bacacier 46/150	0,63	10	1,20	4,79	0,98	6,55	1,81	14,26
		40	1,27	5,07	1,09	7,31	1,68	20,83
	1,00	10	3,74	12,43	3,02	20,12	4,92	52,04
		40	3,92	13,03	3,36	22,40	4,71	78,14

- Example of an interaction diagram M/R (profile 18/76 – 0,63 mm – 10 mm width of support):

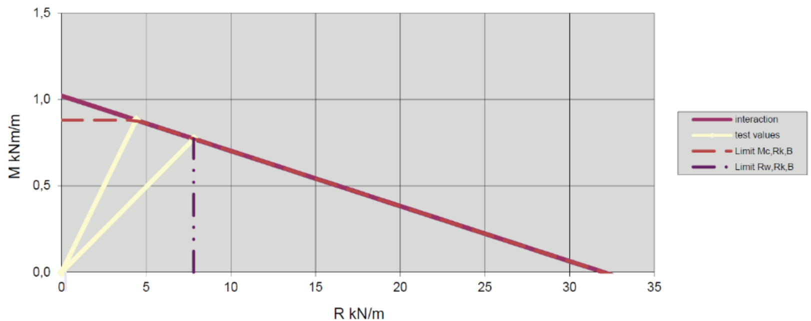

The project has received financial support from the European Community (RFCS programme) under grant agreement No 754092

Acquired data through GRISPE project

- Examples of failure:

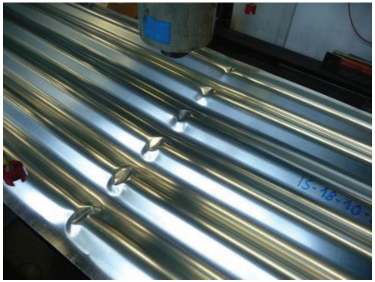

Profile 18.76 – 0,63 mm / 10 mm width of support

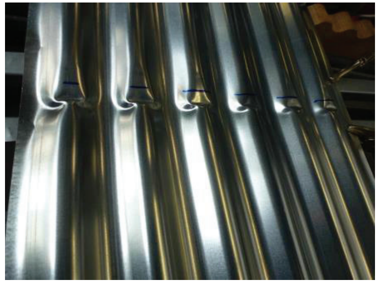

Profile 18.76 – 0,63 mm/ 40 mm width of support

Profile 46.150 – 1,00 mm / 10 mm width of support

Profile 46.150 – 1,00 mm / 40 mm width of support

The project has received financial support from the European Community (RFCS programme) under grant agreement No 754092

Acquired data through GRISPE project

- Intermediate support tests for “uplift” loading:

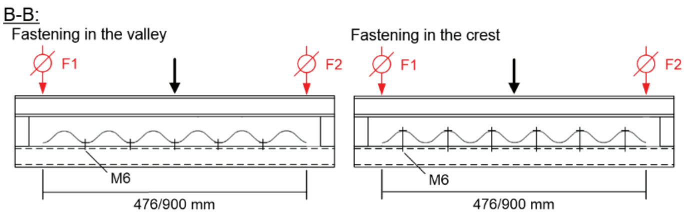

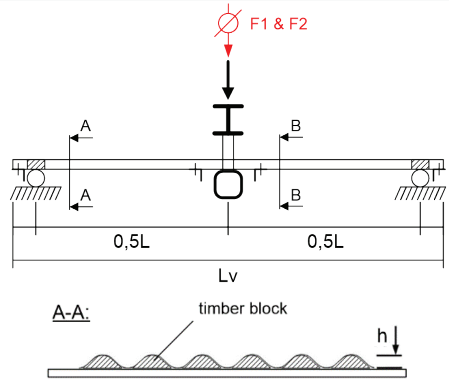

- Test setup and typical load/displacement curve:

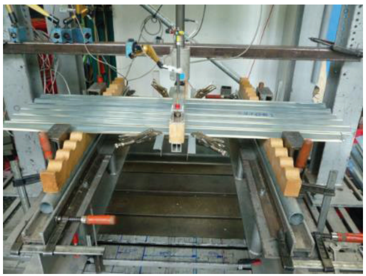

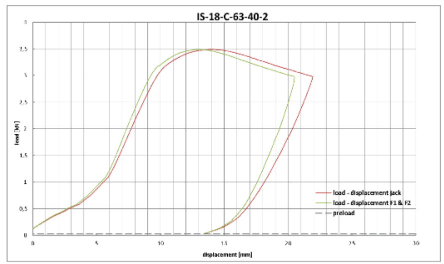

The project has received financial support from the European Community (RFCS programme) under grant agreement No 754092

Acquired data through GRISPE project

- Support reaction and bending moment at support for the “uplift” case are determined using the same formula as for downward loading

- Failure dominated by local deformations or buckling of the compressed part

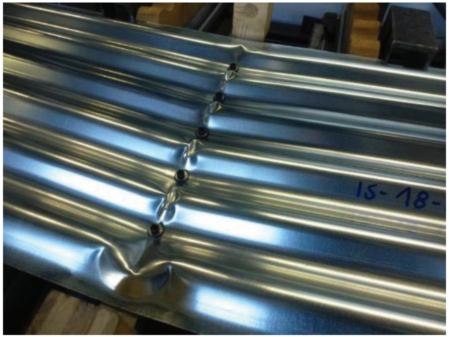

Profile 18.76 – 0,63 mm – fixing in valley

Profile 18.76 – 0,63 mm – fixing in crest

The project has received financial support from the European Community (RFCS programme) under grant agreement No 754092

Acquired data through GRISPE project

- Characteristic M/R-combinations:

Profile	nominal thickness t mm	fixing config-uration	maximum bending moment $M_{c,Rk,B}$ kNm/m	corresp. support reaction R_1 kN/m	corresp. bending moment M_2 kNm/m	max. support reaction $R_{w,Rk,B}$ kN/m	interaction parameter $M^0_{Rk,B}$ kNm/m	interaction parameter $R^0_{Rk,B}$ kN/m
Bacacier 18/76	0,63	crest	0,85	4,23	0,74	7,52	0,98	31,22
		valley	1,06	5,31	1,13	11,41	1,06	∞
	1,00	crest	2,13	8,50	1,87	18,83	2,34	94,17
		valley	2,26	9,02	2,33	23,40	2,26	∞
Bacacier 46/150	0,63	crest	0,99	3,95	0,84	5,64	1,34	15,16
		valley	2,36	9,43	2,34	15,62	2,36	∞
	1,00	crest	3,59	10,22	3,08	13,67	5,11	34,39
		valley	5,62	16,01	5,44	24,16	5,62	∞

- Behaviour of M/R-combinations and failure are strongly affected by the fixing mode

The project has received financial support from the European Community (RFCS programme) under grant agreement No 754092

Acquired data through GRISPE project

- Fixing on the crest of the waves:
  - Failure occurred by a combination of local deformations under the heads of the screws + local buckling of compressed parts

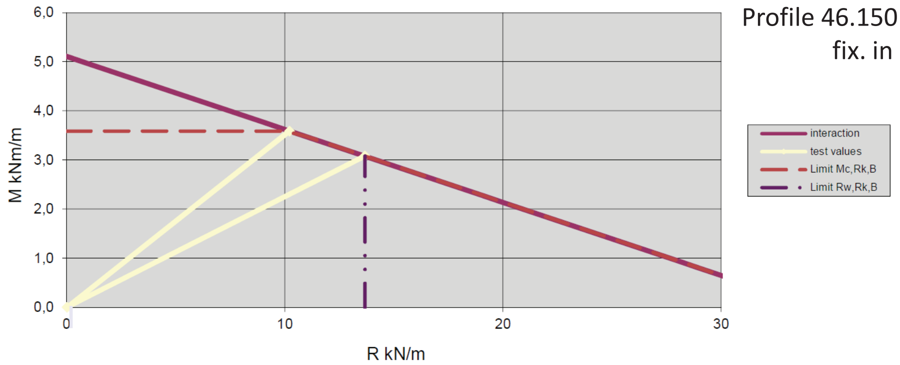

Profile 46.150 – 1,00 mm – fix. in crest

  - Interaction diagram shows a considerable influence of the support reaction on the bending moment

The project has received financial support from the European Community (RFCS programme) under grant agreement No 754092

Acquired data through GRISPE project

- Fixing in the valleys:
  - Local buckling of compressed parts of the cross section leads to failure and determinates the ultimate bending moment
  - No local compression of the cross section

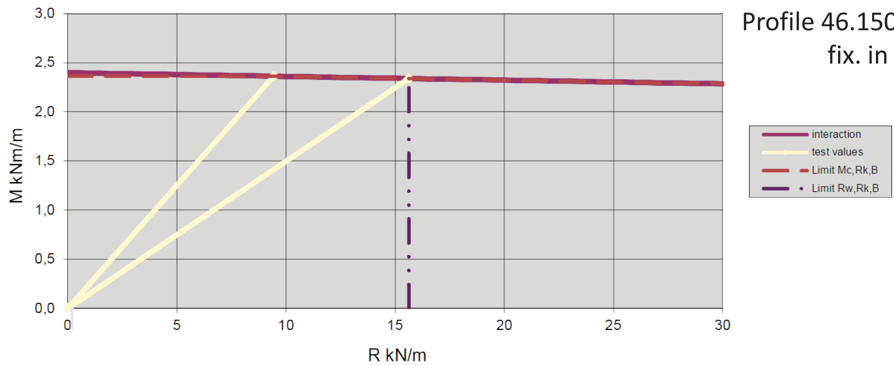

Profile 46.150 – 1,00 mm – fix. in valley

- Interaction diagram is more or less horizontal ⇨ bending moment capacity isn't reduced with increasing support reaction

The project has received financial support from the European Community (RFCS programme) under grant agreement No 754092

Acquired data through GRISPE project

- Comparison of the bearing capacity at internal supports – downward and uplift loading – step 1 – Physical aspect:
  - Bending moment and support reaction act simultaneously ⇨ failure occurs by a combined solicitation
  - Bending moment ⇨ local buckling (compressed area) or yielding
  - Support reaction ⇨ local deformation and shear stresses
  - Local deformations reduce more or less the bending moment capacity

The project has received financial support from the European Community (RFCS programme) under grant agreement No 754092

Acquired data through GRISPE project

- Comparison of the bearing capacity at internal supports – downward and uplift loading – step 2 – diagram comparison:

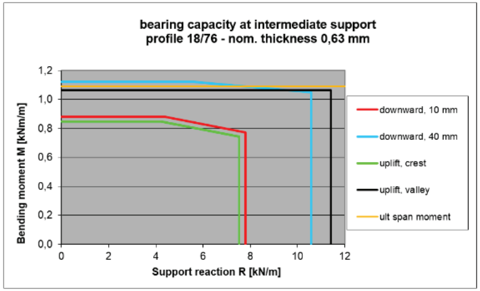

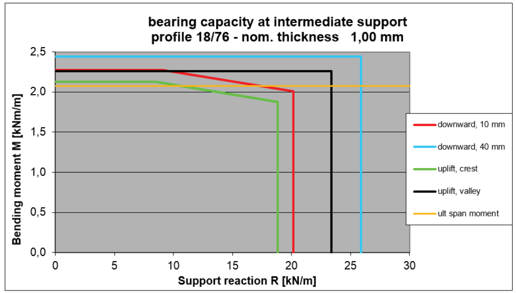

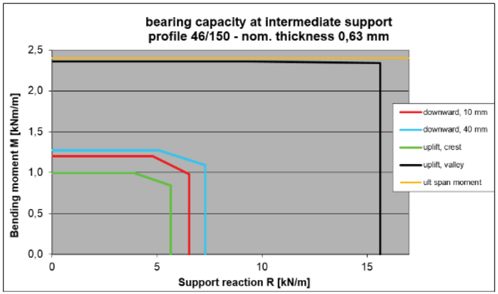

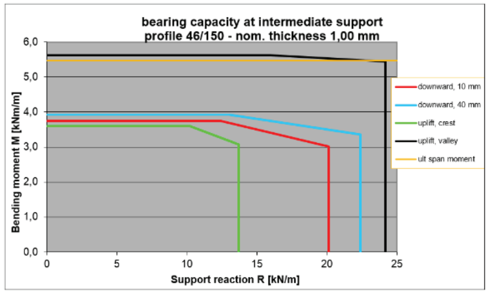

The project has received financial support from the European Community (RFCS programme) under grant agreement No 754092

Acquired data through GRISPE project

- Comparison of the bearing capacity at internal supports – downward and uplift loading – step 3 – influence factors (1/2):
  - Thin sheets are very sensitive to local loads ⇦ R/t ratio influence the reduction of the ultimate bending moment
  - The larger the pitch the bigger the influence of the support reaction
  - Influence of the width of the support isn't very big
  - The punctual "support" by the heads of the screws is even less resistant as the linear support performed by a purlin or wall rail
  - If the support reaction acts as a tension force on the cross section ⇨ no effect on the bending moment

The project has received financial support from the European Community (RFCS programme) under grant agreement No 754092

Acquired data through GRISPE project

- Comparison of the bearing capacity at internal supports – downward and uplift loading – step 3 – influence factors (1/2):
  - Intermediate support tests for "uplift" loading with fixing in the valley:
    - no real interactive influence of the line load on the bending moment
    - bending moment capacity isn't reduced with increasing support reaction
  - Intermediate support tests under downward loading + "uplift" loading with fixing on the crest:
    - For 76/150 profile (great R/t ratios):
      - Bending moment at support is strongly influenced by support reaction
      - Bending moment at support is often considerably smaller than the bending moment in span
    - For 18/76 profile (smaller R/t ratios than for 76/150): No reduction compared to the bending moment capacity in span

The project has received financial support from the European Community (RFCS programme) under grant agreement No 754092

Acquired data through GRISPE project

- End support test for downward loading:

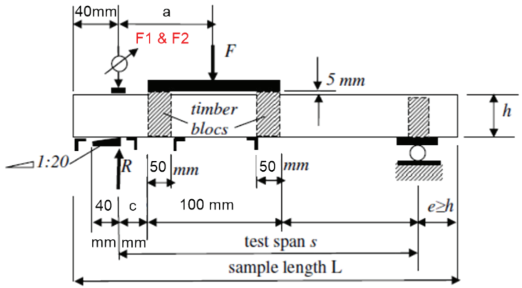

- Test setup and typical load/displacement curve:

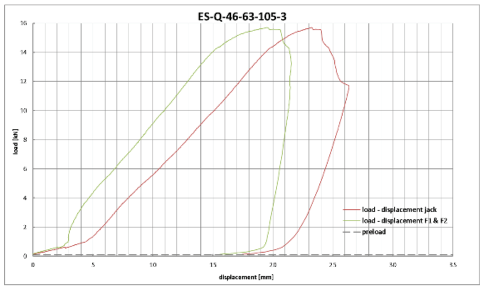

The project has received financial support from the European Community (RFCS programme) under grant agreement No 754092

Acquired data through GRISPE project

- End support reaction: $$R_{w,Rk,A} = \frac{F_{u,k}}{b_V} \cdot \frac{(s-a)}{s}$$

  - $R_{w,Rk,A}$ characteristic support reaction at end support
  - $F_{u,k}$ characteristic load (including preload)
  - b_V width of the test specimen
  - a distance between load axis and support axis
  - s span length

  - The self-weight of the test specimen is neglected

- Test results:

Profile	nominal thickness t mm	support width $L_{a,A}$ mm	overhang c mm	support reaction $R_{w,Rk,A}$ kN/m
Bacacier 18/76	0,63 1,00	0 0	40 40	18,13 40,09
Bacacier 46/150	0,63 1,00	0 0	40 40	13,26 39,20

The project has received financial support from the European Community (RFCS programme) under grant agreement No 754092

Acquired data through GRISPE project

- Failure dominated by local deformations at the support and local buckling of the compressed parts of the cross section in the load axis (where bending moment becomes a maximum)

- Examples of failure:

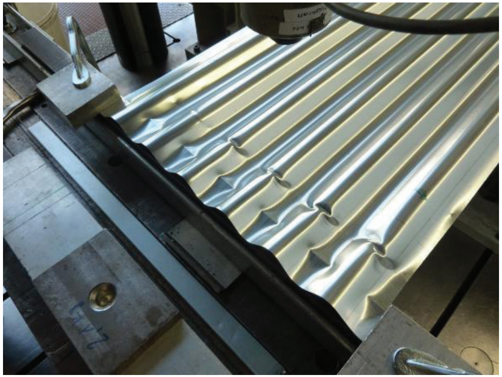

Successive failure at support by local deformation and in the load application area by local buckling (due to bending moment)

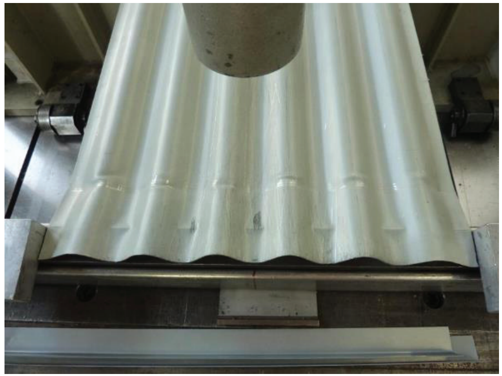

Successive failure at support and in the span, load and local deformations at support can't be increased

The project has received financial support from the European Community (RFCS programme) under grant agreement No 754092

Acquired data through GRISPE project

- Load test to determine the shear resistance:

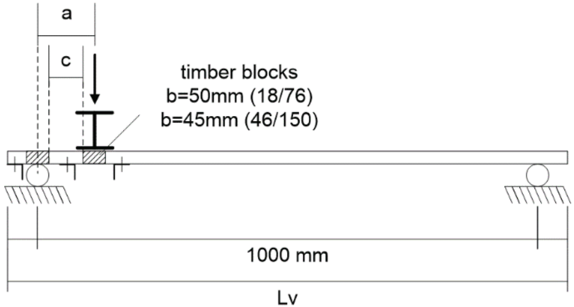

- Test setup and typical load/displacement curve:

The project has received financial support from the European Community (RFCS programme) under grant agreement No 754092

Acquired data through GRISPE project

- Maximum shear force at the support: $$V_{w,Rk} = \frac{F_{u,k}}{b_V} \cdot \frac{(s-a)}{s}$$

  - $V_{w,Rk}$ characteristic shear force at end support
  - $F_{u,k}$ characteristic load (including preload)
  - b_V width of the test specimen
  - a distance between load axis and support axis
  - s span length

  - the self-weight of the test specimen is neglected

- Test results:

Profile	nominal thickness t mm	support width $L_{a,A}$ mm	overhang c mm	support reaction $R_{w,Rk,A}$ kN/m	shear resistance $V_{w,Rk}$ kN/m
Bacacier 18/76	0,63	0	40	18,13	18,77
Bacacier 46/150	0,63	0	40	13,26	16,78

The project has received financial support from the European Community (RFCS programme) under grant agreement No 754092

Acquired data through GRISPE project

- Failure dominated by local buckling of the compressed parts of the cross section in the load axis (where bending moment becomes a maximum). No local deformations at the support are visible.

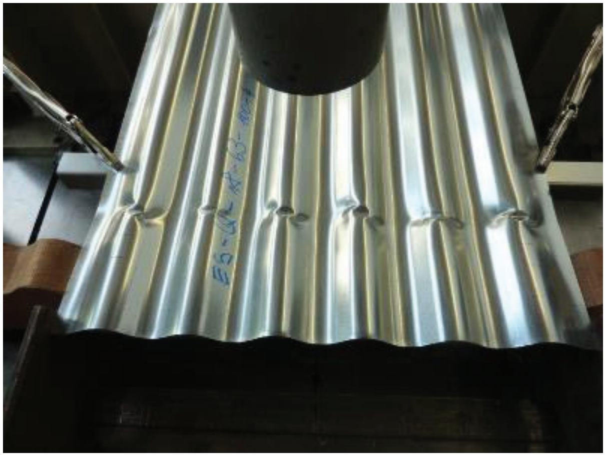

The project has received financial support from the European Community (RFCS programme) under grant agreement No 754092

Calculation method for corrugated sheets

The project has received financial support from the European Community (RFCS programme) under grant agreement No 754092

Calculation method for corrugated sheets

- Design procedure for the bending moment capacity:

- First step: limit ratio for R/t

- If $R/t < 0{,}04 \times E/f_{yb}$ ⇨ the cross section need not be checked for local buckling

- In this case, the characteristic bending moment is determined by:

$$M_{c,Rk} = W_y \cdot f_{yb}$$

- With W_y the section modulus of the gross cross section

The project has received financial support from the European Community (RFCS programme) under grant agreement No 754092

Calculation method for corrugated sheets

- If $R/t \geq 0{,}04 \times E/f_{yb}$ ⇨ the characteristic bending moment can be calculated using the reduced compressive stress σ_c (StBK-N5): $M_{c,Rk} = W_y \cdot \sigma_c$

For SLS : the moment of inertia I_y should be calculated using reduced stress $f_{yb}/1{,}5$

$$W_y = \frac{4 \cdot I_y \cdot t}{(b_R \cdot h_w/2)}$$

- With:
  - the slenderness ratio: $\alpha = \sqrt{f_{yb}/\sigma_{elr}}$
  - the buckling stress: $\sigma_{elr} = 0{,}60 \cdot \eta \cdot E \cdot t/R$
  - coefficient η: $\eta = 0{,}19 + 0{,}67/\sqrt{1 + R/(100 \cdot t)}$
  - for $\alpha \leq 0{,}30$: $\sigma_c = f_{yb}$
  - for $0{,}30 < \alpha < 1{,}10$: $\sigma_c = (1{,}126 - 0{,}419 \cdot \alpha) \cdot f_{yb}$
  - For $1{,}10 \leq \alpha$: $\sigma_c = (0{,}8/\alpha^2) \cdot f_{yb}$
  - Ultimate compressive stress with respect to buckling of the section of the profile:

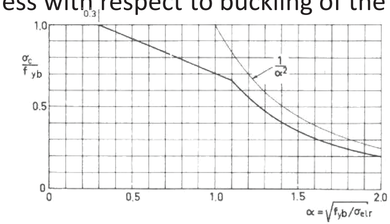

The project has received financial support from the European Community (RFCS programme) under grant agreement No 754092

Calculation method for corrugated sheets

- Simplified method for the bending moment for restricted application (tank formula):
- When conditions:
  - Profile installed as single span girder <u>and</u>
  - Uniformly distributed loads <u>and</u>
  - Ratio $R/t \leq 0{,}1 \cdot E/f_{yb}$ <u>and</u>
  - Steel core thickness $t_{cor} \geq 0{,}55$ mm <u>and</u>
  - Profile height 18 mm $\leq h \leq$ 46 mm <u>and</u>
  - Profile pitch 76 mm $\leq p \leq$ 150 mm
- Are respected, the following procedure may be adopted:
  - Moment of inertia per unit width: $I_y = 0{,}13 \cdot t \cdot h^2$
  - Section modulus per unit width: $W_y = 0{,}26 \cdot t \cdot h$
  - Characteristic bending moment: $M_{c,Rk} = W_y \cdot f_{yb}$

The project has received financial support from the European Community (RFCS programme) under grant agreement No 754092

Calculation method for corrugated sheets

- Comparison of the single span test values with the calculated values:

Profile	Nominal thickness t	steel core t_{cor}	yield strength f_{yb}	Test	calculation			
				span moment $M_{c,Rk,F}$	tanks $M_{c,Rk,F}$	StBkN5 $M_{c,Rk,F}$	elastic Moment $M_{c,Rk,F}$	plastic Moment $M_{c,Rk,F}$
	mm	mm	N/mm²	kNm/m	kNm/m	kNm/m	kNm/m	kNm/m
Bacacier 18/76	0,63	0,523	333,7	1,09	0,817	0,875	0,912	1,151
	1,00	0,943	402,0	2,08	1,774	1,968	1,980	2,500
Bacacier 46/150	0,63	0,520	364,3	2,41	2,266	2,233	2,411	3,143
	1,00	0,933	409,0	5,47	4,564	4,725	4,857	6,332

- For the bending moment resistance at internal support under “uplift” loading with fixing in valley:

$$M_{c,Rk,B} = M_{c,Rk,F}$$

- For the bending moment resistance at internal support under “uplift” loading with fixing on crest and for downward loading:

  Test results are not sufficient to conclude a design rule for the M/R interaction

The project has received financial support from the European Community (RFCS programme) under grant agreement No 754092

Conclusion

The project has received financial support from the European Community (RFCS programme) under grant agreement No 754092

Calculation method for corrugated sheets

- This presentation proposes two design approaches for the corrugated sheets in bending
- First method is based on a Swedish approach
- Second method consider the tank approach defined already in the Eurocode ⇦ with a field of application calibrated on the tests done during GRISPE project

The project has received financial support from the European Community (RFCS programme) under grant agreement No 754092

Calculation method for corrugated sheets

- For the behaviour of corrugated sheets on intermediate support:
  - The results don't show a clear rule as too many parameter interfere
  - More tests are necessary to reach a viable conclusion
  - Reduction of the ultimate bending moment is influenced by:
    - R/t ratio;
    - Pitch of the cross section;
    - Width of the support;
    - Size of the support reaction/load, location and direction of the load (sensitivity of section against local loads)
- For the shear behaviour and reaction on support: results don't allow to find a law

The project has received financial support from the European Community (RFCS programme) under grant agreement No 754092

Thank you for your attention

The project has received financial support from the European Community (RFCS programme) under grant agreement No 754092

GRISPE PLUS

VALORISATION OF KNOWLEDGE FOR SPECIFIC PROFILED STEEL SHEETS

Cracow University of technology, Warszawska 24
Cracow, POLAND

CURVED PROFILES

Irene PUNCELLO, Silvia CAPRILI, Walter SALVATORE

University of Pisa, Department of Civil and Industrial Engineering

THURSDAY 14TH June 2018

The project has received financial support from the European Community (RFCS programme) under grant agreement No 754092

INTRODUCTION

CURVED PROFILES can be obtained through three different processes:

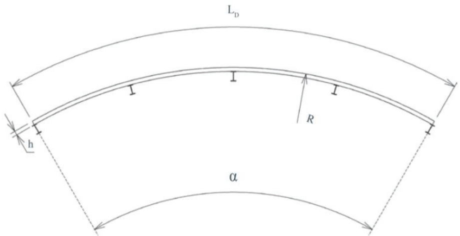

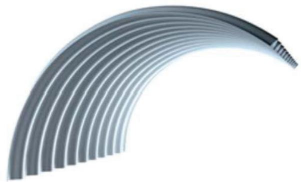

ROLL FORMING – Variant A

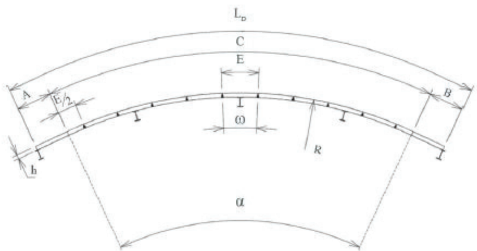

BY CRUSHING OF THE INNER FLANGE – Variant B

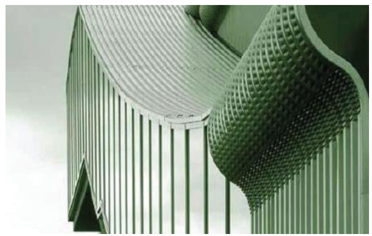

THROUGH IN SITU BENDING PROCESS – Variant C

The project has received financial support from the European Community (RFCS programme) under grant agreement No 754092

INTRODUCTION

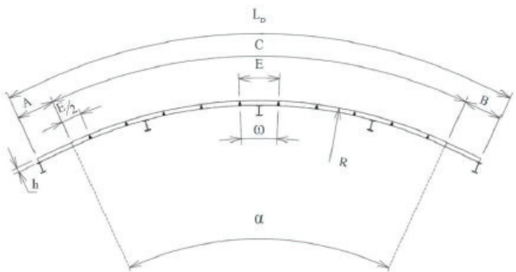

Variant B - CRUSHING OF THE INNER FLANGE

- This case (**VARIANT B**) is usually associated to <u>small span length</u> when adopted, and consequently not considered in the present research project.

THROUGH IN SITU BENDING PROCESS – Variant C

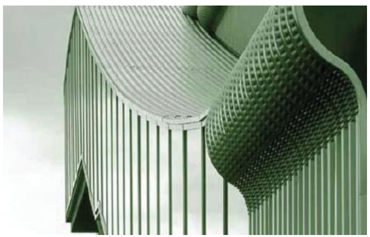

- This case (**VARIANT C**) is usually associated to <u>large curvature/bending radius</u> applied to the profile. The design can be consequently executed following the standard prescriptions imposed by **<u>Eurocode 3 (EN1993-1:2005)</u>** for flat profiles.

Variants B and C were then not considered in the main framework of GRISPE project

The project has received financial support from the European Community (RFCS programme) under grant agreement No 754092

INTRODUCTION

MAIN FOCUS OF GRISPE RESEARCH PROJECT

Investigation of the structural performance of **curved profiles obtained through a continuous roll-forming process** (**VARIANT A**). The structural performance shall be evaluated with reference to the bearing capacity of the corresponding flat profiles.

ROLL-FORMING process

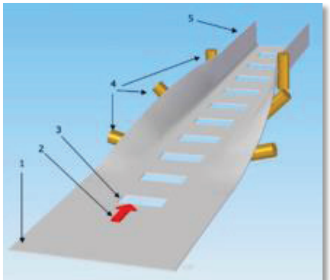

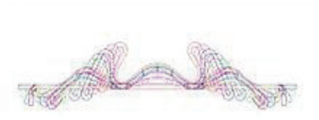

- Type of rolling process involving the **continuous bending of a long strip of sheet metal (typically coiled steel) into a desired cross-section**.
- The strip passed through sets of rolls mounted on consecutive stands, each set performing only an **incremental part** of the bend, until the desired cross-section (profile) is obtained.
- Roll forming is used for producing constant-profile parts with long lengths and in large quantities.-
- Roll-formed sections advantages over **extrusion** process: **components can be lighter, with thinner walls and stronger**, having been work hardened in a **cold state**. The roll forming process is more rapid than extrusion process.

The project has received financial support from the European Community (RFCS programme) under grant agreement No 754092

INTRODUCTION

MAIN FOCUS OF GRISPE RESEARCH PROJECT

Investigation of the structural performance of **curved profiles obtained through a continuous roll-forming process** (**VARIANT A**). The structural performance shall be evaluated with reference to the bearing capacity of the corresponding flat profiles.

ROLL-FORMING process

- The effects of the process on the **material's properties** are ***minimal***. The physical and chemical properties virtually don't change, but the process may cause work-hardening, micro-cracks, or thinning at bends when discussing the mechanical properties of the material.
- What was investigated in GRISPE project was the modification of the ***structural performance (bearing capacity)*** of the obtained curved profile with respect to flat profiles **(plastic deformations developing in the extreme fibres of the cross section may alter the bearing capacity)**

Data presented in the current scientific literature refer to variation of the bearing capacity of curved profiles respect to flat profiles around **10%/20%/30%**

Two situations investigated in GRISPE:

- **BENDING CAPACITY**
- **BENDING+AXIAL CAPACITY**

The project has received financial support from the European Community (RFCS programme) under grant agreement No 754092

ADOPTED METHODOLOGY

To evaluate the modifications induced by the roll-forming process on the bearing capacity of flat profiles (into curved ones), the following methodology was adopted inside GRISPE research project.

1

SELECTION OF THE TYPOLOGIES OF PROFILES

- Trapezoidal and sinusoidal sheets

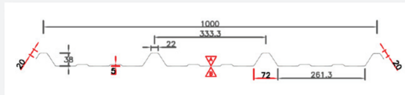

2

ORGANIZATION OF THE EXPERIMENTAL TESTS' CAMPAIGN

- Definition of the test setup
- Definition of the loading history to be applied
- Execution of tests with two different configurations
- Interpretation of results

3

ELABORATION OF DESIGN MODELS AND GUIDELINES

- Simple indications for design of curved profiles (M; M+N)
- Comparison with prescriptions proposed by DIN standards

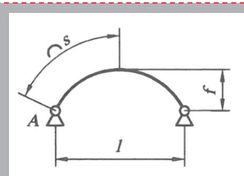

The project has received financial support from the European Community (RFCS programme) under grant agreement No 754092

SELECTION OF CURVED PROFILES

- **Trapezoidal profile with stiffener 39/333 (Arcelor Mittal)**

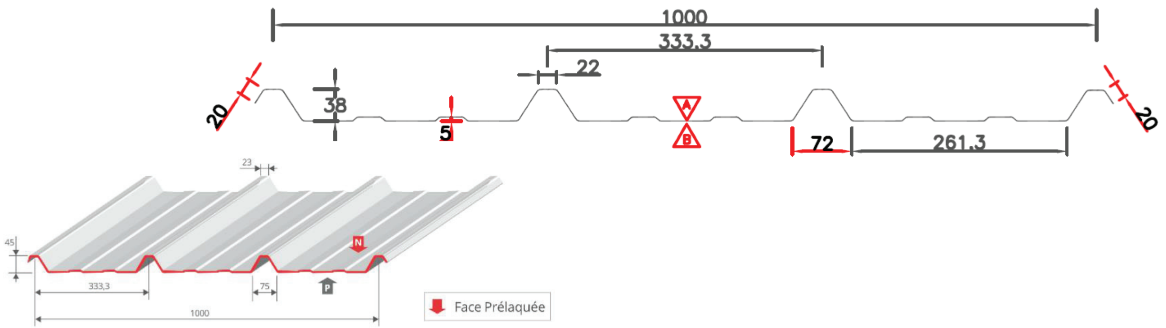

- **Sinusoidal profile 18/76 (Bacacier)**

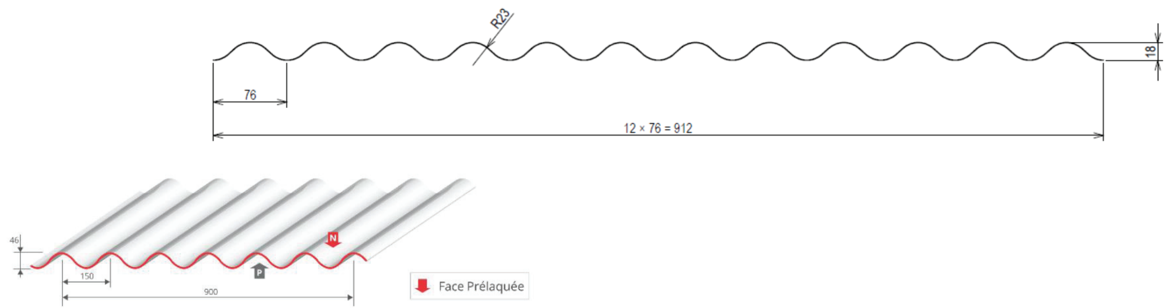

The project has received financial support from the European Community (RFCS programme) under grant agreement No 754092

SELECTION OF CURVED PROFILES

- **Trapezoidal profile 39/333 (Arcelor Mittal)**

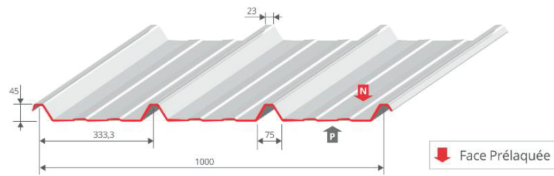

- **Sinusoidal profile 18/76 (Bacacier)**

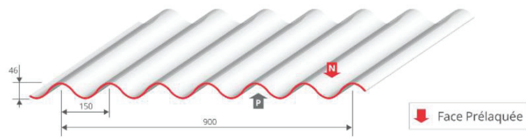

The tested specimens manufactured by Bacacier and Arcelor Mittal consist of **steel sheetings** according to **EN 10346:2009**, which are formed to curved corrugated sheets and curved trapezoidal sheets using the following section heights and overall widths by **roll-forming**:

Type of profile	Steel grade according to EN 10346:2009	Height [mm]	Width [mm]	Thickness [mm]
Bacacier 18/76	S320GD	18	912	0,63 and 1.00
Arcelor Mittal 39/333	S320GD	39	1000	0.63 and 1.00

The project has received financial support from the European Community (RFCS programme) under grant agreement No 754092

SELECTION OF CURVED PROFILES

A wide test program was performed to determine the **load-bearing capacity of curved profiles in bending for different bending radii.**

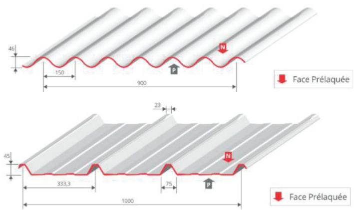

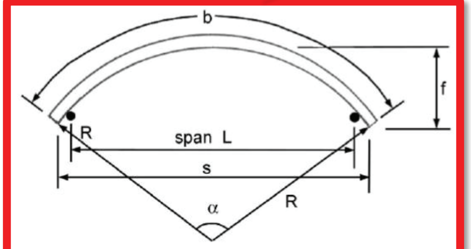

Type of test	Profile	R [m]	b [mm]	Span L [mm]	s [mm]	f [mm]	α [°]	Number of tests
Single span positive bending test	18/76 t_N = 0.63 mm	∞	2200	2000	2200	0	0	3
		20.0	2201			30	6.31	2
		10.0	2204			61	12.63	2
		4.0	2229			154	31.92	2
	18/76 t_N = 1.00 mm	∞	3200	3000	3200	0	0	1
		20.0	3203			64	9.18	4
		10.0	3214			129	18.41	3
		4.0	3292			334	47.16	3
	39/333 t_N = 0.63 mm	∞	3200	3000	3200	0	0	3
		20.0	3203			64	9.18	2
		10.0	3214			129	18.41	2
		6.0	3239			217	30.93	3
	39/333 t_N = 1.00 mm	∞	4200	4000	4200	0	0	2
		20.0	4208			111	12.05	2
		10.0	4232			223	24.24	2
		6.0	4291			380	40.98	2
Single span positive bending test with horizontal support	39/333 t_N = 0.63 mm	6.0	3239	3000	3200	217	30.93	2
		6.0	4291	4000	4200	380	40.97	3
		6.0	5300	5000	5129	576	50.61	3

The project has received financial support from the European Community (RFCS programme) under grant agreement No 754092

SETUP OF EXPERIMENTAL TESTS

SELECTION OF THE TESTING CONFIGURATIONS

Two different configurations were selected for the execution of the experimental tests, respectively for the analysis of the structural performance of the curved profile under only **BENDING ACTIONS** and under the condition of **COMBINED BENDING AND AXIAL FORCES**.

BENDING ACTIONS:
SINGLE SPAN TESTS

- Evaluation of the **mid-span bearing capacity** of the curved profile (with reference to the original flat one).
- Definition of an opportune scheme for restraints
- Application of a uniformly distributed loading action

A

COMBINED BENDING AND AXIAL ACTIONS:
SINGLE SPAN TESTS WITH HORIZONTAL SUPPORTS

- Evaluation of the **mid-span bearing capacity** of the curved profile (with reference to the original flat one).
- Definition of an opportune scheme for restraints (arch system, M+N)
- Application of a uniformly distributed loading action

B

The project has received financial support from the European Community (RFCS programme) under grant agreement No 754092

PRELIMINARY CHARACTERIZATION OF MATERIAL PROPERTIES

- 3 specimens per sheet and per thickness were worked out, from coupons extracted by the tested trapezoidal sheets or directly delivered by the producer.
- **Tensile tests were executed according to EN 6892-1:2009.**
- The determination of the yield strength $\mathbf{R_{p0.2}}$ and the tensile strength $\mathbf{R_m}$ was based upon the measured sheet thickness without zinc coating.

Profile	Nominal thickness t_N [mm]	Core thickness t_K [mm]	Yield strength $R_{p0,2}$ [N/mm²]	Tensile strength R_m [N/mm²]	Elongation at fracture $A_{L=80mm}$ [%]
18/76	0.63	0.53	330	456	26.2
		0.53	329	457	26.0
		0.52	329	456	25.4
	1.00	0.99	342	387	29.3
		1.00	346	387	27.6
		0.99	358	392	27.9
39/333	0.63	0.58	406	430	27.6
		0.58	411	430	26.4
		0.58	408	431	27.0
	1.00	0.96	379	425	24.7
		0.96	384	427	24.5
		0.95	382	426	25.4

The project has received financial support from the European Community (RFCS programme) under grant agreement No 754092

SELECTION OF THE TESTING CONFIGURATIONS

BENDING ACTIONS: SINGLE SPAN TESTS

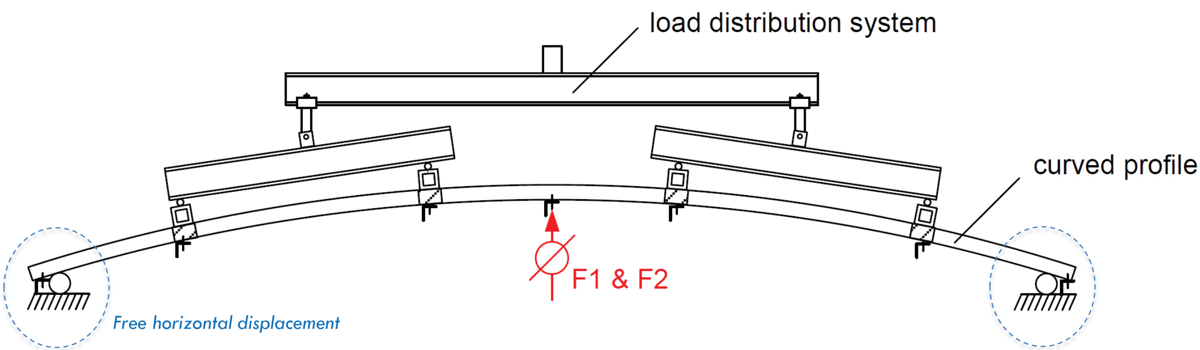

- **Determination of MID-SPAN MOMENT RESISTANCE: Single span tests** for load case "gravity loading" (positive bending) were performed with uniformly distributed load simulated by **four line loads**.
- The load was introduced into the valleys of the corrugated sheets or the bottom flanges of the trapezoidal sheets via **transverse steel sections and timber blocks**. The transverse steel sections were clamped with the profile.
- The test specimens are placed on supports which are **movable in horizontal direction**. Therefore, **no axial forces can appear in the apex of the curved specimen** where the bending moment becomes a maximum.

The project has received financial support from the European Community (RFCS programme) under grant agreement No 754092

SELECTION OF THE TESTING CONFIGURATIONS

BENDING ACTIONS: SINGLE SPAN TESTS

Trapezoidal sheet 39/333

The project has received financial support from the European Community (RFCS programme) under grant agreement No 754092

SELECTION OF THE TESTING CONFIGURATIONS

BENDING ACTIONS: SINGLE SPAN TESTS

Sinusoidal sheet 18/76

The project has received financial support from the European Community (RFCS programme) under grant agreement No 754092

SELECTION OF THE TESTING CONFIGURATIONS

BENDING ACTIONS: SINGLE SPAN TESTS

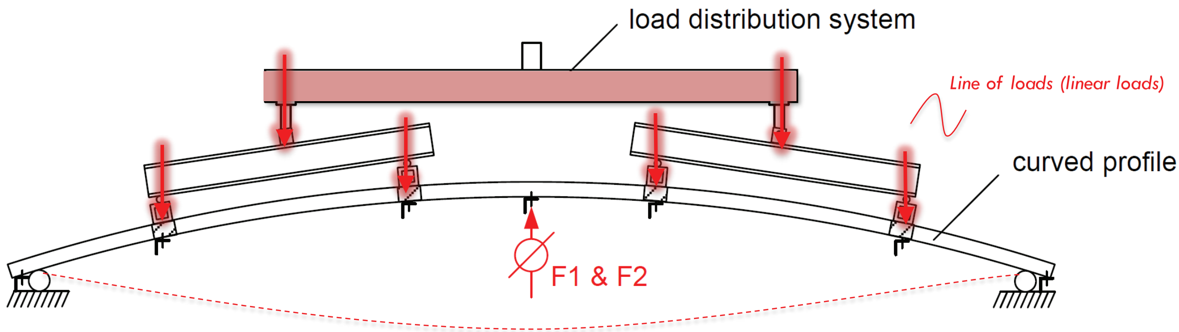

- In order to reduce the friction between the transverse steel beams at the supports of the load distribution system oil was used.
- The load was applied in **deflection-control** with a speed **of 6 mm/min to 15 mm/min**. The load was measured continuously using a load cell with a maximum capacity of 50 kN.
- The deflections were measured continuously in mid-span by two trip **wire displacement sensors,** under the bottom flanges.

The project has received financial support from the European Community (RFCS programme) under grant agreement No 754092

TESTS' RESULTS AND INTERPRETATION

BENDING ACTIONS: SINGLE SPAN TESTS

CORRUGATED SHEETS 18/76

Test	Span [mm]	t_N [mm]	b [mm]	Measured t_N incl. zinc coating [mm]	Measured height f [mm]		Measured width b [mm]	Preload [kN]	F_{max} [kN]
SSP-18-0-063-1[1)]	2000	0.63	2200	0.57	0	0	894	0.29	3.71
SSP-18-0-063-2[1)]				0.56	0	0	895		4.07
SSP-18-0-063-3[1)]				0.56	0	0	890		3.91
SSP-18-30-063-1[1)]			2201	0.59	40	47	890	0.29	3.97
SSP-18-30-063-2[1)]				0.55	40	48	892		3.93
SSP-18-61-063-1[1)]			2204	0.56	45	56	888		4.11
SSP-18-61-063-2[1)]				0.56	48	60	890		4.01
SSP-18-154-063-1[2)]			2229	0.56	120	115	890	0.49	4.98
SSP-18-154-063-2[2)]				0.55	120	120	895		4.86
SSP-18-0-100-1[1)]	3000	1.00	3200	1.00	0	0	887	0.35	-
SSP-18-0-100-2				-	-	-	-	-	-
SSP-18-64-100-1[2)]			3203	0.99	75	60	885	0.49	-
SSP-18-64-100-2[2)]				0.99	70	70	885		-
SSP-18-64-100-3[2)]				0.99	64	60	885		-
SSP-18-64-100-4[2)]				0.99	60	65	885		-
SSP-18-129-100-1[2)]			3214	1.01	110	120	885	0.49	-
SSP-18-129-100-2[2)]				1.00	110	125	885		-
SSP-18-129-100-3[2)]				0.99	90	85	885		-
SSP-18-334-100-1[2)]			3292	1.00	320	300	885	0.80	-
SSP-18-334-100-2[2)]				1.00	325	295	885		-
SSP-18-334-100-3[2]				1.00	315	300	885		-

- Failure occurred by **local buckling of the crest** (corrugated sheets) in the span generally for thickness 0.63 mm.
- Failure by **plastic deformation** occurred in all tests of the corrugated sheets (profile 18/76) with a nominal thickness of $\mathbf{t_N}$ **= 1.00 mm**, <u>none F_{max} value is then determined.</u>

<u>*The load Fmax indicates the failure load including preload, but without self-weight of the test specimen*</u>

*1) test setup for flat profiles, 2) test setup for curved profiles, *) test setup for curved profiles without oil at supports of the load distribution system*

The project has received financial support from the European Community (RFCS programme) under grant agreement No 754092

TESTS' RESULTS AND INTERPRETATION

BENDING ACTIONS: SINGLE SPAN TESTS

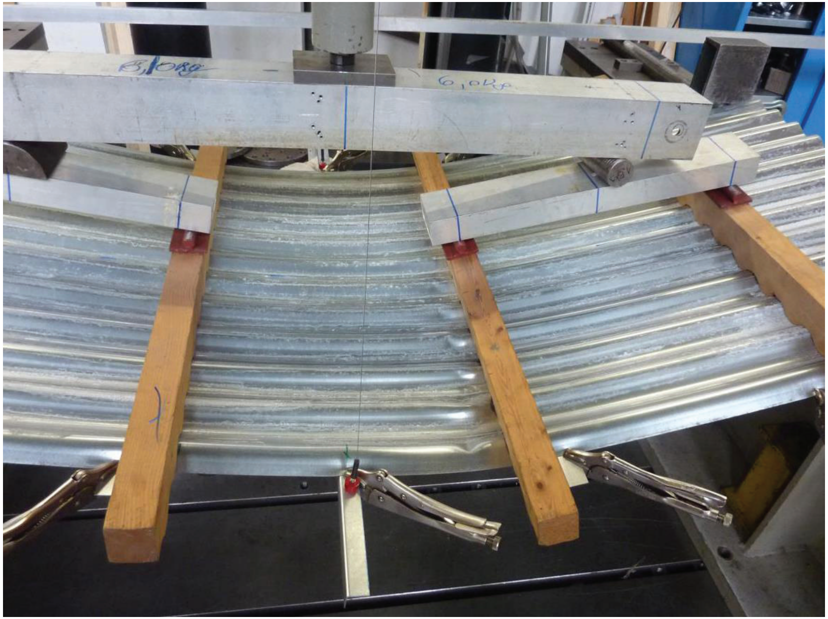

CORRUGATED SHEETS 18/76

- Failure mode (**local buckling**) of profile 18/76, t_N = **0.63 mm**

The project has received financial support from the European Community (RFCS programme) under grant agreement No 754092

TESTS' RESULTS AND INTERPRETATION

BENDING ACTIONS: SINGLE SPAN TESTS

CORRUGATED SHEETS 18/76

- Failure mode (**plastic deformation)** of profile 18/76 $\mathbf{t_N}$ **= 1.00 mm**

The project has received financial support from the European Community (RFCS programme) under grant agreement No 754092

TESTS' RESULTS AND INTERPRETATION

BENDING ACTIONS: SINGLE SPAN TESTS

CORRUGATED SHEETS 18/76

The project has received financial support from the European Community (RFCS programme) under grant agreement No 754092

TESTS' RESULTS AND INTERPRETATION

BENDING ACTIONS: SINGLE SPAN TESTS

Load-deflection curve (local buckling occurred – 0.63 mm)

CORRUGATED SHEETS 18/76

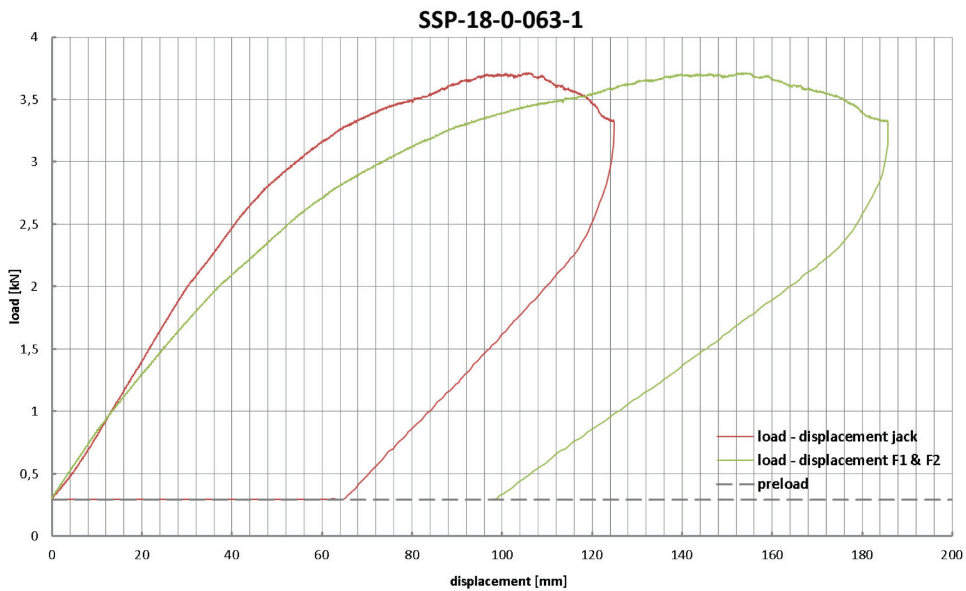

The project has received financial support from the European Community (RFCS programme) under grant agreement No 754092

TESTS' RESULTS AND INTERPRETATION

BENDING ACTIONS: SINGLE SPAN TESTS

Test	Span [mm]	t_N [mm]	b [mm]	Measured t_N incl. zinc coating [mm]	Measured height f [mm]		Measured width b [mm]	Preload [kN]	F_{max} [kN]
SSP-39-0-063-1[1)]	3000	0.63	3200	0.66	0	0	668	0.43	2.09
SSP-39-0-063-2[1)]				0.65	0	0	660		2.03
SSP-39-0-063-3[2)]				0.65	0	0	670	0.40	1.85
SSP-39-64-063-1[1)]			3203	0.66	37	34	660	0.43	1.92
SSP-39-64-063-2[1)]				0.66	34	32	663		1.96
SSP-39-129-063-1[1)]			3214	0.65	116	116	663	0.48	1.84
SSP-39-129-063-2[1)]				0.65	116	120	661		1.85
SSP-39-217-063-1[2)]			3239	0.64	205	200	670	0.49	1.61
SSP-39-217-063-2[2)]				0.66	205	205	670		1.56
SSP-39-217-063-3[2)]				0.68	210	210	668		1.65
SSP-39-0-100-1[1)]	4000	1.00	4200	1.02	0	0	665	0.71	2.80
SSP-39-0-100-2[1)]				1.01	0	0	668		2.81
SSP-39-111-100-1[1)]			4208	1.01	74	82	668		2.78
SSP-39-111-100-2[1)]				1.02	74	80	668		2.72
SSP-39-223-100-1[2)]			4232	1.02	190	190	670	0.49	2.81
SSP-39-223-100-2[2)]				1.03	190	190	670		2.82
SSP-39-380-100-1[2)]			4291	1.03	320	327	670	0.49	2.82
SSP-39-380-100-2[2)]				1.04	325	315	670		2.85

Trapezoidal Sheet 39/333

Failure occurred by **local buckling of upper flange** (trapezoidal sheets) in the span; in this case no problem of plastic deformation like in the case of sinusoidal sheet.

The load F_{max} indicates the failure load including preload, but without self-weight of the test specimen

The project has received financial support from the European Community (RFCS programme) under grant agreement No 754092

TESTS' RESULTS AND INTERPRETATION

BENDING ACTIONS: SINGLE SPAN TESTS

Trapezoidal Sheet 39/333

- Failure mode (**local buckling of the upper flange**) of profile 39/333 with arch stitch h = 217 mm

The project has received financial support from the European Community (RFCS programme) under grant agreement No 754092

TESTS' RESULTS AND INTERPRETATION

BENDING ACTIONS: SINGLE SPAN TESTS

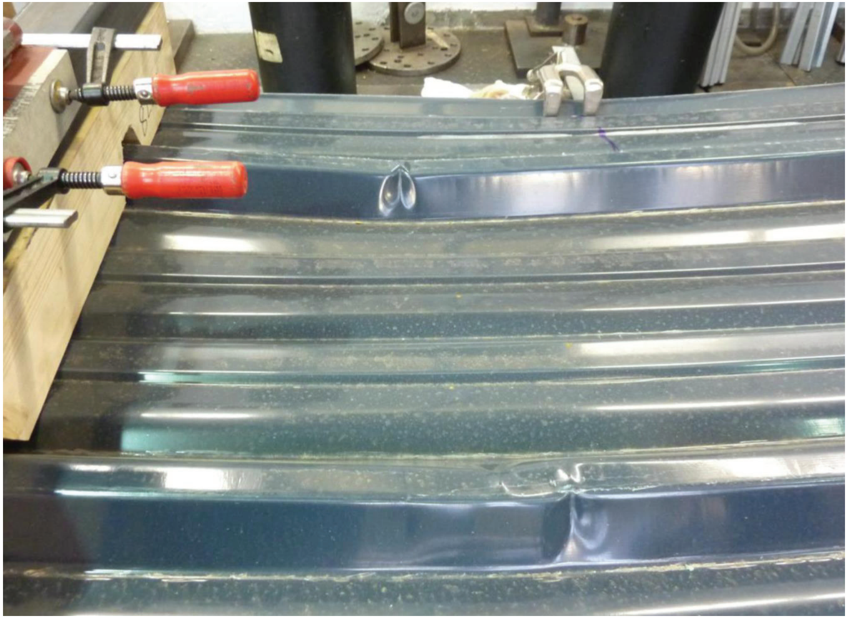

Trapezoidal Sheet 39/333

- Failure mode (**local buckling of the upper flange**) of profile 39/333

The project has received financial support from the European Community (RFCS programme) under grant agreement No 754092

SETUP OF EXPERIMENTAL TESTS

B

SELECTION OF THE TESTING CONFIGURATIONS

COMBINED BENDING AND AXIAL ACTIONS:
SINGLE SPAN TESTS WITH HORIZONTAL SUPPORTS

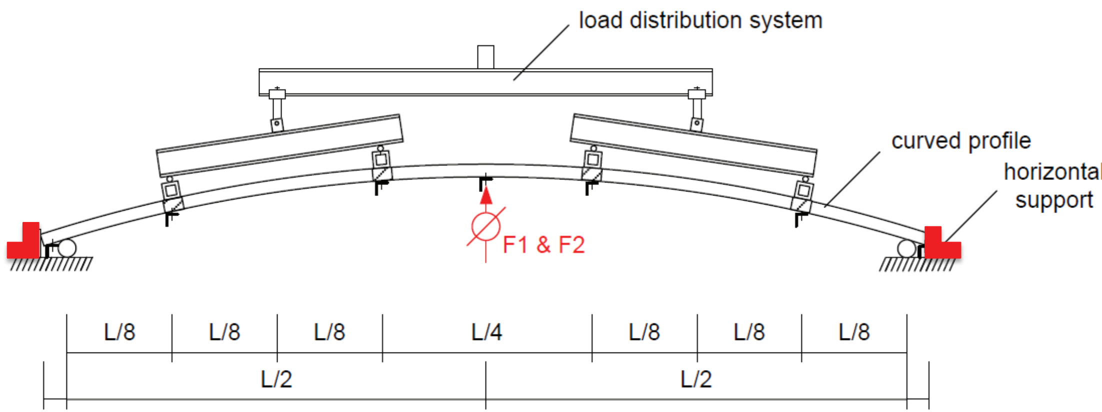

- Tests performed on curved profiles placed on **horizontally fixed supports**.
- The profile works as an **ARCH**, stressed by **bending moments and axial combined forces**.
- By varying the span of the specimen, different slopes are performed and consequently **different ratios bending moment/axial compression**.

The project has received financial support from the European Community (RFCS programme) under grant agreement No 754092

SELECTION OF THE TESTING CONFIGURATIONS

COMBINED BENDING AND AXIAL ACTIONS:
SINGLE SPAN TESTS WITH HORIZONTAL SUPPORTS

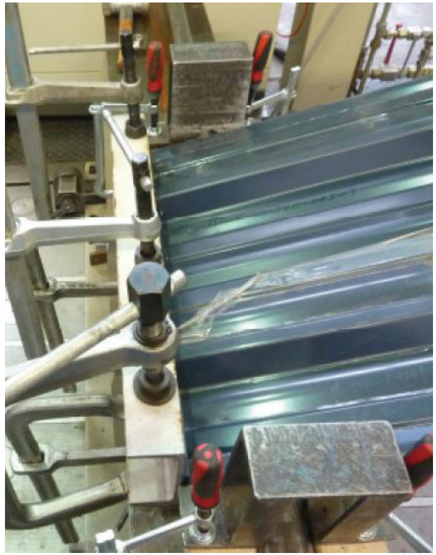

The project has received financial support from the European Community (RFCS programme) under grant agreement No 754092

TESTS' RESULTS AND INTERPRETATION

COMBINED BENDING AND AXIAL ACTIONS: SINGLE SPAN TESTS WITH HORIZONTAL SUPPORTS

Results of single span tests of profile 39/333 with horizontal support

Test	Span [mm]	Measured t_N incl. zinc coating [mm]	Measured height f [mm]		Measured width b [mm]	Preload [kN]	F_{max} [kN]
SSP-H-39-217-063-1[1)]	3000	0.66	200	210	670	0.49	9.12
SSP-H-39-217-063-2[1)]		0.66	205	210	670		8.95
SSP-H-39-380-063-1[1)]	4000	0.66	330	350	670	0.49	9.49
SSP-H-39-380-063-2[1)]		0.66	340	350	670		11.43
SSP-H-39-380-063-3[1)]		0.66	335	345	370		11.03
SSP-H-39-576-063-1[1)]	5000	0.65	460	465	665	0.49	5.67
SSP-H-39-576-063-2[1)]		0.67	450	455	668		5.17
SSP-H-39-576-063-3[1)]		0.67	460	465	665		6.83

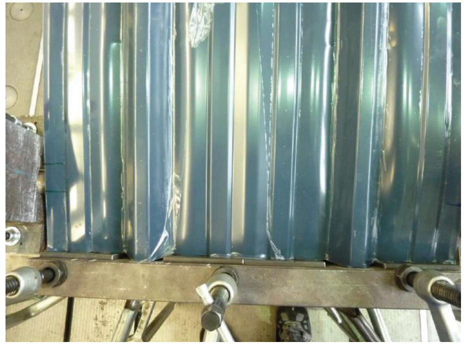

Plastic deformations were observed in correspondence of the horizontal supports were the sheet is fixed

The project has received financial support from the European Community (RFCS programme) under grant agreement No 754092

TESTS' RESULTS AND INTERPRETATION

COMBINED BENDING AND AXIAL ACTIONS: SINGLE SPAN TESTS WITH HORIZONTAL SUPPORTS

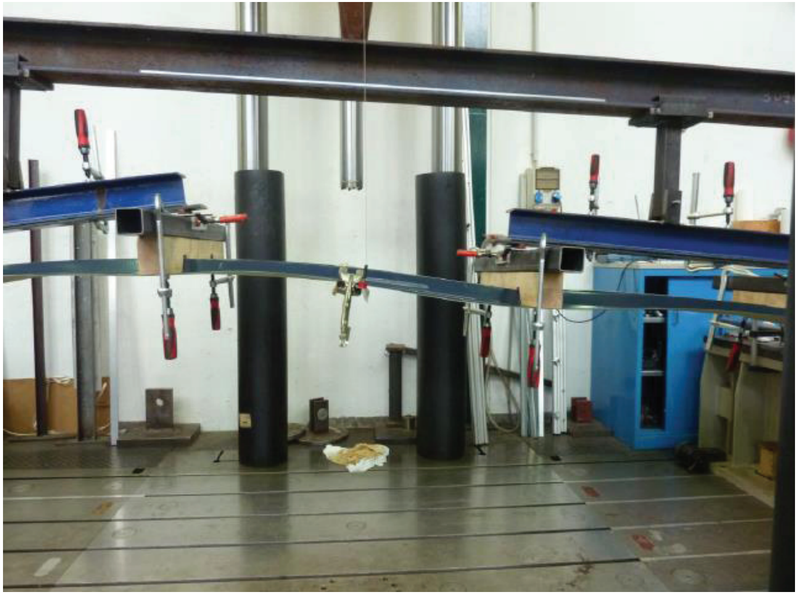

Trapezoidal Sheet 39/333

- Failure mode (**buckling of the arch**) for arch stitch h = 217 mm and h = 380 mm

The project has received financial support from the European Community (RFCS programme) under grant agreement No 754092

TESTS' RESULTS AND INTERPRETATION

COMBINED BENDING AND AXIAL ACTIONS: SINGLE SPAN TESTS WITH HORIZONTAL SUPPORTS

Trapezoidal Sheet 39/333

- Failure mode for specimen SSP-H-576-063-1, side view

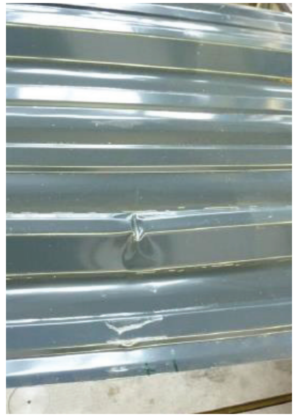

The project has received financial support from the European Community (RFCS programme) under grant agreement No 754092

TESTS' RESULTS AND INTERPRETATION

COMBINED BENDING AND AXIAL ACTIONS: SINGLE SPAN TESTS WITH HORIZONTAL SUPPORTS

Load-Deflection curve

SSP-H-39-217-063-1

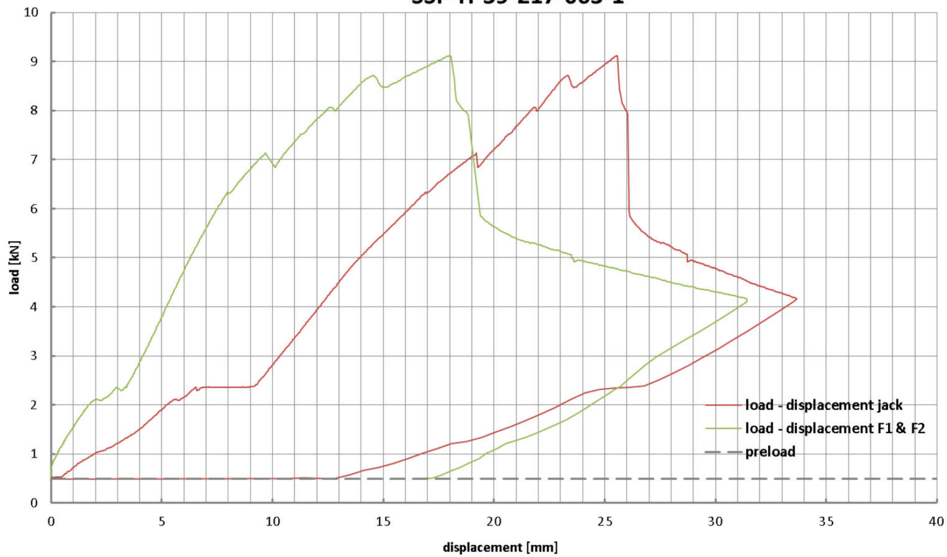

The project has received financial support from the European Community (RFCS programme) under grant agreement No 754092

BEARING CAPACITY ASSESSMENT

SPECIMENS SUBJECTED TO ONLY BENDING ACTIONS

Evaluation of the mid-span bending resistance

$$M_{c,Rk,F} = \frac{F_{u,k}}{b_v} \cdot \frac{L}{8} + \gamma \cdot L_v \cdot \frac{[2L - L_v]}{8}$$

- *$M_{c,Rk,F}$ characteristic bending moment in span (kNm/m)*
- *$F_{u,k}$ characteristic load in kN (including preload)*
- *b_V width of the specimen (here: b_V = 0,912 or 1,00 m)*
- *L_V length of the specimen (here: L_V = 2,20 or 3,20 or 4,20 m)*
- *L span length (here: L = 2,00 or 3,00 or 4,00 m)*

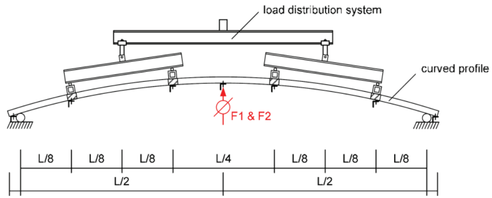

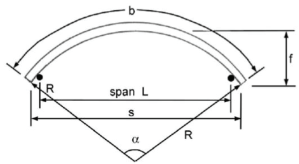

Bacacier 18/76-0,63			Bacacier 18/76-1,00			Arcelor 39/333-0,63			Arcelor 39/333-1,00		
R m	1/R 1/m	$M_{c,Rk,F}$ kNm/m	R m	1/R 1/m	$M_{c,Rk,F}$ kNm/m	R m	1/R 1/m	$M_{c,Rk,F}$ kNm/m	R m	1/R 1/m	$M_{c,Rk,F}$ kNm/m
flat	0,000	1,057	flat	0	1,727	flat	0	0,785	flat	0	1,539
11,5	0,087	1,071	17,2	0,058	1,736	32,9	0,030	0,767	25,8	0,039	1,513
9,6	0,104	1,100	10,6	0,094	1,674	9,7	0,103	0,733	10,6	0,094	1,544
4,3	0,234	1,327	3,8	0,264	1,661	5,6	0,180	0,647	6,4	0,157	1,554

The project has received financial support from the European Community (RFCS programme) under grant agreement No 754092

SPECIMENS SUBJECTED TO ONLY BENDING ACTIONS

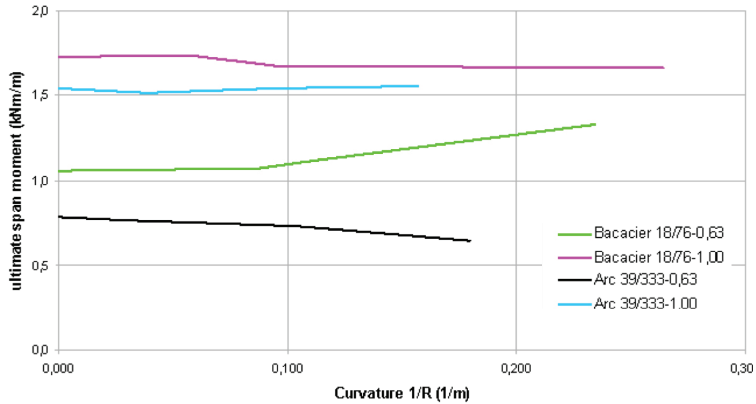

Bacacier 18/76-0,63			Bacacier 18/76-1,00			Arcelor 39/333-0,63			Arcelor 39/333-1,00		
R m	1/R 1/m	$M_{c,Rk,F}$ kNm/m	R m	1/R 1/m	$M_{c,Rk,F}$ kNm/m	R m	1/R 1/m	$M_{c,Rk,F}$ kNm/m	R m	1/R 1/m	$M_{c,Rk,F}$ kNm/m
flat	0,000	1,057	flat	0	1,727	flat	0	0,785	flat	0	1,539
11,5	0,087	1,071	17,2	0,058	1,736	32,9	0,030	0,767	25,8	0,039	1,513
9,6	0,104	1,100	10,6	0,094	1,674	9,7	0,103	0,733	10,6	0,094	1,544
4,3	0,234	1,327	3,8	0,264	1,661	5,6	0,180	0,647	6,4	0,157	1,554

The project has received financial support from the European Community (RFCS programme) under grant agreement No 754092

SPECIMENS SUBJECTED TO ONLY BENDING

Design proposition for curved profiles: conclusions coming from the analysis of tests 'results

1. The curving process by bending or by roll-forming creates **plastic deformations in the extreme fibres of the cross section.** This generates internal stresses that can influence the bending moment capacity of the profile. Anyway, **test results evidenced a rather small and not uniform influence on the bearing capacity.**
2. **For the profiles with thickness 1,0 mm, the curvature (1/R) doesn't change the bending moment capacity.**
3. **For the profiles with thickness 0,63 mm,** the bending moment capacity is affected in both senses:

   + 25 % for the sinusoidal profile 18/76

   - 15 % for the trapezoidal profile 39/333

4. With respect to this indifferent behaviour and regarding the low sensitivity of the bending moment capacity **it is proposed to reduce the bending moment capacity by 10 % compared to the bending moment capacity of the flat profile**. This reduction factor is an additional safety factor to cover the indifferent scattering; it is not a mechanically based coefficient.

$$M_{c,Rk,F}\,(\text{curved profiles}) = 0.90 \cdot M_{c,Rk,F}\,(\text{flat profiles})$$

The project has received financial support from the European Community (RFCS programme) under grant agreement No 754092

SPECIMENS SUBJECTED TO ONLY BENDING ACTIONS

Design proposition for curved profile conclusions concerning tests 'results

Comparison between the values directly derived from experimental tests on curved profiles and assumed design value (design proposition elaborated in GRISPE)- the design proposition for bending is **CONSERVATIVE**

profile	nominal thickness t (mm)	radius of curvature R (m)	charact. bending moment (test value) $M_{c,Rk,F}$ (kNm/m)	design proposition $0,9 * M_{c,Rk,F\ (flat)}$ (kNm/m)	ratio design/test
Bacacier 18/76	0,63	flat	1,057		
		11,5	1,071	0,951	0,89
		9,6	1,100	0,951	0,86
		4,3	1,327	0,951	0,72
	1,00	flat	1,727		
		17,2	1,736	1,554	0,89
		10,6	1,674	1,554	0,93
		3,8	1,661	1,554	0,94
Arcelor 39/333	0,63	flat	0,785		
		32,9	0,767	0,707	0,92
		9,7	0,733	0,707	0,96
		5,6	0,647	0,707	1,09
	1,00	flat	1,539		
		25,8	1,513	1,385	0,92
		10,6	1,544	1,385	0,90
		6,4	1,554	1,385	0,89

The project has received financial support from the European Community (RFCS programme) under grant agreement No 754092

BEARING CAPACITY ASSESSMENT

SPECIMENS SUBJECTED TO COMBINED M+N

- The static system of the test specimen is **hyperstatic;** the internal forces don't depend only upon the applied load, but also on the **stiffness parameters** of the beam and its supports.
- The statistic evaluation is applied on the failure loads in order to determine an individual characteristic (failure) load for each subset.

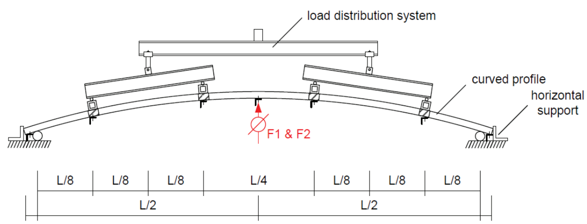

The problem in this case is more complicated and shall be solved in an indirect way, since the internal forces depend on several factors that are not immediately known, such as:

- **EA and EJ of the profile section**
- **K (C) of the horizontal restraints positioned at the ends of the profile.**

NUMERICAL SIMULATIONS

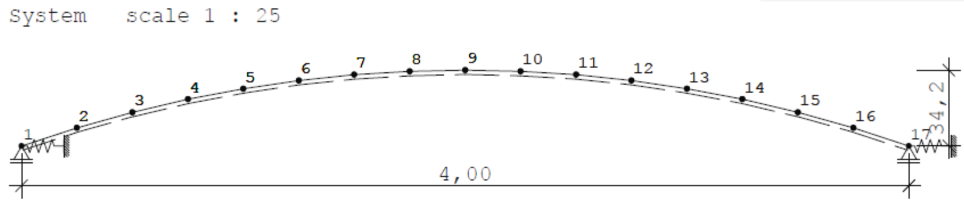

The project has received financial support from the European Community (RFCS programme) under grant agreement No 754092

SPECIMENS SUBJECTED TO COMBINED M+N

MODEL for SIMULAIONS: The curved profile is approximated as a polygonal line

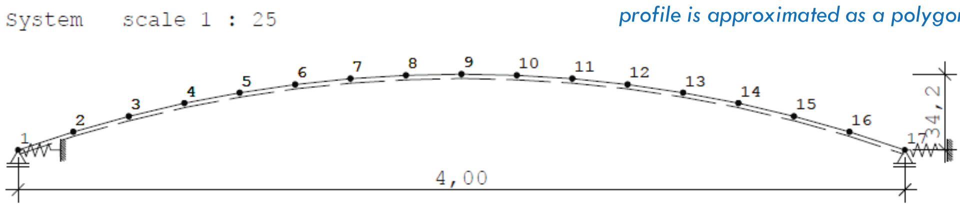

PARAMETERS CONSIDERED IN THE NUMERICAL SIMULATIONS

- **Spring stiffness of the horizontal support**
  fixed ($C = \infty$)
  C = 20 kN/m/cm
  C = 10 kN/m/cm
  Cind (29 > 88 kN/m/cm)

Note: neglecting the displacements at the ends leads to unsafe values (bending underestimated)

The spring stiffness Cind is different for each arch; this value is calibrated according to the condition, that the calculated vertical deflection at summit is the same as measured in the test family.

- **Cross section properties**
  gross cross section Ag , Jg
  effective cross section Aef , Jef

The project has received financial support from the European Community (RFCS programme) under grant agreement No 754092

CALIBRATION OF SUPPORT STIFFNESS

1. For each test **the deflection at mid span** is evaluated, as well as the **ultimate load corresponding to failure;** as a consequence, the overall stiffness of the specimen **$C_{f,i}$** can be evaluated as:

$$C_{f,i} = F_u / f_{max}$$

2. The mean value of the stiffness of the specimens achieved form tests **C_f** is considered as representative for this family and can be evaluated as:

$$C_f = \mathrm{mean}(C_{f,i})$$

3. Using the overall stiffness value of the family, a midspan deflection under characteristic failure load can be calculated, which is considered as representative for this family. Since the internal forces of the arch are calculated for the unit width, the result should be multiplied with the width of the test specimen.

$$f_{eq} = F_{u,k} / C_f \cdot b_v$$

test no. SSP-H-39-…	F_u kN	deflection f_{max} at mid-span (mm)	L m	b_V m	overall stiffness specimen $C_{f,i}$ (kN/mm)	mean value stiffness C_f	repr. deflection (mm) for $F_{u,k}$, width 1 m
217-063-1	9,12	18,0	3,00	0,667	0,507	0,444	16,6
217-063-2	8,95	23,5	3,00	0,667	0,381		
576-063-2	5,17	14,1	5,00	0,667	0,367		
576-063-3	6,83	18,0	5,00	0,667	0,379		

*Calculating the arch with the software, **the spring stiffness of the horizontal support is varied and finally locked to a value, for which the calculated midspan deflection under characteristic failure load corresponds to the deflection feq.***

This spring stiffness of the horizontal support is the above mentioned Cind.

The project has received financial support from the European Community (RFCS programme) under grant agreement No 754092

SPECIMENS SUBJECTED TO COMBINED M+N: Evaluation of internal M/N forces

Test setup/ span	Cross section	spring stiffness at support (kN/m/cm)	Failure load	displacements (cm)		support reactions (kN/m)		M- / N-values (kNm/m, kN/m)		
								at load point near to summit		at support
			(kN/m)	f_h (support)	f_v (summit)	R_h	R_v	max M	corresp N	max N
1 / 3,00 m	gross	fixed	11,03	0,00	0,11	20,46	5,52	0,17	20,62	21,19
		68,0	11,03	0,28	1,67	18,81	5,52	0,49	18,98	19,60
		20,0	11,03	0,79	4,55	15,76	5,52	1,08	15,94	16,65
		10,0	11,03	1,28	7,33	12,82	5,52	1,65	13,01	13,80
	effective	fixed	11,03	0,00	0,41	20,35	5,52	0,19	20,51	21,08
		88,0	11,03	0,22	1,66	19,64	5,52	0,33	19,80	20,40
		20,0	11,03	0,88	5,33	17,57	5,52	0,73	17,74	18,39
		10,0	11,03	1,55	9,08	15,46	5,52	1,14	15,64	16,35
2 / 4,00 m	gross	fixed	12,77	0,00	0,08	19,13	6,39	0,25	19,35	20,16
		62,0	12,77	0,30	1,45	18,64	6,39	0,40	18,87	19,70
		20,0	12,77	0,88	4,10	17,69	6,39	0,71	17,92	18,80
		10,0	12,77	1,64	7,56	16,45	6,39	1,11	16,69	17,62
	effective	fixed	12,77	0,00	0,39	19,09	6,39	0,26	19,31	20,13
		79,0	12,77	0,24	1,44	18,88	6,39	0,33	19,11	19,93
		20,0	12,77	0,91	4,51	18,29	6,39	0,51	18,53	19,37
		10,0	12,77	1,76	8,33	17,56	6,39	0,75	17,80	18,68
3 / 5,00 m	gross	fixed	6,62	0,00	0,02	9,23	3,31	0,16	9,36	9,81
		29,0	6,62	0,31	1,34	9,01	3,31	0,26	9,14	9,60
		20,0	6,62	0,45	1,91	8,91	3,31	0,30	9,04	9,50
		10,0	6,62	0,86	3,67	8,61	3,31	0,43	8,74	9,22
	effective	fixed	6,62	0,00	0,23	9,22	3,31	0,16	9,35	9,80
		33,0	6,62	0,28	1,33	9,12	3,31	0,21	9,09	9,70
		20,0	6,62	0,45	2,07	9,05	3,31	0,24	9,18	9,63
		10,0	6,62	0,89	3,91	8,88	3,31	0,31	9,01	9,48

The project has received financial support from the European Community (RFCS programme) under grant agreement No 754092

DIN 18807 APPROACH FOR THE EVALUATION OF M/N INTERACTION

In case of compression force the following equation can be applied:

$$\frac{N_D}{N_{d,D}} \cdot \left[1 + 0{,}5 \cdot \alpha \cdot \left(1 - \frac{N_D}{N_{d,D}}\right)\right] + \frac{M}{M_d} \leq 1$$

N_D design value of compressive force
M design value of bending moment
Md design resistance of bending moment
N_{dD} design resistance of compressive force

$$\alpha = \frac{L_{cr}}{i_{ef} \cdot \pi} \cdot \sqrt{\frac{f_{y,k}}{E}}$$

L_{cr} buckling length
i_{ef} radius of gyration of the effective cross section

PROBLEM

- In the **M-N-interaction formula,** the coefficient α should be limited to 1 if **α > 1.**
- Anyway, this limit is not valid when the slenderness ratio α is used to determine the ultimate compressive stress with respect to overall buckling.
- **Hereafter, the DIN-procedure for combined bending moment/axial compression, adapted to curved profiles is described in detail organizing it into 4 different steps.**

The project has received financial support from the European Community (RFCS programme) under grant agreement No 754092

DIN 18807 APPROACH FOR THE EVALUATION OF M/N INTERACTION

- **Step 1: <u>Determination of the internal forces of the arch under characteristic failure load (= design load)</u>** under consideration of the horizontal spring stiffness C at the supports (M and N depends on C).

Test setup/ span	Cross section	spring stiffness at support (kN/m/cm)	Failure load (kN/m)	displacements (cm) f_h (support)	f_v (summit)	support reactions (kN/m) R_h	R_v	M- / N-values (kNm/m, kN/m) at load point near to summit: max M	corresp N	at suppor t: max N
1 / 3,00 m	gross	fixed	11,03	0,00	0,11	20,46	5,52	0,17	20,62	21,19
		68,0	11,03	0,28	1,67	18,81	5,52	0,49	18,98	19,60
		20,0	11,03	0,79	4,55	15,76	5,52	1,08	15,94	16,65
		10,0	11,03	1,28	7,33	12,82	5,52	1,65	13,01	13,80
	effective	fixed	11,03	0,00	0,41	20,35	5,52	0,19	20,51	21,08
		88,0	11,03	0,22	1,66	19,64	5,52	0,33	19,80	20,40
		20,0	11,03	0,88	5,33	17,57	5,52	0,73	17,74	18,39
		10,0	11,03	1,55	9,08	15,46	5,52	1,14	15,64	16,35
2 / 4,00 m	gross	fixed	12,77	0,00	0,08	19,13	6,39	0,25	19,35	20,16
		62,0	12,77	0,30	1,45	18,64	6,39	0,40	18,87	19,70
		20,0	12,77	0,88	4,10	17,69	6,39	0,71	17,92	18,80
		10,0	12,77	1,64	7,56	16,45	6,39	1,11	16,69	17,62

Evaluation of the values of M and N corresponding to the failure load

- **Step 2: <u>Determination of the buckling length Lcr</u>.** The buckling length of a circle-shaped arch can be found in the literature, for instance <u>DIN 18800 part 2</u>:

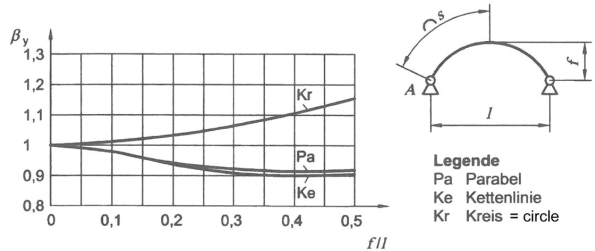

The project has received financial support from the European Community (RFCS programme) under grant agreement No 754092

DIN 18807 APPROACH FOR THE EVALUATION OF M/N INTERACTION

- **Step 3: Determination of design resistance to compressive axial force**

$$N_{d,D} = min\left(\sigma_{cd} \cdot A_{ef}; 0{,}8\sigma_{elg} \cdot A_g\right)$$

Ideal buckling force

$$maxN_{dD} = 0{,}8 \cdot \sigma_{elg} \cdot A_g = 0{,}8 \cdot \frac{\pi^2 \cdot E \cdot J_g}{L_{cr}^2}$$

Critical buckling force

$$ultN_{dD} = \sigma_{cd} \cdot A_{ef}$$

Slenderness ratio

$$\alpha = \frac{L_{cr}}{i_{ef} \cdot \pi} \cdot \sqrt{\frac{f_{y,k}}{E}}$$

α	σ_{cd}/β_S
$\alpha \leq 0{,}30$	1,00
$0{,}30 < \alpha \leq 1{,}85$	$1{,}126 - 0{,}419 \cdot \alpha$
$1{,}85 < \alpha$	$1{,}2/\alpha^2$

- **Step 4: Final interaction M/N and final assessment**

$$\frac{N_D}{N_{d,D}} \cdot \left[1 + 0{,}5 \cdot \alpha \cdot \left(1 - \frac{N_D}{N_{d,D}}\right)\right] + \frac{M_D}{M_{d,D}} \leq 1$$

The project has received financial support from the European Community (RFCS programme) under grant agreement No 754092

FINAL CONCLUSIONS

For curved profiles with only bending actions it is proposed to reduce the bending moment capacity by 10 % compared to the bending moment capacity of the flat profiles.

For curved profiles with horizontal support (arch: M+N) it is proposed to use the following design procedure:

1. The internal forces of the arch (bending moments, axial forces) should be calculated using the gross cross section values Ag and Jg of the profiled sheeting.
2. ***The horizontal displacement at supports may not be neglected.*** As greater the displacement is estimated, the internal forces become more unfavourable. Therefore it is necessary to take into account the horizontal displacement **by modelling the support with a horizontal spring**. The spring stiffness, which depends on the substructure and the fixing of the profiled sheeting, should be adjusted, that the calculated horizontal displacements meet the real values. To avoid unsafe design, the spring stiffness should not be over-estimated. Under-estimation of the spring stiffness leads to an over-estimation of the horizontal displacements and in consequence to a design on the safe side.
3. The bending moment – axial compression – interaction should be calculated with the interaction formula of DIN 18807, **but without limitation of α to 1**.

Please note that the design model is verified only for arches with symmetric loading.

The project has received financial support from the European Community (RFCS programme) under grant agreement No 754092

Cracow Workshop, 14.06.2018

CURVED PROFILES

THANK YOU FOR YOUR ATTENTION!

The project has received financial support from the European Community (RFCS programme) under grant agreement No 754092

GRISPE PLUS

VALORISATION OF KNOWLEDGE
FOR SPECIFIC PROFILED STEEL SHEETS

Assembled profiles

Ph. D. Thibault RENAUX – Joris Ide

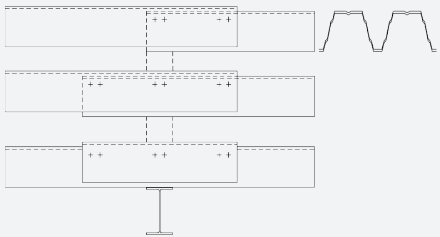

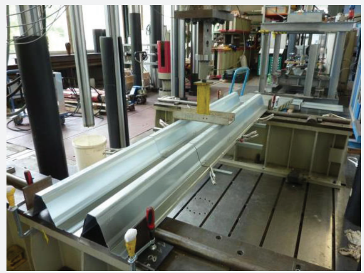

The project has received financial support from the European Community (RFCS programme) under grant agreement No 754092

Agenda

- Participant presentation
- Component description and application field
- Acquired data through GRISPE project
- Design and calculation method for assembled profiles
- Software and design manual
- Conclusion

The project has received financial support from the European Community (RFCS programme) under grant agreement No 754092

Presentation of Joris Ide Group

The project has received financial support from the European Community (RFCS programme) under grant agreement No 754092

Presentation of Joris Ide Group

An entrepreneurial growth story

1985
Establishment of Joris Ide NV

1994
Acquisition of Mafer (B)

1996
Establishment of Profinord (FR) and Balex Metal (PL)
Acquisition of Perma System (B)

2000
Acquisition of stake in SBP (FR) and Europe Twintile (B)

2001
Establishment of Megaprofil Romania and JORIS IDE Auvergne (FR)

2002
First sandwichpanel on continuous line
Acquisition of CBI (FR)

2004
Acquisition of stake in Isometall (B)
Establishment of JORIS IDE Hungary

2005
Acquisition of Lacafer and JORIS IDE Bourgogne (FR)
Establishment of JORIS IDE UK and Megaprofil Croatia

2006
Partnership with Ergon Capital Partners
Establishment of JORIS IDE Sud Ouest (FR) and Megaprofil Russia

2008
Acquisition of VDB Profiel (NL)

2009
Acquisition of 100% in Europe Twintile

2010
Start-up of satellite JI Sud Ouest: in Toulouse (FR)

2011
Start-up of satellite JI Auvergne in Sorgues (FR)
Opening Akkerstraat site (wall & cold store sandwich panel line)
Start up of JORIS IDE Energy

2012
Start-up of JORIS IDE Façade: architectural facade systems
Establishment JORIS IDE Deutschland (DE)

2013
Launch of Joris Ide Est

2014
Launch of new building Joris Ide Façade

2016
Autonomous integration in Kingspan Group

The project has received financial support from the European Community (RFCS programme) under grant agreement No 754092

Presentation of Joris Ide Group

- 18 manufacturing in 8 countries
- More than 1000 employees
- 250 trucks delivering 1000 customers per day in Europe
- Export division worldwide
- Commercial presence spread over 16 countries

The project has received financial support from the European Community (RFCS programme) under grant agreement No 754092

Presentation of Joris Ide Group

- Insulated roof solution PIR/Mineral Wool:

JI Roof 1000

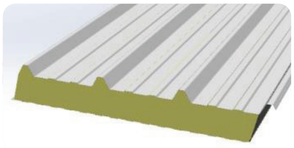

JI Vulcasteel Roof

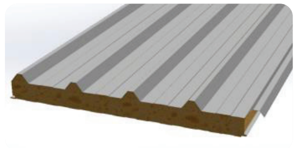

JI Ecopanel

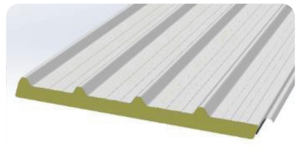

JI Permapan

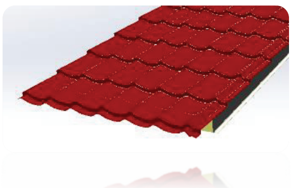

JI Onduroof 1000

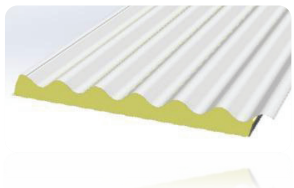

JI Vulcasteel Roof 3C

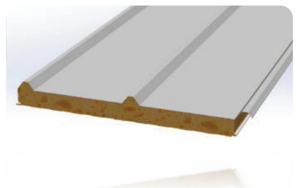

The project has received financial support from the European Community (RFCS programme) under grant agreement No 754092

Presentation of Joris Ide Group

- Insulated wall solution PIR/Mineral Wool:

JI Wall 1000 SF E

JI Wall 1000 SF F

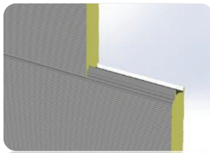

JI Wall 1000 SF MR

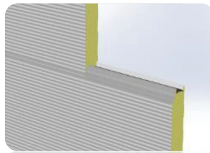

JI Wall 1000 SF P

JI Vulcasteel Wall 1000 SF E

JI Vulcasteel Wall 1000 SF F

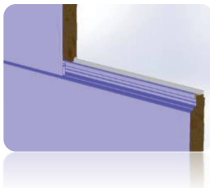

JI Vulcasteel Wall 1000 SF MR

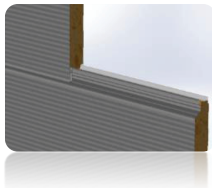

JI Vulasteel Wall 1000 SF P

The project has received financial support from the European Community (RFCS programme) under grant agreement No 754092

Presentation of Joris Ide Group

Non insulated architectural façade solutions:

JI Grégale
(300 to 600 mm)

JI Ponant
(300 to 500 mm)

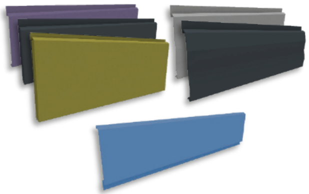

JI Breva
(1200 to 6000 mm)

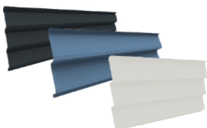

JI Ouragan
(1200 to 6000 mm)

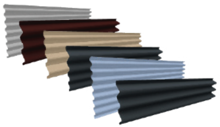

JI Suroit
(1200 to 6000 mm)

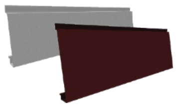

JI Tornade progress
(1200 to 6000 mm)

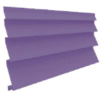

JI Brise
(1200 to 6000 mm)

JI Sonora
(1200 to 6000 mm)

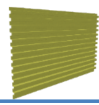

JI Boréas XLS
(500 to 1250 mm)

JI Boréas XL
(500 to 1000 mm)

The project has received financial support from the European Community (RFCS programme) under grant agreement No 754092

Presentation of Joris Ide Group

- Profiles and purlins:

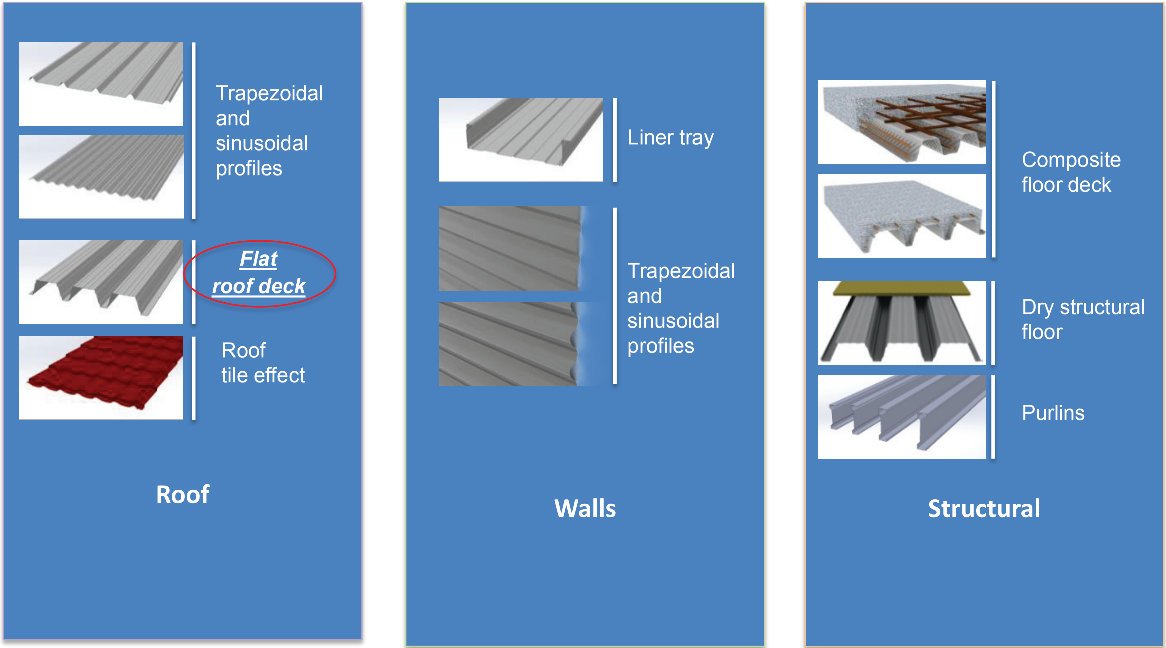

The project has received financial support from the European Community (RFCS programme) under grant agreement No 754092

Component description and application field

The project has received financial support from the European Community (RFCS programme) under grant agreement No 754092

Component description and application field

- Trapezoidal steel deck used for flat roofing:

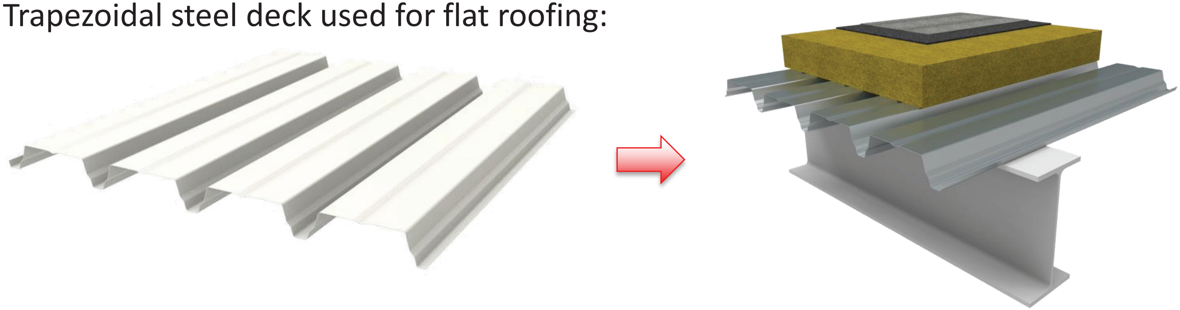

The project has received financial support from the European Community (RFCS programme) under grant agreement No 754092

Component description and application field

- Better performance ⇨ 2 (or more) spans configuration:

- Reasons driving to have a reduction of performance:
  - Local area on roof with more elevated loading (“Wind + Snow” effect)

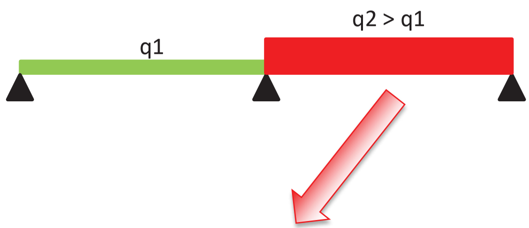

How avoid increasing thickness ?

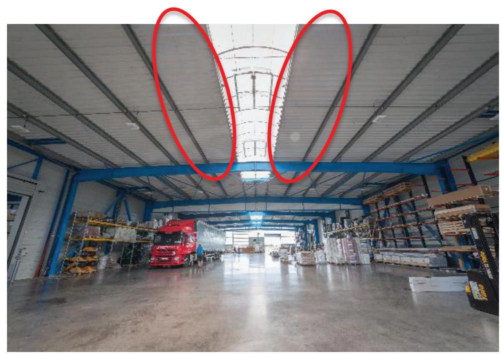

The project has received financial support from the European Community (RFCS programme) under grant agreement No 754092

Component description and application field

- Isostatic case due to location changes of:
  - natural lighting
  - smoke extractors

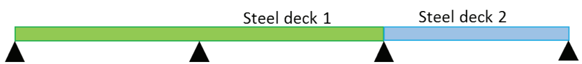

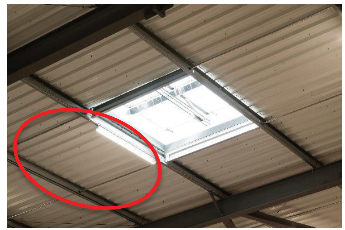

- Consequences:
  - Steel deck is locally on 2 supports
  - Characteristic resistance values not sufficient

⇒ How avoid increasing thickness ?

The project has received financial support from the European Community (RFCS programme) under grant agreement No 754092

Component description and application field

- Can Eurocode provides solutions ?
  - Actually : NO
  - But some guidance or information are allowable

- Objective of GRISPE : propose solution and design procedure
  - Assemblies for roof profiles (statically effective overlapping)
  - Consequence on the intermediate support behaviour

The project has received financial support from the European Community (RFCS programme) under grant agreement No 754092

Component description and application field

- Joint according to DIN 18807-3 (DIN):
  - Statically effective overlapping
  - Permitted in the area of support (moment resisting connection)
  - Ultimate limit state of the whole structure remains unaltered
  - 2 variants :

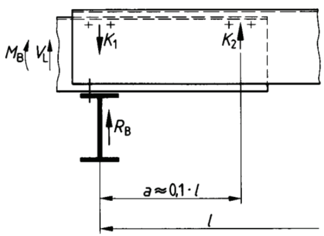

Cantilevered end of profile underneath

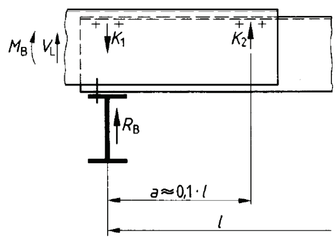

Cantilevered end of profile on top

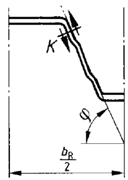

The project has received financial support from the European Community (RFCS programme) under grant agreement No 754092

Component description and application field

- Joint according to DIN 18807-3 (DIN), and included in EN 1090-4 § B.8:
  - Design of sheeting and connections as follow:

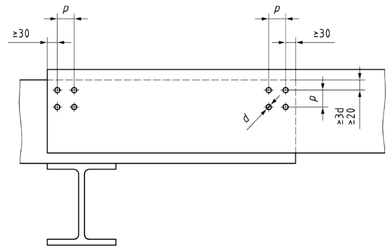

- Cantileverd end of profiled sheets underneath:

$$K = maxK_i = \frac{|M_B|}{2 \cdot a \cdot \sin\varphi} \cdot b_R$$

- Cantileverd end of profiled sheets on top:

$$K = maxK_i = \frac{\left|\frac{M_B}{a} + V_L\right|}{2 \cdot \sin\varphi} \cdot b_R$$

If obverlapping region is considered as continuous:

a ≥ 0,08 L_{max}

or 0,065 L_{max} ≤ a ≤ 0,11 L_{max}

and:
a ≤ 0,15 Lmin

The project has received financial support from the European Community (RFCS programme) under grant agreement No 754092

Component description and application field

- Overlap joint (OL):
  - Statically effective overlapping
  - Permitted in the area of support (moment resisting connection)
  - Overlapping length 2·a at both sides of the support
  - Load-bearing capacity increases compared with a single continuous profile

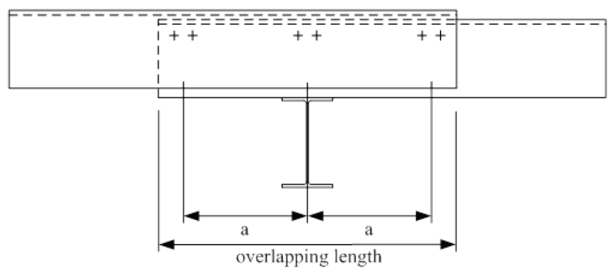

The project has received financial support from the European Community (RFCS programme) under grant agreement No 754092

Component description and application field

- Continuous profile with local reinforcement (CR):
  - Statically effective overlapping
  - Permitted in the area of support (moment resisting connection)
  - Overlapping length 2·a at both sides of the support
  - Load-bearing capacity increases compared with a single continuous profile

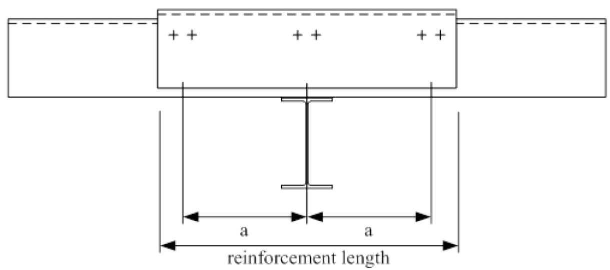

The project has received financial support from the European Community (RFCS programme) under grant agreement No 754092

Acquired data through GRISPE project

The project has received financial support from the European Community (RFCS programme) under grant agreement No 754092

Acquired data through GRISPE project

- Summary of tested assemblies:
  - Continuous
  - DIN
  - OL
  - CR

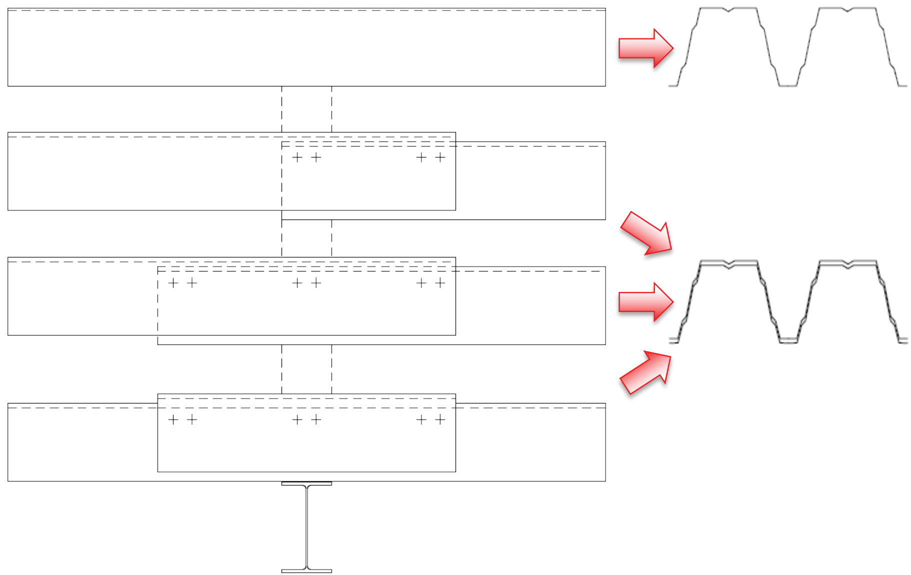

The project has received financial support from the European Community (RFCS programme) under grant agreement No 754092

Acquired data through GRISPE project

- Tested profiles (higher and smaller angle of the web:

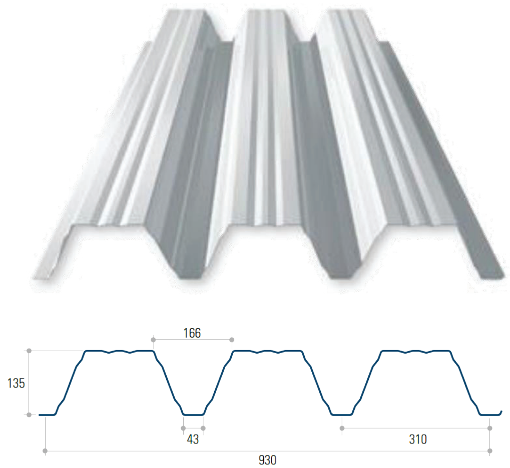

Joris Ide 137/310

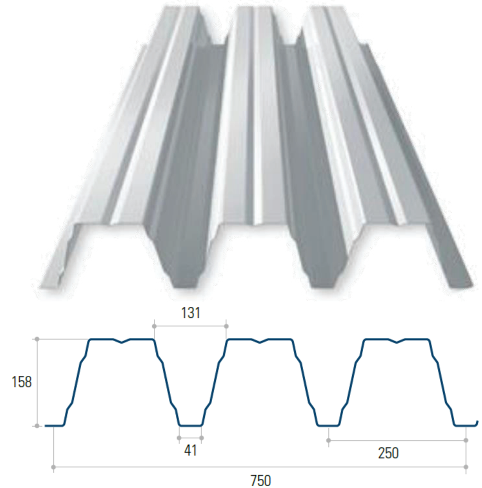

Joris Ide 158/250

- 2 thicknesses: 0,75 mm and 1,00 mm

The project has received financial support from the European Community (RFCS programme) under grant agreement No 754092

Acquired data through GRISPE project

- To study the load-bearing behaviour at intermediate support (M_{rd}, $R_{w,Rd}$) ⇨ 3-point bending tests were carried out according to EN 1993-1-3 § A.2.4:

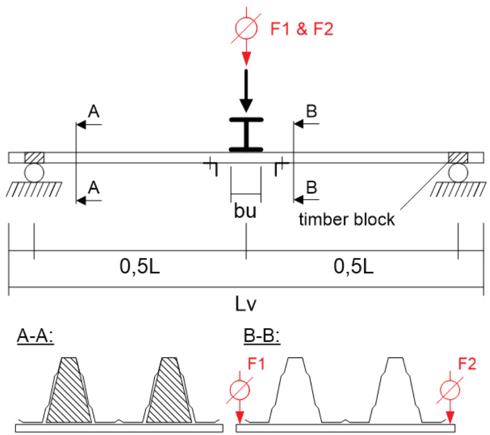

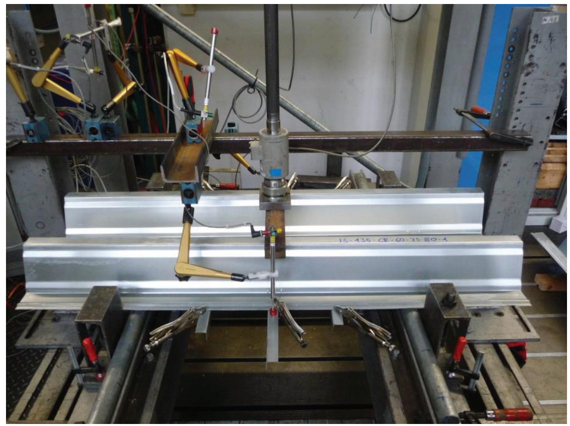

The project has received financial support from the European Community (RFCS programme) under grant agreement No 754092

Acquired data through GRISPE project

- Parameters of the tests:
  - 3 types of assemblies (+ reference)
  - Sheet thickness (0,75 mm & 1,00 mm)
  - Profile type (135/310 & 158/250)
  - Support width b_u (60 mm & 160 mm)
  - Span length (800 mm to 3 200 mm)

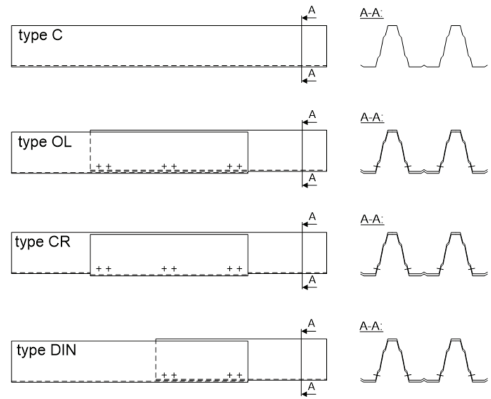

- Campaign of 71 tests for both profiles
- Tests supplemented with tensile tests

The project has received financial support from the European Community (RFCS programme) under grant agreement No 754092

Acquired data through GRISPE project

- Self weight of test specimens:

profile	thickness t (mm)	self-weight (kN/m²)
JID 137.310.930	0,75	0,097
	1,00	0,129
JID 158.250.750	0,75	0,120
	1,00	0,160

- Adjustment of test values considering real characteristics and number of tests:

  - According EN 1993-1-3 § A.6.2:

$$R_{adj,i} = R_{obs,i}/\mu_R \qquad \mu_R = \left(\frac{f_{yb,obs}}{f_{yb}}\right)^{\alpha}\left(\frac{t_{obs,cor}}{t_{cor}}\right)^{\beta}$$

  - According EN 1993-1-3 §

$$R_k = R_m +/- k\,s$$

n	4	5	6	8	10	20	30	∞
k	2,63	2,33	2,18	2,00	1,92	1,76	1,73	1,64

$$s = \left[\sum_{i=1}^{n}\left(R_{adj,i} - R_m\right)^2 / (n-1)\right]^{0,5}$$

The project has received financial support from the European Community (RFCS programme) under grant agreement No 754092

Acquired data through GRISPE project

- Support reaction for intermediate support test: $R_{w,Rk,B} = F_{u,k}/b_V$
- Bending moment at support: $M_{c,Rk,B} = R_{w,Rk,B} \cdot \frac{L}{4} + \frac{g \cdot L_V \cdot (2L - L_V)}{8}$
  - $R_{w,Rk,B}$ characteristic support reaction at intermediate support
  - $M_{c,Rk,F}$ characteristic bending moment at intermediate support
  - $F_{u,k}$ characteristic load (including preload)
  - b_V width of the test specimen (0,620 or 0,500 mm)
  - L_V length of the test specimen (1 200 to 3 600 mm)
  - L span length (800 to 3 200 mm)
  - q self-weight of the test specimen
- M/R diagram interaction :

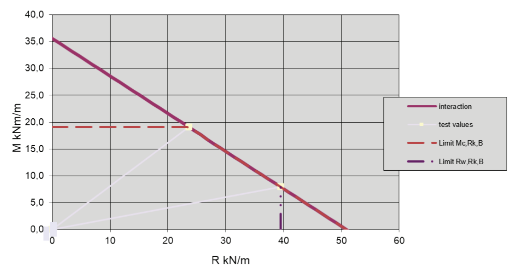

The project has received financial support from the European Community (RFCS programme) under grant agreement No 754092

Acquired data through GRISPE project

- Typical failure of the continuous profile:

- Local impression and buckling at the support (maximum bending moment)

The project has received financial support from the European Community (RFCS programme) under grant agreement No 754092

Acquired data through GRISPE project

- Typical failure of the joint according to DIN:

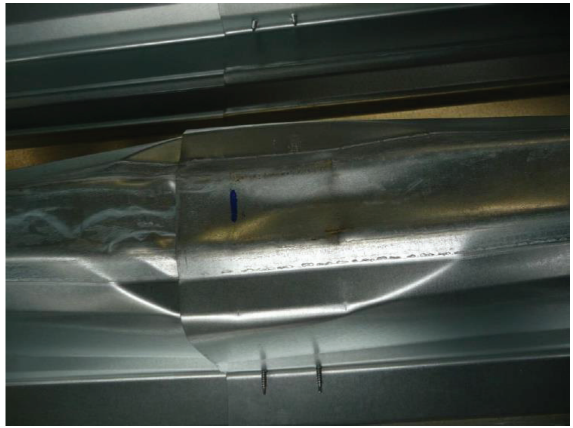

- Local impression and buckling at the support (maximum bending moment)

The project has received financial support from the European Community (RFCS programme) under grant agreement No 754092

Acquired data through GRISPE project

- Typical failure of the joint according to DIN:

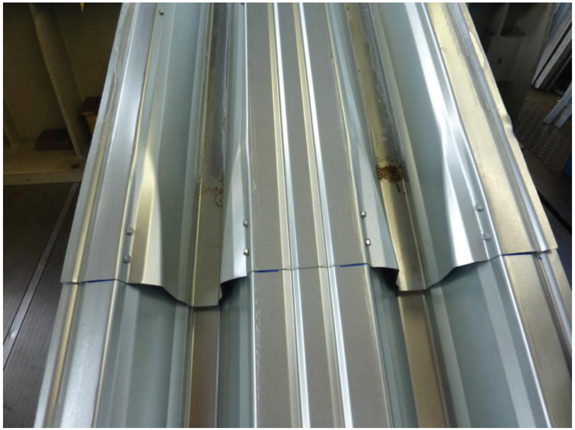

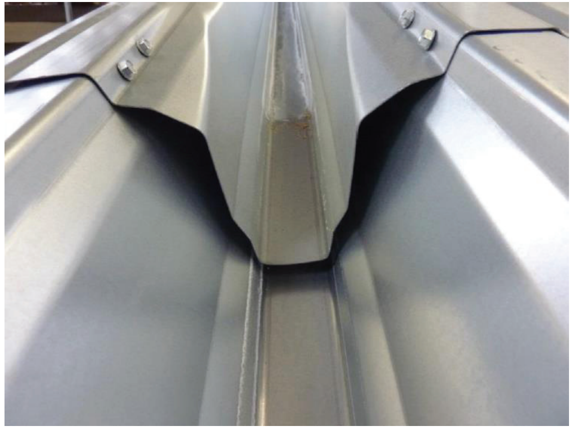

- Slope difference of the overlapping parts created by local web-crushing at the end of overlap ⇨ overlap too short (only in variant cantilevered end of profile on top)

The project has received financial support from the European Community (RFCS programme) under grant agreement No 754092

Acquired data through GRISPE project

- Typical failure of the joint according to DIN:

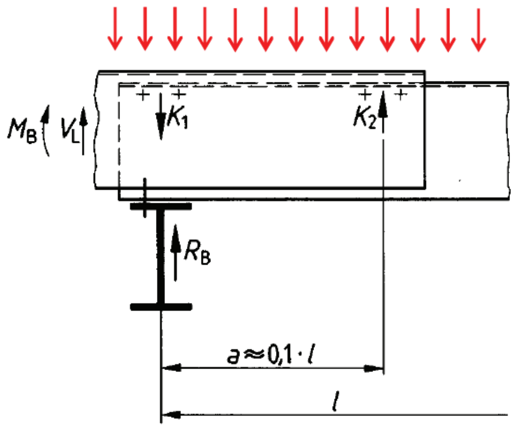

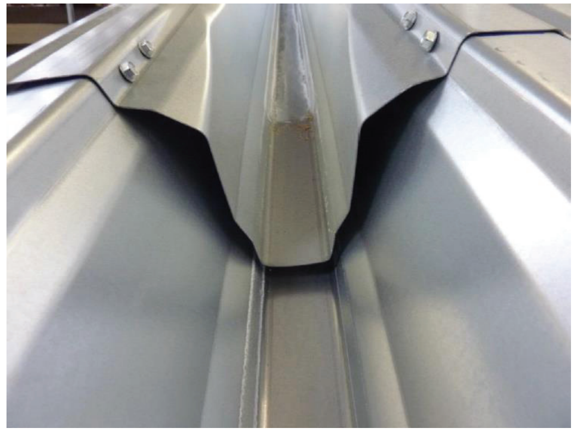

- Slope difference of the overlapping parts created by local web-crushing at the end of overlap ⇨ overlap too short (only in variant cantilevered end of profile on top)

The project has received financial support from the European Community (RFCS programme) under grant agreement No 754092

Acquired data through GRISPE project

- Typical failure of the overlap joint and the continuous profile with local reinforcement (same behaviour):

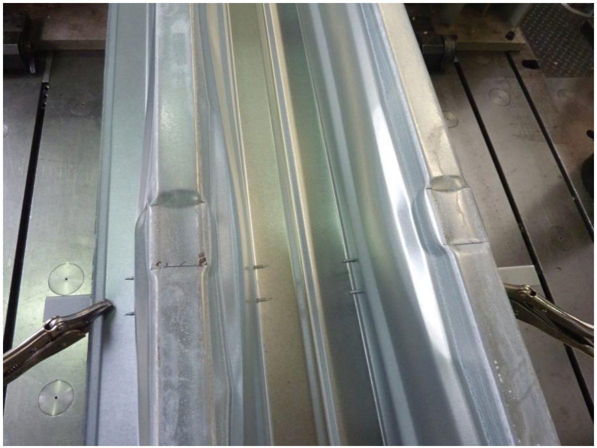

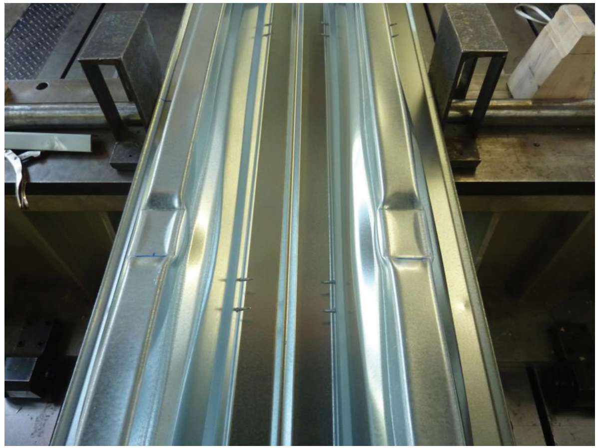

- Local impression and buckling at the support (maximum bending moment)

The project has received financial support from the European Community (RFCS programme) under grant agreement No 754092

Acquired data through GRISPE project

- Tests result and analyse for profile 137.310 – 0,75 mm – b_u = 60 mm:

Profile	137.310	thickness	0,75 mm	support width	60 mm
Type of assembly	bending moment $M_{c,Rk,B}$	relative bending moment	shear force at end of overlap F	0.5 R_{wRkB}	ratio F/(0,5 R_{wRkB})
-	kNm/m	%	kN/m	kN/m	-
Continuous	6,463	100,0	-	11,45	-
DIN a = 0,5 m	5,703	88,2	11,41	11,45	1,00
DIN a = 0,7 m	-	-	-	-	-
OL a = 0,5 m	12,247	189,5	12,25	11,45	1,07
OL a = 0,7 m	-	-	-	-	-
CR a = 0,5 m	12,230	189,2	12,23	11,45	1,07

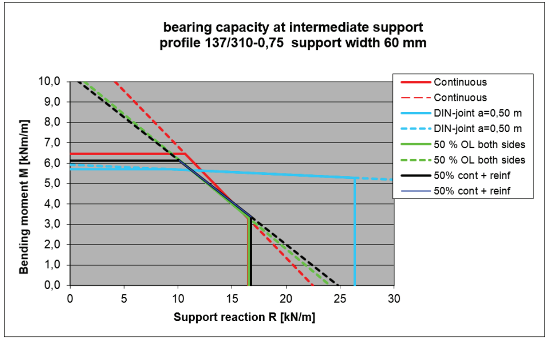

- DIN joint:
  - Bearing capacity mostly greater than continuous profile
  - Maximum moment remain 10 % below comparing continuous profile

- Overlap (OL) and continuous with reinforcement (CR):
  - Maximum support reaction = 2 x continuous profile
  - Maximum moment: small gap of 10 %

The project has received financial support from the European Community (RFCS programme) under grant agreement No 754092

Acquired data through GRISPE project

- Tests result and analyse for profile 137.310 – 0,75 mm – b_u = 160 mm:

Profile	137.310	thickness	0,75 mm	support width	160 mm
Type of assembly	bending moment $M_{c,Rk,B}$	relative bending moment	shear force at end of overlap F	0.5 R_{wRkB}	ratio F/(0,5 R_{wRkB})
-	kNm/m	%	kN/m	kN/m	-
Continuous	8,031	100,0	-	11,45	-
DIN a = 0,5 m	5,823	72,5	11,65	11,45	1,02
DIN a = 0,7 m	8,068	100,5	11,53	11,45	1,01
OL a = 0,5 m	13,100	163,1	13,10	11,45	1,14
OL a = 0,7 m	15,219	189,5	10,87	11,45	0,95
CR a = 0,5 m	13,188	164,2	13,19	11,45	1,15

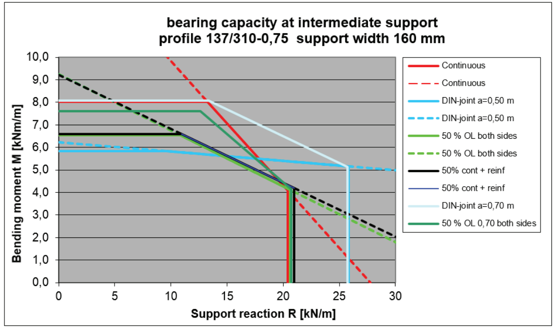

- DIN joint:
  - Maximum moment same than moment for b_u = 60 mm for a = 0,5 m
  - Maximum moment same than continuous profile for a = 0,7 m

- Overlap (OL): same behaviour

The project has received financial support from the European Community (RFCS programme) under grant agreement No 754092

Acquired data through GRISPE project

- Tests result and analyse for profile 137.310 – 0,75 mm – b_u = 160 mm:
  - When overlap is too short (a = 0,5 m): prior failure by web crippling at the end of the overlap:

  - To avoid prior failure: overlap should be sufficiently long
  - The shear force at the end of the overlap doesn't exceed the web crippling capacity ⇨ shear force depends directly from the overlap length
  - DIN-joint: $F = M_{c,Rk,B}/a$
  - OL and CR: $F = M_{c,Rk,B}/(2 \cdot a)$

The project has received financial support from the European Community (RFCS programme) under grant agreement No 754092

Acquired data through GRISPE project

- Tests result and analyse for profile 137.310 – 1,00 mm – b_u = 60 mm:

Profile	137.310	thickness	1,00 mm	support width	60 mm
Type of assembly	bending moment $M_{c,Rk,B}$	relative bending moment	shear force at end of overlap F	0.5 R_{wRkB}	ratio F/(0,5 R_{wRkB})
-	kNm/m	%	kN/m	kN/m	-
Continuous	10,625	100,0	-	20,47	-
DIN a = 0,5 m	12,599	118,6	25,20	20,47	1,23
DIN a = 0,7 m	-	-	-	-	-
OL a = 0,5 m	20,270	190,8	20,27	20,47	0,99
OL a = 0,7 m	-	-	-	-	-
CR a = 0,5 m	20,866	196,4	20,87	20,47	1,02

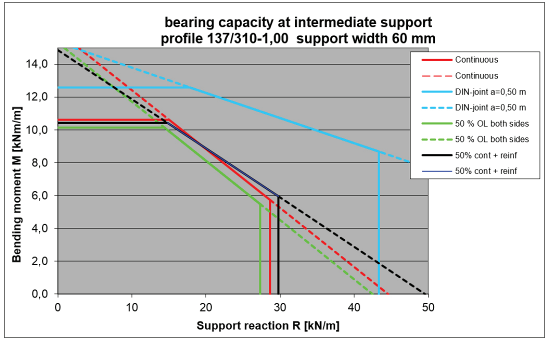

- DIN joint:
  - At least on the same level as the continuous profile (even with the short overlap (0,50 m)

- Overlap (OL) and reinforcement (CR):
  - Nearly the doubled resistance of the continuous profile

The project has received financial support from the European Community (RFCS programme) under grant agreement No 754092

Acquired data through GRISPE project

- Tests result and analyse for profile 137.310 – 1,00 mm – b_u = 160 mm:

Profile	137.310	thickness	1,00 mm	support width	160 mm
Type of assembly	bending moment $M_{c,Rk,B}$	relative bending moment	shear force at end of overlap F	0.5 R_{wRkB}	ratio F/(0,5 R_{wRkB})
-	kNm/m	%	kN/m	kN/m	-
Continuous	13,194	100,0	-	20,47	-
DIN a = 0,5 m	13,751	104,2	27,50	20,47	1,34
DIN a = 0,7 m	-	-	-	-	-
OL a = 0,5 m	20,884	158,3	20,88	20,47	1,02
OL a = 0,7 m	23,864	180,9	17,05	20,47	0,83
CR a = 0,5 m	22,274	168,8	22,27	20,47	1,09

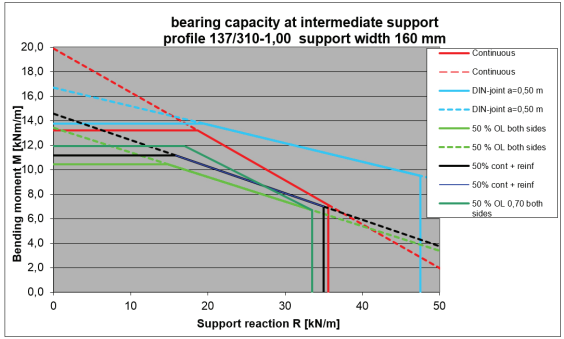

- DIN joint:
  - At least on the same level as the continuous profile (even with the short overlap (0,50 m)
- Overlap (OL) and reinforcement (CR):
  - Achieve 160 % and 170 % of the resistance of the continuous profile

The project has received financial support from the European Community (RFCS programme) under grant agreement No 754092

Acquired data through GRISPE project

- Tests result and analyse for profile 158.250:
  - 0,75 mm – b_u = 60 mm
  - 1,00 mm – b_u = 60 mm
  - 1,00 mm – b_u = 160 mm

  Same conclusion than for profile 137.310 – 1,00 mm – b_u = 60 mm

- Tests result and analyse for profile 158.250 – 0,75 mm – b_u = 160 mm:
  - DIN-joint: overlap length upgrade to ≈ 0,80 m to reach bending of continuous profile
  - OL and CR joints: achieve 150 % of continuous profile ⇨ overlap of 0,8 m allow 170 %

The project has received financial support from the European Community (RFCS programme) under grant agreement No 754092

Acquired data through GRISPE project

- Analysis of tests results – necessary overlap a (m):

Profile	thickness	support width	Shear force V in the joint [kN/m]			necessary overlap a [m]		
	t [mm]	l_a [mm]	DIN	OL	CR	DIN	OL	CR
137/310 a = 0,50 m	0,75	60	11,41	12,25	12,23	0,57	0,53	0,53
		160	11,65	13,10	13,19	0,69	0,61	0,61
	1,00	60	25,20	20,27	20,87	0,42	0,52	0,51
		160	27,50	20,88	22,27	0,48	0,63	0,59
158/250 a = 0,60 m	0,75	60	19,68	16,62	16,13	0,51	0,60	0,62
		160	18,40	16,24	17,93	0,69	0,79	0,71
	1,00	60	36,23	29,75	28,97	0,53	0,64	0,66
		160	37,37	30,96	29,74	0,60	0,73	0,76

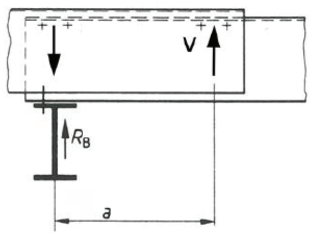

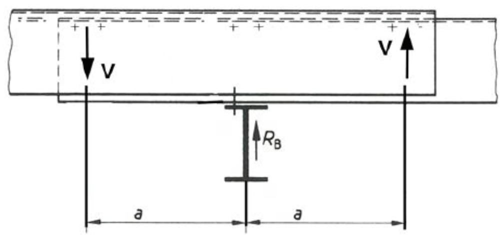

The project has received financial support from the European Community (RFCS programme) under grant agreement No 754092

GRISPE PLUS

Design and Calculation method for assembled profiles

The project has received financial support from the European Community (RFCS programme) under grant agreement No 754092

Design and calculation method for assembled profiles

- ***For ALL studied joint (DIN, OL, CR):***

- Edge and hole spacings for statically effective overlapping

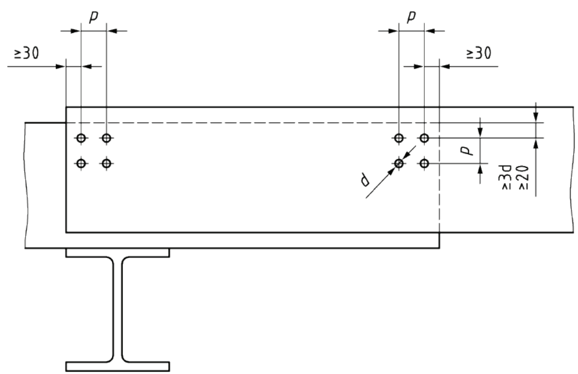

The project has received financial support from the European Community (RFCS programme) under grant agreement No 754092

Design and calculation method for assembled profiles

- ***<u>Assembled profiles with "DIN-joint" – cantilevered end of profile on top</u>*** :

- Step 1 ⇨ Verification with the characteristic values ($M_{Rd,B}$, $R_{w,Rd,B}$) of the continuous profile in the support axis + taking account of the influence of support reaction (M-R interaction)

- Step 2 ⇨ Check of the free end of the cantilever = does the line load Fed introduced by the connections K_i may create web crippling ?

  - Uplift loading = positive moment ⇨ no additional verification of web-crippling

  - Downward loading = negative moment:

    - Additional verification of web-crippling at the end of the cantilever:

$$F_{Ed} = M_{B,Ed}/a < 0{,}5\ R_{w,Rk,B}$$

    - With $R_{w,Rk,B}$ the ultimate support reaction at intermediate supports in the opposite profile position (in general negative position) for the maximum support width, in general l_{aB} = 160 mm ⇦ GRISPE determined that is suitable for this verification.

The project has received financial support from the European Community (RFCS programme) under grant agreement No 754092

Design and calculation method for assembled profiles

- ***<u>Assembled profiles with “DIN-joint ” – cantilevered end of profile on top</u>*** :

- Step 3 ⇨ Verification of the connection K_{Ed} (in one web):

$$K_{Ed} = \max K_i = \frac{\left| \frac{M_{B,Ed}}{a} + V_{L,Ed} \right|}{2 \cdot \sin \varphi} \cdot b_R \leq \Sigma F_{V,Rd}$$

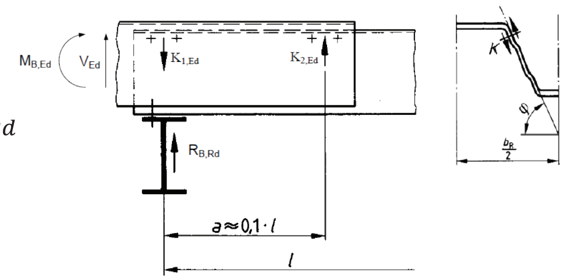

- With $\Sigma\, F_{V,Rd}$ the schear resistance of the screws

The project has received financial support from the European Community (RFCS programme) under grant agreement No 754092

Design and calculation method for assembled profiles

- ***Assembled profiles with "DIN-joint" – cantilevered end of profile underneath***:

- Step 1 ⇨ Verification with the characteristic values ($M_{Rd,B}$, $R_{w,Rd,B}$) of the continuous profile in the support axis + taking account of the influence of support reaction (M-R interaction)

- Step 2 ⇨ Check of the free end of the cantilever = does the line load Fed introduced by the connections Ki may create web crippling ?

  - Uplift loading = positive moment ⇨ no additional verification of web-crippling

  - Downward loading = negative moment ⇨ no additional verification of web-crippling

The project has received financial support from the European Community (RFCS programme) under grant agreement No 754092

Design and calculation method for assembled profiles

- ***<u>Assembled profiles with "DIN-joint" – cantilevered end of profile underneath</u>***:

- Step 3 ⇨ Verification of the connection K_{Ed} (in one web):

$$K_{Ed} = \max K_i = \frac{\left|\frac{M_{B,Ed}}{a}\right|}{2 \cdot \sin\varphi} \cdot b_R \leq \Sigma F_{V,Rd}$$

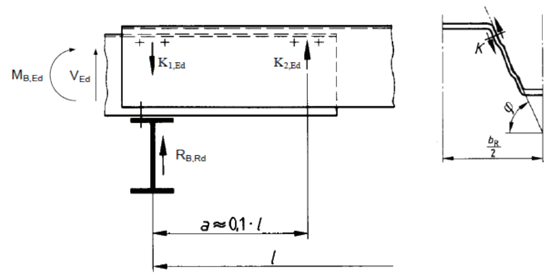

- With $\Sigma F_{V,Rd}$ the schear resistance of the screws

The project has received financial support from the European Community (RFCS programme) under grant agreement No 754092

Design and calculation method for assembled profiles

- ***Assembled profiles with “Overlap-joint ”*** :
- Step 1 ⇨ Determination of the bending moment distribution under desing loads like for continuous sheets ⇨ $M_{B,Ed}$ / $R_{B,Ed}$ / $M_{1,Ed}$ / $M_{2,Ed}$:

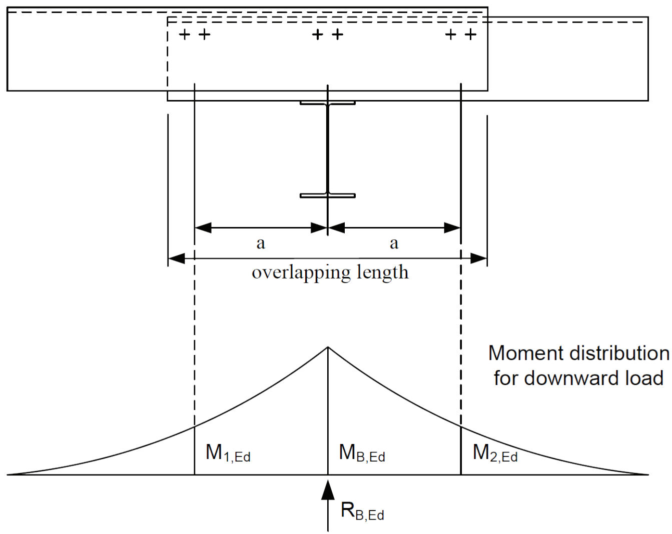

The project has received financial support from the European Community (RFCS programme) under grant agreement No 754092

Design and calculation method for assembled profiles

- ***Assembled profiles with "Overlap-joint"*** :
- Step 2 ⇨ Verification of the profiles at the support axis with 90 % of the resistance of the overlapping profiles:
  - $M_{B,Ed} \leq 0{,}9\ \Sigma M_{B,Rd}$
  - $R_{B,Ed} \leq 0{,}9\ \Sigma R_{w,B,Rd}$
  - M-R interaction

- Step 3 ⇨ Verification of the continuous profiles at the ends of the overlap with $M_{1,Ed}$, or $M_{2,Ed}$, and the line loads introduced by K_i: $F_{Ed} = M_{B,Ed}/2a$:
  - For downward loading: F_{Ed} = tension force on the webs ⇨ Check the M-V interaction
  - For uplift loading: F_{Ed} = compression force on the webs ⇨ Check the M-R interaction
  - Resistance values of the profile in the opposite position at intermediate supports are considered for thes verifications

The project has received financial support from the European Community (RFCS programme) under grant agreement No 754092

Design and calculation method for assembled profiles

- ***<u>Assembled profiles with "Overlap-joint "</u>*** :
- Step 4 ⇨ Check of the free end of the cantilever = does the line load Fed introduced by the connections K_i may create web crippling ?
  - Uplift loading = positive moment ⇨ no additional verification of web-crippling
  - Downward loading = negative moment:
    - Additional verification of web-crippling at the end of the cantilever:

$$F_{Ed} = M_{B,Ed}/(2 \cdot a) < 0{,}5\ R_{w,Rk,B}$$

    - With $R_{w,Rk,B}$ the ultimate support reaction at intermediate supports in the opposite profile position (in general negative position) for the maximum support width, in general l_{aB} = 160 mm ⇦ GRISPE determined that is suitable for this verification.
    - No web crippling possible at the end of the cantilever underneath

The project has received financial support from the European Community (RFCS programme) under grant agreement No 754092

Design and calculation method for assembled profiles

- ***<u>Assembled profiles with "Overlap-joint "</u>*** :

- Step 5 ⇨ Verification of the connection K_{Ed} (in one web):

$$K_{Ed} = \max K_i = \frac{\left| M_{B,Ed} \right|}{4 \cdot a \cdot \sin\varphi} \cdot b_R \leq \Sigma F_{V,Rd}$$

- With $\Sigma F_{V,Rd}$ the schear resistance of the screws

The project has received financial support from the European Community (RFCS programme) under grant agreement No 754092

Design and calculation method for assembled profiles

- ***Assembled profiles with “Reinforcement-joint ”*** :
- Step 1 ⇨ Determination of the bending moment distribution under desing loads like for continuous sheets ⇨ $M_{B,Ed}$ / $R_{B,Ed}$ / $M_{1,Ed}$ / $M_{2,Ed}$:

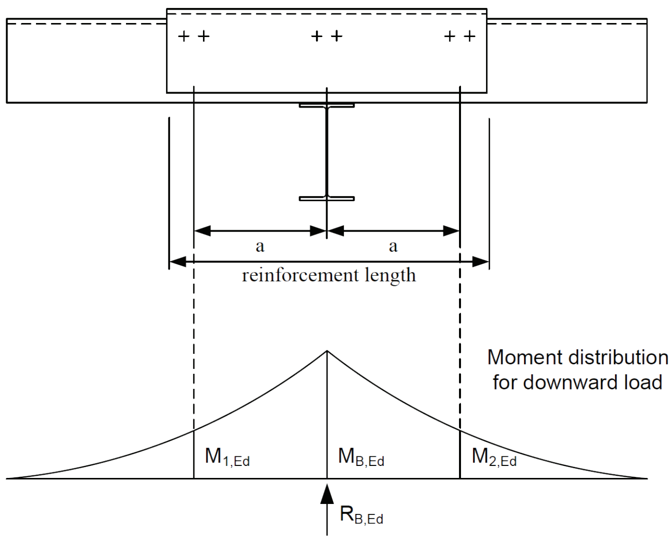

The project has received financial support from the European Community (RFCS programme) under grant agreement No 754092

Design and calculation method for assembled profiles

- ***Assembled profiles with “Reinforcement-joint ”*** :
- Step 2 ⇨ Verification of the profiles at the support axis with 90 % of the resistance of the overlapping profiles:
  - $M_{B,Ed} \leq 0{,}9\ \Sigma M_{B,Rd}$
  - $R_{B,Ed} \leq 0{,}9\ \Sigma R_{w,B,Rd}$
  - M-R interaction
- Step 3 ⇨ Verification of the continuous profiles at the ends of the overlap with $M_{1,Ed}$, or $M_{2,Ed}$, and the line loads introduced by K_i: $F_{Ed} = M_{B,Ed}/2a$:
  - For downward loading: F_{Ed} = tension force on the webs ⇨ Check the M-V interaction
  - For uplift loading: F_{Ed} = compression force on the webs ⇨ Check the M-R interaction
  - Resistance values of the profile in the opposite position at intermediate supports are considered for thes verifications

The project has received financial support from the European Community (RFCS programme) under grant agreement No 754092

Design and calculation method for assembled profiles

- ***<u>Assembled profiles with "Reinforcement-joint"</u>*** :
- Step 4 ⇨ Check of the free end of the cantilever = does the line load Fed introduced by the connections K_i may create web crippling ?
  - Uplift loading = positive moment
    - ⇨ no additional verification of web-crippling
    - No web crippling possible at the end of both cantilevers
  - Downward loading = negative moment:
    - Additional verification of web-crippling at the end of the cantilever:

$$F_{Ed} = M_{B,Ed}/(2 \cdot a) < 0{,}5\ R_{w,Rk,B}$$

    - With $R_{w,Rk,B}$ the ultimate support reaction at intermediate supports in the opposite profile position (in general negative position) for the maximum support width, in general l_{aB} = 160 mm ⇦ GRISPE determined that is suitable for this verification.

The project has received financial support from the European Community (RFCS programme) under grant agreement No 754092

Design and calculation method for assembled profiles

- ***Assembled profiles with “Reinforcement-joint ”*** :

- Step 5 ⇨ Verification of the connection K_{Ed} (in one web):

$$K_{Ed} = \max K_i = \frac{|M_{B,Ed}|}{4 \cdot a \cdot \sin\varphi} \cdot b_R \leq \Sigma F_{V,Rd}$$

- With $\Sigma F_{V,Rd}$ the schear resistance of the screws

The project has received financial support from the European Community (RFCS programme) under grant agreement No 754092

GRISPE PLUS

Software and design manual

The project has received financial support from the European Community (RFCS programme) under grant agreement No 754092

Software and design manual

- Excel software developed during GRISPE project :

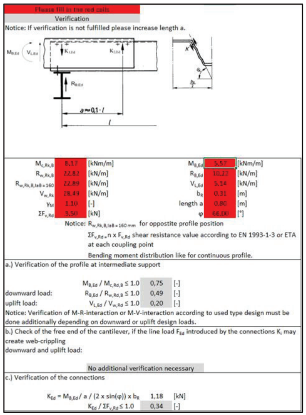

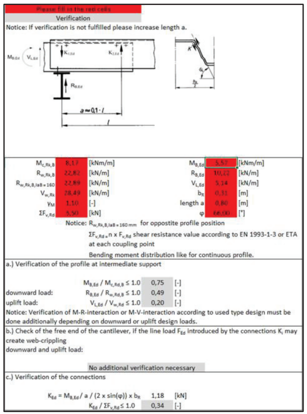

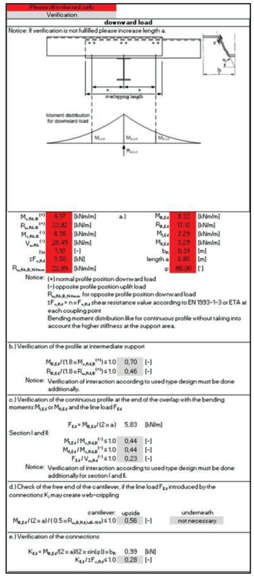

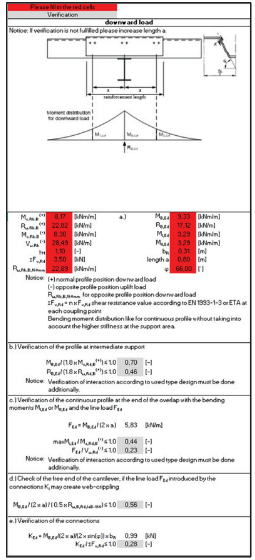

The project has received financial support from the European Community (RFCS programme) under grant agreement No 754092

Software and design manual

- Design manual:
  - Description of design method;
  - Analytical examples;
  - Comparison between Excel software and analytical results.


Design Manual for Assembled profiles

GRISPE PLUS

GRISPE PLUS
VALORISATION OF KNOWLEDGE
FOR SPECIFIC PROFILED STEEL SHEETS

DESIGN MANUAL FOR ASSEMBLED PROFILES

RFCS funded – agreement N° 754092

FINAL VERSION

1

The project has received financial support from the European Community (RFCS programme) under grant agreement No 754092

Conclusion

The project has received financial support from the European Community (RFCS programme) under grant agreement No 754092

Conclusion

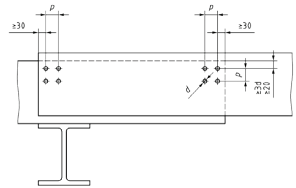

- DIN-joint:
  - provides the same load bearing capacity as continuous profile with an overlap sufficiently long
  - Overlap length should be designed in a way that web crippling at the end of the overlap is excluded
  - The sufficient overlap length should be checked by an additional verification of the shear force at the end of the overlap

The project has received financial support from the European Community (RFCS programme) under grant agreement No 754092

Conclusion

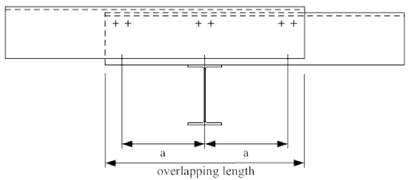

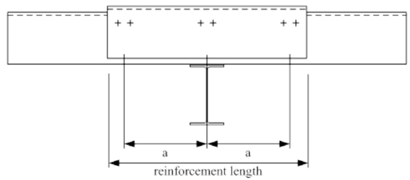

- Assemblies with double cross section (OL and CR):
  - Provides 90 % of the resistance of the continuous profile (to be multiplied by 2 ⇦ 2 cross section assembled)
  - Overlap length should be designed in a way that web crippling at the end of the overlap is excluded
  - The sufficient overlap length should be checked by an additional verification of the shear force at the end of the overlap

The project has received financial support from the European Community (RFCS programme) under grant agreement No 754092

All documents at:
www.grispeplus.eu

The project has received financial support from the European Community (RFCS programme) under grant agreement No 754092

Thank you for your attention

The project has received financial support from the European Community (RFCS programme) under grant agreement No 754092

GRISPE PLUS

VALORISATION OF KNOWLEDGE
FOR SPECIFIC PROFILED STEEL SHEETS

GRISPE WORKSHOP
Interactive section

David Izabel
14 June 2018
RFCS Project

The project has received financial support from the European Community (RFCS programme) under grant agreement No 754092

Contence

1. Draft clauses for steel decks with embossments /indentations
2. Draft clauses for steel decks with outwards stiffener
3. Draft clauses for corrugated sheetings
4. Draft clauses for liner trays with s_1 >1m
5. Draft clauses for assembled profiles
6. Draft clauses for curved profiles
7. Draft clauses for perforated profiles
8. Draft clauses for holed profiles
9. Draft clauses for plank profiles

The project has received financial support from the European Community (RFCS programme) under grant agreement No 754092

1. Draft clauses for steel decks with embossments /indentations

The project has received financial support from the European Community (RFCS programme) under grant agreement No 754092

1. Draft clauses for steel decks with embossments /indentations

Design thickness t_{red}

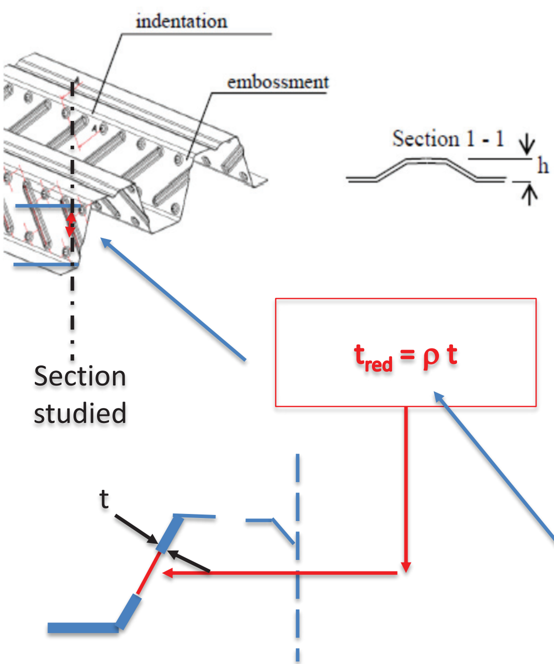

$t_{red} = \rho t$

$\rho = Ah + B$

Table 5.3: Valles of coefficients A and B (equation (5.43)

Type of local deformation	t (mm)	h (mm)	A	B
Indentation	0.71	0 - 1.5	-0.533	1.000
		1.5 - 2.75	-0.112	0.368
		2.75 - 4.0	-0.025	0.128
	0.96	0 - 1.5	-0.467	1.000
		1.5 - 2.75	-0.186	0.580
		2.75 - 4.0	-0.020	0.122
	1.21	0 - 1.5	-0.401	1.000
		1.5 - 2.75	-0.260	0.792
		2.75 - 4.0	-0.015	0.116
Embossment	0.71	0 - 1.5	-0.267	1.000
		1.5 - 2.75	-0.056	0.684
		2.75 - 4.0	-0.013	0.564
	0.96	0 - 1.5	-0.234	1.000
		1.5 - 2.75	-0.093	0.790
		2.75 - 4.0	-0.010	0.561
	1.21	0 - 1.5	-0.201	1.000
		1.5 - 2.75	-0.130	0.896
		2.75 - 4.0	-0.008	0.558

The project has received financial support from the European Community (RFCS programme) under grant agreement No 754092

2. Draft clauses for steel decks with outwards stiffener

The project has received financial support from the European Community (RFCS programme) under grant agreement No 754092

2. Draft clauses for steel decks with outwards stiffener

Design stress distribution

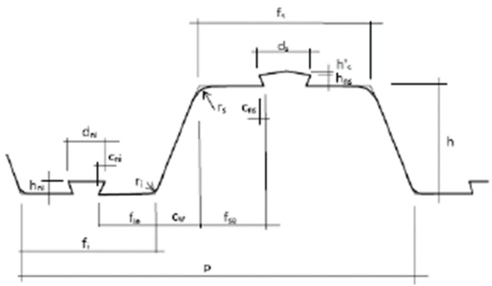

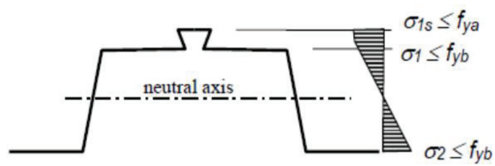

- if the yield stress is reached in the lower flange then $\sigma_2 = f_{yb}$ and $\sigma_1 < f_{yb}$
- if the yield stress is reached in the upper flange then $\sigma_1 = f_{yb}$ and $\sigma_2 < f_{yb}$

The project has received financial support from the European Community (RFCS programme) under grant agreement No 754092

3. Draft clauses for corrugated sheetings

The project has received financial support from the European Community (RFCS programme) under grant agreement No 754092

3. Draft clauses for corrugated sheetings

Design stress

$M_{c,Rk} = W_y * \sigma_c$

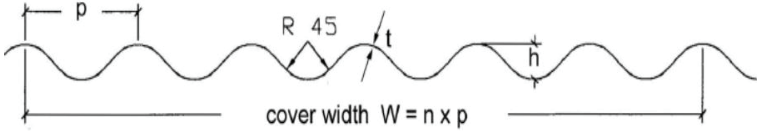

Solution 1

Solution 2

Simplified procedure for restricted application range

If the conditions

- profile installed as single span girder <u>and</u>
- uniformly distributed loads <u>and</u>
- ratio $R/t \le 0{,}1 * E / f_{yb}$ <u>and</u>
- steel core thickness $t_{cor} \ge 0{,}55$ mm <u>and</u>
- profile height 18 mm $\le h \le$ 46 mm <u>and</u>
- profile pitch 76 mm $\le p \le$ 150 mm

are met, the following simplified procedure may be adopted:

moment of inertia per unit width $J_y = 0{,}13 * t * h^2$

section modulus per unit width $W_y = 0{,}26 * t * h$

characteristic bending moment: $M_{c,Rk} = W_y * f_{yb}$

coefficient η $\quad \eta = 0{,}19 + 0{,}67 / \sqrt{1 + R / 100 * t}$

buckling stress $\quad \sigma_{elr} = 0{,}60 * \eta * E * t / R$

slenderness ratio: $\quad \alpha = \sqrt{f_{yb} / \sigma_{elr}}$

for $\alpha \le 0{,}30$ $\quad \sigma_c = f_{yb}$

for $0{,}30 < \alpha < 1{,}10$ $\quad \sigma_c = \left| 1{,}126 - 0{,}419 * \alpha \right| * f_{yb}$

for $1{,}10 \le \alpha$ $\quad \sigma_c = \left| 0{,}8 / \alpha^2 \right| * f_{yb}$

If $r/t > 0{,}04 * E / f_{yb}$: The characteristic bending moment should be calculated using the reduced compressive stress σ_c $\quad M_{c,Rk} = W_y * \sigma_c$

If $r/t \le 0{,}04 * E / f_{yb}$: The cross section needs not be checked for local buckling

characteristic bending moment: $\quad M_{c,Rk} = W_y * f_{yb}$

4. Draft clauses for liner trays with s_1 >1m

The project has received financial support from the European Community (RFCS programme) under grant agreement No 754092

4. Draft clauses for liner trays with s_1 >1m

Design coef β_b

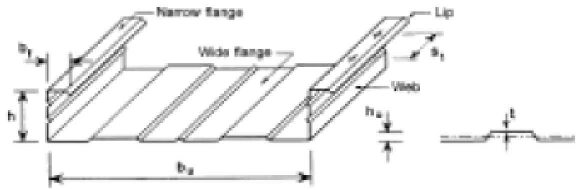

s_1 > 1m

$s_{1,1}$ technical sheet (known)
$s_{1,2}$ new spacing > 1m

$$M_{c,Rk,2} = M_{c,Rk,1} * \frac{N_{R,k,2}}{N_{R,k,1}} = M_{c,Rk,1} * \beta_b$$

Known

$N_{R,k,1}$ characteristic compression force of the small flanges of the liner trays, calculated with the buckling length $l = s_{1,1}$

Usually $s_{1,1}$ = 621 mm by testing

Usually $s_{1,1}$ = 300 mm by calculation

UnKnown

$N_{R,k,2}$ characteristic compression force of the small flanges of the liner trays, calculated with the buckling length $l = s_{1,2}$

Usually $s_{1,2}$ = max 2000mm (work site)

The project has received financial support from the European Community (RFCS programme) under grant agreement No 754092

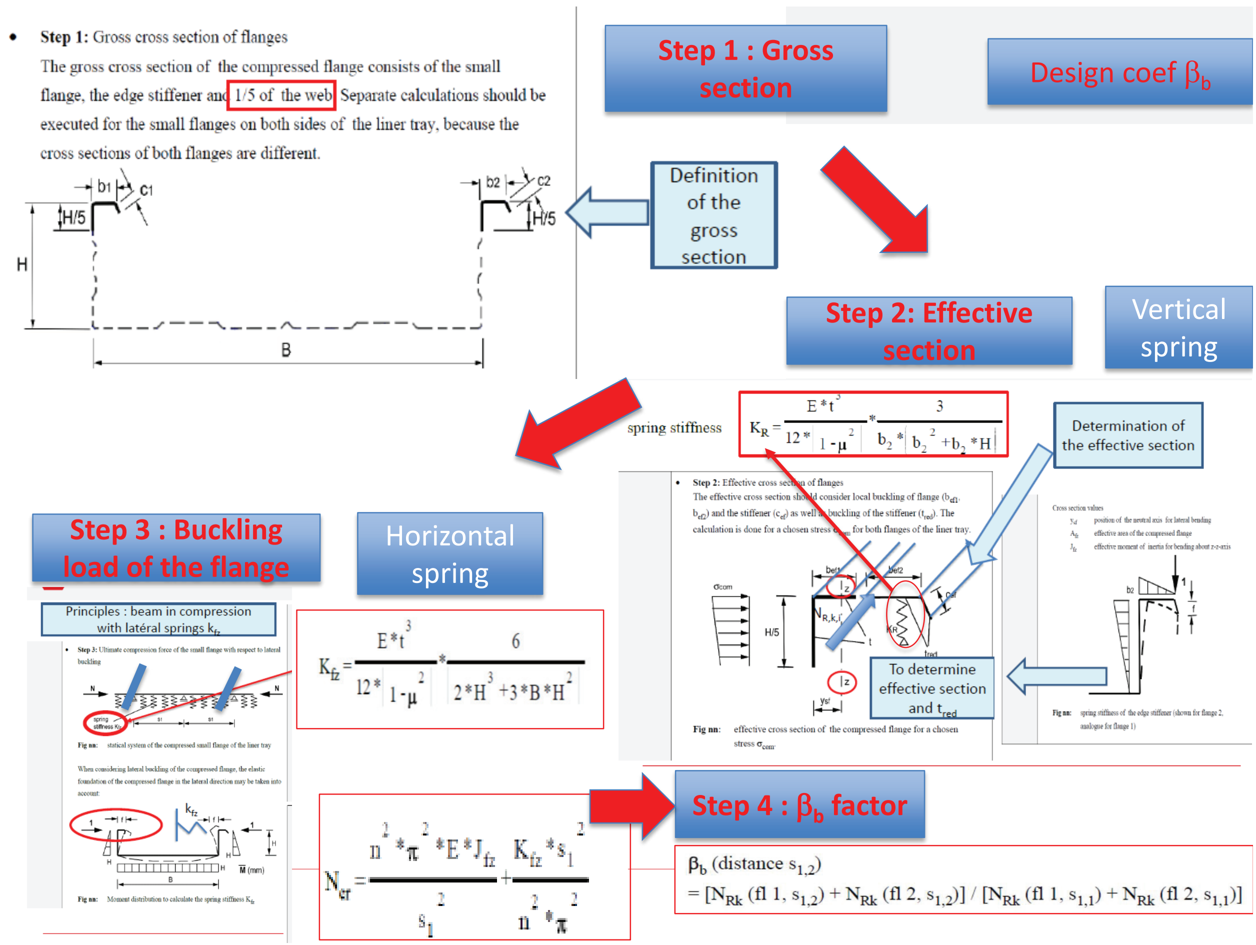
Step 1: Gross cross section of flanges
The gross cross section of the compressed flange consists of the small flange, the edge stiffener and 1/5 of the web. Separate calculations should be executed for the small flanges on both sides of the liner tray, because the cross sections of both flanges are different.
b1
c1
H/5
b2
c2
H
B
Step 1 : Gross section
Design coef β_b
Definition of the gross section
Step 2: Effective section
Vertical spring
spring stiffness
$K_R = \frac{E*t^3}{12*(1-\mu^2)} * \frac{3}{b_2*(b_2^2+b_2*H)}$
Determination of the effective section
Step 2: Effective cross section of flanges
To determine effective section and t_{red}
Fig nn: effective cross section of the compressed flange for a chosen stress σ_{com}
Step 3 : Buckling load of the flange
Horizontal spring
Principles : beam in compression with latéral springs k_{fz}
$K_{fz} = \frac{E*t^3}{12*(1-\mu^2)} * \frac{6}{2*H^3+3*B*H^2}$
Step 4 : β_b factor
$N_{cr} = \frac{n^2*\pi^2*E*J_{fz}}{s_1^2} + \frac{K_{fz}*s_1^2}{n^2*\pi^2}$
β_b (distance $s_{1,2}$)
$= [N_{Rk}(fl\ 1, s_{1,2}) + N_{Rk}(fl\ 2, s_{1,2})] / [N_{Rk}(fl\ 1, s_{1,1}) + N_{Rk}(fl\ 2, s_{1,1})]$

5. Draft clauses for assembled profiles

The project has received financial support from the European Community (RFCS programme) under grant agreement No 754092

5. Draft clauses for assembled profiles

Design process

1. cantilever above

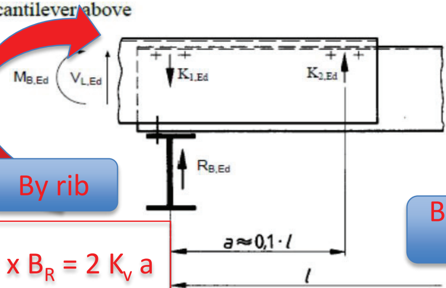

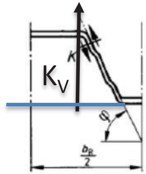

By rib

$M \times B_R = 2\, K_v\, a$

kN.m/m

B_R distance between two ribs

4 Types of assemblies

2. cantilever underneath

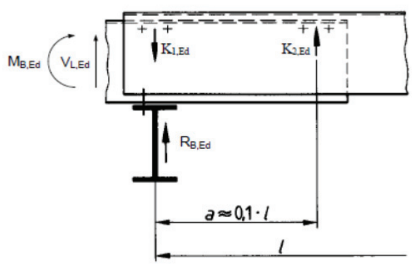

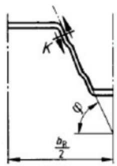

3. Overlap joint

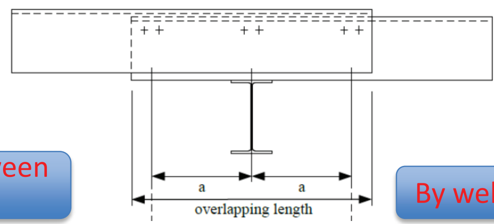

By web

$$K_{Ed} = \max K_i = \frac{\left|\frac{M_{B,Ed}}{a} + V_{L,Ed}\right|}{2 \ast \sin\varphi} \ast b_R \text{ (Verification in one web)}$$

$$\frac{K_{Ed}}{F_{V,Rd}} \leq 1{,}0$$

with $F_{V,Rd}$ shear resistance of the screws

4. Continuous profile with local reinforcement

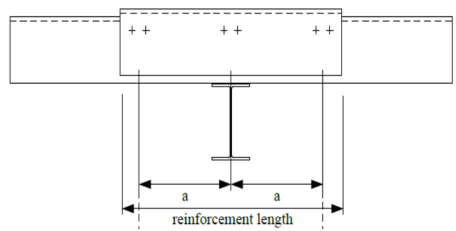

The project has received financial support from the European Community (RFCS programme) under grant agreement No 754092

6. Draft clauses for curved profiles

The project has received financial support from the European Community (RFCS programme) under grant agreement No 754092

6.1 Draft clauses for curved profiles

Interaction formula M/N+buckling

Take into account horizontal spring of the support

$$\boxed{\frac{N_{c,Ed}}{N_{c,Rd}} \cdot \left[1 + 0{,}5 \cdot \alpha \cdot \left(1 - \frac{N_{c,Ed}}{N_{c,Rd}}\right)\right] + \frac{M_{c,Ed}}{M_{c,Rd}} \leq 1}$$

α Not limited to 1

$$\boxed{\alpha = \sqrt{\frac{f_{y,b}}{\sigma_{cr}}} = \frac{s_K}{i_{ef} \cdot \pi} \cdot \sqrt{\frac{f_{y,b}}{E}}}$$

with:

$N_{c,Ed}$ compressive force,

$N_{c,Rd}$ resistance for compressive force,

$M_{c,Ed}$ bending moment,

$M_{c,Rd}$ resistance for bending moment,

α factor dependent on section and geometry.

$$\boxed{N_{c,Rd} = min(0{,}8 \cdot \sigma_{cr,gr} \cdot A_{gr} \; ; \; \sigma_c \cdot A_{eff})}$$

With:

$\sigma_{cr,gr}$ buckling stress in the gross section A_{gr}: $\sigma_{cr,gr} = \pi^2 \cdot E/(s_K/I_{gr})^2$,

I_{gr} second moment of area of the gross cross-section,

with:

σ_{cr} buckling stress in the effective cross section,

s_K buckling length: $s_K = \beta \cdot s$,

i_{ef} radius of inertia of the effective cross section: $i_{ef} = \sqrt{I_{eff}/A_{eff}}$

s half arc length as showned in figure 1,

β half arc length as showned in figure 1,

The project has received financial support from the European Community (RFCS programme) under grant agreement No 754092

6.2 Draft clauses for curved profiles

Bending resistance :How to pass from flat profile to curved profile

6.5 Curved profiled sheeting without arch effect

(1) For the design of the bending moment resistance of the curved profiled sheeting the following formula apply

$$\boxed{M_{c,Rd}(curved\,profile) = 0{,}9 \cdot M_{c,Rd}(flat\,profile) \qquad (6.40)}$$

The field of application is given in the table xx below :

Type of profile	Nominal thickness of the sheeting (mm)	Radius of curvarure R (m)
Corugated profile	0,63	$4{,}3 \leq R \leq 11{,}50$
	1,00	$3{,}80 \leq R \leq 17{,}20$
Trapezoidal profile	0,63	$5{,}60 \leq R \leq 32{,}9$
	1,00	$6{,}40 \leq R \leq 25{,}80$

Table xx field of application of the formula (6.40)

The project has received financial support from the European Community (RFCS programme) under grant agreement No 754092

7. Draft clauses for perforated profiles

The project has received financial support from the European Community (RFCS programme) under grant agreement No 754092

7. Draft clauses for perforated profiles

Effective thicknesses in the area of the perforation

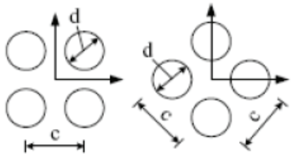

Gross section

for triangular pattern: $t_{a,\mathrm{eff}} = 1{,}18\,t\left(1 - \frac{0{,}9d}{a}\right)$ ... (10.25a)

for square pattern: $t_{a,eff} = 1{,}09t\left(1 - \frac{0{,}84d}{a}\right)$ ... (10.25b)

where:
d is the diameter of the perforations;
a is the spacing between the centres of the perforations.

(3) Provided that $0{,}2 \leq d/a \leq 0{,}9$ effective section properties may be calculated using Section 5, but replacing t by $t_{b,\mathrm{eff}}$ obtained from:

for triangular pattern: $t_{b,\mathrm{eff}} = t\sqrt[3]{1{,}18\left(1 - \frac{d}{a}\right)}$ ... (10.26a)

for square pattern: $t_{b,eff} = 0{,}98t\sqrt[3]{\left(1 - \frac{0{,}93d}{a}\right)}$ ... (10.26b)

Effective section

(4) The resistance of a single web to local transverse forces may be calculated using 6.1.9, but replacing t by $t_{c,\mathrm{eff}}$ obtained from:

for triangular pattern: $t_{c,\mathrm{eff}} = t\left[1 - \left(\frac{d}{a}\right)^2 \frac{s_{per}}{s_w}\right]^{3/2}$ ... (10.27a)

for square pattern: $t_{c,eff} = t\left[1 - 0{,}866\left(\frac{d}{a}\right)^2 \frac{s_{per}}{s_w}\right]^{3/2}$ ... (10.27b)

Resistance of single web

The project has received financial support from the European Community (RFCS programme) under grant agreement No 754092

8. Draft clauses for holed profiles

The project has received financial support from the European Community (RFCS programme) under grant agreement No 754092

8. Draft clauses for holed profiles

Design principle

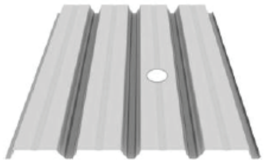

The top flange is considered as an oustanding element

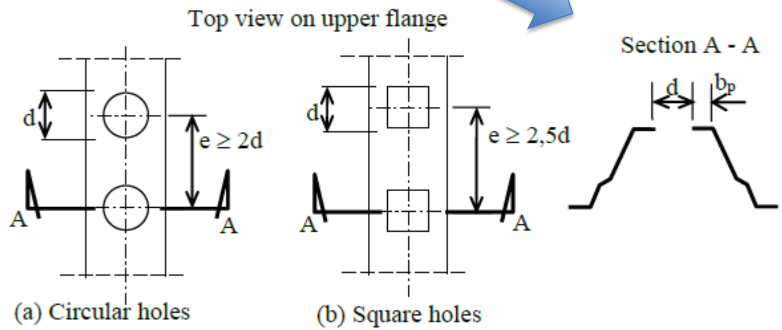

Fig. 10.16: Sheeting with circular (a) or square (b) holes in flange

(2) Range of validity :

a) trapezoidal profiled sheets;
b) no more than two holes by span in a flange, with minimum distances according to the Figure 10.16;
c) only uniformly distributed loads are permitted.

The project has received financial support from the European Community (RFCS programme) under grant agreement No 754092

9. Draft clauses for plank profiles

The project has received financial support from the European Community (RFCS programme) under grant agreement No 754092

9. Draft clauses for plank profiles

Principle :Planck = Liner tray + specifical verification of the dislocation

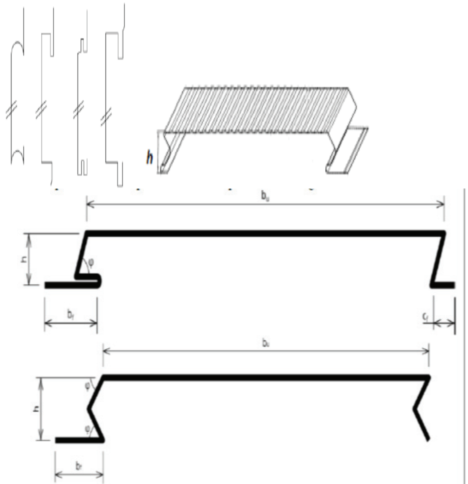

Table 10.7: Range of validity for plank profiles

0,75 mm ≤	t_{nom}	≤ 1 mm
	b_f	≤ 40 mm
25 mm ≤	h	≤ 30 mm
	b_u	≤ 300mm
	φ	≤ 60°
11 mm ≤	c_f	

=

Correction of α for action on support

(5) The value of the coefficient α should be obtained from the following:

a) for Category 1 :

- for sheeting profiles: $\alpha = 0{,}075$ ... (6.20a)
- for liner trays and hat sections: $\alpha = 0{,}057$ ... (6.20b)
- for plank profiles: $\alpha = 0{,}115$ ... (6.20c)

b) for Category 2:

- for sheeting profiles: $\alpha = 0{,}15$ ... (6.20d)
- for liner trays and hat sections: $\alpha = 0{,}115$ ... (6.20e)
- for plank profiles: $\alpha = 0{,}115$ ... (6.20f)

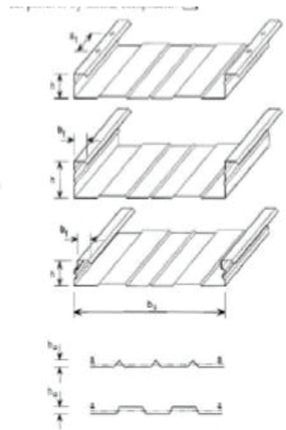

Figure 10.9: Typical geometry for liner trays

The project has received financial support from the European Community (RFCS programme) under grant agreement No 754092

9. Draft clauses for plank profiles

verification of the dislocation

(2) To avoid dislocation of the joint of plank profile, we must verify :

$$q_{Ed} \leq q_{Rd}$$

(3) The load resistance regarding joint dislocation of a plank profile is :

$$\boxed{q_{Rd} = \frac{0{,}8 \cdot 2 \cdot E \cdot 1000 \cdot t^3 \cdot \delta_{\lim}}{b_u \cdot \left(12 \cdot (1-\nu^2) \cdot \sqrt{\left(\frac{2 \cdot b_f{}^3}{3}\right)^2 + \left[b_f \cdot \left(\frac{b_u \cdot h}{3} + \frac{h^2}{2}\right)\right]^2}\right)}}$$

Where:

- For clip joint:

$$\delta_{\lim} = c_f$$

- For chevron shaped joint:

$$\delta_{\lim} = \frac{h}{2 \cdot \tan\varphi}$$

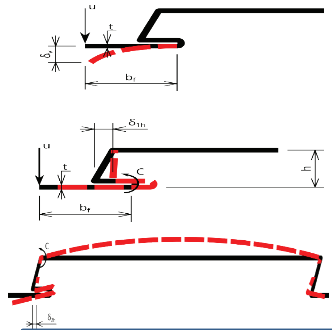

To cover the dislocation phenomenon = analysis of possible displacements with plank geometry

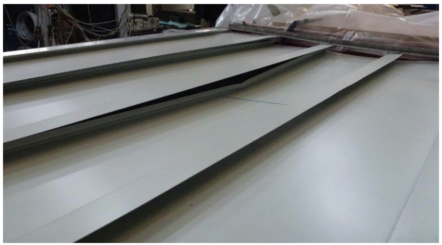

The project has received financial support from the European Community (RFCS programme) under grant agreement No 754092

GRISPE PLUS

VALORISATION OF KNOWLEDGE
FOR SPECIFIC PROFILED STEEL SHEETS

GRISPE WORKSHOP
Proposals for the inclusion of 9 calculation methods into EN 1993-1-3

David Izabel
14 june 2018
RFCS Project

The project has received financial support from the European Community (RFCS programme) under grant agreement No 754092

Contence

1. Draft clauses for steel decks with embossments /indentations
2. Draft clauses for steel decks with outwards stiffener
3. Draft clauses for liner trays with s_1 >1m
4. Draft clauses for assembled profiles
5. Draft clauses for corrugated sheetings
6. Draft clauses for curved profiles
7. Draft clauses for perforated profiles
8. Draft clauses for holed profiles
9. Draft clauses for plank profiles

The project has received financial support from the European Community (RFCS programme) under grant agreement No 754092

1) Draft clauses for steel decks with embossments/indentations

- Embossements/Indantations

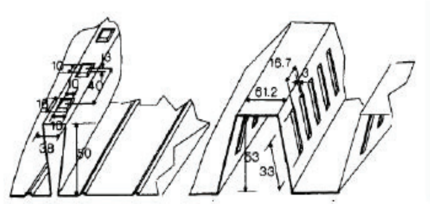

Fig 1

New clause

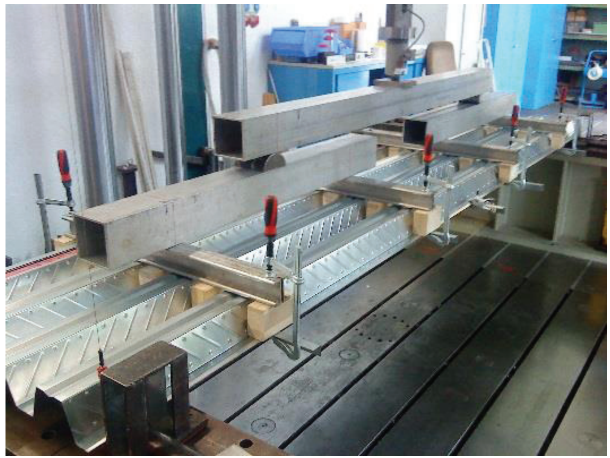

The project has received financial support from the European Community (RFCS programme) under grant agreement No 754092

Profile sheets with indentations and/or embossements

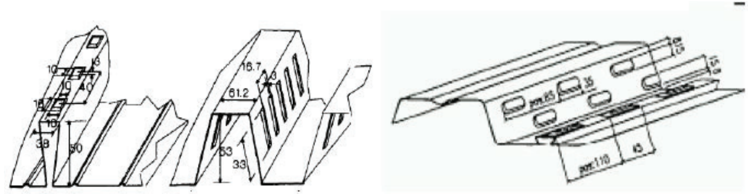

Fig 1

AM-1-3-2013- GRISPE2	
Subject	Effective section of sheeting with indentation and/or embossment
Clause No./ Subclause No./ Annex	Section 5, adding new section 5.7
Reason for amendment	Composite behaviour between profiled sheeting and concrete is ensured by means of mechanical interlock provided by local deformations in the profile such as indentations or embossments. The clause 9.4.1 (1) of EN 1994-1-1 stipulates that the design of the profiled steel sheeting as shuttering should be in accordance with EN1993-1-3. The sheeting used in composite slabs is subjected to a simultaneous action of traction and bending. However, the current version EN 1993-1-3 does not provide the information on the taking into account the indentations or embossments in calculation of the effective section under this action.

The project has received financial support from the European Community (RFCS programme) under grant agreement No 754092

New section 5.7 for sheeting with indentations and embossements

Proposed change	Add a new section: 5.7 Sheeting with indentations or embossments (1) The effective width of plane wall with indentations or embossments should be first calculated according to 5.5.1(2) (2) In the second step, the indentation or embossment located on the effective part of the wall should be taken into account reducing the effective thickness by mean of a reduction factor considering the embossments / indentations (Fig. 5.15) as plate elements with a reduced thickness $\boxed{t_{red} = \rho * t}$ where: $\boxed{\rho = A*h + B}$ ... (5.43) h is height of the indentation / embossment (see figure 5.15) A and B are coeeficients given in table 5.3.

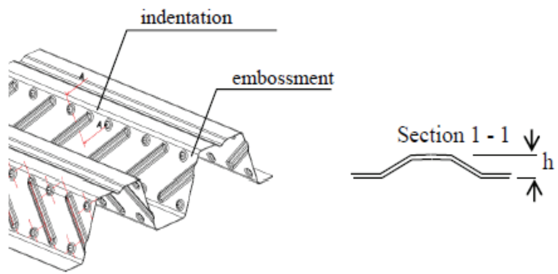

Figure 5.15 Exemple of sheeting with indentations and embossments

Results of GRISPE

The embossement is taken into account by a ρ coefficient applied on the thickness and on the length of the embossement

The project has received financial support from the European Community (RFCS programme) under grant agreement No 754092

New section 5.7 for sheeting with indentations and embossements

Results of GRISPE

Tabulated vales of ρ

Table 5.3: Valles of coefficients A and B (equation (5.43)

Type of local deformation	t (mm)	h (mm)	A	B
Indentation	0.71	0 - 1.5	-0.533	1.000
		1.5 - 2.75	-0.112	0.368
		2.75 - 4.0	-0.025	0.128
	0.96	0 - 1.5	-0.467	1.000
		1.5 - 2.75	-0.186	0.580
		2.75 - 4.0	-0.020	0.122
	1.21	0 - 1.5	-0.401	1.000
		1.5 - 2.75	-0.260	0.792
		2.75 - 4.0	-0.015	0.116
Embossment	0.71	0 - 1.5	-0.267	1.000
		1.5 - 2.75	-0.056	0.684
		2.75 - 4.0	-0.013	0.564
	0.96	0 - 1.5	-0.234	1.000
		1.5 - 2.75	-0.093	0.790
		2.75 - 4.0	-0.010	0.561
	1.21	0 - 1.5	-0.201	1.000
		1.5 - 2.75	-0.130	0.896
		2.75 - 4.0	-0.008	0.558

For intermediate thickness 0.71 mm $\leq t < 0.96$ mm the reduction factor ρ may be deremina-ted by means of linear interpolation between 0.71 mm and 0.96 mm

For intermediate thickness 0.96 mm $\leq t < 1.21$ mm the reduction factor ρ may be deremina-ted by means of linear interpolation between 0.96 mm and 1.21 mm

The project has received financial support from the European Community (RFCS programme) under grant agreement No 754092

Background – for sheeting with embossements and indentations

Background information	RFCS research project GRISPE: C. FAUTH (KIT) "WP1 Test report of steel trapezoidal sheeting with and without embossments and outward stiffeners ", GRISPE D1.3, 2014 A. PALISSON (Sokol Palisson Consultants) "WP1 TEST ANALYSIS AND INTER-PRETATION", GRISPE D1.4, 2015 A. PALISSON (Sokol Palisson Consultants) " WP1 Background guidance for EN 1993-1-3 to design of special shape sheeting with outwards stiffeners in the flange", GRISPE D1.6, June 2015
	Proposal from A. Palisson, D. Izabel, L. Sokol

The project has received financial support from the European Community (RFCS programme) under grant agreement No 754092

Indentations and embossement – bending support reaction

AM-1-3-2013- GRISPE3	
Subject	Resistance of sheeting with indentations or embossment to combined bending moment and local load or support reaction
Clause No./ Subclause No./ Annex	Section 6.1.11, adding new clause (2)
Reason for amendment	The clause 9.4.1 (1) of EN 1994-1-1 stipulates that the design of the profiled steel sheeting as shuttering should be in accordance with EN1993-1-3. The sheeting used in composite slabs is subjected to a simultaneous action of traction and bending. However, the current version EN 1993-1-3 does not provide the information on the taking into account the indentations or embossments in calculation of the effective section under this action.
Proposed change	Add a new clause: (2) In case of sheeting with indentations or embossments, the quations (6.28a), (6.28b) and (6.28c) from the AMD-1-3-2013-14 may be used with: $M_{c,Rd}$ = resistance moment determined considering the identations and/or embossments according to the Amendment AM-1-3-2013-XX $R_{w,Rd}$ = local transverse resistance determined without considering the identations and/or embossments

Results of GRISPE

For the design at internal support

Reduced thicknesses

No modifications

The project has received financial support from the European Community (RFCS programme) under grant agreement No 754092

Background

Background information	RFCS research project GRISPE: C. FAUTH (KIT) "WP1 Test report of steel trapezoidal sheeting with and without embossments and outward stiffeners ", GRISPE D1.3, 2014 A. PALISSON (Sokol Palisson Consultants) "WP1 TEST ANALYSIS AND INTER-

	PRETATION", GRISPE D1.4, 2015 A. PALISSON (Sokol Palisson Consultants) " WP1 Background guidance for EN 1993-1-3 to design of special shape sheeting with outwards stiffeners in the flange", GRISPE D1.6, June 2015
	Proposal from A. Palisson, D. Izabel, L. Sokol

The project has received financial support from the European Community (RFCS programme) under grant agreement No 754092

2) Draft clauses for steel decks with outward stiffener

Outward stiffener

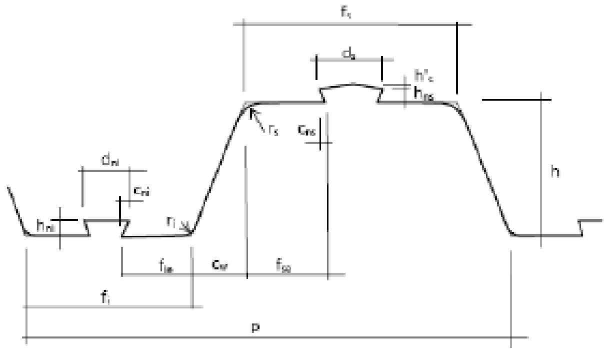

New clause

The project has received financial support from the European Community (RFCS programme) under grant agreement No 754092

Steel decking with outward stiffener

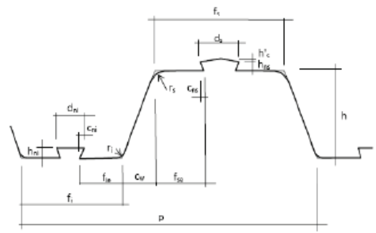

AM-1-3-2013-GRISPE1	
Subject	Taking into account of intermediate outward stiffener in the sheeting flange
Clause No./ Subclause No./ Annex	Section 5.5.3.3, new clause 5.5.3.3(12)
Reason for amendment	In current practice of composite slabs, in order to increase the horizontal shear resistance between the steel sheeting and concrete, the outward intermediate stiffeners in dovetail form are used in the upper flange. However, the current version EN 1993-1-3 does not provide information on the taking into account this kind of stiffener in calculation of the bending resistance of the section.

The project has received financial support from the European Community (RFCS programme) under grant agreement No 754092

New clause 5.5.33

Proposed change	Add a new clause:

(12) In case of flange with intermediate outward stiffener, which the width not exceeds the 1/3 of the flange width, such as shown in the Fig. 5.11a, the calculation of the effective section is performed considering if the yield stress is reached in the upper or lower flange:

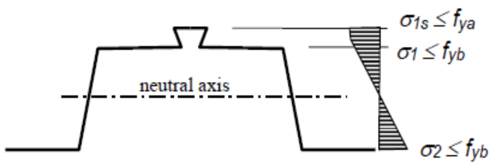

- if the yield stress is reached in the lower flange then $\sigma_2 = f_{yb}$ and $\sigma_1 < f_{yb}$
- if the yield stress is reached in the upper flange then $\sigma_1 = f_{yb}$ and $\sigma_2 < f_{yb}$

In calculation, the stress σ_{1s} in the stiffener may be defined according to equation (3.2), clause 3.2.2(6). As a safe simplification, the stress σ_{1s} may be limited to the f_{yb} value.

The critical buckling stress $\sigma_{cr,s}$ for the stiffener should be obtained from the equation (5.19).

Results of GRISPE

Value of the stress to be taken into account for the outward stiffener

The project has received financial support from the European Community (RFCS programme) under grant agreement No 754092

Background

Background information	RFCS research project GRISPE: C. FAUTH (KIT) "WP1 Test report of steel trapezoidal sheeting with and without embossments and outward stiffeners ", GRISPE D1.3, 2014 A. PALISSON (Sokol Palisson Consultants) "WP1 TEST ANALYSIS AND INTERPRETATION", GRISPE D1.4, 2015 A. PALISSON (Sokol Palisson Consultants) " WP1 Background guidance for EN 1993-1-3 to design of special shape sheeting with outwards stiffeners in the flange", GRISPE D1.6, June 2015
	Proposal from A. Palisson, D. Izabel, L. Sokol

The project has received financial support from the European Community (RFCS programme) under grant agreement No 754092

3) Draft clause for liner tray (s_1>1m)

- Liner trays with s_1 >1m

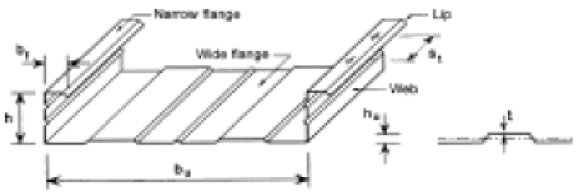

s_1 > 1m

Curent clause has to be completed

The project has received financial support from the European Community (RFCS programme) under grant agreement No 754092

Liner tray design with 300 mm $\leq s_1 \leq$ 2000 mm

AM-1-3-2016-04	
Subject	Influence of the fixing distance s_1 on the bending moment capacity of liner trays. Improvement of the coefficient β_b and extension of the application range
Clause No/ Subclause No/ Annex	10.2.2.3
Reason for Amendment	The actual design rule to take into account the effect of the fixing distance s_1 is rather conservative, and furthermore limited to a maximum fixing distance $s_1 = 1000$ mm. Both aspects will be improved.

The project has received financial support from the European Community (RFCS programme) under grant agreement No 754092

Bending resistant proportional with β_b

Proposed Change	The ultimate positive bending moment of the liner trays (wide flange in tension) is generally determined by the ultimate compression forces of the small flanges. The compressed flanges are stabilized against lateral buckling by the connections between liner tray and outer cladding; the fixing distance s_1 determines the buckling length of the compressed flange and therefore the ultimate compression forces of the small flanges and in consequence also the ultimate bending moment. The ultimate bending moment ist approximately proportional to the compression resistance of the small flanges. The reduction coefficient $\boldsymbol{\beta_b}$ to respect the fixing distance s1 corresponds approximately to the reduction of the compression resistance of the small flanges. Ultiamte bending moment $M_{c,Rk,2} = M_{c,Rk,1} * \frac{N_{R,k,2}}{N_{R,k,1}} = M_{c,Rk,1} * \beta_b$

$s_{1,1}$ technical sheet (known)
$s_{1,2}$ new spacing > 1m

$N_{Rk,1}$ Critical compression force for $s_{1,1}$
$N_{Rk,2}$ Critical compression force for $s_{1,2}$

New β_b

Results of GRISPE

The project has received financial support from the European Community (RFCS programme) under grant agreement No 754092

$M_{c,Rk,1}$ bending positive moment for $s_{1,1}$ =300mm (calculation)

The different values of $s_{1,1}$ => Design by calculation

with:

$M_{c,Rk,1}$ (already known) ultimate positive bending moment of the liner trays for a fixing distance $s_{1,1}$

Design by calculation: The bending moment $M_{c,Rk,1}$ is the calculated ultimate bending moment for the fixing distance $s_{1,1}$ = 300 mm according to Clause 10.2.2.2 ($\beta_b = 1{,}0$)

Design by calculation

Usually $s_{1,1}$ = 300 mm

Results of GRISPE

The project has received financial support from the European Community (RFCS programme) under grant agreement No 754092

$M_{c,Rk,1}$ bending positive moment for $s_{1,1}$ =621 mm(testing)

The different values of $s_{1,1}$ => Design by testing

Design by testing: The bending moment $M_{c,Rk,1}$, which is determined by testing, is related to the distance $s_{1,1}$, which was chosen for the tests. This fixing distance $s_{1,1}$ is mentioned in the technical documents of the liner tray (often: s_1 = 621 mm = 3 ribs of the cladding profile 35/307)

Results of GRISPE

Design by testing

Usually $s_{1,1}$ = 621 mm

The project has received financial support from the European Community (RFCS programme) under grant agreement No 754092

$M_{c,Rk,2}$ bending positive moment for $s_{1,1}$ = 2000 maxi

maximum values of $s_{1,2}$ => 2 m

	$M_{c,Rk,2}$	(unknown) ultimate positive bending moment of the liner trays for a fixing distance $s_{1,2}$ The bending moment $M_{c,Rk,2}$ is the recalculated ultimate bending moment for the interesting fixing distance $s_{1,2}$. The interesting fixing distance $s_{1,2}$ corresponds to the foreseen fixing distance in a specific application. The fixing distance $s_{1,2}$ should not exceed max s_1 = 2000 mm

Results of GRISPE

Bending moment resistance for $s_{1,2}$ = **2000 mm max.**

The project has received financial support from the European Community (RFCS programme) under grant agreement No 754092

New definition of β_b

Principle: determine a new β_b coefficient fonction of the ratio of the critical compression force of the free flange of the liner tray

Results of GRISPE

$\beta_b = \frac{N_{R,k,2}}{N_{R,k,1}}$ reduction coefficient for fixing distances $s_1 \geq s_{1,1}$

$N_{R,k,1}$ characteristic compression force of the small flanges of the liner trays, calculated with the buckling length $l = s_{1,1}$

$N_{R,k,2}$ characteristic compression force of the small flanges of the liner trays, calculated with the buckling length $l = s_{1,2}$

Critical compression force calculated for each distance of the spacers $s_{1,1}$ and $s_{1,2}$

The calculation of the characteristic compression force of the small flanges of the liner trays should respect the following principles:

The project has received financial support from the European Community (RFCS programme) under grant agreement No 754092

Step 1 – Gross cross section of flange

- **Step 1:** Gross cross section of flanges

  The gross cross section of the compressed flange consists of the small flange, the edge stiffener and 1/5 of the web Separate calculations should be executed for the small flanges on both sides of the liner tray, because the cross sections of both flanges are different.

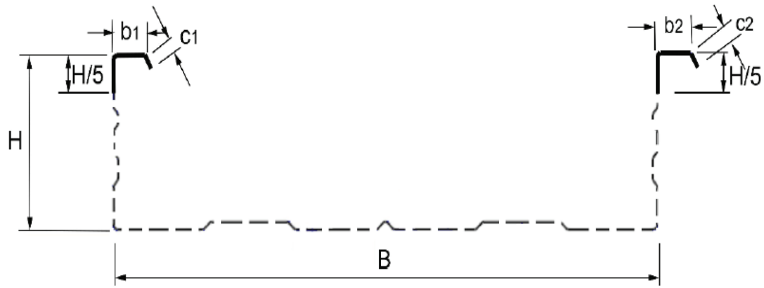

Fig nn: Liner tray, definition of the gross cross sections of the compressed flanges

Definition of the gross section

The project has received financial support from the European Community (RFCS programme) under grant agreement No 754092

Step 2 – Effective cross section of flanges

spring stiffness
$$K_R = \frac{E * t^3}{12 * (1 - \mu^2)} * \frac{3}{b_2 * (b_2^2 + b_2 * H)}$$

Determination of the effective section

- **Step 2:** Effective cross section of flanges
  The effective cross section should consider local buckling of flange (b_{ef1}, b_{ef2}) and the stiffener (c_{ef}) as well as buckling of the stiffener (t_{red}). The calculation is done for a chosen stress σ_{com} for both flanges of the liner tray.

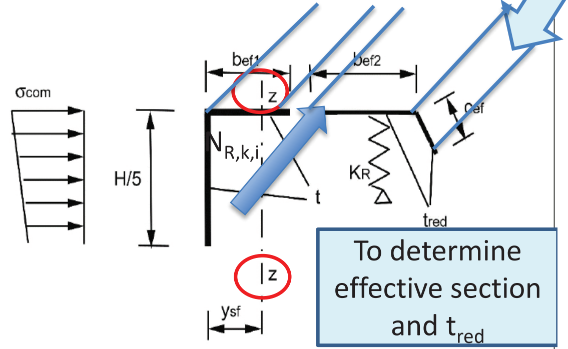

To determine effective section and t_{red}

Fig nn: effective cross section of the compressed flange for a chosen stress σ_{com}.

Cross section values
y_{sf} position of the neutral axis for lateral bending
A_{fz} effective area of the compressed flange
J_{fz} effective moment of inertia for bending about z-z-axis

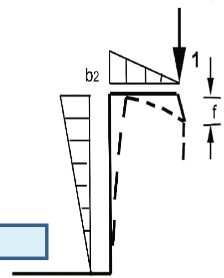

Fig nn: spring stiffness of the edge stiffener (shown for flange 2, analogue for flange 1)

The project has received financial support from the European Community (RFCS programme) under grant agreement No 754092

Step 3 – Ultimate compression force

Principles : beam in compression with latéral springs k_{fz}

- **Step 3:** Ultimate compression force of the small flange with respect to lateral buckling

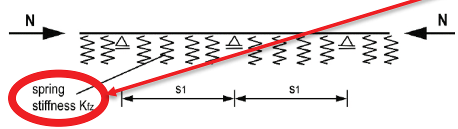

Fig nn: statical system of the compressed small flange of the liner tray

When considering lateral buckling of the compressed flange, the elastic foundation of the compressed flange in the lateral direction may be taken into account:

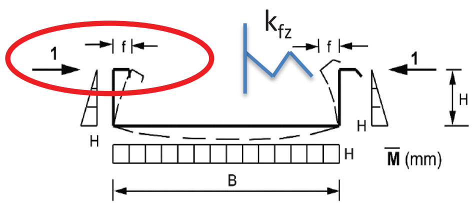

Fig nn: Moment distribution to calculate the spring stiffness K_{fz}

6.3.1.1

spring stiffness $K_{fz} = \frac{E*t^3}{12*(1-\mu^2)} * \frac{6}{2*H^3+3*B*H^2}$

critical axial force $N_{cr} = \frac{n^2*\pi^2*E*J_{fz}}{s_1^2} + \frac{K_{fz}*s_1^2}{n^2*\pi^2}$

Normally, the axial force is a minimum for n = 1 (n = number of buckling waves between neighboured fixings).

The ultimate axial compression force N_{Rk} is calculated according to EN 1993-1-1 clause 6.3.1.1. Hereby, buckling curve a_0 may be used.

Buckling Curve a_0

ultimate axial force $N_{Rk} = X(a_0) * N_{pl}$

$N_{b,Rd} = \frac{\chi A_{eff} f_y}{\gamma_{M1}}$ $= X(a_0) * A_{fz} * f_{yb}$

ultimate compressive stress $\sigma_k = X(a_0) * f_{yb}$

If σ_k is different from the initially chosen stress σ_{com}, the calculation should be repeated from step 2 using $\sigma_{com} = \sigma_k$ until the stress σ_{com}, which is the basis for the effective cross section, and the buckling stress of the compressed flange σ_k have converge

eventual calibration of the effective section with σ_k

Analogue calculations should be executed for both flanges of the liner tray.

The project has received financial support from the Europe

Step 4 – Reduction coefficient β_b

Results of GRISPE

- **Step 4:** Reduction coefficient β_b

  The calculation according step 2 and step 3 is done for both flanges and for both fixing distances $s_{1,1}$ and $s_{1,2}$. The reduction coefficient for the fixing distance $s_{1,2}$ is

  $$\beta_b \text{ (distance } s_{1,2}) = [N_{Rk} (\text{fl } 1, s_{1,2}) + N_{Rk} (\text{fl } 2, s_{1,2})] / [N_{Rk} (\text{fl } 1, s_{1,1}) + N_{Rk} (\text{fl } 2, s_{1,1})]$$

Ultiamte bending moment

$$M_{c,Rk,2} = M_{c,Rk,1} * \frac{N_{R.k.2}}{N_{R.k.1}} = M_{c,Rk,1} * \beta_b$$

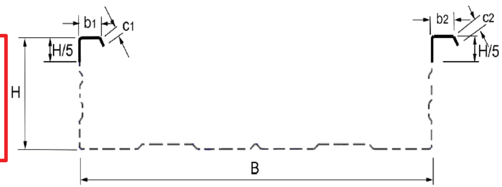

The project has received financial support from the European Community (RFCS programme) under grant agreement No 754092

Background

Background Information	[1] D2.5 Background and draft annexes for EN 1993-1-3 for liner trays, 31.10.2015, KIT

The project has received financial support from the European Community (RFCS programme) under grant agreement No 754092

4) Draft clauses for assembled profiles

- Assembled profiles

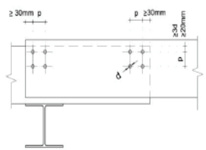

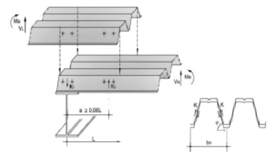

Fig 6

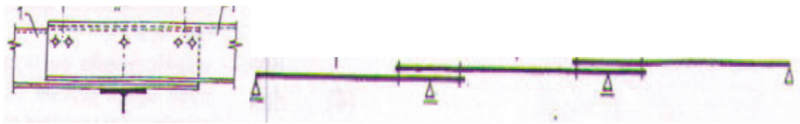

Fig 7

New paragraph have to be added

The project has received financial support from the European Community (RFCS programme) under grant agreement No 754092

New clause to be added

AM-1-3-2016-08	
Subject	Assembled trapezoidal profiles (statically effective overlapping)
Clause No/ Subclause No/ Annex	
Reason for Amendment	No data in the actual version of EN 1993-1-3

The project has received financial support from the European Community (RFCS programme) under grant agreement No 754092

Cantilever above

Proposed Change

1. cantilever above

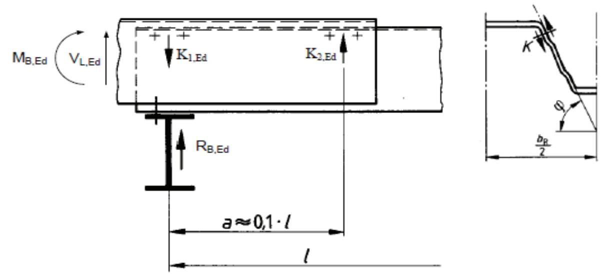

a) Verification of the profile with the design resistance values ($M_{Rd,B}$, $R_{w,Rd,B}$) of the continuous profile in the support axis taking into account the influence of support reaction (M-R-interaction).

b) Check of the free end of the cantilever, if the line load introduced by the connections K_i may create web crippling

- Downward load = negative bending moment
web crippling at the end of the cantilever
$F_{Ed} = M_{B,Ed}/(2a) < 0,5\ R_{w,Rd,B}$
$R_{w,Rd,B}$ is the ultimate support reaction at intermediate supports in the opposite profile position (in general negative position) for the max. support width, in general l_{aB} = 160 mm (determined in GRISPE [1], that the design resistance $R_{w,Rd,B}$(160 mm) is suitable for this verification)

- Uplift load = positive bending moment
No web crippling possible at the end of the cantilever necessary

Results of GRISPE

Based on Grispe and DIN

Principles : bending moment split in two forces : M/a = F

The project has received financial support from the European Community (RFCS programme) under grant agreement No 754092

Cantilever above

c) Verification of the connections K_{Ed}

$$K_{Ed} = \max K_i = \frac{\left|\frac{M_{B,Ed}}{a} + V_{L,Ed}\right|}{2 * \sin\varphi} * b_R \text{ (Verification in one web)}$$

$$\frac{K_{Ed}}{F_{v,Rd}} \leq 1{,}0$$

with $F_{v,Rd}$ shear resistance of the screws

Results of GRISPE

Based on Grispe and DIN

The project has received financial support from the European Community (RFCS programme) under grant agreement No 754092

Cantilever underneath

2. cantilever underneath

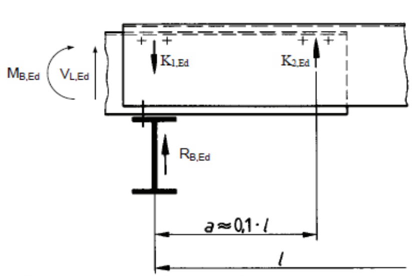

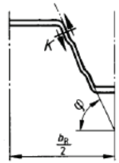

a) Verification of the profile with the design resistance values ($M_{Rd,B}$, $R_{w,Rd,B}$) of the continuous profile in the support axis taking into account the influence of support reaction (M-R-interaction).

b) Check of the free end of the cantilever, if the line load introduced by the connections K_i may create web crippling

- Downward load = negative bending moment
No web crippling possible at the end of the cantilever
- Uplift load = positive bending moment
No web crippling possible at the end of the cantilever

c) Verification of the connections K_{Ed}

$K_{Ed} = \max K_i = \frac{|M_{B,Ed}|}{2 * a * \sin \varphi} * b_R$ (Verification in one web)

$\frac{K_{Ed}}{F_{v,Rd}} \leq 1{,}0$

with $F_{v,Rd}$ shear resistance of the screws

Results of GRISPE

Based on GRISPE and DIN

The project has received financial support from the European Community (RFCS programme) under grant agreement No 754092

Overlap Joint

3. Overlap joint

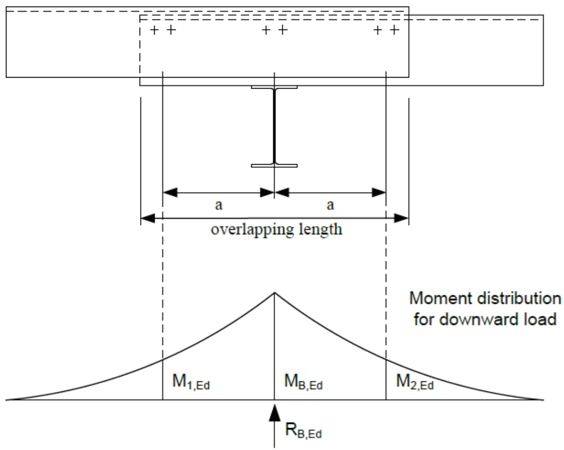

a) Determination of the bending moment distribution under design loads like for continuous sheets (The influence of the higher bending stiffness at the overlapping area, which is partly compensated by the slip and/or elastic deformations at the connections, is neglected). Results: $M_{B,Ed}$; $R_{B,Ed}$; $M_{1,Ed}$; $M_{2,Ed}$

b) Verification of the profiles at the support axis with 90 % of the resistance of the overlapping profiles (factor 0,9 determined in GRISPE [1]) taking into account the influence of the support reaction (M-R-interaction): $M_{B,ED} \leq 0{,}9 \sum M_{Rd,B}$; $R_{B,ED} \leq 0{,}9 \sum R_{wRd,B}$; M-R-interaction

Results of GRISPE

Based on GRISPE and DIN

The project has received financial support from the European Community (RFCS programme) under grant agreement No 754092

Overlap Joint

c) Verification of the continuous profiles at the ends of the overlap with the bending moments $M_{1,Ed}$ or $M_{2,Ed}$ and the line loads introduced by the connections K_i: $F_{Ed} = M_{B,Ed} / (2\ a)$. Depending of the direction of the load F_{Ed} relative to the web of the profile, the M-R-interaction or the M-V-interaction has to be verified.

For downward load, F_{Ed} is acting as a tension force on the webs of the continuous profiles; M-V-interaction has to be verified.

For uplift load, F_{Ed} is acting as a compression force on the webs of the continuous profiles; M-R-interaction has to be verified.

In both load cases, the resistance values of the profile in the opposite position at intermediate supports apply for these verifications.

d) Check of the free end of the cantilever, if the line load introduced by the connections K_i may create web crippling

- Downward load = negative bending moment
  web crippling at the end of the upside cantilever

Results of GRISPE

Based on Grispe and DIN

The project has received financial support from the European Community (RFCS programme) under grant agreement No 754092

Overlap Joint

$F_{Ed} = M_{B,Ed}/(2a) < 0{,}5\ R_{w,Rd,B}$

$R_{w,Rd,B}$ is the ultimate support reaction at intermediate supports in the opposite profile position (in general negative position) for the max. support width, in general $l_{aB} = 160$ mm (determined in GRISPE [1], that the design resistance $R_{w,Rd,B}$(160 mm) is suitable for this verification)

No web crippling possible at the end of the cantilever underneath

- Uplift load = positive bending moment

No web crippling possible, neither at the upside cantilever nor at the cantilever underneath.

e) Verification of the connections K_{Ed} with

$$K_{Ed} = \max K_i = \frac{|M_{B,Ed}|}{2 * a * \sin\varphi} * b_R \text{ (Verification in one web)}$$

$$\frac{K_{Ed}}{F_{v,Rd}} \leq 1{,}0$$

with $F_{v,Rd}$ shear resistance of the screws

Results of GRISPE

Based on Grispe and DIN

The project has received financial support from the European Community (RFCS programme) under grant agreement No 754092

Continous profiles with local reinforcement

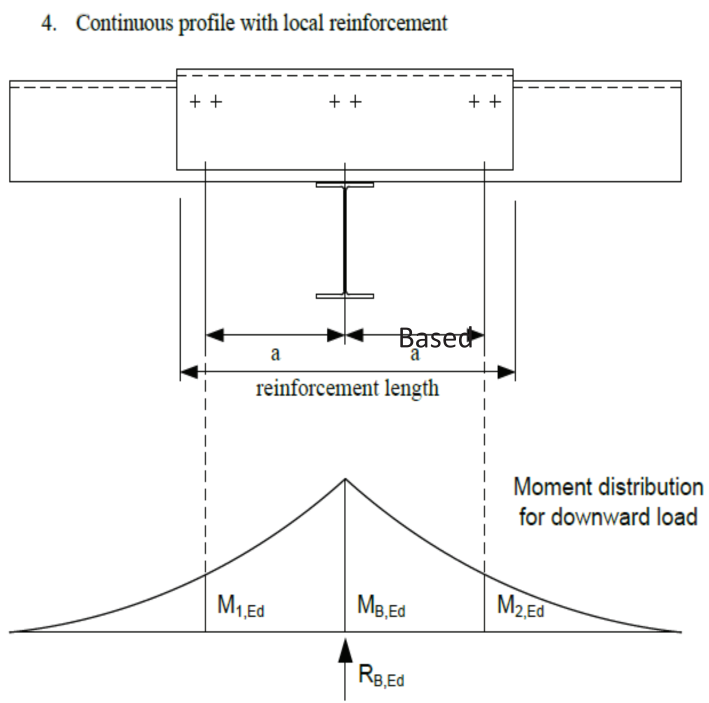

Results of GRISPE

Based on GRISPE and DIN + complementary clause about the shear force (web crippling)

The project has received financial support from the European Community (RFCS programme) under grant agreement No 754092

Continous profiles with local reinforcement

a) Determination of the bending moment distribution under design loads like for continuous sheets (The influence of the higher bending stiffness at the overlapping area, which is partly compensated by the slip and/or elastic deformations at the connections, is neglected). Results: $M_{B,Ed}$; $R_{B,Ed}$; $M_{1,Ed}$; $M_{2,Ed}$

b) Verification of the profiles at the support axis with 90 % of the resistance of the overlapping profiles (factor 0,9 determined in GRISPE [1]) taking into account the influence of the support reaction (M-R-interaction): $M_{B,ED} \leq 0,9 \sum M_{Rd,B}$; $R_{B,ED} \leq 0,9 \sum R_{wRd,B}$; M-R-interaction

Results of GRISPE

Based on GRISPE and DIN + complementary clause about the shear force (web crippling)

The project has received financial support from the European Community (RFCS programme) under grant agreement No 754092

Continous profiles with local reinforcement

	c) Verification of the continuous profile at the ends of the overlap with the bending moments $M_{1,Ed}$ or $M_{2,Ed}$ and the line loads introduced by the connections K_i: $F_{Ed} = M_{B,Ed} / (2\ a)$. Depending of the direction of the load F_{Ed} relative to the web of the profile, the M-R-interaction or the M-V-interaction has to be verified. For downward load, F_{Ed} is acting as a tension force on the webs of the continuous profile; M-V-interaction has to be verified. For uplift load, F_{Ed} is acting as a compression force on the webs of the continuous profile; M-R-interaction has to be verified. In both load cases, the resistance values of the profile in the opposite position at intermediate supports apply for these verifications.

Results of GRISPE

Based on GRISPE and DIN + complementary clause about the shear force (web crippling)

The project has received financial support from the European Community (RFCS programme) under grant agreement No 754092

Continous profiles with local reinforcement

d) Check of the free end of the cantilever, if the line load introduced by the connections K_i may create web crippling

- Downward load = negative bending moment

web crippling at the end of both cantilevers

$F_{Ed} = M_{B,Ed}/(2a) < 0,5\ R_{w,Rd,B}$

$R_{w,Rd,B}$ is the ultimate support reaction at intermediate supports in the opposite profile position (in general negative position) for the max. support width, in general $l_{aB} = 160$ mm (determined in GRISPE [1], that the design resistance $R_{w,Rd,B}$(160 mm) is suitable for this verification)

- Uplift load = positive bending moment

No web crippling possible at the end of both cantilevers

e) Verification of the connections K_{Ed} with

$$K_{Ed} = \max K_i = \frac{|M_{B,Ed}|}{2*a*\sin\varphi} * b_R \text{ (Verification in one web)}$$

$$\frac{K_{Ed}}{F_{V,Rd}} \leq 1{,}0$$

with $F_{V,Rd}$ shear resistance of the screws

Results of GRISPE

Based on GRISPE and DIN + complementary clause about the shear force (web crippling)

The project has received financial support from the European Community (RFCS programme) under grant agreement No 754092

Continous profiles with local reinforcement

	Edge and hole spacings for statically effective overlapping (1.-4.) 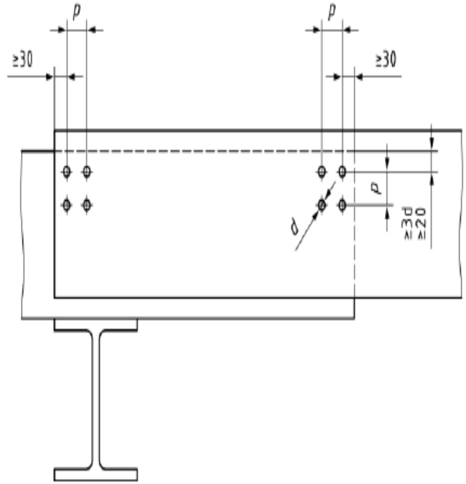
Background Information	[1] D2.5 Background and draft annexes for EN 1993-1-3 for assembled profiles, 31.10.2015, KIT

Results of GRISPE

Based on GRISPE and DIN + complementary clause about the shear force (web crippling)

The project has received financial support from the European Community (RFCS programme) under grant agreement No 754092

Background

Background Information	[1] D2.5 Background and draft annexes for EN 1993-1-3 for assembled profiles, 31.10.2015, KIT

The project has received financial support from the European Community (RFCS programme) under grant agreement No 754092

5) Draft clauses for corrugated sheeting

- Corrugated profiles

New paragraph have to be created

The project has received financial support from the European Community (RFCS programme) under grant agreement No 754092

New clauses

AM-1-3-2016-05	
Subject	Load bearing capacity / characteristic values of corrugated profiles with sinusoidal or similar cross section
Clause No/ Subclause No/ Annex	
Reason for Amendment	No design rules by calculation available in EN 1993-1-3

The project has received financial support from the European Community (RFCS programme) under grant agreement No 754092

Approach 1

Proposed Change	In order to calculate the bending stiffnes and the ultimate bending moment for corrugated profils with sinusoidal or similar cross section, two approaches are proposed **1. Generally applicable design procedure with respect to local buckling in the compressed are:** 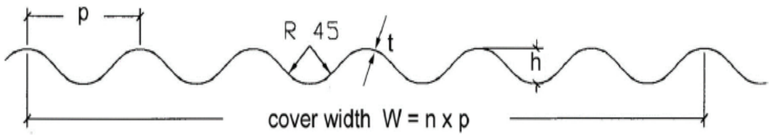 **Fig nn:** Typical cross section, definition of parameters • If $r/t \leq 0{,}04 * E / f_{yb}$: The cross section needs not be checked for local buckling characteristic bending moment: $M_{c,Rk} = W_y * f_{yb}$

Results of GRISPE

Based on Swedish approach + GRISPE

The project has received financial support from the European Community (RFCS programme) under grant agreement No 754092

Approach 1

Results of GRISPE

From gross section

- If $r/t > 0{,}04 * E / f_{yb}$: The characteristic bending moment should be calculated using the reduced compressive stress σ_c

  $M_{c,Rk} = W_y * \sigma_c$

  with:

  slenderness ratio: $\alpha = \sqrt{f_{yb} / \sigma_{elr}}$

  buckling stress $\sigma_{elr} = 0{,}60 * \eta * E * t / R$

  coefficient η $\eta = 0{,}19 + 0{,}67 / \sqrt{1 + R / 100 * t}$

  for $\alpha \leq 0{,}30$ $\sigma_c = f_{yb}$

  for $0{,}30 < \alpha < 1{,}10$ $\sigma_c = (1{,}126 - 0{,}419 * \alpha) * f_{yb}$

  for $1{,}10 \leq \alpha$ $\sigma_c = (0{,}8 / \alpha^2) * f_{yb}$

The project has received financial support from the European Community (RFCS programme) under grant agreement No 754092

Approach 1

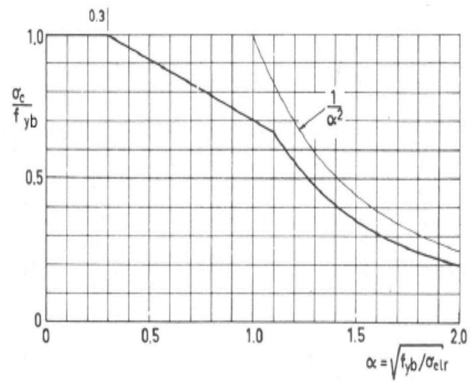

Fig nn: ultimate compressive stress with respect to local buckling of the cylindrical part of the profile

The moment of inertia, which is used to calculate deformations in serviceability limit state, should be calculated using the same procedure as for bending moment, but with reduced stress f_{yb} / 1,5.

Results of GRISPE

Curve to determine α

The project has received financial support from the European Community (RFCS programme) under grant agreement No 754092

Approach 2 - Simplified

2. Simplified procedure for restricted application range

If the conditions

- profile installed as single span girder and
- uniformly distributed loads and
- ratio $R/t \leq 0{,}1 * E / f_{yb}$ and
- steel core thickness $t_{cor} \geq 0{,}55$ mm and
- profile height 18 mm $\leq h \leq$ 46 mm and
- profile pitch 76 mm $\leq p \leq$ 150 mm

are met, the following simplified procedure may be adopted:

moment of inertia per unit width $J_y = 0{,}13 * t * h^2$

section modulus per unit width $W_y = 0{,}26 * t * h$

characteristic bending moment: $M_{c,Rk} = W_y * f_{yb}$

Results of GRISPE

Based on EN 1993-4-1 tank

The project has received financial support from the European Community (RFCS programme) under grant agreement No 754092

6) Draft clauses for curved profiles

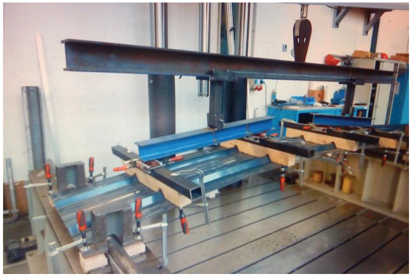

- Curved profiles

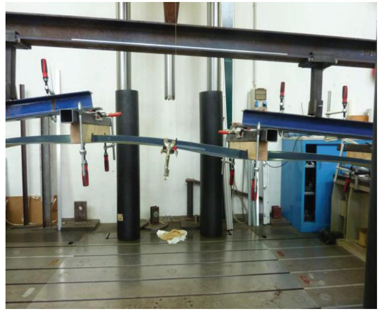

New paragraph have to be added

The project has received financial support from the European Community (RFCS programme) under grant agreement No 754092

New clauses 1.1(7) and 6.4

AM-1-3-2013-XX	
Subject	Design by calculation of curved profiles
Clause No./ Sub-clause No./ Annex	Section 1.1, adding new clause 1.1(7) Section 6, adding new section 6.4

The project has received financial support from the European Community (RFCS programme) under grant agreement No 754092

Arch – new paragraph

Results of GRISPE

Based on GRISPE tests and DIN formulation

Pro-posed change

Add a new clause:

1.1 (7) EN 1993-1-3 covers curved profiles.

Add a new section:

6.4 Curved profiles

(1) If the internal forces and moments are determined using first-order theory, verification must be carried out following the fictitious bar method. Clauses (2) and (3) are applied.

(2) In the case of compressive forces the following criterion may be used:

$$\boxed{\frac{N_{c,Ed}}{N_{c,Rd}} \cdot \left[1 + 0{,}5 \cdot \alpha \cdot \left(1 - \frac{N_{c,Ed}}{N_{c,Rd}}\right)\right] + \frac{M_{c,Ed}}{M_{c,Rd}} \leq 1}$$

with:

$N_{c,Ed}$ compressive force,

$N_{c,Rd}$ resistance for compressive force,

$M_{c,Ed}$ bending moment,

$M_{c,Rd}$ resistance for bending moment,

α factor dependent on section and geometry.

$$\boxed{\alpha = \sqrt{\frac{f_{y,b}}{\sigma_{cr}}} = \frac{s_K}{i_{ef} \cdot \pi} \cdot \sqrt{\frac{f_{y,b}}{E}}}$$

with:

σ_{cr} buckling stress in the effective cross section,

s_K buckling length: $s_K = \beta \cdot s$,

i_{ef} radius of inertia of the effective cross section: $i_{ef} = \sqrt{I_{eff}/A_{eff}}$

s half arc length as showned in figure 1,

β half arc length as showned in figure 1,

The project has received financial support from the European Community (RFCS programme) under grant agreement No 754092

Arch New paragraph

Results of GRISPE

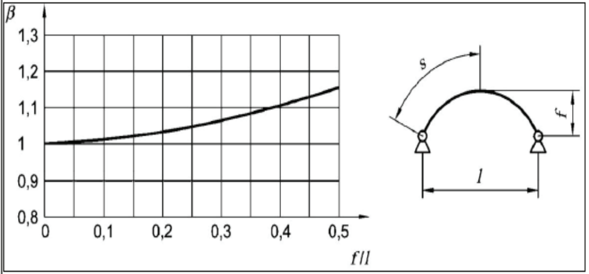

Figure 1: Arc characterisctics and determination of the factor β.

The resistance of compressive force is determined by:

$$\boxed{N_{c,Rd} = min\left(0{,}8 \cdot \sigma_{cr,gr} \cdot A_{gr}\,;\, \sigma_c \cdot A_{eff}\right)}$$

With:

$\sigma_{cr,gr}$ buckling stress in the gross section A_{gr}: $\sigma_{cr,gr} = \pi^2 \cdot E/\left(s_K/I_{gr}\right)^2$,

I_{gr} second moment of area of the gross cross-section,

σ_c critical stress in compression following table below:

α	$\sigma_c/f_{y,b}$
$\alpha \leq 0{,}30$	1,00
$0{,}30 < \alpha \leq 1{,}85$	$1{,}126 - 0{,}419 \cdot \alpha$
$1{,}85 < \alpha$	$1{,}2/\alpha^2$

(3) In the case of tensile forces, the following criterion may be used:

$$\boxed{\frac{N_{Ed}}{N_{t,Rd}} + \frac{M_{c,Ed}}{M_{c,Rd}} \leq 1}$$

With:

N_{Ed} axial tension,

$N_{t,Rd}$ design resistance of a cross-section for uniform tension (6.1.2).

(4) If the internal forces and moments are determined using second-order theory, the followed criterion may be used for the verification of the cross section under compressive forces:

$$\boxed{\frac{N_{c,Ed}}{N_{c,Rd}} + \frac{M_{c,Ed}}{M_{c,Rd}} \leq 1}$$

The verification under tensile forces remains unchanged using criterion defined at clause (3).

The project has received financial support from the European Community (RFCS programme) under grant agreement No 754092

Background

Back-ground infor-mation	RFCS research project GRISPE: DIN 18807 part 1 “Trapezoidal steel sheeting – General requirements and determination of loadbearing capacity by calculation” DIN 18807 part 3 “Trapezoidal steel sheeting – Structural analisys and design” DIN 18800 part 2 “Steel structures – Stability – Buckling of bars and skeletal structures” C. FAUTH (KIT) “Test report – Curved Profiles – Main Part", GRISPE D2.3, 2015 C. FAUTH (KIT) “Test report – Curved Profiles – Annex”, GRISPE D2.3, 2015 R. HOLZ (IFLSSON Consultants) “WP2 TEST ANALYSIS AND INTERPRETATION", GRISPE D2.4, XXXX C. FAUTH (KIT) " WP2 Background guidance for EN 1993-1-3 curved profiles", GRISPE D2.6, 2016
	Proposal from R. Holz, D. Izabel, T. Renaux

The project has received financial support from the European Community (RFCS programme) under grant agreement No 754092

Strength of curved profiles without arch effect

6.5 Curved profiled sheeting without arch effect

(1) For the design of the bending moment resistance of the curved profiled sheeting the following formula apply

$$\boxed{M_{c,Rd}(curved\,profile) = 0{,}9 \cdot M_{c,Rd}(flat\,profile) \qquad (6.40)}$$

The field of application is given in the table xx below :

Type of profile	Nominal thickness of the sheeting (mm)	Radius of curvarure R (m)
Corugated profile	0,63	4,3 ≤ R ≤ 11,50
	1,00	3,80 ≤ R ≤ 17,20
Trapezoidal profile	0,63	5,60 ≤ R ≤ 32,9
	1,00	6,40 ≤ R ≤ 25,80

Table xx field of application of the formula (6.40)

The project has received financial support from the European Community (RFCS programme) under grant agreement No 754092

Strength of curved profiles without arch effect

Background information	RFCS research project GRISPE: C. Fauth (KIT), WP2 Background guidance for EN 1993-1-3 curved profiles, GRISPE D2.6, October 2015
	Proposal from R. Holz, D. Izabel, T. Renaux

The project has received financial support from the European Community (RFCS programme) under grant agreement No 754092

7) Draft clauses for perforated profiles

- Perforated profiles

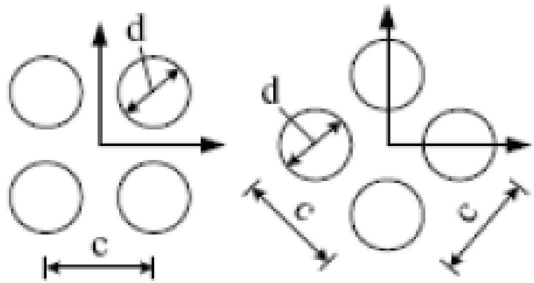

Article 10.4 have to be completed

The project has received financial support from the European Community (RFCS programme) under grant agreement No 754092

Perforated profile

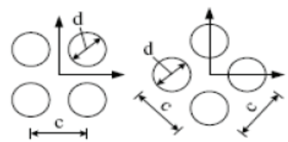

AM-1-3-2013- GRISPE4	
Subject	Perforated sheeting
Clause No./ Subclause No./ Annex	Section 10.4
Reason for amendment	The current version EN 1993-1-3 provides the design rules sheeting with triangular equilateral distribution of perforation. In practice the sheeting with square distribution of perforation is often used, but the information is missing as to the design rules for this case.

The project has received financial support from the European Community (RFCS programme) under grant agreement No 754092

Actual version of the clause 10.4 of EN 1993-1-3

Proposed change

The section 10.4 currently states:

10.4 Perforated sheeting

(1) Perforated sheeting with the holes arranged in the shape of equilateral triangles may be designed by calculation, provided that the rules for non-perforated sheeting are modified by introducing the effective thicknesses given below.

NOTE: These calculation rules tend to give rather conservative values. More economical solutions might be obtained from design assisted by testing, see Section 9.

(2) Provided that $0{,}2 \leq d / a \leq 0{,}9$ gross section properties may be calculated using 5, but replacing t by $t_{a,eff}$ obtained from:

$$t_{a,eff} = 1{,}18t\left(1 - \frac{0{,}9d}{a}\right) \qquad \text{... (10.25)}$$

where:

d is the diameter of the perforations;

a is the spacing between the centres of the perforations.

(3) Provided that $0{,}2 \leq d / a \leq 0{,}9$ effective section properties may be calculated using Section 5, but replacing t by $t_{b,eff}$ obtained from:

$$t_{b,eff} = t\sqrt[3]{1{,}18(1 - d / a)} \qquad \text{... (10.26)}$$

(4) The resistance of a single web to local transverse forces may be calculated using 6.1.7, but replacing t by $t_{c,eff}$ obtained from:

$$t_{c,eff} = t\left[1 - (d / a)^2 s_{per} / s_w\right]^{3/2} \qquad \text{... (10.27)}$$

where:

s_{per} is the slant height of the perforated portion of the web;

s_w is the total slant height of the web.

Replace the Section 10.4 with:

curent version of EN 1993-1-3

The project has received financial support from the European Community (RFCS programme) under grant agreement No 754092

Perforated profiles (new version of the clause 10.4)

10.4. Perforated sheeting

(1) Sheeting with the perforation arranged in the shape of equilateral triangles or sheeting with perforation in the flange or in the web arranged in squares, may be designed by calculation, provided that the rules for non-perforated sheeting are modified by introducing the effective thicknesses given below.

NOTE: These calculation rules tend to give rather conservative values. More economical solutions might be obtained from design assisted by testing, see Section 9.

(2) Provided that $0,2 \leq d/a \leq 0,9$ gross section properties may be calculated using 5.1, but replacing t by $t_{a,eff}$ obtained from:

Results of GRISPE

for triangular pattern: $t_{a,eff} = 1,18\,t \left(1 - \dfrac{0,9d}{a}\right)$ ... (10.25a)

for square pattern: $t_{a,eff} = 1,09t \left(1 - \dfrac{0,84d}{a}\right)$ ... (10.25b)

where:

d is the diameter of the perforations;

a is the spacing between the centres of the perforations.

Updating of the existing formula with the square distribution

The project has received financial support from the European Community (RFCS programme) under grant agreement No 754092

Perforated profiles (new version of the clause 10.4)

Results of GRISPE

Principe : use a reduced thickness in the area of the perforations

(3) Provided that $0{,}2 \leq d/a \leq 0{,}9$ effective section properties may be calculated using Section 5, but replacing t by $t_{b,eff}$ obtained from:

for triangular pattern: $$t_{b,eff} = t \sqrt[3]{1{,}18\left(1-\frac{d}{a}\right)} \quad \ldots (10.26a)$$

for square pattern: $$t_{b,eff} = 0{,}98t \sqrt[3]{\left(1-\frac{0{,}93d}{a}\right)} \quad \ldots (10.26b)$$

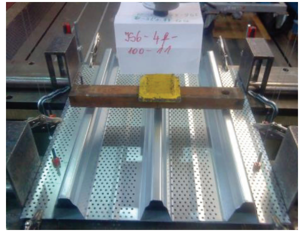

(4) The resistance of a single web to local transverse forces may be calculated using 6.1.9, but replacing t by $t_{c,eff}$ obtained from:

for triangular pattern: $$t_{c,eff} = t\left[1-\left(\frac{d}{a}\right)^2\frac{s_{per}}{s_w}\right]^{3/2} \quad \ldots (10.27a)$$

for square pattern: $$t_{c,eff} = t\left[1-0{,}866\left(\frac{d}{a}\right)^2\frac{s_{per}}{s_w}\right]^{3/2} \quad \ldots (10.27b)$$

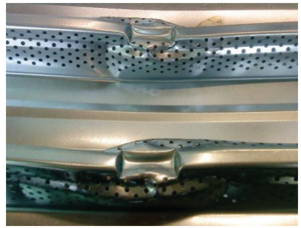

where:

s_{per} is the slant height of the perforated portion of the web;

s_w is the total slant height of the web.

The project has received financial support from the European Community (RFCS programme) under grant agreement No 754092

Background for perforated profile

Background information	RFCS research project GRISPE: C. FAUTH (KIT) "WP3 Test report", GRISPE D3.2, 2015 A. PALISSON (Sokol Palisson Consultants) "WP3 TEST ANALYSIS AND INTERPRETATION", GRISPE D3.4, 2015 A. PALISSON (Sokol Palisson Consultants) "WP3 Background guidance for EN 1993-1-3 to design of sheeting with perforations or with a hole", GRISPE D3.5, November 2015
	Proposal from A. Palisson, D. Izabel, L. Sokol

The project has received financial support from the European Community (RFCS programme) under grant agreement No 754092

8) Profiles with a hole in the flange

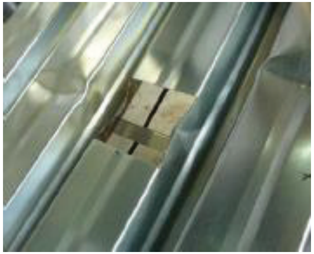

Holed profiles

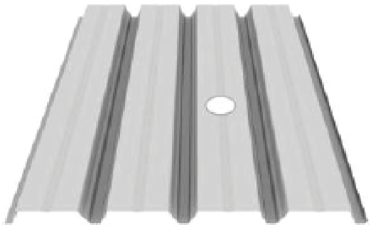

AM-1-3-2013- GRISPE5		
Subject	Sheeting with a hole in the flange	
Clause No./ Subclause No./ Annex	New section section 10.5	New clause Article 10.5 has to be added on « sheeting with an hole in the flange «
Reason for amendment	In practice the square or circular holes in compressed flange are often required for the passage of services, but the information is missing for the design rules for this case.	

The project has received financial support from the European Community (RFCS programme) under grant agreement No 754092

Holed profiles – Draft new clause 10.5

AM-1-3-2013- GRISPE5	
Subject	Sheeting with a hole in the flange
Clause No./ Subclause No./ Annex	New section section 10.5
Reason for amendment	In practice the square or circular holes in compressed flange are often required for the passage of services, but the information is missing for the design rules for this case.
Proposed change	Add a new Section 10.5: **10.5 Sheeting with a hole in the flange** (1) In case of a circular or rectangular hole in the compressed upper flange, the effective width of this flange is determined considering the portions of flange adjacent to the webs as outstand elements with width b_p (see figure 10.16). 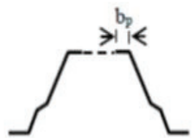 Fig. 10.16: Cross section passing by center of the hole in the flange of sheeting

Results of GRISPE

Taken into account the hole as an outstanding element

The project has received financial support from the European Community (RFCS programme) under grant agreement No 754092

Calibration of the amendement

Add a new Section 10.5:

10.5 Sheeting with a hole in the flange

(1) In case of a circular or square hole in the compressed upper flange, the effective width of the flange parts adjacent to the webs may be determined considering them as as outstand elements of width b_p (see figure 10.16).

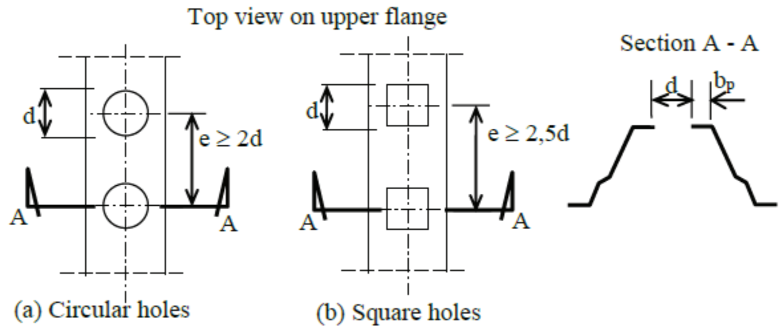

Fig. 10.16: Sheeting with circular (a) or square (b) holes in flange

(2) Range of validity :

a) trapezoidal profiled sheets;
b) no more than two holes by span in a flange, with minimum distances according to the Figure 10.16;
c) only uniformly distributed loads are permitted.

TC250 Sc3 group EN 1993--3

New field of application

The project has received financial support from the European Community (RFCS programme) under grant agreement No 754092

Background Holed profiles

Background information	RFCS research project GRISPE: C. FAUTH (KIT) "WP3 Test report", GRISPE D3.2, 2015 A. PALISSON (Sokol Palisson Consultants) "WP3 TEST ANALYSIS AND INTER-PRETATION", GRISPE D3.4, 2015 A. PALISSON (Sokol Palisson Consultants) "WP3 Background guidance for EN 1993-1-3 to design of sheeting with perforations or with a hole", GRISPE D3.5, November 2015
	Proposal from A. Palisson, D. Izabel, L. Sokol

The project has received financial support from the European Community (RFCS programme) under grant agreement No 754092

9) Draft clauses for planks

Plank profiles

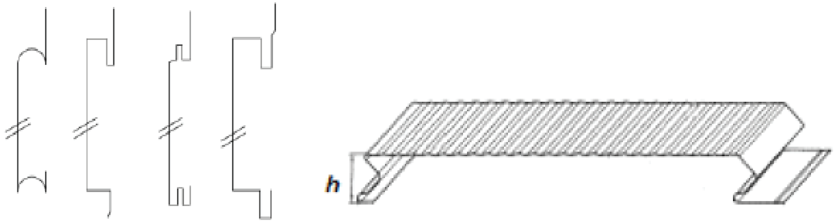

Modification of existing clauses for liner tray to cover planks
Creation of new article to cover the phenomenon of the dislocation of the joint

The project has received financial support from the European Community (RFCS programme) under grant agreement No 754092

Clause 6.1.7.3 (5) Eurocode 3 part 1.3

AM–1-3–2016–XX	
Subject	Scope of the formulas
Clause No. / Subclause No. / Annex	Clause 6.1.7.3 (5)
Reason for amendment	Scope of the formulas enlarged to plank profiles
Proposed change	The actual clause is: (5) The value of the coefficent α should be obtained from the following: a) for Category 1: - for sheeting profiles: $\alpha = 0{,}075$ ... (6.20a) - for liner trays and hat sections: $\alpha = 0{,}057$ ... (6.20b) b) for Category 2: - for sheeting profiles: $\alpha = 0{,}15$ ... (6.20c) - for liner trays and hat sections: $\alpha = 0{,}115$ ... (6.20d) The new clause should be: (5) The value of the coefficient α should be obtained from the following: a) for Category 1 : – for sheeting profiles: $\alpha = 0{,}075$ ... (6.20a) – for liner trays and hat sections: $\alpha = 0{,}057$ ... (6.20b) – for plank profiles: $\alpha = 0{,}115$ ... (6.20c) b) for Category 2: – for sheeting profiles: $\alpha = 0{,}15$ ... (6.20d) – for liner trays and hat sections: $\alpha = 0{,}115$ ... (6.20e) – for plank profiles: $\alpha = 0{,}115$ ... (6.20f)
Background information	D4.5 – Background guidance for EN 1993-1-3

Global behaviour on support

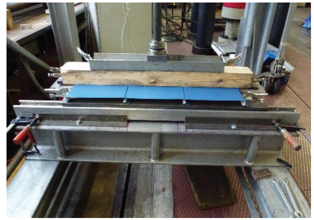

To adapt the support resistant capacity to planks

The project has received financial support from the European Community (RFCS programme) under grant agreement No 754092

Plank – integration in the Eurocode 3 1.3

AM–1-3–2016–XX	
Subject	Scope of the formulas
Clause No. / Subclause No. / Annex	Title 10.2
Reason for amendment	Scope of the formulas enlarged to plank profiles
Proposed change	Actual title is : **10.2 Liner trays restrained by sheeting** The title should be : **10.2 Liner trays restrained by sheeting and plank profiles**
Background information	D4.5 – Background guidance for EN 1993-1-3

The project has received financial support from the European Community (RFCS programme) under grant agreement No 754092

Clause 10.2.1 (1) to be completed

AM–1-3–2016–XX	
Subject	Scope of the formulas
Clause No. / Subclause No. / Annex	Clause 10.2.1 (1)
Reason for amendment	Scope of the formulas enlarged to plank profiles
Proposed change	The actual clause says: (1) Liner trays should be large channel-type sections, with two narrow flanges, two webs and one wide flange, generally as shown in figure 10.9. The two narrow flanges should be laterally restrained by attached profiled steel sheeting or by steel purlin or by similar component. 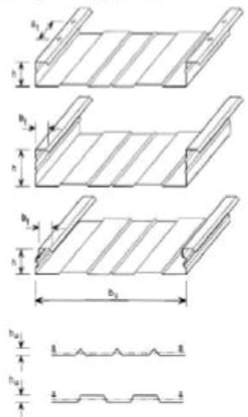 Figure 10.9: Typical geometry for liner trays The following text should be added: Plank profiles should be large channel type section with two webs and a flat wide flange. The joint between planks can be a clip one or chevron shaped as shown in figure 10.10. 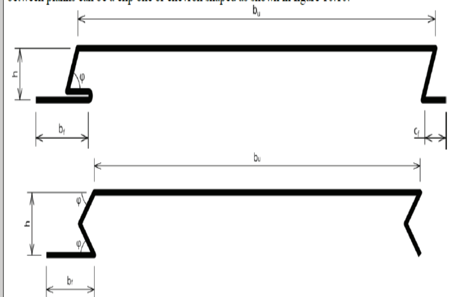 Figure 10.10: Typical geometry for plank profiles
Background information	D4.5 – Background guidance for EN 1993-1-3

To apply the liner-tray formulation to planks

The project has received financial support from the European Community (RFCS programme) under grant agreement No 754092

Clause 10.2.1 (2) to be completed

AM–1-3–2016–XX	
Subject	Scope of the formulas
Clause No. / Subclause No. / Annex	Clause 10.2.1 (2)
Reason for amendment	Scope of the formulas enlarged to plank profiles
Proposed change	The actual clause says: (2) The resistance of the webs of liner trays to shear forces and to local transverse forces should be obtained using 6.1.5 to 6.1.11, but using the value of $M_{c,Rd}$ given by (3) or (4). Change the clause for: (2) The resistance of the webs of liner trays and plank profiles to shear forces and to local transverse forces should be obtained using 6.1.5 to 6.1.11, but using the value of $M_{c,Rd}$ given by (3) or (4).
Background information	D4.5 – Background guidance for EN 1993-1-3

Global behaviour

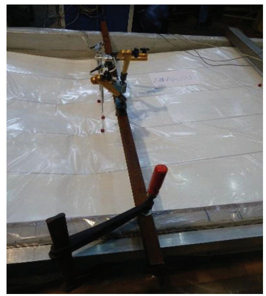

The project has received financial support from the European Community (RFCS programme) under grant agreement No 754092

Clause 10.2.1 (3) to be completed

AM–1-3–2016–XX	
Subject	Scope of the formulas
Clause No. / Subclause No. / Annex	Clause 10.2.1 (3)
Reason for amendment	Scope of the formulas enlarged to plank profiles
Proposed change	The actual clause states that: (3) The moment resistance $M_{c,Rd}$ of a liner tray may be obtained using 10.2.2 provided that: - the geometrical properties are within the range given in table 10.6; - the depth h_u of the corrugations of the wide flange does not exceed $h/8$, where h is the overall depth of the liner tray. The following text and table should be added: The moment resistance $M_{c,Rd}$ of a plank profile may be obtained using 10.2.2 provided that the geometrical properties are within the range given in table 10.7 **Table 10.7: Range of validity for plank profiles** 0,75 mm ≤ t_{nom} ≤ 1 mm b_f ≤ 40 mm 25 mm ≤ h ≤ 30 mm b_u ≤ 300mm φ ≤ 60° 11 mm ≤ c_f
Background information	D4.5 – Background guidance for EN 1993-1-3

To cover the full range of planks geometry

The project has received financial support from the European Community (RFCS programme) under grant agreement No 754092

Clause 10.2.1.4 (to be completed)

AM–1-3–2016–XX	
Subject	Scope of the formulas
Clause No. / Subclause No. / Annex	Clause 10.2.1 (4)
Reason for amendment	Scope of the formulas enlarged to plank profiles
Proposed change	The actual clause says: (4) Alternatively the moment resistance of a liner tray may be determined by testing provided that it is ensured that the local behaviour of the liner tray is not affected by the testing equipment. Change the clause for: (2) Alternatively the moment resistance of a liner tray or plank profile may be determined by testing provided that it is ensured that the local behaviour of the liner tray or plank profile is not affected by the testing equipment.
Background information	D4.5 – Background guidance for EN 1993-1-3

The project has received financial support from the European Community (RFCS programme) under grant agreement No 754092

New clause 10.2.3

AM–1-3–2016–XX	
Subject	Non dislocation of the plank joints
Clause No. / Subclause No. / Annex	New clause 10.2.3
Reason for amendment	Specific verification for joints of the plank profiles
Proposed change	The following clause should be added : **10.2.3 Non dislocation of the joint for plank profiles** (1) Dislocation of the joints for plank profiles is particular failure mode (2) To avoid dislocation of the joint of plank profile, we must verify : $q_{Ed} \leq q_{Rd}$ (3) The load resistance regarding joint dislocation of a plank profile is : $q_{Rd} = \frac{0{,}8 \cdot 2 \cdot E \cdot 1000 \cdot t^3 \cdot \delta_{\lim}}{b_u \cdot \left(12 \cdot (1-\nu^2) \cdot \sqrt{\left(\frac{2 \cdot b_f{}^3}{3}\right)^2 + \left[b_f \cdot \left(\frac{b_u \cdot h}{3} + \frac{h^2}{2}\right)\right]^2}\right)}$ Where: – For clip joint: $\delta_{\lim} = c_f$ – For chevron shaped joint: $\delta_{\lim} = \frac{h}{2 \cdot \tan\varphi}$
Background information	D4.5 – Background guidance for EN 1993-1-3

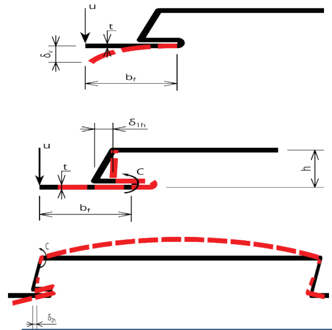

To cover the dislocation phenomenon = analysis of possible displacements with plank geometry

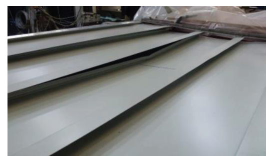

The project has received financial support from the European Community (RFCS programme) under grant agreement No 754092

Next steps

- Assembled profiles : in discussion in the preparation group of the amendement of the EC3 1.3 (murge Grispe + Swedish approach + EN 1090-4 approach)
- Holed profiles : murge Grispe approach and German approach (reinforcement of hole) and EN 1090-4 approach
- Other Grispe amendements on the TC 250 Sc3 table

The project has received financial support from the European Community (RFCS programme) under grant agreement No 754092